

R-66

# ASTROGEOLOGIC STUDIES

## ANNUAL PROGRESS REPORT

July 1, 1965 to July 1, 1966

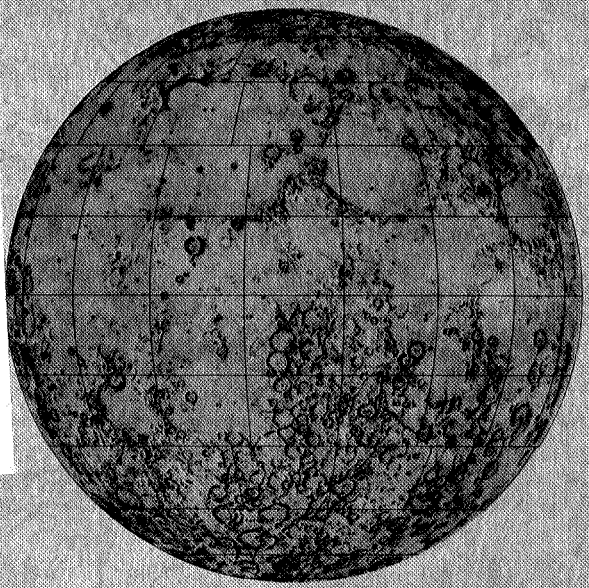
GPO PRICE \$ \_\_\_\_\_

CFSTI PRICE(S) \$ \_\_\_\_\_

Hard copy (HC) 3.00

Microfiche (MF) .65

ff 653 July 65



PART A  
LUNAR AND PLANETARY INVESTIGATIONS

**N67-31934 N67-31955**

(ACCESSION NUMBER) (THRU)

10 417 1

(PAGES) (CODE)

CR-86649 30

(NASA CR OR TMX OR AD NUMBER) (CATEGORY)

FACILITY FORM 602

DEPARTMENT OF THE INTERIOR

---

UNITED STATES GEOLOGICAL SURVEY

3A  
ASTROGEOLOGIC STUDIES,

4 ANNUAL PROGRESS REPORT

July 1, 1965 to

July 1, 1966<sup>9</sup>

Δ PART A: <sup>b</sup>LUNAR AND PLANETARY INVESTIGATIONS

3 December 1966

This preliminary report is distributed without editorial and technical review for conformity with official standards and nomenclature. It should not be quoted without permission.

This report concerns work done on behalf of the  
National Aeronautics and Space Administration

DEPARTMENT OF THE INTERIOR  
UNITED STATES GEOLOGICAL SURVEY

39

## CONTENTS

## PART A LUNAR AND PLANETARY INVESTIGATIONS

	Page
Introduction . . . . .	ix
SECTION I Published maps . . . . .	1
Summary of geology of the Pitatus region of the Moon. by N. J. Trask and S. R. Titley . . . . .	3 ✓
Introduction . . . . .	3
Stratigraphy . . . . .	3
Structure . . . . .	7
References . . . . .	8
The geology of Mare Serenitatis region of the Moon. by M. H. Carr . . . . .	11 ✓
Introduction . . . . .	11
Stratigraphy . . . . .	11
Structure . . . . .	15
References . . . . .	16
Geologic history of the Mare Humorum region of the Moon. by S. R. Titley . . . . .	17 ✓
Summary of the geology of the Hevelius region of the Moon. by J. F. McCauley . . . . .	23 ✓
Stratigraphy and structure . . . . .	23
Geologic history . . . . .	27
Luna 9 landing site . . . . .	28
References . . . . .	28
Summary of the geology of the Copernicus quadrangle of the Moon. by H. H. Schmitt, N. J. Trask, and E. M. Shoemaker . . . . .	31 ✓
Introduction . . . . .	31
Stratigraphy . . . . .	31
The crater Copernicus . . . . .	35

Copernicus quadrangle--Continued	Page
Dark-halo craters . . . . .	38
References . . . . .	38
Summary of the geology of the Seleucus quadrangle	
of the Moon, by H. J. Moore . . . . .	41 ✓
Introduction. . . . .	41
Stratigraphy. . . . .	41
Lineations and faults . . . . .	49
References . . . . .	49
Geology of the Julius Caesar and Mare Vaporum	
quadrangles, by Don E. Wilhelms and Elliot	
C. Morris.. . . . .	51 ✓
Introduction . . . . .	51
Stratigraphy . . . . .	51
Structure . . . . .	57
Geologic history. . . . .	60
References. . . . .	61
SECTION 11--Preliminary maps and other geologic	
studies. . . . .	63
A comparison of two terrestrial grabens with the	
lunar rilles Rima Ariadaeus and Rimae Hypatia	
I and II, by George I. Smith . . . . .	65 ✓
Introduction, . . . . .	65
Terrestrial grabens . . . . .	65
Lunar rilles Rima Ariadaeus and Rima Hypatia . . . . .	75
Comparison of terrestrial and lunar features . . . . .	82
Origin of terrestrial and lunar features. . . . .	82
References cited . . . . .	84
Seismic energy as an agent of morphologic	
modification on the Moon, by S. R. Titley. . . . .	87
Introduction . . . . .	87
Sources and nature of lunar seismicity . . . . .	88
Nature of lunar surface materials . . . . .	91

3

Seismic energy.. Continued	Page
Surface seismic effects on Earth and their relationships to the Moon . . . . .	94
Evidence of lunar seismic effects . . . . .	99
Summary., . . . . .	99
References cited . . . . .	101
Preliminary report on the geology of the Plato quadrangle of the Moon. by J. W. M'Gonigle and D. L. Schleicher . . . . .	
	105 ✓
Introduction . . . . .	105
Description of rock units . . . . .	105
Age relation of Unit 2 . . . . .	110
Structure . . . . .	110
Geologic history . . . . .	112
References. . . . .	113
Preliminary geologic summary of the Cassini quadrangle of the Moon. by Norman J Page. . . . .	
	115 ✓
Introduction . . . . .	115
Stratigraphy . . . . .	115
Special features . . . . .	118
Structure . . . . .	119
References . . . . .	120
Probable igneous relations in the floor of the crater J. Herschel. by G. E. Ulrich . . . . .	
	123 ✓
Introduction . . . . .	123
Morphology of features . . . . .	123
Geologic interpretation . . . . .	126
Conclusions . . . . .	130
References cited . . . . .	131
Structure of the Triesnecker-Hipparchus region. by T. W. Offield . . . . .	
	133 ✓
Introduction . . . . .	133
Regional setting . . . . .	138

Triesnecker-Hipparchus--Continued	Page
Distribution of lineaments. . . . .	138
Nature of lineaments. . . . .	147
Relative ages of lineaments . . . . .	149
Origin of lineament pattern . . . . .	150
References. . . . .	153
SECTION III--Lunar and planetary physics . . . . .	155
The theory of radiative transfer in the lunar surface. by Robert L. Wildey . . . . .	157 ✓
Maximum polarization values of some lunar geologic units. by N. J. Trask. . . . .	163 J
Spatial filtering of astronomical photographs. by Robert L. Wildey . . . . .	169 ✓
Application of moiré patterns to lunar mapping. by David Cummings and H. A. Pohn . . . . .	183 ✓
Introduction . . . . .	183
Screens and technique . . . . .	184
Application of moiré patterns to lunar photograph interpretation . . . . .	185
Conclusions . . . . .	185
References. . . . .	187
The processing of photoclinometric data. by Alexander J. Swartz. . . . .	189 ✓
The nocturnal heat sources of the surface of the Moon. by Robert L. Wildey. . . . .	195 ✓
Summary . . . . .	195
Introduction. . . . .	195
Observations. . . . .	197
Analysis. . . . .	200
Conclusions . . . . .	207
References . . . . .	208

	Page
A photoelectric-photographic map of the normal albedo of the Moon. by H. A. Pohn and R. L. Wildey . . .	211 ✓
Introduction. . . . .	211
The observations . . . . .	214
Absolute calibration . . . . .	215
The absolute albedo map . . . . .	220
Acknowledgments . . . . .	224
Appendix A . . . . .	225
Appendix B . . . . .	229
References . . . . .	231
SECTION IV--Summary of telescopic lunar stratigraphy.	
by Don E. Wilhelms . . . . .	
Introduction . . . . .	237
Application of stratigraphic principles to the Moon . . . . .	239
The lunar stratigraphic column . . . . .	251
Interpretative summary . . . . .	295
References . . . . .	298

## INTRODUCTION

This Annual Report is the seventh of a series describing the results of research conducted by the U.S. Geological Survey on behalf of the National Aeronautics and Space Administration. The report is in four volumes corresponding to four main areas of research: Part A, Lunar and Planetary Investigations (with a map supplement); Part B, Crater Investigations; Part C, Cosmic Chemistry and Petrology; and Part D, Space Flight Investigations. An additional volume presents abstracts of the papers in Parts A, B, C, and D.

The long-range objectives of the astrogeologic studies program are to determine and map the stratigraphy and structure of the Moon's crust, to work out from these the sequence of events that led to the present condition of the Moon's surface, and to determine the processes by which these events took place. Work that leads toward these objectives includes a program of lunar geologic mapping; studies on the discrimination of geologic materials on the lunar surface by their photometric, polarimetric, and infrared properties; field studies of structures of impact, explosive, and volcanic origin; laboratory studies on the behavior of rocks and minerals subjected to shock; and study of the chemical, petrographic and physical properties of materials of possible lunar origin and the development of special techniques for their analysis.

Part A, Lunar and Planetary Investigations, consists of four sections of text and a map supplement. Preliminary maps of seven quadrangles at a scale of 1:1,000,000 are included in the map supplement; five are located in the northwest quadrant of the Moon and two in the southeast. These maps represent the first extensions of lunar geologic mapping beyond the equatorial belt (lat 32° N.-32° S., long 70° E.-70° W.) that was covered in previous years. Three maps in the equatorial belt at a scale of 1:500,000 are also

included in the map supplement, and structural maps of two others are shown as text figures.

The first text section is a collection of geologic summaries of eight maps at a scale of 1:1,000,000 published or in press during the present report period. In addition to these, two other quadrangle maps were published in this period, Montes Apenninus and Aristarchus, but their geology was summarized in previous annual reports in articles by Hackman (1962-63 rept. , p. 1-8) and Moore (1962-63 rept., p. 33-45; 1963-64 rept. , p. 42-51). Some of the eight quadrangle maps summarized in this section are accompanied by summary texts in their published form: Copernicus, Hevelius, Mare Humorum, Mare Vaporum, and Seleucus. The others-- Julius Caesar, Pitatus, and Mare Serenitatis--do not have summary texts in their published form. Two quadrangles, Julius Caesar and Mare Vaporum, are geologically similar and thus are discussed in one article in this report.

The second section includes two topical studies, summaries or special studies of the geology in three of the seven quadrangles covered by preliminary maps in this report, and a structural study of two 1:500,000-scale quadrangles.

The third section comprises seven articles describing studies in lunar and planetary physics that are in support of the geologic mapping program.

The fourth section is an extensive summary of lunar stratigraphic concepts and of stratigraphic units that appeared on preliminary maps produced through the annual report period preceding this one and on revised published versions of some of these same maps.

SECTION I  
PUBLISHED MAPS

N67-51935

SUMMARY OF THE GEOLOGY OF THE  
PITATUS REGION OF THE MOON

By N. J. Trask and S. R. Titley

INTRODUCTION

The Pitatus region in the southwest part of the equatorial belt (lat 16"-32" S., long 10"-30" W.) includes parts of three geologic provinces: the eastern rim of the Humorum basin, a small part of the southern lunar highlands, and the western part of the Mare Nubium (fig. 1) (Titley, 1964b; Trask and Titley, 1966). Bullialdus, one of the larger post-mare craters, is a prominent feature in the central part of the region.

STRATIGRAPHY

The top of the widespread mare material of the Procellarum Group of Imbrian age is the most satisfactory stratigraphic datum in the region. The more rugged topography of the terrae is embayed by the mare material at many places and appears to be older except for some local deposits. Stratigraphic units are not well shown on the terrae, and the classification of the terrae employed on the geologic map of the region (Trask and Titley, 1966) is based on a qualitative analysis of the local terrain.

Positive relief features dominate the topography around the Humorum basin and form a widespread area of hummocky terrain, first recognized by Titley (1964a) and Titley and Eggleton (1964). The hummocks diminish in size outward from the rim of the basin, and in the Pitatus region in the area southeast of Mercator grade to very small hills that are strung out in lines or are themselves linear and radial to the center of the basin. The progressive and systematic changes in this hummocky terrain warrant its designation as a formation, the Vitello Formation, with type area near the younger crater Vitello in the southwest part of the Humorum basin (Trask and Titley, 1966; Titley, 1967). The hummocky topography

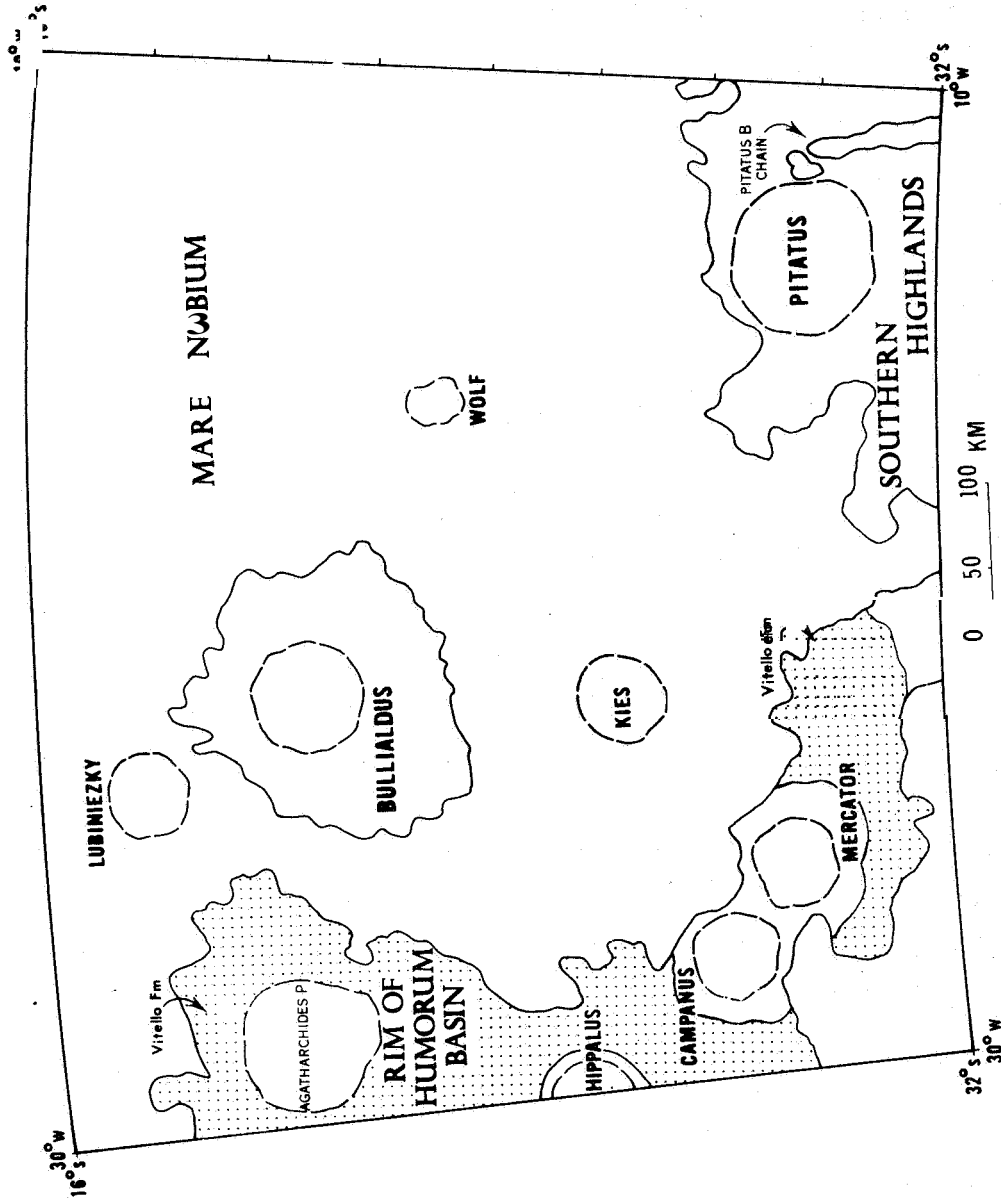


Figure 1.--Sketch showing major geographic features of the Pitatus region and the extent of the Vitello Formation (possible ejecta from the Humorum basin). Dashed lines indicate rim crests of major craters.

of the Vitello Formation may be partly due to the uneven texture of a blanket of material ejected from the Humorum basin by impact and partly to a structural fabric developed at the time of formation of the basin in materials that predated the basin. The Vitello Formation records the event or series of events that gave rise to the Humorum basin. The Vitello has more superposed craters on it than the Fra Mauro Formation, which surrounds the Imbrium basin, and the rim of the Humorum basin is dissected by structural elements such as faults and lineaments to a greater degree than the rim of the Imbrium basin. For these reasons, the Humorum basin is believed to be older than the Imbrium basin. The Vitello Formation is therefore pre-Imbrian.

Highly dissected craters whose overall topography is similar to that of the Vitello are evidently older than the Humorum basin; Agatharchides P is the best example in the Pitatus region. Also, elongate smooth-appearing hills and ridges that stand above the surrounding hummocky terrain are probably the expression of structurally uplifted blocks of pre-basin material and have been mapped as pre-Imbrian ridges and hills; any impact-produced ejecta that may have been deposited on such blocks has either slumped off or is relatively thin.

Undissected circular craters superposed on the Vitello Formation are younger than the Humorum basin. Materials of craters in this category that are also filled with mare material, such as Campanus and Mercator, form another well-defined stratigraphic unit and are referred to the Gassendi Group of Imbrian and pre-Imbrian age, named for the large crater Gassendi in the northern part of the Humorum basin (Trask and Titley, 1966; Titley, 1964a, 1967).

The topography of the southern lunar highlands in the southeast corner of the Pitatus region in many respects is similar to that around the Humorum basin. Positive relief features dominate the terrain and range in size from large smooth-appearing hills and ridges down to hummocks that are barely discernible at the telescope. Many of the hummocks are aligned parallel to adjacent lineaments.

Small pits are present in some places. The time of development of this topography relative to the standard lunar stratigraphic column is not known. The rim of the large mare-filled crater Pitatus (diameter 90 km) appears to be covered except for narrow strips on its northwest and eastern sides by hummocky material which extends outward from the crater for a distance of several crater diameters. The impression is strong that the covering material is volcanic, composed of flows and pyroclastic materials that were relatively viscous and conformed only slightly to the underlying topography. The material is similar to the Kant plateau-forming material described by Milton (in press). Concentric chain craters and rilles on both the raised rim of Pitatus and the mare material covering the floor suggest that the crater itself may have been the site of eruption of much of this material. Whether Pitatus was originally an impact crater or is entirely volcanic can only be surmised.

East of and tangential to the rim of Pitatus is a strikingly aligned set of irregularly shaped but sharp-rimmed craters--Gauricus M, and Pitatus B, N, P, and G. These have often been cited as a volcanic chain (for example, Green, 1963). The alinement appears to be too strong to have formed by random impact; the craters in the chain are too large to be secondary impact craters from any nearby primary. The craters have been assigned to the Gassendi Group because they are partly filled and partly embayed by smooth-appearing plains-forming material resembling material which at some places elsewhere on the terrae is of Imbrian age. Activity along this chain could conceivably have extended into post-mare time, however.

The Procellarum Group in Mare Nubium exhibits a wide range of albedo and, except where covered by rays and diffuse bright streaks radial to Tycho, can be divided into four subunits according to albedo. The darkest unit includes some of the darkest material on the Moon (Rowan and West, 1965), and the lightest has an unusually high albedo for mare material. The darker units have fewer visible craters than the lighter units. The many ghost craters and islands of terra in Mare Nubium indicate that the Procellarum is relatively thin in this region (Titley, 1964b).

Deposition of the mare material was followed by further cratering. Bullialdus is the largest post-mare crater in the region; it has a rugged, hummocky rim with concentric ridges close to the rim crest, more gentle radial ridges farther from the crest, and a surrounding field of small radially disposed satellitic craters. Bullialdus has a few very faint rays (Titley, 1964b) and may be a relatively young Eratosthenian crater. Rays from the younger Copernican crater Tycho cross the rim, wall, and floor of Bullialdus. Lying on many of the Tycho rays, especially at the proximal ends, are small craters, 2 to 5 km in diameter, arranged in clusters or lines radial to Tycho. These are interpreted as secondary impact craters formed by fragments ejected at the time of the Tycho impact. Similar craters also occur outside of well-defined rays and are labeled Tycho secondaries, although with an additional degree of uncertainty.

#### STRUCTURE

Numerous scarps, ridges, and lineaments in the Pitatus region are related to both the Humorum basin and the more random system of linear features on the southern lunar highlands. The Humorum basin, like the Imbrium basin, is surrounded by a series of concentric arches and troughs (Hartmann and Kuiper, 1962; Titley, 1967). One arch passes through the western part of the Pitatus region in the area southwest of Agatharchides P and northwest of Campanus. On the arch are several grabens, also concentric to the basin, that cut both the terra and mare material. The concentric grabens appear to be offset slightly by later grabens trending northeast-southwest (Titley, 1964b).

On the rest of the terrae, linear features trend both northeast and northwest, though with a wide range of directions in detail. Especially prominent is the sharp scarp extending southeast from Mercator; it is interpreted as an old fault scarp in the terra against which the younger mare material has abutted. Northeast- and northwest-trending scarps and troughs appear to be reinforced

where they coincide with the direction radial to Mare Humorum, as in the area west of Lubiniezky and in the area southeast of Mercator. Much of the hummocky terrain in the terrae may have developed by repeated movement along these structural elements with concurrent slumping and erosion of surface materials to produce the rounded forms visible today. The numerous mare ridges also have a wide range of orientations with poorly developed maximums in the north-east, northwest, and north directions; they almost certainly reflect buried structural features in the subjacent terrae. Collectively, the structural features indicate that the history of the region is complex and involves tectonism, subsidence, basin filling, and further subsidence (Titley, 1964b).

#### REFERENCES

- Green, Jack, 1963, The geology of the lunar base: New York Acad. Sci. Annals, v. 105, p. 489-626.
- Hartmann, W. L., and Kuiper, G. P., 1962, Concentric structures surrounding lunar basins: Arizona Univ. Lunar and Planetary Lab. Commun., v. 1, no. 12, p. 51-72.
- Milton, D. J., in press, Geologic map of the Theophilus region of the Moon: U.S. Geol. Survey Misc. Geol. Inv. Map.
- Rowan, L. C., and West, Mareta, 1965, A preliminary albedo map of the lunar equatorial belt, in Astrogeologic Studies Ann. Prog. Rept., July 1, 1964-July 1, 1965, pt. A: U.S. Geol. Survey open-file rept., p. 101-113.
- Titley, S. R., 1964a, A summary of the geology of the Mare Humorum quadrangle of the Moon, in Astrogeologic Studies Ann. Prog. Rept., Aug. 25, 1962-July 1, 1963, pt. A: U.S. Geol. Survey open-file rept., p. 64-74,
- \_\_\_\_\_ 1964b, Stratigraphic and structural relationships in the Pitatus quadrangle and adjacent parts of the Moon, in Astrogeologic Studies Ann. Prog. Rept., July 1, 1963-July 1, 1964, pt. A: U.S. Geol. Survey open-file rept., p. 90-101.

Titley, S. R. , 1967, Geologic map of the Mare Humorum region of the Moon: U.S. Geol. Survey Misc. Geol. Inv. Map 1-495.

Titley, S. R., and Eggleton, R. E., 1964, Description of an extensive hummocky deposit around the Humorum basin, in Astrogeologic Studies Ann. Prog. Rept., July 1, 1963-July 1, 1964, pt. A: U.S. Geol. Survey open-file rept., p. 85-89.

Trask, N. J., and Titley, S. R., 1966, Geologic map of the Pitatus region of the Moon: U.S. Geol. Survey Misc. Geol. Inv. Map 1-485.

120me 3

N67-31936

3 THE GEOLOGY OF THE MARE SERENITATIS REGION  
OF THE MOON 6

By M. H. Carr 8

8 same as first draft.  
P. 11-16 CS  
20me

INTRODUCTION

The Mare Serenitatis region in the northeast quadrant of the lunar disk (lat 16"-32" N., long 10"-30" E.) includes most of Mare Serenitatis and some terra areas to the south and east (fig. 1). The dominant geologic units exposed in the region are various subunits of the Procellarum Group. Older units are exposed on the terra, and younger units occur around rilles at the edge of the mare and locally around craters. The most striking geologic features of the region are the differences in albedo of the Procellarum Group, the materials of low albedo associated with rilles at the edge of the mare, and the pattern of ridges and rilles concentric with the Serenitatis basin.

STRATIGRAPHY

The Serenitatis basin appears to have formed before the Imbrium basin. Part of the arc formed by the Apennine and Caucasus Mountain<sup>1</sup> is concentric with the Imbrium basin and is probably related to the formation of that basin. The fact that this arc cuts across the western edge of Mare Serenitatis is evidence that that basin formed before the Imbrium basin. In addition, typical Fra Mauro Formation, presumably ejecta from the Imbrium basin, is found southwest of Mare Serenitatis on the Haemus and Apennine Mountains, but an analogous unit derived from the Serenitatis basin has not been found anywhere. Ejecta from the Serenitatis basin, if it ever existed, would be so modified by now as to be unrecognizable. Similarly, no structures

---

<sup>1</sup>For convenience, English names are used instead of the Latin names that appear on the ACIC topographic maps.

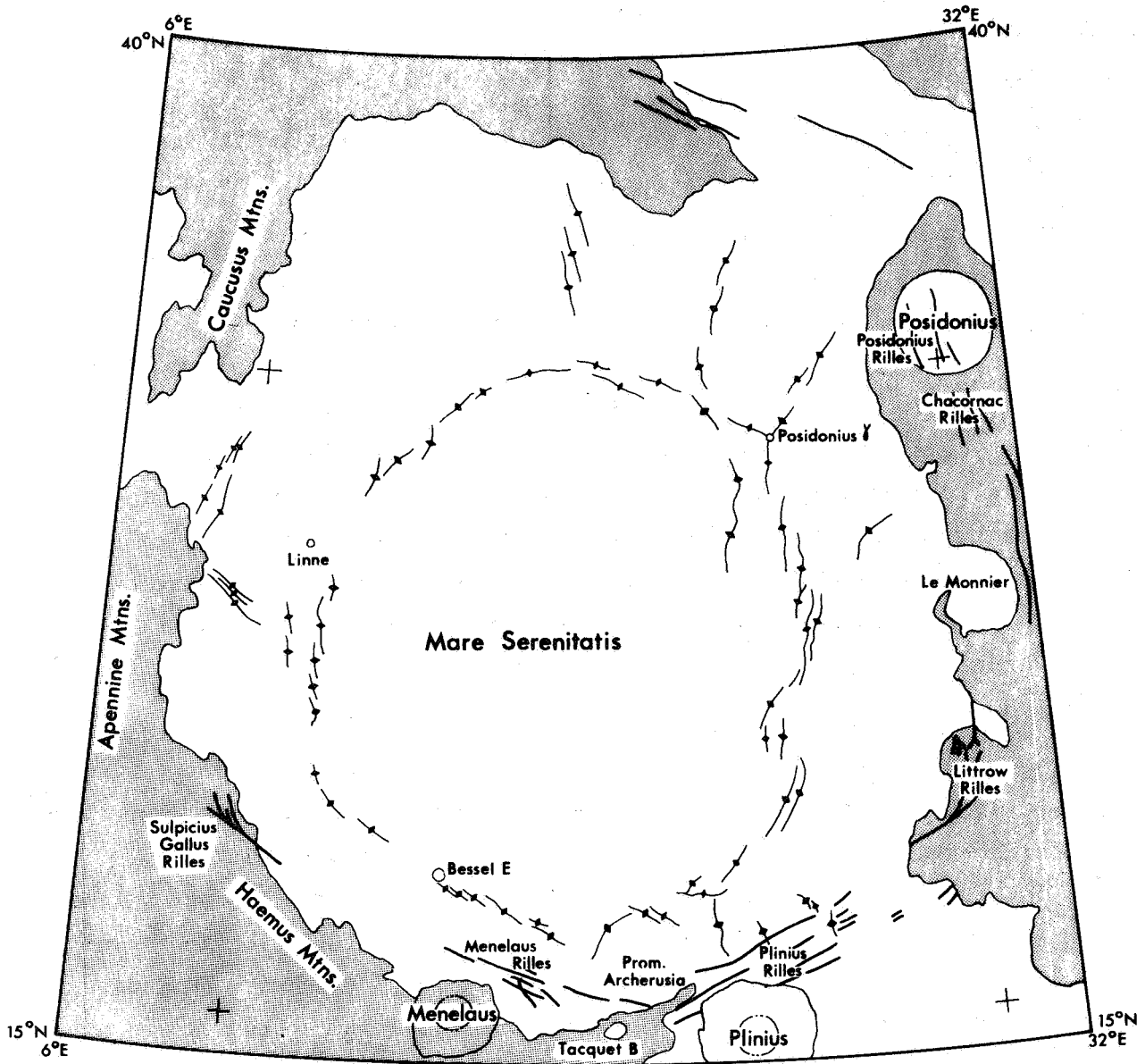


Figure 1.--Sketch of Mare Serenitatis showing concentric rilles and radial mare ridges outside an inner circle of concentric mare ridges. Stipple indicates terra. Ticks near lower right- and left-hand corners indicate corners of geologic map of Mare Serenitatis region (Carr, 1966). Scale 1:5,000,000.

that are radial to Mare Serenitatis analogous to the Imbrium sculpture have been reported in the literature or clearly identified by the author.

The ages of the Serenitatis and Imbrium basins and the mare filling provide a basis for determining the relative ages of craters in the area. No craters older than the Serenitatis basin are recognized. Craters that are probably older than the Imbrium basin, exemplified by Le Monnier and Tacquet B, have low, almost nonexistent rims that lack the hummocky topography characteristic of the rims of younger craters. Their crater shape has been maintained despite their proximity to the Serenitatis basin, and they are therefore considered to be younger than that basin. Tacquet B is covered with Fra Mauro Formation and is therefore clearly pre-Imbrian. Other craters that predate the present mare surface appear fresher and probably formed after the Imbrium basin. Posidonius, the most prominent example, has a well-defined hummocky rim. Although there is no conclusive evidence of an Imbrian age, the resemblance of Posidonius to other Imbrian craters suggests that it is in fact Imbrian.

The post-mare craters resemble those found elsewhere on the surfaces of the maria. The locations of some suggest internal origins; unusually large numbers lie along the Sulpicius Gallus and Menelaus Rilles; and Posidonius  $\gamma$ , one of the brightest ray craters in Mare Serenitatis, lies at the junction of two mare ridges.

Around the edge of Mare Serenitatis, several units occur which have low albedo and are closely associated with rilles (Carr, 1965). The Sulpicius Gallus Formation (Carr, 1966) occurs around the Sulpicius Gallus Rilles and covers both the terra and mare; it is believed to be a thin layer of post-Procenian Group volcanic material whose origin is closely related to formation of the Sulpicius Gallus Rilles. Other units with low albedo occur near the Menelaus Rilles (Tacquet Formation of Carr, 1966) and the Littrow Rilles and probably represent the final stages in the filling of the Serenitatis basin with volcanic materials. The surface topography

of these units near the Menelaus and Littrow Rilles, their scarp-like contacts with the rest of the mare, their close association with rilles, and the large numbers of craters on the rilles suggest that they are volcanic in origin and younger than the Procellarum Group.

The Procellarum Group itself has been divided into four albedo units. That different parts of Mare Serenitatis have different albedos is obvious from any full Moon photograph. Some albedo changes are abrupt along a well-defined line; others are gradational. To aid in mapping the different albedo units, isodensitometer tracings were made of a photograph of Mare Serenitatis taken close to full Moon (Lick Observatory Plate L-18, Jan. 17, 1946, 7:51 U.T.). Sharp contacts were drawn on the basis of a visual examination of several near full Moon photographs; gradational contacts were drawn from the isodensitometer measurements. In cooperation with H. A. Pohn and R. L. Wildey and using a photoelectric photometer, direct telescopic measurements were made of the reflectivity of different parts of Mare Serenitatis at phase angles of  $4''$  and  $7^\circ$ . These 'measurements were used to calibrate the isodensitometer tracings and to provide absolute values for the albedos of the different units of the Procellarum Group.

The differences in albedo are believed to correspond to differences in the underlying geologic units and not merely to differences in the surface material, a few millimeters thick, that scatters incident light. This is particularly true of the contact between the dark, marginal materials and the lighter materials in the central part of the mare; this contact coincides with a low scarp north and northeast of Areherusia Promontory and northwest of the Menelaus Rilles. The lighter material is on the low side of the scarp. The coincidence of albedo contacts with topographic relief suggests strongly that the albedo units are true stratigraphic units. The striking concentric pattern of the marginal albedo units implies that their distribution is structurally controlled and constitutes further evidence that they are related

to the underlying geologic units. The different albedo units probably correspond to formations of the Procellarum Group of different ages. The mare material around the Menelaus and Littrow Rilles is younger than the Procellarum Group and has a very low albedo. By analogy, it is suggested that within the Procellarum Group the unit with the lowest albedo is the youngest and the one with the highest albedo is the oldest.

#### SIRUCTURE

Some of the structural features found around other lunar basins are missing around the Serenitatis basin. It lacks the conspicuous concentric scarps that are characteristic of fresh-appearing basins such as Imbrium, Nectaris, and Orientale (Hartmann and Kuiper, 1962; Hartmann, 1963). There is a faint indication of a scarp concentric to the center of Mare Serenitatis in the terra to the east of the mare in the Macrobius quadrangle (Pohn, 1965). This, however, is a very subdued feature compared with the Altai Scarp concentric to the Nectaris basin or the Cordillera Mountains concentric to the Orientale basin. The absence of prominent concentric scarps and troughs probably indicates that the Serenitatis basin is older than basins possessing these features. It also suggests that some process is causing the destruction of the concentric features with time. Isostatic readjustment, meteoritic bombardment, and mass wasting are possible mechanisms.

Mare Serenitatis does have a well-developed concentric rille and mare ridge system (fig. 1). An almost complete circle of ridges occurs within the mare; outside this circle ridges occur that are radial to the center of the basin. The pattern of an inner circle of ridges and radial ridges outside it is similar to that observed in Mare Imbrium and indicates strong control of the location of the ridges by the underlying structure of the basin. Mare Serenitatis is also almost completely girdled by concentric rilles: the Sulpicius Gallus, Menelaus, Plinius, Littrow, Chacornac, and Posidonius Rilles, to name those on the south and

east. The rilles to the south lie within the mare, but to the east and north they are in the terra just beyond the margin of the mare. Only in the west are concentric rilles absent, and this probably results from the dominant effect of the Imbrium basin.

#### REFERENCES

- Carr, M. H. , 1965, Dark volcanic materials and rille complexes in the north central region of the moon, in Astrogeologic studies Ann. Prog. Rept. , July 1964-July 1965, pt. A: U.S. Geol. Survey open-file rept., p. 35-43.
- \_\_\_\_\_, 1966, Geologic map of the Mare Serenitatis region of the Moon: U.S. Geol. Survey Misc. Geol. Inv. Map 1-489.
- Hartmann, W. K. , 1963, Radial structures surrounding lunar basins, I; the Imbrium system: Arizona Univ. Lunar and Planetary Lab. Commun. , v. 2. no. 24, p. 1-15.
- Hartmann, W. K., and Kuiper, G. P., 1962, Concentric structures surrounding lunar basins: Arizona Univ. Lunar and Planetary Lab. Commun. v. 1, no. 12, p. 51-66.
- Pohn, H. A. , 1965, The Serenitatis Bench and Bond Formation, in Astrogeologic Studies Ann. Prog. Rept., July 1964-July 1965, pt. A: U.S. Geol. Survey open-file rept., p. 9-12.

1  
3  
N67-31937

3  
GEOLOGIC HISTORY OF THE MARE HUMORUM REGION  
OF THE MOON

By S. R. Titley

same p 11-21 RS  
same

The principal feature of the Mare Humorum region (fig. 1) is the circular mare-filled Humorum basin, approximately 330 km in diameter. The basin formed early in the history of the Moon and was later flooded by mare material. Impact cratering with attendant erosion and aggradation, episodic volcanism, and faulting have also occurred in the region. The inferred history of the Humorum basin is similar to that of the Imbrium basin (Shoemaker and Hackman, 1962; Titley, 1963), but the more subdued topography and the greater density of craters on the rim of the Humorum basin suggest that it is older than the Imbrium basin.

The earliest history of the region has been mostly obscured by formation of the basin and later events. A few large craters, such as Agatharchides, Mersenius P, and a large, nameless, nearly circular crater in the northwest probably predate the formation of the basin because they are extensively eroded and sculptured and because they appear to be partly covered by ejecta from the basin. Prior to formation of the Humorum basin the region was probably topographically similar to the highly cratered terra of the southern part of the earthside hemisphere.

The geologic relations suggest that the basin was formed by the impact of a large body. The whole complex concentric structure probably originated at the time of or shortly after the impact. It consists of a series of roughly concentric depressed benches and troughs and several elevated arcs of rugged fractured blocks (Hartmann and Kuiper, 1962), all of which ring a relatively deep

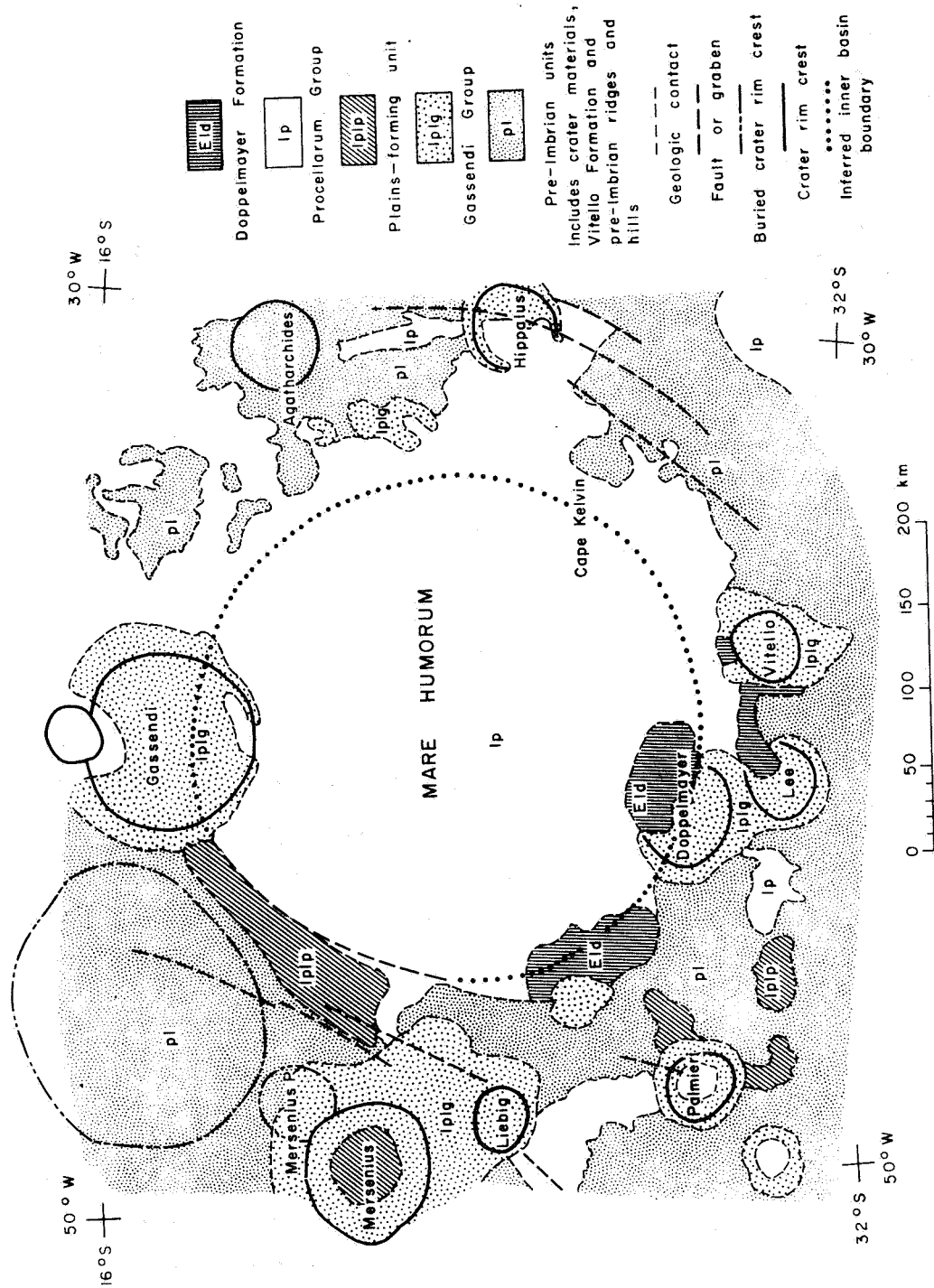


Figure 1.--Generalized geology of the Mare Humorum region of the Moon, showing distribution of principal regional stratigraphic units.

basin, which lacks islands of pre-basin terra material. The bench surrounding it is partly covered by mare material and contains islands and peninsulas of terra. Outside the bench is a discontinuous raised scarp, most pronounced in the rugged highlands southeast of Cape Kelvin and southwest of the crater Gassendi. This scarp is the inner face of a generally mountainous belt, locally sloping gently outward, which is one of the several elevated arcs. Surrounding the belt is a discontinuous trough that includes the lowlands south of the crater Mersenius, southwest of the crater Doppelmayer, and in the southeast corner of the map area. Another discontinuous elevated arc, mostly outside the mapped region, surrounds this trough. The concentric structure probably continued to form by isostatic adjustment and faulting long after the impact.

Surrounding the basin and mantling much of the deformed and cratered terrain is the hummocky material of the Vitello Formation, which is interpreted to be ejecta produced by the impact that created the basin. In many places this unit has been eroded away or buried. Beyond the map region the Vitello Formation occurs in elongate isolated exposures radial to the basin. Material with the topographic characteristics of the Vitello can be identified at a distance of at least one basin diameter from the center of Mare Humorum (Titley and Eggleton, 1964). The Vitello Formation was probably deposited on uplifted blocks of the surrounding mountainous belt, but the highest blocks have not retained the characteristic appearance of this covering unit. The surface material on such blocks may be either part of the older cratered terrain or Vitello Formation materials that have been smoothed by erosion and downslope movement of loose material.

Sufficient time elapsed between basin formation and the last stages of basin filling for a group of craters, including Gassendi, Doppelmayer, Lee, and Vitello, to form on the basin floor and rim. All are flooded, at least in part, by mare materials and therefore their stratigraphic relation to the Humorum basin is analogous to that of craters of the Archimedian Series to the Imbrium basin

(Hackman, 1966). They are more numerous, however, than Archimedean craters and probably span an interval from pre-Imbrian to Imbrian. The materials of this group are designated the Gassendi Group.

Extensive aggradation on the terra probably accompanied formation of the craters of the Gassendi Group and may be occurring at the present time but with diminished intensity. The aggradation resulted from the deposition of generally smooth plains-forming material upon earlier topographic forms on crater floors and in intermontane depressions of the terra. The plains-forming material may be a mixture consisting predominantly of volcanic flows and pyroclastic deposits and of lesser amounts of relatively fine ejecta from near and distant craters. It appears to have partially covered the floors and mantled the outer rims of pre-Imbrian and Gassendi Group craters and buried topographically low deposits of the Vitello Formation.

Flooding and partial filling of the Humorum basin and Gassendi Group craters by mare material constitute the next major recognizable event. The relatively flat and smooth mare material covers all of the inferred original circular basin as well as surrounding low areas. Clearly later than the structural basin which it fills, it is correlated with the Procellarum Group, which makes up most of the lunar maria and probably consists of volcanic flows and pyroclastic materials. It has been divided into subunits (not shown in fig. 1) on the basis of relative albedo. The albedo variations probably represent differences in either composition or relative age of the various units.

On the south and southwest edges of Mare Humorum, extremely dark materials of possible volcanic origin mantle the rims of craters such as Doppelmayer and cover some areas of Procellarum Group mare material. These materials, named the Doppelmayer Formation, may be contemporaneous with part of the Procellarum Group or may postdate it entirely. The position of the Doppelmayer Formation on the edge of the basin suggests a control by basin structure.

Next, craters formed on the 'mare' material that had flooded the basin. Some of these belong to a class of post-Procellarum Group rayless craters whose materials are assigned to the **Eratosthenian** System. They may have once had rays which darkened with time and disappeared. Rayless craters of similar size and morphology occur on the terra, but because their stratigraphic relation to the Procellarum Group is indeterminate, they may be either Eratosthenian or Imbrian.

The youngest features in the region are a class of craters having well-developed ray systems which overlie all older units. They occur on both terra and mare surfaces; their materials are assigned to the Copernican System.

#### REFERENCES

- Hackman, R. J., 1966, Geologic map of the Montes Apenninus region of the Moon: U.S. Geol. Survey Misc. Geol. Inv. Map 1-453.
- Hartmann, W. K., and Kuiper, G. P., 1962, Concentric structures surrounding lunar basins: Arizona Univ. Lunar and Planetary Lab. Commun., v. 1, no. 12, p. 51-72.
- Shoemaker, E. M., and Hackman, R. J., 1962, Stratigraphic basis for a lunar time scale, in Kopal, Zdenek, and Mikhailov, Z. K., eds., The Moon--Symposium of the Internat. Astron. Union: London, Academic Press, p. 289-300.
- Titley, S. R., 1963, A summary of the geology of the Mare Humorum quadrangle of the Moon, in Astrogeologic Studies Ann. Prog. Rept., Aug. 1962-July 1963, pt. A: U.S. Geol. Survey open-file report, p. 64-72.
- Titley, S. R., and Eggleton, R. E., 1964, Description of an extensive hummocky deposit around the Humorum basin, in Astrogeologic Studies Ann. Prog. Rept., July 1963-July 1964, pt. A; U.S. Geol. Survey open-file report, p. 85-89.

N67-31938

SUMMARY OF THE GEOLOGY  
OF THE HEVELIUS REGION OF THE MOON

By J. F. McCauley

The Hevelius region is in the west-central part of Oceanus Procellarum, about 1,200 km from the center of Mare Imbrium. Three distinct topographic and geologic provinces are recognized in the region (fig. 1).

STRATIGRAPHY AND STRUCTURE

Province one, west of Oceanus Procellarum and at the west edge of this region, is part of a large area of cratered terra that extends to Mare Orientale, which is at the extreme west edge of the earthside hemisphere and approximately 1,000 km southwest of the Hevelius region. The surface material of this terra (Hevelius Formation) is of intermediate to high albedo and within the crater Hevelius is relatively smooth with a faintly braided to fine hummocky texture and numerous superposed small pits. Westward from the Hevelius region, toward Mare Orientale, the old craters of this terra appear to be progressively more deeply buried, and the terrain is more hummocky (McCauley, 1964). Apparently this terra is covered by a blanket of material that extends continuously from the edge of Mare Orientale, where it is thickest, into the Hevelius region, where it is relatively thin and only partly subdues the larger subjacent topographic features such as the crater Hevelius. This blanketing material is interpreted to be ejecta produced by an impact that formed the Orientale basin, believed to be the youngest of the large mare basins. Numerous northeast-trending lineaments (McCauley, 1967) and mare-embayed troughs in the region appear to be part of a structural pattern radial to the Orientale basin (Hartmann and Kuiper, 1962).

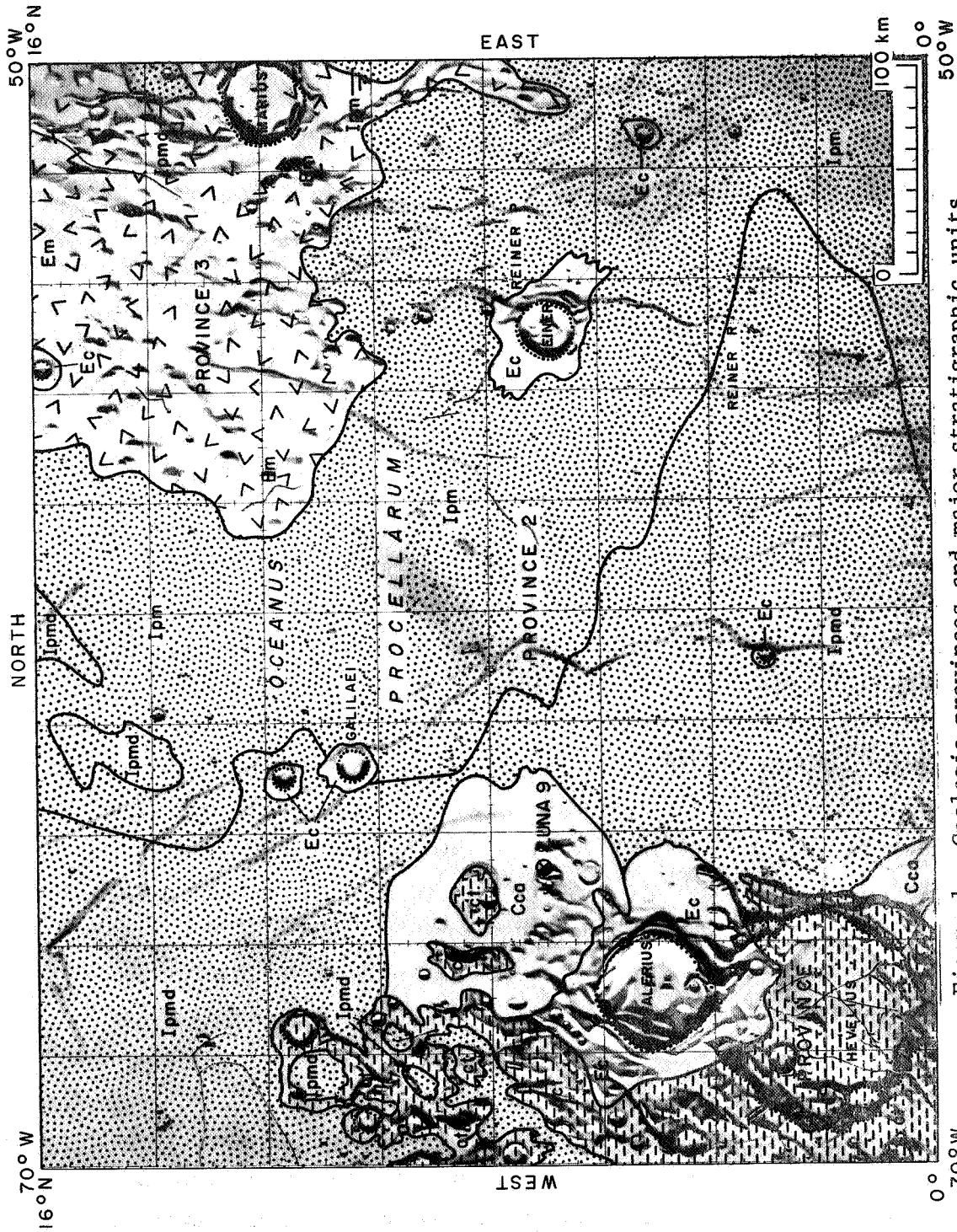


Figure 1.--Geologic provinces and major stratigraphic units of the Hevelius region.



Province two, in the center of the region, is a mare plain. The mare material is thickest in the north-central part of the region near the crater Galilaei, where a series of northwest-trending mare ridges is present but no trace of subjacent features can be seen. The mare material thins to the west, where it embays older craters and northeast-trending troughs; it also appears to thin to the south and southeast, where ghost craters such as Reiner P and Reiner R occur. The depression now occupied by the mare plain probably resulted from structural subsidence of an old cratered terra like that of province one. In the mare plain, two major stratigraphic units of regional extent have been recognized. One (Ipm) has an intermediate albedo, contains numerous dunes, and is correlated with the mare material of the Procellarum Group in the Kepler region to the east (Hackman, 1962). The other (Ipmd) is generally darker and less cratered; it occurs mostly along the west margins of Oceanus Procellarum and is interpreted as a thin veneer covering the older mare material. Unit Ipmd may be post-Imbrian in age. Both units are probably volcanic. Numerous dark-rimmed craters assigned to the Eratosthenian System, 2-5 km in diameter, occur on the mare plain, and about one-third of these lie on mare ridges. Bright-rimmed craters assigned to the Copernican System also occur throughout the area but are generally smaller (2-3 km in diameter) and about half as numerous. Most or all bright-rimmed craters and the majority of the dark-rimmed craters are probably of impact origin; the latter are inferred to be older than the former. The large number of dark-rimmed craters on ridges, however, suggests that many of these may be of internal origin. Relative albedo cannot be used to determine the relative age of these craters. One of the youngest units recognized in the region is the Cavalerius Formation, a dark blanketing unit which overlaps the terra-mare contact and is probably composed of pyroclastic material.

Province three, in the northeastern part of the region, is a large southward-dipping plateau, generally several hundred meters higher than the adjacent 'mare. Rising from the plateau are numerous domes of two types: one, broad and low; the other, higher and steeper. The plateau and domes are interpreted to be a volcanic complex consisting of intercalated lava and ash deposits erupted from numerous vents at the crests of both types of domes (McCauley, 1965). The Marius Group is clearly superposed on the mare material of the Procellarum Group along a sinuous scarp marking its northern contact in the adjacent Seleucus quadrangle. The crater density of the Marius Group is markedly lower than that of the Procellarum Group of Imbrian age in its type area (Kepler region) to the east (craters 1-2 km in diameter are almost 10 times less numerous). Lower crater density and superposition on the Procellarum Group indicate that the Marius Group is post-Imbrian in age. An Eratosthenian age is assigned to it because it is locally overlain by faint Copernican ray material.

#### GEOLOGIC HISTORY

The oldest recognizable event in the Hevelius region was extensive cratering of the old terra surface; Hevelius is an example of such a crater. The western part of the area was then covered by a thin blanket of impact ejecta (Hevelius Formation) from the Orientale basin, and this new surface was again cratered. The earlier of these craters were partly flooded, and the entire central and northwestern parts of the region subsided and were inundated by mare material, first of the Procellarum Group, later by darker material which may be younger than the Procellarum Group. Volcanism of a different type occurred later in the northeastern part of the region and produced numerous domes of two types with smooth undulating local deposits between (Marius Group). After these events, cratering by impact and also probably by volcanism continued throughout the entire region during the Eratosthenian and Copernican Periods. Deposition of the pyroclastic

material of the Cavalerius Formation is among the most recent events. Also, slumping has produced one of the youngest units present in the region: Copernican slope material.

#### LUNA 9 LANDING SITE

Luna 9, a surface probe of the USSR, soft landed in the Hevelius region on February 3, 1966, at 21:45 hours (Moscow time), and during the following 2 1/2 days transmitted a series of high-resolution panoramic television pictures. According to the best current estimate, Luna 9 landed in the vicinity of lat 7°00' N. and long 64°33' W. (fig. 1), probably on young dark volcanic material of the Cavalerius Formation, either in the plains where it covers mare material or on one of the broad hills nearby where it covers older crater rim deposits. Alternatively, it could have landed on one of the local occurrences of Copernican slope material on the flanks of the hills. The pictures released to date show an intricate, undulating rubbly surface with fragments ranging in size from the limit of resolution (several millimeters) to angular blocks about 25 cm across. The sharply angular nature of the blocks suggests that they are composed of material at least weakly cohesive (Moore, 1966) and that they have not undergone significant erosion either by micrometeorites or sputtering since deposition on this surface. Numerous craters, most of which are rimless, can also be recognized; these range from a few centimeters to several meters in diameter.

#### REFERENCES

- Hackman, R. J., 1962, Geologic map and sections of the Kepler region of the Moon: U.S. Geol. Survey Misc. Geol. Inv. Map 1-355.
- Hartmann, W. K., and Kuiper, G. P., 1962, Concentric structures surrounding lunar basins: Ariz. Univ. Lunar and Planetary Lab. Commun., v. 1, no. 12, p. 51-72.

- McCauley, J. F. , 1964, The stratigraphy of the Mare Orientale region of the Moon, in Astrogeologic Studies Ann, Prog. Rept. , Aug. 1962-July 1963, pt. A; U.S. Geol. Survey open-file report, p. 86-93.
- \_\_\_\_\_ 1965, The Marius Hills volcanic complex, in Astrogeologic Studies Ann. Prog. Rept. , July 1964-July 1965, pt. A: U.S. Geol. Survey open-file report, p. 115-122.
- \_\_\_\_\_ 1967, Geologic map of the Hevelius region of the Moon: U.S. Geol. Survey Misc. Geol. Inv. Map I-491.
- Moore, H. J., 1966, Cohesion of material on the lunar surface, in Ranger VIII and IX, pt. 2, Experimenters' analyses and interpretations: Jet Propulsion Lab. , Tech. Rept. 32-800, Pasadena, p. 263-270.

*12/10/62*

N67-31939

3 SUMMARY OF THE GEOLOGY OF THE COPERNICUS  
QUADRANGLE OF THE MOON

By H. H. Schmitt, N. J. Trask,  
and E. M. Shoemaker

*8 done P 31-31  
RS  
2/10/62*

INTRODUCTION

The Copernicus quadrangle in the west-central part of the equatorial belt (lat 0"-16" N. , long 10"-30" W.) lies on the southern edge of the Mare Imbrium basin. The large rayed crater Copernicus, 90 km in diameter, is the most prominent feature (fig. 1) ; its ray system extends over much of the western half of the visible side of the Moon. The first detailed preliminary lunar geologic map, based on telescopic photographs and observations, was of the Copernicus region (Shoemaker, 1962; Shoemaker and Hackman, 1962). Improved photographs, studied by Schmitt and Trask, and additional telescopic observations by Schmitt have added new stratigraphic units and provided an improved picture of the albedo pattern around Copernicus. The new results have been incorporated in the completed geologic map of the quadrangle (Schmitt, Trask, and Shoemaker, in press).

STRATIGRAPHY

The complex topography of the terrae reflects the earliest decipherable history of the Copernicus quadrangle, which involves the genesis of the Mare Imbrium basin. The terrae are traversed by scarps, grabens, and ridges, the most prominent of which are oriented north-northeast and north-northwest. These linear features are part of the system of Imbrian sculpture which is approximately radial to the center of the basin and extends outward from the basin around its entire periphery (Hartmann, 1963). The extent and regularity of this system of fractures suggest that the Imbrium basin formed by a single catastrophic event.

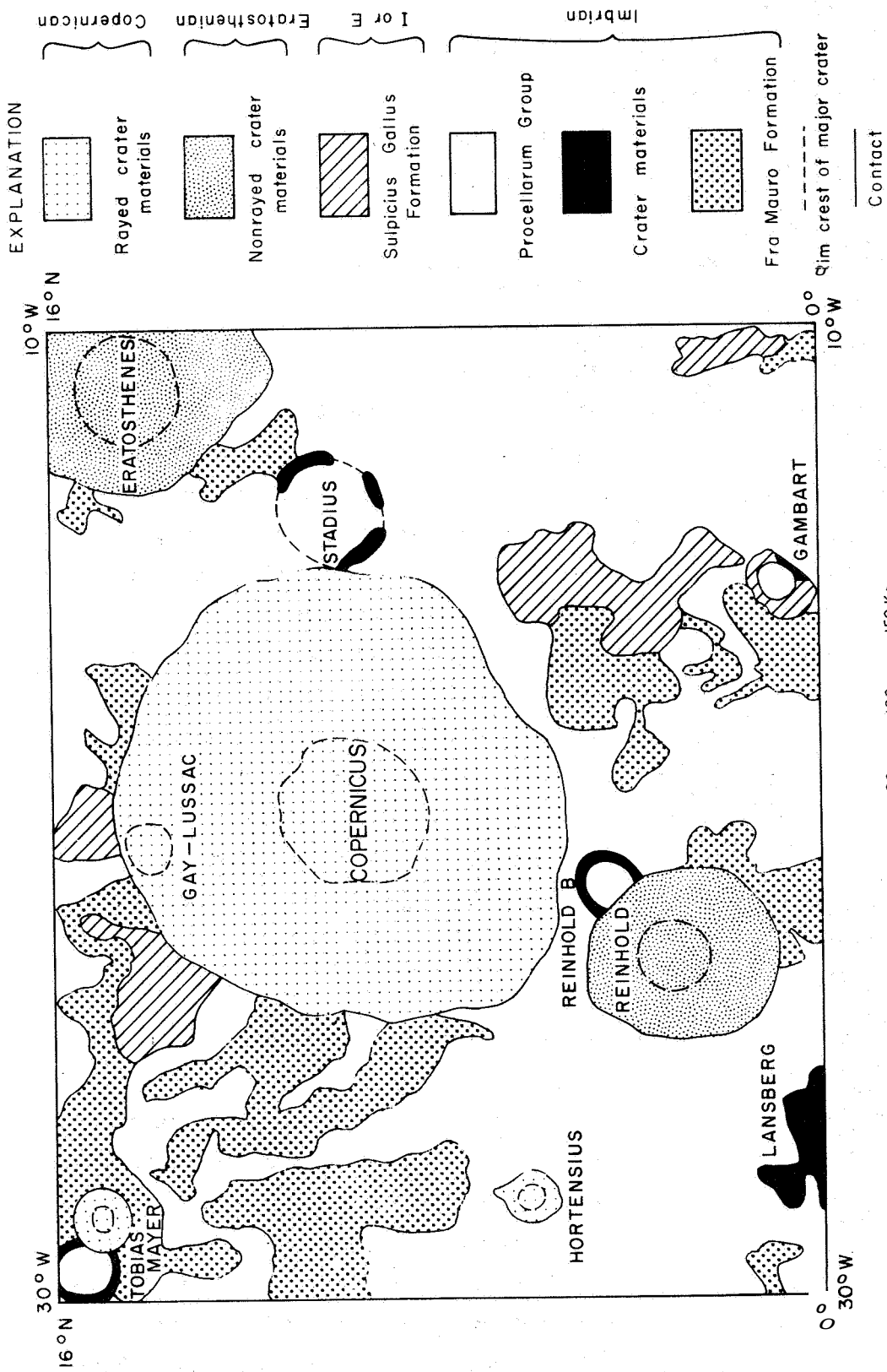


Figure 1.--Sketch showing geology and principal craters of the Copernicus quadrangle.  
Scale 1:4,000,000.

The hilly to gently rolling terrain between the elements of the Imbrian sculpture system has been mapped as the Fra Mauro Formation. The exposures of the Fra Mauro are continuous with the type locality in the Rhiphaeus Mountains region directly to the south (Eggleton, 1965). The Fra Mauro Formation occurs in a pattern concentric with the Imbrium basin; in general, the hills diminish in size outward from the edge of the basin and grade outward to a gently rolling topography with ridges radial to the basin.

Two members of the Fra Mauro Formation are recognized in the Copernicus quadrangle: (1) the hummocky member, consisting of closely spaced relatively steep-sided hummocks up to 5 km in diameter, and (2) the smooth member, consisting of smooth-appearing ridges, hills, and plateaus without numerous hummocks. The Fra Mauro Formation appears to be an ejecta blanket created by the impact that formed the Imbrium basin, although in the Copernicus quadrangle limited exposures of the formation make it difficult to distinguish hills that are part of such a blanket from structurally uplifted blocks of pre-Imbrian material. The ridges, hills, and plateaus of the smooth member have been mapped as expressions of pre-Imbrian topography buried by ejecta. In places, the hills and ridges of the Fra Mauro Formation form a circular pattern which suggests craters that predated the Imbrian event and were highly dissected by the Imbrian sculpture.

Between the formation of the Imbrium basin and the flooding of the basin by mare material, a number of craters formed in the quadrangle. Lansberg, Stadius, Tobias Mayer, Reinhold B, Gambart, and Gay-Lussac are the chief members of this class; they were not affected by Imbrium sculpture and are filled or partly embayed by mare material. The origin of these Imbrian craters is uncertain. The narrow smooth rim crests and lack of well-defined crater rim deposits on some of them (for example, Gambart and Reinhold B) suggest that they *may* be calderas, although similar characteristics might result from isostatic rebound and erosion of impact craters. Lansberg closely resembles Eratosthenes and Copernicus and is probably of impact origin.

Materials of the Procellarum Group make up the widespread flat dark mare plains. The relatively smooth upper surface of this unit closely follows the curvature of the Moon, and the material appears to have filled most preexisting depressions to approximately the same level. The mare material apparently had considerable fluidity at the time of its formation and could spread widely from a few eruptive centers. On the other hand, its presence in isolated low areas within the Fra Mauro Formation and inside many unbroken Imbrian craters also indicates a multiplicity of feeder channels from depth over a broad region. The mare material probably consists of a mixture of lava and volcanic ash flows.

Very dark apparently thin materials of the Sulpicius Gallus Formation overlapping both terra and mare material were first mapped in the Mare Serenitatis region by Carr (1966) and occur in other isolated patches to the east of the Copernicus quadrangle. Same materials in the Copernicus quadrangle are correlated with the formation on the basis of their similar characteristics and stratigraphic position. In the large exposure directly to the southeast of Copernicus, the topography of the formation includes some low dunes; elsewhere it is flat or exhibits the hummocky topography of the Fra Mauro Formation but is smoother and more subdued. Within all the exposures of the formation, there are abundant small dark spots, readily apparent on recent high-resolution Earth-based full Moon photographs; some of the dark areas surround small craters and others have no resolvable crater within them. The materials of the Sulpicius Gallus Formation are probably volcanic in origin and may have resulted from a continuation of the activity that gave rise to the maria. The formation may be the same age as the Procellarum Group; however, some parts of it appear to be superposed on and therefore younger than some parts of the Procellarum.

Post-mare craters in the Copernicus region include the large well-defined craters Copernicus, Eratosthenes and Reinhold, as well as many smaller craters. The ray system of Copernicus overlaps the rim materials of Eratosthenes and Reinhold, which are almost

rayless. In general, the rays from large craters overlap large rayless craters everywhere on the Moon. Two systems of post-'mare crater materials have therefore been established for the Moon, both with type areas in the Copernicus quadrangle: the Eratosthenian System including large rayless craters with type area in the crater Eratosthenes, and the Copernican System including rayed craters with type area in the crater Copernicus. Also included in the Copernican System are dark-halo craters that are superposed on the 'rays' of Copernicus and are therefore younger. Dark-halo craters are especially abundant in the Copernicus quadrangle, as shown by recent high-resolution full Moon photographs from the U.S. Naval Observatory, Flagstaff. Only craters clearly superposed on rays are definitely of Copernican age.

#### THE CRATER COPERNICUS

Copernicus is a large fresh-appearing crater favorably located near the center of the lunar disk for detailed studies of its ray pattern, albedo, and morphology. Shoemaker (1962) related the ray pattern to the profusion of elongate depressions and small craters (maximum diameter 5 km) surrounding the crater. The depressions and small craters are mapped as satellitic craters; many of them lie at the proximal ends of ray elements. Shoemaker showed that the disposition of many of the satellitic craters in looplike patterns could be caused by the impact of fragments ejected along ballistic trajectories from structural blocks bounded by zones of weakness surrounding a shock epicenter at the center of Copernicus. He concluded that Copernicus is an impact crater, that the satellitic craters are secondary impact craters, and that the rays are formed mostly by ejecta from Copernicus and from the secondary impact craters on the rays.

The normal albedo of the rays and materials of Copernicus is shown on the map prepared by Pohn and Wildey and included in the map supplement to this report. The albedo pattern around the crater is clearly intricate. The albedo of the floor, wall, and

inner hummocky rim of Copernicus is higher than that of the mare material on which the Copernicus rays are superposed. The albedo of the rim materials decreases gradually outward; the rays, which appear to be extensions of the rim material, have albedos that are only slightly higher than those of the surrounding mare material. In addition to this pronounced outward variation in albedo, there are lesser variations in the direction normal to the radial. These appear as radiating streaks of light and dark material. The material on the south rim of the crater is relatively dark, and the material on the north rim is relatively bright. There are other smaller streaks of relatively dark material on the northwest and northeast parts of the rim. Parts of the wall and floor are also darker than their surroundings. Full Moon photographs show a contact separating darker from brighter material cutting across the rim, wall, and floor in the southwest part of the crater.

An impact that formed Copernicus would probably have occurred on the contact between the Procellarum Group and the Fra Mauro Formation. Mapping of these two units outside the limits of the rim material of Copernicus shows that the mare material embays the Fra Mauro in a complex pattern but that in general, a northeast-southwest line running through the center of the crater would have divided the bulk of the Fra Mauro on the northwest from the Procellarum Group on the southeast. The relatively dark and light materials on the rim, wall, and floor of the crater are probably reflections of these inhomogeneities in the target rocks. The pattern of ejection of material would be expected to be complex; in a very general way, materials of the Procellarum Group would be ejected to the south and materials of the Fra Mauro Formation to the north. The rate of darkening of these contrasting materials under bombardment by solar radiation and particles would differ and the present complex pattern of albedo would result.

In addition to systematic variations in albedo, several morphologic provinces, partly correlative with albedo, can be delineated in and around Copernicus. The exterior rim has three facies:

(1) an inner hummocky facies with rugged, concentric to branching ridges, (2) an intermediate radial facies with ridges approximately radial to the center of the crater, and (3) an outer cratered facies, with very low radial ridges and many interspersed low-rimmed partly covered satellitic craters. Very low ridges of the outer facies extend radially outward as far as 150 km from the rim crest of the crater. The outer limit of the outer facies coincides with a dropoff in the abundance of satellitic craters. The high concentric ridges near the rim crest probably represent buckled and uplifted segments of bedrock deformed by the impact and covered with a layer of ejecta; the radial ridges represent stringers and clots of ejecta that maintained coherence during flight.

The topography of the crater walls consists of relatively level benches crossing hummocky slopes and is probably the result of nearly concentric normal faulting, landsliding, and local slumping which began soon after the crater first formed. The upper contacts of the walls are locally characterized by arcuate concave-inward slump planes. Both the floors and central peaks are probably the highly brecciated and shocked remains of the rocks at the site of impact. The central peaks are thought to have been created by rebound immediately after impact.

Differences in the morphology of the floor of the crater may partly reflect the inferred heterogeneity of the target rocks. Smooth floor material is confined to that side of the contact that was originally occupied by the Fra Mauro Formation and underlying pre-Imbrian materials; the hummocky floor material is largely on the side originally occupied by the Procellarum Group and subjacent feeders. This suggests that the initially shocked and broken Fra Mauro Formation was more pulverized during impact and more easily smoothed and slumped afterward than the more coherent rocks of the Procellarum Group.

## DARK-HALO CRATERS

The dark-halo craters in the quadrangle may be partly volcanic, similar to the structurally controlled dark-halo craters on the floor of Alphonsus photographed by the Ranger IX mission, and partly impact craters that have brought to the surface darker underlying material. The stratigraphic column includes dark units such as the Sulpicius Gallus Formation with a high density of dark-halo craters; other dark layers may be present. Shoemaker (1962) has presented evidence that the albedo of material newly exposed at the surface of the Moon progressively decreases with time. The dark material partly surrounding the craters Eratosthenes and Reinhold is probably near the final stage of such darkening. Material on the rim of the younger crater Copernicus is much brighter. The relatively low albedo of the maria is a derived characteristic rather than intrinsic to the material itself, and repeated cratering of a surface should result in a complex layering of dark and light materials. Material of the dark-halo craters on the rim of Copernicus is too dark to have been derived from the underlying rim material, however, and its albedo is low probably because its composition is different from the surrounding material. Volcanic ash from these craters may have formed a thin dusting over parts of the southern rim of Copernicus where albedo is lower than average.

## REFERENCES

- Carr, M. H. , 1966, Geologic map of the Mare Serenitatis region of the Moon: U.S. Geol. Survey Misc. Geol. Inv. Map 1-489.
- Eggleton, R. E., 1965, Geologic map of the Rhipaeus Mountains region of the Moon: U.S. Geol. Survey Misc. Geol. Inv. Map 1-458.
- Hartmann, W. K. , 1963, Radial structures surrounding lunar basins, I: the Imbrium system: Arizona Univ. Lunar and Planetary Lab. Commun., v. 2, no. 24, p. 1-15.

- Schmitt, H. H. , Trask, N. J. , and Shoemaker, E. M. , in press,  
Geologic map of the Copernicus quadrangle of the Moon: **U.S.**  
Geol. Survey Misc. Geol. Inv. Map 1-515.
- Shoemaker, E. M., 1962, Interpretation of lunar craters, in Kopal,  
Zdenek, ed., Physics and astronomy of the Moon: London,  
Academic Press , p. 283-359.
- Shoemaker, E. M. , and Hackman, R. J. , 1962, Stratigraphic basis for  
a lunar time scale, in Kopal, Zdenek, and Mikhailov, Z. K.,  
eds., The Moon--Symposium 14 of the International Astronomical  
Union: London, Academic Press, p. 289-300.

1 same 3 N67-31940

3 SUMMARY OF THE GEOLOGY OF THE SELEUCUS QUADRANGLE  
OF THE MOON 6

By H. J. Moore 6

same p 50 R  
2010

INTRODUCTION

The Seleucus quadrangle (fig. 1) lies in the northwestern part of Oceanus Procellarum, a large mare area of irregular shape in the western part of the earthside hemisphere of the Moon. Material of the 'mare occupies most of the quadrangle. Craters ranging from 1 to 44 km in diameter are scattered over the smooth mare surface; in addition, a few isolated hills and ridges rise above the mare. In the east-central part of the quadrangle, the Aristarchus plateau slopes gently westward and merges with the surrounding surface of Oceanus Procellarum. The plateau, which is red in overall color (Wood, 1912), contains many unique features, such as Vallis Schr'dteri and areas where occasional bright reddish glows have been seen (Greenacre, 1965, p. 811-816).

STRATIGRAPHY

Volcanism and impact cratering have contributed to the formation of the surface features of the quadrangle throughout its interpretable geologic history. The materials present can be roughly classified into three major time-stratigraphic units, although sharp time boundaries between the time-stratigraphic units do not exist. The classification is similar to the one used in the Copernicus quadrangle by Shoemaker and Hackman (1962); the time-stratigraphic units are: the Imbrian System, the Eratosthenian System, and the Copernican System. The boundaries between each system are spanned by stratigraphic units composed of volcanic materials. A few units cannot be placed in a system, such as pre-

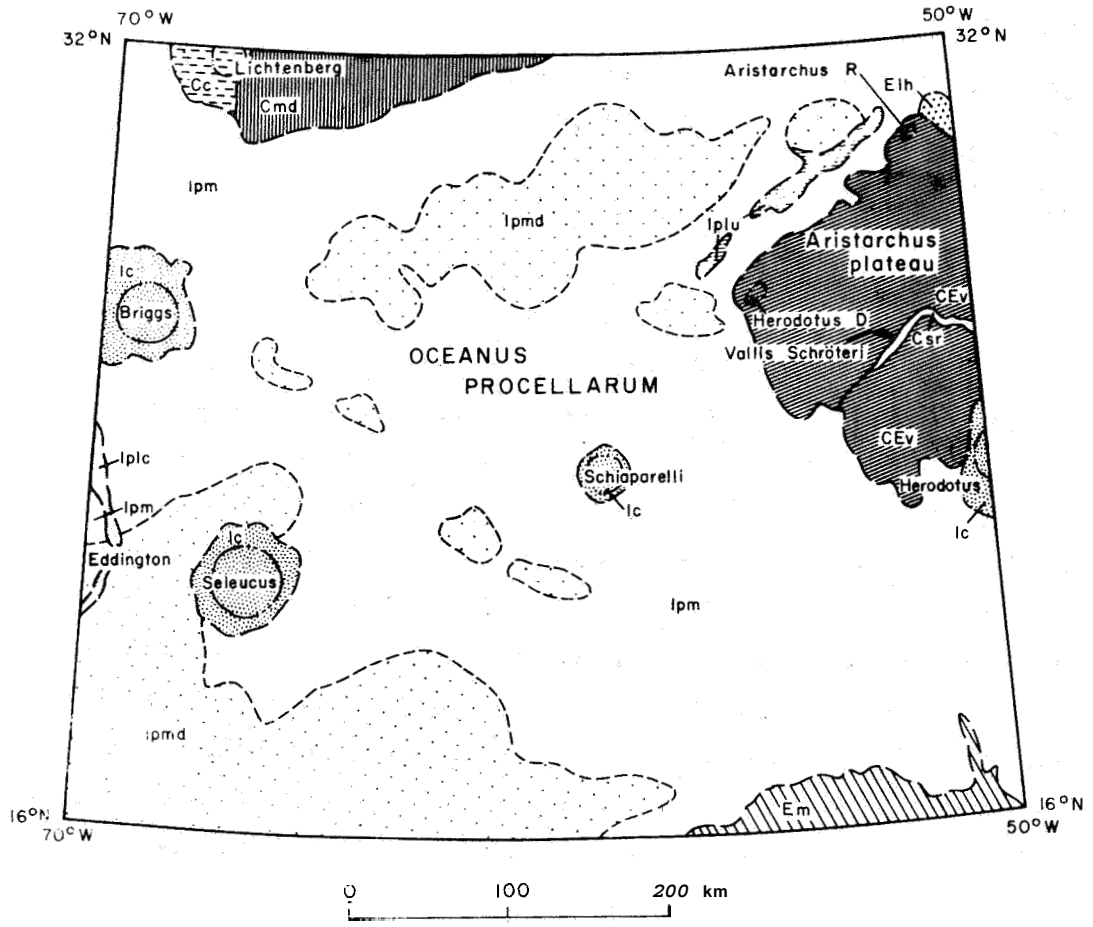
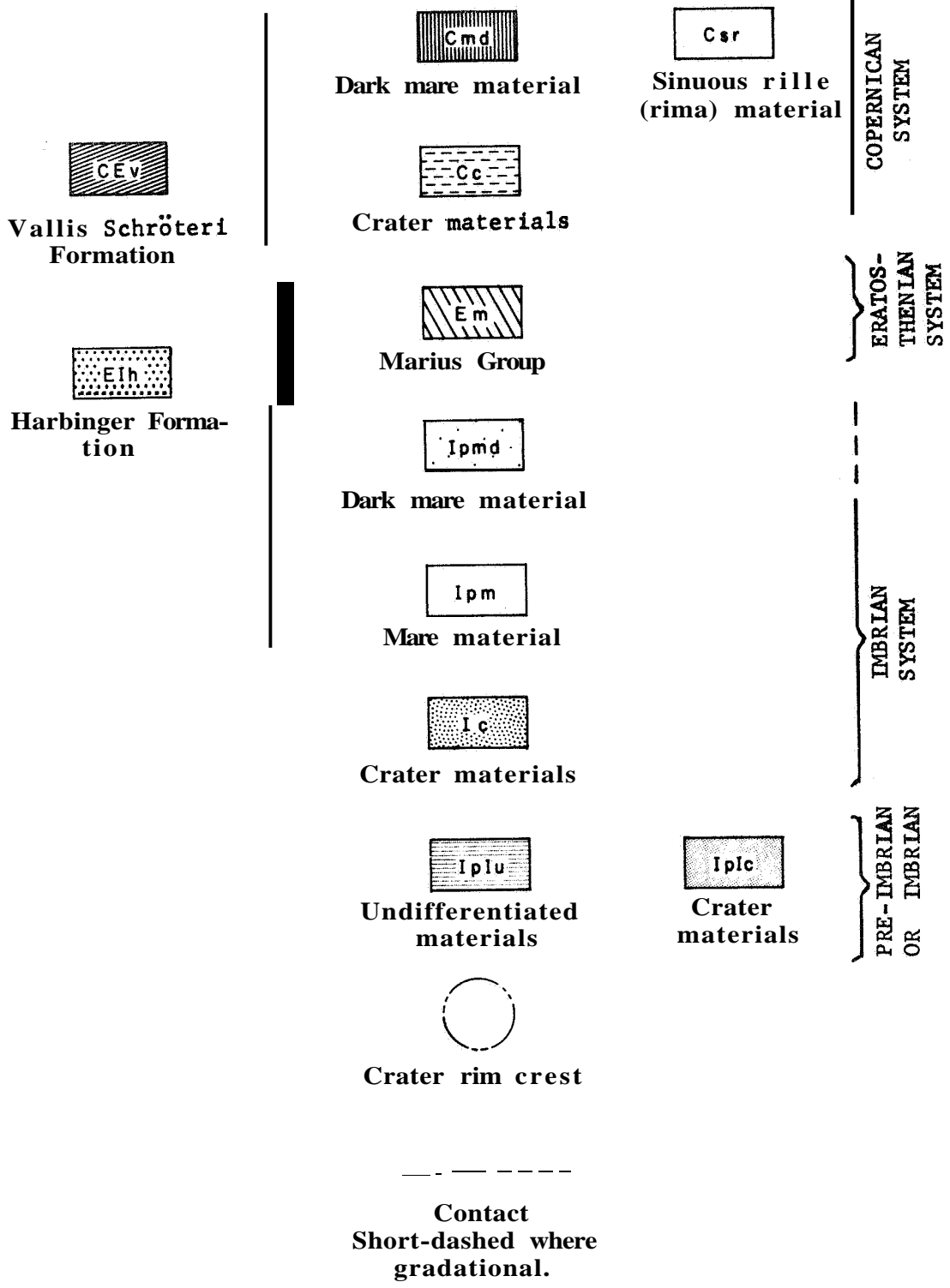


Figure 1.--Generalized geology of the Seleucus quadrangle of the Moon, showing selected stratigraphic units.



Imbrian or Imbrian units. Correlations, age relations, and interpretations for the units are discussed below.

Photographic evidence collected by the U. S. S. R. 's Luna 9 (Lebedinsky, 1966) and the United States' Ranger series and Surveyor I (California Inst. Technology, 1966, pls. B-88, P-12; Jaffe and others, 1966; Natl. Aeronautics and Space Adm., 1966) has shown that the lunar surface in other areas has been significantly modified and altered on a fine scale by impact cratering. Preliminary evaluation of photographic evidence from the U.S.S.R. 's Luna 13, which landed in the Seleucus quadrangle, suggests that such modification has occurred also in this quadrangle (Anderson, 1966). Thus, unmodified materials of the units mapped in the Seleucus quadrangle may not occur at the surface but at a depth which depends on the degree of modification. This depth may range from a few millimeters to tens of meters or more. The degree of modification should increase with the age of the material, local concentrations of rays, and proximity to large impact craters.

#### Ere-Imbrian or Imbrian units

A lower age limit of the oldest crater materials in the quadrangle (unit IpIc), such as those which form the rim of the crater Eddington, and the undifferentiated materials (unit IpIu) cannot be established because they are not in contact with the Fra Mauro Formation, the unit that defines the base of the Imbrian System. However, the deformed and modified appearance of the crater Eddington suggests that it is very old and is probably pre-Imbrian in age. That part of unit IpIu which is nearly contiguous with the Fra Mauro Formation in the Aristarchus region is tentatively correlated with the Fra Mauro. Units IpIc and IpIu are generally surrounded, embayed, or filled by mare material and therefore are older than mare material.

#### Imbrian System

Crater rim, floor, and peak materials (unit Ic) of the craters Briggs, Seleucus, and Schiaparelli are placed in the Imbrian System.

These materials are partly covered with mare material and yet the craters appear fresher and less deformed and modified than pre-Imbrian craters elsewhere on the Moon. The craters Briggs and Seleucus were probably produced by the impacts of large bodies from space, since radial ridges and a hummocky ejecta blanket can be seen along the crater flanks. The peculiar internal annular structure and apparently smooth flanks of Schiaparelli are distinctive, so that a volcanic origin is possible.

Mare material, which covers most of the Seleucus quadrangle, is divided into two units. The first unit, mare material of the Procellarum Group (Ipm), has a higher albedo and density of superposed rays than the second, designated dark mare material of the Procellarum Group (unit Ipmd). The Procellarum Group in the type area is in the Imbrian System by definition; however, dark mare material is superposed on lighter mare material and, although tentatively assigned to the Imbrian, may be partly Eratosthenian or partly Copernican (McCauley, 1967). At least one patch of dark mare material embays the Copernican crater Lichtenberg (discussed later). Both units of mare material and their associated domes probably represent volcanic ash flows, ash falls, or lava flows.

#### Rock-Stratigraphic Units Spanning the Imbrian and Eratosthenian Systems

A small area in the northeast part of the quadrangle is mapped as the Harbinger Formation (ETh), which was originally defined in the Aristarchus region (Moore, 1965). This formation is Imbrian in the Seleucus quadrangle, but mapping in the Aristarchus region has shown that it is partly contemporaneous with and partly younger than mare material. Although the contiguous area in the Aristarchus region was mapped as Fra Mauro Formation and not Harbinger Formation, subsequent studies have shown that it is Harbinger. The materials of the Harbinger Formation are probably volcanic (Moore, 1964). In the Seleucus quadrangle, topography suggests that the

materials are associated with a partly buried rille about the width of Vallis Schr'dteri.

#### Eratosthenian System

The Eratosthenian System comprises crater materials and volcanic material. The crater materials (not shown in fig. 1) occur in and around craters that are younger than the mare material but have no associated rays. The radial ridges of the superposed rim material extend out over the mare material, and if any rays were once present they have been degraded and modified and are no longer visible. Most of the craters may be the result of impacts, but some, especially those on mare ridges, may be volcanic in origin. Volcanic material makes up the smooth undulating Marius Group (unit Em) (McCauley, 1967), which occupies only a small area in the southeastern part of the Seleucus quadrangle.

#### Rock-Stratigraphic Units Spanning the Eratosthenian and Copernican Systems

The Vallis Schr'dteri Formation (unit CEv) occurs on the Aristarchus plateau. This formation, first mapped in the adjacent Aristarchus region (Moore, 1965), is divided in the Seleucus quadrangle into five units: hummocky member, dome material, cone-crater material, dark-smooth member, and low-rimmed crater material. In general the dark-smooth member and low-rimmed crater material are younger than the other materials. Relative ages of units not in contact are inferred from apparent amount of superposed ray material. Where superposition relations are observed, these units, with the possible exception of the hummocky member in one place, appear to overlie the Procellarum Group. With this possible exception, the materials formed during the Eratosthenian and Copernican Periods.

The hummocky member has higher albedo than the smooth member and also has some superposed rays. The unit appears to be superposed on mare material along the northwest edge of the Aristarchus plateau. Along the southwestern margin of the plateau, the age relations between the hummocky member and mare material are not

clear. Although the mare material there has a greater density of superposed rays, parts of the hummocky member could be contemporaneous with mare material. A small patch of the hummocky member extends into the adjacent Aristarchus region where it was not previously mapped. The member probably consists of a thin layer of volcanic material mantling a preexisting hummocky surface.

Dome material forms convex-upward domical surfaces with a small crater near the apex; cone-crater material forms the rims and surrounding flanks of irregular high-rimmed craters. These materials are probably volcanic. For example, the cone-crater Aristarchus R is at the apex of an elliptical dome probably composed of volcanic flows and ejecta, and the double cone-crater Herodotus D has coarse lobes extending down its flanks which probably represent lava flows; they are too coarse to be radial ridges and hummocks of an impact crater the size of Herodotus D (7 km). Some material from Herodotus D extends out upon mare material on the north edge of the plateau. Materials of cone-craters and domes generally have more superposed rays than dark-smooth material and are thus generally older.

Material of the dark-smooth member is superposed on material of the hummocky member and is younger. Only a few areas of the dark-smooth member have superposed rays and the member may therefore be of Copernican age. Patches of this member are superposed on the mare material of the Procellarum Group (unit Ipm) along the north flanks of the Aristarchus plateau. A small patch of this material extends into the adjacent Aristarchus region where it was not previously mapped. The dark-smooth member probably represents volcanic ash falls, and ash flows or lava flows.

In general, low-rimmed craters are unrayed and superposed on hummocky material. Some of the larger low-rimmed craters are associated with the dark-smooth member and are contemporaneous with it. Some low-rimmed craters along the northwest edge of the Aristarchus plateau are apparently the source of material of the dark-smooth member that occurs on the mare surface and on the

adjacent hummocky member. The low rims of these craters are similar to rims of terrestrial maar craters.

The diverse morphologies, distribution, and age relations of materials making up the Vallis Schröteri Formation suggest that the Aristarchus plateau is a volcanic field with a long and complex history characterized by diverse volcanic processes. The transitory red spots sighted in this region (Greenacre, 1965) may be evidence of present-day volcanism but these spots have not been satisfactorily explained.

#### Copernican System

Copernican crater materials are scattered across the quadrangle; their bright materials and surrounding rays are superposed on many of the units discussed above. The rays and hummocky ejecta blankets around the large craters suggest that the craters were produced by impacts. Secondary craters (not shown in fig. 1) are probably also of impact origin, because they are associated with rays from larger craters and have ejecta plumes radial to the parent crater or parallel to rays that are clearly related to the parent crater.

Dark mare material (unit C<sub>md</sub>) occurs in the northwest part of the map area. This material has covered the ejecta and rays of the Copernican crater Lichtenberg (unit C<sub>c</sub>) along the crater's southeast flanks. Thus, this dark mare material is classed as Copernican. A few craters are superposed on this material, and one of these may be partly buried by even younger material. This dark mare material, which covers thousands of square kilometers, can best be ascribed to volcanism. Since this dark material is Copernican, some areas of dark mare material assigned to the Procellarum Group (I<sub>pmd</sub>) might be Copernican instead of Imbrian.

Sinuuous rille (rima) material (unit C<sub>sr</sub>) is exposed in Vallis Schröteri on the Aristarchus plateau and extends into the Aristarchus region, where it terminates within the Cobra Head Formation. Vallis Schröteri may be a graben or a channel produced by the flow of volcanic material.

## LINEATIONS AND FAULTS

Four sets of lineations are present in the Aristarchus plateau. The most conspicuous set, which is radial to the Imbrium basin, trends N. 40"-60" E. **Two** other well-developed sets trend N. 30"-40" E. and N. 30°-40° W. These lineations are expressed by ridges, scarps, and rilles. The fourth set, which trends north-south, is expressed by some rilles. Displacements have occurred along many of the lineations throughout the history of the Aristarchus plateau. An additional lineament, trending N. 75° E. , may be present near and parallel to the southern contact of unit Cnd.

## REFERENCES

- Anderson, R. H., 1966, Moon soil found similar to Earth: New York **Times**, Dec. 31, 1966, p. 6c.
- California Institute of Technology, Jet Propulsion Laboratory, 1966, Ranger IX photographs of the Moon: U.S. Natl. Aeronautics and Space Adm. Spec. Pub. 112.
- Greenacre, J. , 1965, The 1963 Aristarchus events, in Whipple, H. E. , ed., Geological problems in lunar research: New York Acad. Sci. Annals, v. 123, art. 2, p. 367-1257.
- Jaffe, L. D., and others, 1966, Surveyor I: Preliminary results: Science, v. 152, no. 3730, p. 1737-1750.
- Lebedinsky, A. I., 1966, Scientific results of processing of panoramas obtained from photographs of the lunar surface taken from "Luna 9": U.S.S.R. Acad. Sci., contract NAS-5-9299, 7 p.
- McCauley, J. F., 1967, Geologic map of the Hevelius region of the Moon: U.S. Geol. Survey Misc. Geol. Inv. Map 1-491.
- Moore, H. J. , 1964, A possible volcanic complex near the Harbinger Mountains of the Moon, in Astrogeologic Studies Ann. Prog. Rept. , Aug. 1963-1964, pt. A: U.S. Geol. Survey open-file report, p. 42-51.

- Moore, H. J. , 1965., Geologic map of the Aristarchus region of the Moon: U.S. Geol. Survey Misc. Geol. Inv. Map 1-465.
- National Aeronautics and Space Administration, 1966, Photo 66-H-934, released June 16, 1966.
- Shoemaker, E. M., and Hackman, R. J., 1962, Stratigraphic basis for a lunar time scale, in Kopal, Zdenek, and Mikhailov, Z. K., eds. , The Moon--Internat. Astron. Union Symposium 14: London, Academic Press , p. 289-300.
- Wood, R. W. , 1912, Selective absorption of light on the Moon's surface and lunar petrography: Astrophys. Jour., v. 36, p. 75-84.

N67-31941

3 GEOLOGY OF THE JULIUS CAESAR AND MARE VAPORUM QUADRANGLES

6  
Don E. Wilhelms and Elliot C. Morris

INTRODUCTION

The adjoining Julius Caesar and Mare Vaporum quadrangles (fig. 1) lie in the central part of the equatorial belt (lat 0°-16° N., long 30° E.-10° W.) southeast of the Imbrium basin. Stratigraphic units and structures peripheral to the craterlike Imbrium basin and related to it are the principal geologic features of the terra of both quadrangles. One of the mare areas within the quadrangles, Sinus Medii, occupies part of a trough that is concentric with the Imbrium basin. The other principal maria, Mare Tranquillitatis, Mare Vaporum, and Sinus Aestuum, lie within craterlike basins that apparently developed independently from the Imbrium basin and antedate it. A high arch of terra, the Montes Haemus, and an adjacent topographically low zone are related to the Serenitatis basin northeast of the area. The Julius Caesar quadrangle (Morris and Wilhelms, 1967) was the first of the two quadrangles to be mapped, and later mapping in the Mare Vaporum quadrangle (Wilhelms, in prep.) has led to revised interpretations of some stratigraphic units.

STRATIGRAPHY

The stratigraphic column of the quadrangles, as in much of the central part of the visible hemisphere, is divided by two extensive units into three main parts. Units older than the Fra Mauro Formation (fig. 1) (Eggleton, 1965) are pre-Imbrian. The Fra Mauro and units younger than it but older than the top of the Procellarum Group (which comprises 90 percent of the mare material shown in fig. 1) belong to the Imbrian System. Units younger than the Procellarum Group are post-Imbrian and belong to the Eratosthenian and Copernican Systems.

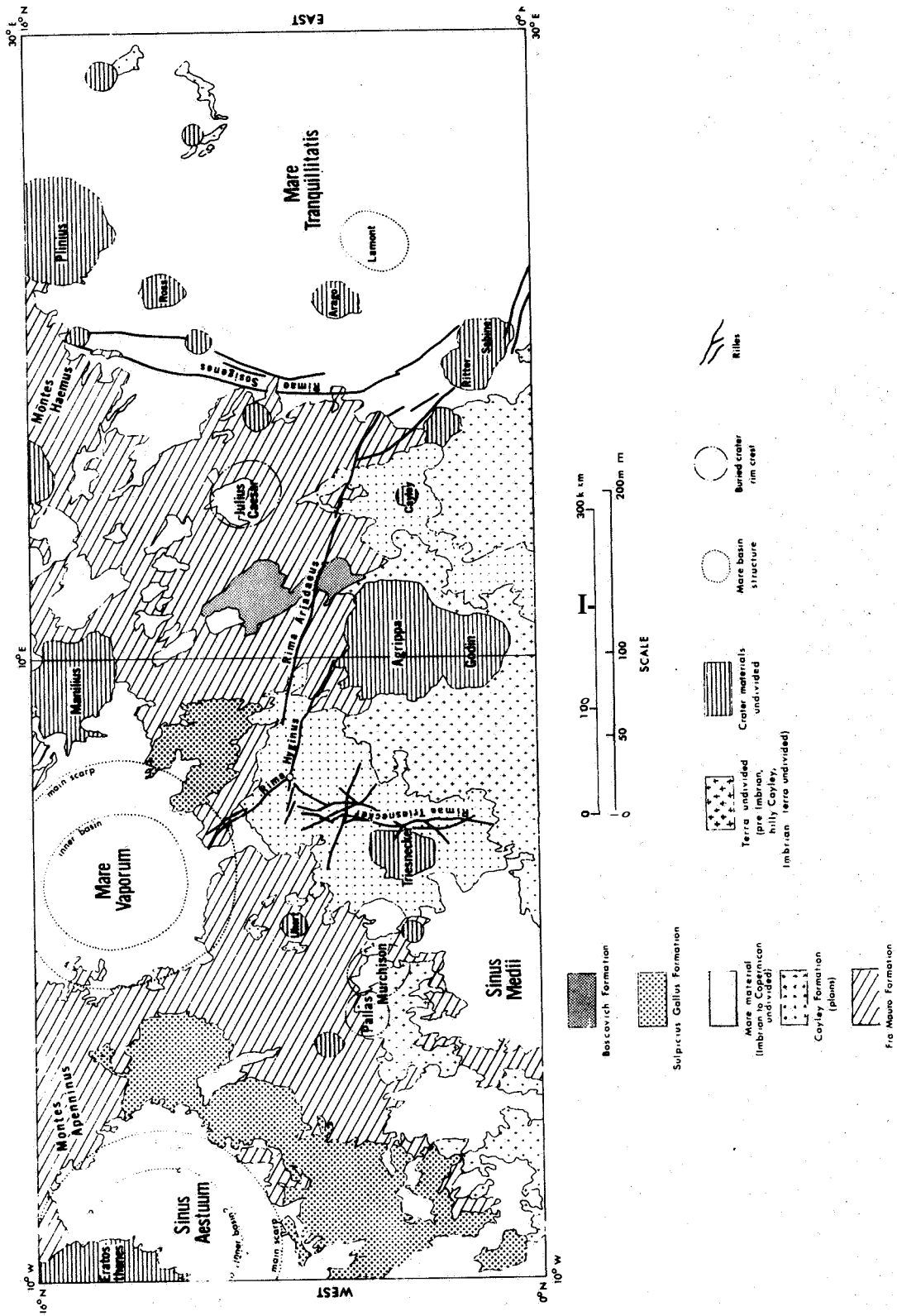


Figure 1 --Geologic sketch map of Mare Vaporum and Julius quadrangles.

Several craters, the exposed margins of the Tranquillitatis, Vaporum, and Aestuum basins, and probably the floors of these basins, are covered by Fra Mauro Formation. These craters and basins are therefore pre-Imbrian.

Regional relations strongly suggest that the Fra Mauro Formation, which occurs in much of the terra surrounding the Imbrium basin, is a blanket of debris ejected from the basin (Eggleton, 1965). The surface of this blanket slopes gradually away from the Imbrium outer scarp. The surface texture is gradational: coarsely hummocky close to the basin and smoother farther out, like the texture of rim materials of large fresh craters. The few large craters close to the basin appear to be heavily mantled and structurally deformed. Progressively farther from the basin more craters are visible, and these appear to be less mantled. The topography of the pre-Imbrian crater Julius Caesar (fig. 1) is well accounted for by the interpretation of the Fra Mauro as Imbrium ejecta (Morris, 1964). The northwest flank of the rim, which faces the Imbrium basin, appears to have material piled upon it, whereas the northern interior of the crater is deep, suggesting that it has been shadowed from deposition of the ejecta. The floor is progressively shallower southeastward, and the south rim is also apparently buried. The craters Pallas and Murchison show similar relations but less clearly.

Materials which are younger than the Fra Mauro Formation and therefore assigned to the Imbrian, Eratosthenian, and Copernican Systems are of four types: plains-forming materials, terra-mantling materials, materials with irregular surfaces, and crater materials.

#### Plains-Forming Materials

Materials which form nearly flat surfaces are called plains-forming. They preferentially fill depressions, including mare basins, circumbasin and radial troughs, and large craters, and are divided into rock-stratigraphic units on the basis of albedo and density of superposed craters. The lighter and more cratered are collectively designated the Cayley Formation (type area near

the genetically unrelated crater Cayley, fig. 1); the darker and less cratered are mare materials. Mare materials are further divided into four rock-stratigraphic units, which are named differently on the two maps. On the map of the Julius Caesar quadrangle, all **four** are designated as numbered formations of the Procellarum Group of Imbrian age, whereas in the Mare Vaporum quadrangle only the lighter two units are Procellarum Group and the darker two are designated Eratosthenian or Copernican mare material. After mapping of the Julius Caesar quadrangle was completed, these darker materials in one place in the Mare Vaporum quadrangle were found to embay the rim material of the crater Manilius, which is either Eratosthenian or Copernican in age. The other occurrences in the Mare Vaporum quadrangle are tentatively correlated with this one, and the two darker mare units in the Julius Caesar quadrangle are probably also post-Imbrian. In both quadrangles the dark units occur mainly at the basin margins and in old large craters at low elevations in the *terra*. **Most** mare materials are younger than the Cayley Formation and where exposed at the surface may overlie the Cayley and represent only the final stage of depression filling. The Cayley and mare materials may have the same general composition. Albedo differences may be due only to differences in the degree to which external processes such as cratering, solar radiation, and sputtering have altered the two units. One of the chief alterations may be the creation of small slopes of craters, fault scarps, slump scars, etc.; albedo differences on the slopes may result largely from differences in the amount of fresh rock exposed. Such alteration would be largely a function of age; however, it would be independent of age and anomalously great in areas cratered by secondary impacts from a nearby large crater or in areas of unusual tectonic activity. In the vicinity of Triesnecker, some alteration is a function of age and some is not. Plains-forming materials are little affected by subjacent topographic irregularities and commonly terminate abruptly against higher topographic forms; they may have been emplaced largely as fluid flows. Many contacts, however, are

gradational in detail, suggesting that pyroclastic materials are also present or that debris has moved downslope from higher places onto the plains.

#### Terra-Mantling Materials

Materials which subdue topography but do not obliterate it are called terra-mantling materials. Both light and dark materials of this kind are present. Light mantling materials that are believed to correlate with plains-forming Cayley because of identical albedo and apparent gradual transition in relief are designated the hilly member of the Cayley Formation (not differentiated on fig. 1). Hilly Cayley is similar to the smooth member of the Fra Mauro Formation but is commonly smoother, and many occurrences have sharp contacts with the Fra Mauro. Parts of the hilly Cayley may be volcanic material, probably pyroclastic, because they are uniform, have sharp contacts with adjacent materials, and are near many probable volcanic craters and rilles; but parts may be mass-wasted debris developed on materials of mixed origin.

Material which partly resembles smooth Fra Mauro and hilly Cayley but which appears to subdue topography less and thus may be thinner is called Imbrian terra material, undivided. The origin of much subdued lunar topography is not clear, especially in areas of this unit. The subdued nature may be due to mass wasting of the Fra Mauro, Cayley, or other units so that they are no longer recognizable.

Dark mantling material, much of it darker than any mare material, is more common in the Mare Vaporum quadrangle than in any other visible part of the Moon. Most of this material is correlated with the Sulpicius Gallus Formation (fig. 1) of Imbrian and Eratosthenian age named by Carr (1966), and some parts may be Copernican in age. Some of the Sulpicius Gallus, both in the Mare Vaporum quadrangle and in the type area 150 km to the northeast, appears to overlie the Procellarum but other occurrences are embayed by the Procellarum. Some dark material of Copernican age interrupts rays of the crater Copernicus. The apparent superposition on other

56-57

terrain suggests that these dark materials are pyroclastic. Much of the material surrounding the mapped exposures of Sulpicius Gallus is unusually dark for those materials though not as dark as Sulpicius Gallus, suggesting that thin layers of the pyroclastic material may overlie these materials. This darkening is conspicuous northwest of the Triesnecker area along an extension of the Sinus Medii trough and ends near the quadrangle boundary.

#### Materials with Irregular Surfaces

Two units in the Julius Caesar quadrangle, the Boscovich Formation (fig. 1) and material of steep domes (not shown on fig. 1), are characterized by considerable positive relief. The Boscovich Formation forms stringy ridges approximately parallel to Imbrian sculpture. The ridges probably consist of viscous volcanic materials extruded along sculpture fractures. The steep domes have extremely high albedo, probably because fresh rock is exposed through downslope movement. Many such domes may be volcanic constructional features, whereas others may be structurally isolated bedrock. Similar features in the Mare Vaporum quadrangle are mapped as possible pre-Imbrian materials.

#### Crater Materials

Crater materials fall into several morphologic classes which probably correspond to genetic classes. All large and many small circular or equidimensionally polygonal craters with high sharp rims and concave-upward flanks probably formed by impact. These craters are assigned to time-stratigraphic systems on the assumption that the presence or absence of rays, the magnitude of thermal anomaly at eclipse (Saari, Shorthill, and Fulmer, 1966), and the relation to the Procellarum Group have the same age significance as they do for the type craters of the systems outside the quadrangles. In both quadrangles several large craters have properties transitional between those of typical Eratosthenian and Copernican craters. Plinius, Ross, Arago and several smaller craters in Mare Tranquillitatis lack discrete rays but have light halos and high thermal anomalies typical of Copernican craters. These craters

are mapped as Eratosthenian because of the absence of rays; their high thermal anomalies may be unrelated to age because Mare Tranquillitatis has an overall high thermal signal during eclipse. Agrippa, in the terra, and Manilius, mostly in the terra but partly on mare, have low thermal anomalies typical Of Eratosthenian craters but have faint rays and light halos. Materials of these craters are exposed in both quadrangles. These materials were mapped as Copernican in the Julius Caesar quadrangle because the rays were the prime mapping criterion but are mapped as Eratosthenian or Copernican, undifferentiated, in the Mare Vaporum quadrangle because the thermal data, refined after mapping in Julius Caesar was completed, appear to correlate very well with age in this region.

Other kinds of craters, probably of internal origin, include irregular high-rimmed craters, low-rimmed round or slightly elongate craters, and craters other than satellitic craters alined in chains or along rilles. Three or four craters of these classes in the Mare Vaporum quadrangle, including the chain craters along Rima Hyginus, have high thermal anomalies like those of the Copernican impact craters and may also be relatively young. Some large apparently rimless round craters such as Hyginus or irregular depressions such as those around Ukert may be calderas. Ritter and Sabine, which are round but have low rims and atypically shallow floors and lack satellitic craters, also may be calderas.

In addition to ray craters, dark-halo craters and bright slope material are assigned a Copernican age. The albedo of the slope material apparently is highest on steepest and youngest slopes.

## STRUCTURE

### Mere Basins

Three craterlike mare basins--Tranquillitatis, Vaporum, and Aestuum--and the peripheral structures of two others--Imbrium and Serenitatis--are the dominant structures in the two quadrangles. Several concentric structures are associated with all the basins (Hartmann and Kuiper, 1962). The most conspicuous structure in

each is the edge of the basin proper that encloses most of the mare filling. The Montes Apenninus, in the northwest part of the Mare Vaporum quadrangle (fig. 1), are part of the first high ring outside the Imbrium basin and are bounded north of the quadrangle by a steep scarp that faces northwest toward the basin proper. The Montes Haemus, in the northwest part of the Julius Caesar quadrangle, are part of the first high ring outside the Serenitatis basin. The Montes Haemus are greatly modified by Imbrian structures and are covered with the Fra Mauro Formation. The Serenitatis basin scarp that bounds them on the north is not as high as the Imbrium one. Structures of the Tranquillitatis, Vaporum, and Aestuum basins that correspond to these scarps are the mare-terra contacts, breaks in slope in the terra, and, in the eastern part of Vaporum, a mare terrace higher to the east than in the center of the basin. All these scarplike rings are approximately circular but in places are straight and parallel regional structural trends. The mare-terra contact of Tranquillitatis is especially ragged, and the circular form of this probably shallow basin is best marked by a set of arcuate rilles, the Rimae Sosigenes (fig. 1). (A separate shallow basin may control that part of Mare Tranquillitatis east of the Julius Caesar quadrangle.)

#### Concentric Structures

Concentric structures that lie inside the main basin scarps within the Vaporum, Aestuum, and Tranquillitatis basins are concealed for the most part by mare material, but in Vaporum there are sufficient islands to permit comparison with the better exposures of structures in the Imbrium basin northwest of the quadrangles. Inside the main scarp is a depressed shelflike ring having peninsulas and islands complexly embayed by shallow mare material, and inside this shelf, an inner basin which has no islands and is probably much deeper. The Aestuum basin probably has a similar shelf and inner basin; there are more mare ridges close to the bounding scarp than in the center of the basin, and such ridges are characteristic of the Vaporum and Imbrium shelves. Much of the surface of Mare

Tranquillitatis is covered by a complex system of mare ridges that form the circular feature Lamont or are radial to it. Lamont may mark the inner Tranquillitatis basin.

Concentric structures that lie outside the main basin scarps are commonly conspicuous. One major trough related to the Imbrium basin, 1,100 to 1,200 km from the basin center, includes Sinus Medii and the low plains of the Triesnecker region, and another, 1,300 to 1,500 km from the center of the Imbrium basin, encloses the terra plain in which the type area of the Cayley Formation is located. A similar broad trough related to Serenitatis is probably present southwest of the Montes Haemus and accounts for the general low elevation of a zone in the terra where several old craters are filled with mare material, and for a large embayment of Mare Tranquillitatis into the terra (fig. 1). Concentric structures outside the Aestuum, Tranquillitatis, and Vaporum basins, listed in order of decreasing prominence of the structures, are only narrow grooves and ridges.

#### Radial Scarps and Troughs

A system of scarps and troughs radial to the Imbrium basin (Gilbert, 1893; Hartmann, 1963) and called Imbrian sculpture is conspicuous in the Julius Caesar quadrangle and the east half of the Mare Vaporum quadrangle. These scarps and troughs range in trend from N. 45° W. in the northern part of the Julius Caesar quadrangle to N. 30° W. in the Mare Vaporum quadrangle. They partly control in detail the outlines of the pre-Imbrian basins and the Sinus Medii trough. The close geometric relations of the sculpture to the Imbrium basin suggest that most sculpture is the topographic expression of faults that originated at the time the basin first formed (Shoemaker, 1962, p. 349). Some fault planes may have been reactivated later, and volcanism may have built the rims that bound many of the troughs.

The mare basins are believed to have been produced by the impact of solid bodies. Evidence for this interpretation is their size and circularity and, in the case of Imbrium, the wide extent

of concentric and radial scarps and troughs surrounding it. Also, the surface material around the Imbrium basin, the Fra Mauro Formation, resembles ejecta around lunar and terrestrial impact craters.

#### Minor Structures

Many faults, ridges, and other minor structures are not related to mare basins. The most conspicuous are two systems consisting mainly of rilles (probably grabens) and some mare ridges. One persistent and fresh-appearing en echelon system which includes Rima Ariadaeus, part of Rima Hyginus, and a straight segment of the edge of Mare Vaporum, has an unusual, unexplained trend: N. 70° -75° W. Another fresh and probably young system, the Rimae Triesnecker, trends north-south, but individual segments follow Imbrian sculpture, the Ariadaeus-Hyginus trend, and the long dimension of the Sinus Medii trough. All segments of the Triesnecker system seem to have formed more or less simultaneously, probably as a result of east-west tension caused by upwarp of part of the trough.

#### GEOLOGIC HISTORY

The first decipherable events in this part of the Moon are the formation in pre-Imbrian time of the Tranquillitatis, Serenitatis, Aestuum, and Vaporum basins. The great Imbrium impact then superimposed its concentric and radial structures upon these basins and the intervening cratered terra and covered them with ejecta, the Fra Mauro Formation. Volcanic materials (Cayley Formation) filled depressions, notably a large trough in the Julius Caesar quadrangle, another northwest of Sinus Medii in the Triesnecker area, and irregular depressions in the Ukert area that may be calderas. Other volcanic rocks of the Cayley Formation mantled rugged terrain but did not completely conceal it. Volcanism continued and probably increased greatly toward the end of the Imbrian Period, and flows of mare material (Procellarum Group) almost completed the filling of the old basins and the Sinus Medii trough. Pyroclastic materials (Sulpicius Gallus Formation) were deposited on the terra both before and after deposition of the Procellarum.

During or after deposition of the Sulpicius Gallus Formation, Eratosthenes and several other impact craters formed. These craters lack rays or have very faint ones and have low thermal anomalies; the albedo of their rim materials is low to moderate. Later, either in the Eratosthenian or Copernican Period, impacting bodies formed Plinius, Ross, Arago, Agrippa, and Manilius--craters whose properties make their age determination ambiguous. Dark mare material was then deposited along the margins of basins, covered the floors of some large craters, and embayed the rim deposits of the crater Manilius. In the Copernican Period, impact formed the craters Godin and Triesnecker, which have very extensive bright rays and large thermal anomalies. These craters formed after the emplacement of most, but perhaps not all, of the dark mare material.

At an unknown time, probably late in the Imbrian Period, some of the largest lunar grabens and crater chains, Ariadaeus and Hyginus, began to form along a new tectonic direction--N. 70° -75° W. Also at an unknown time, upwarp of the Sinus Medii trough resulted in splitting of the surface into a reticulate network of cracks, the Triesnecker rilles, along which volcanic craters formed. More recently, dark-halo craters and bright slope material formed. Impact cratering and mass wasting have occurred throughout lunar history and covered all surfaces with a layer of debris.

#### REFERENCES

- Carr, M. H., 1966, Geologic map of the Mare Serenitatis region of the Moon: U.S. Geol. Survey Misc. Geol. Inv. Map 1-489.
- Eggleton, R. E., 1965, Geologic map of the Rhiphaeus Mountains region of the Moon: U.S. Geol. Survey Misc. Geol. Inv. Map 1-458.
- Gilbert, G. K., 1893, The Moon's face--A study of the origin of its features: Philos. Soc. Washington Bull., v. 12, p. 241-292.
- Hartmann, W. K., 1962, Radial structures surrounding lunar basins, I--The Imbrium System: Univ. Arizona Lunar and Planetary Lab. Commun., v. 2, no. 24, p. 1-15.

- Hartmann, W. K., and Kuiper, G. P., 1962, Concentric structures surrounding lunar basins: Univ. Arizona Lunar and Planetary Lab. Commun., v. 1, no. 12, p. 51-66.
- Morris, E. C., 1964, Stratigraphic relations in the vicinity of the crater Julius Caesar, in Astrogeologic Studies Ann. Prog. Rept., August 1962-July 1963, pt. A: U.S. Geol. Survey open-file report, p. 31-32.
- Morris, E. C., and Wilhelms, D. E., 1967, Geologic map of the Julius Caesar quadrangle of the Moon: U.S. Geol. Survey Misc. Geol. Inv. Map 1-510.
- Saari, J. M., Shorthill, R. W., and Fulmer, C. V., 1966, Eclipse isothermal contour map of the Julius Caesar quadrangle and Mare Vaporum quadrangle of the Moon [two separate maps]: Seattle, Washington, Boeing Sci. Research Labs.
- Shoemaker, E. M., 1962, Interpretation of lunar craters, in Kopal, Zdenek, ed., Physics and astronomy of the Moon: London, Academic Press, p. 283-359.

SECTION II  
PRELIMINARY MAPS AND  
OTHER GEOLOGIC STUDIES

N67-31942

12003

3 A COMPARISON OF TWO TERRESTRIAL GRABENS WITH THE LUNAR RILLES  
RIMA ARIADAEUS AND RIMAE HYPATIA I AND II

By George I. Smith

map  
p 5-85 KS  
same

INTRODUCTION

Photogeologic maps were made of the fault systems related to two Quaternary grabens and were compared with maps of the inferred fault patterns in the vicinity of the lunar rilles Rima Ariadaeus and Rima Hypatia I and II. The lunar and terrestrial features have several characteristics in common; this article spotlights these and comments on their possible meanings.

TERRESTRIAL GRABENS

Two exceptionally well preserved grabens in southeast California were chosen for study. One is the Wildrose graben (figs. 1-3) on the east side of Panamint Valley (Maxson, 1950, p. 104 and fig. 1; Jennings, 1958); the other is the Slate Range graben (figs. 4-6) on the east side of Searles Valley (Smith and others, 1967). Both grabens are of Pleistocene age and formed as the result of apparently vertical movement on subparallel faults that cut middle to upper Pleistocene gravels. They are well preserved because the gravels are fairly well indurated and the climate is arid,

Cross sections of these grabens were made under the direction of R. E. Altenhofen, Topographic Division, U. S. Geological Survey. The sections were measured photogrammetrically, and the data were converted by computer to ground position and elevation. The 10 sections across the Wildrose graben (fig. 7) are estimated to be accurate to within 5 feet; the 8 sections across the Slate Range graben (fig. 8) are estimated to be accurate to within 2 feet.

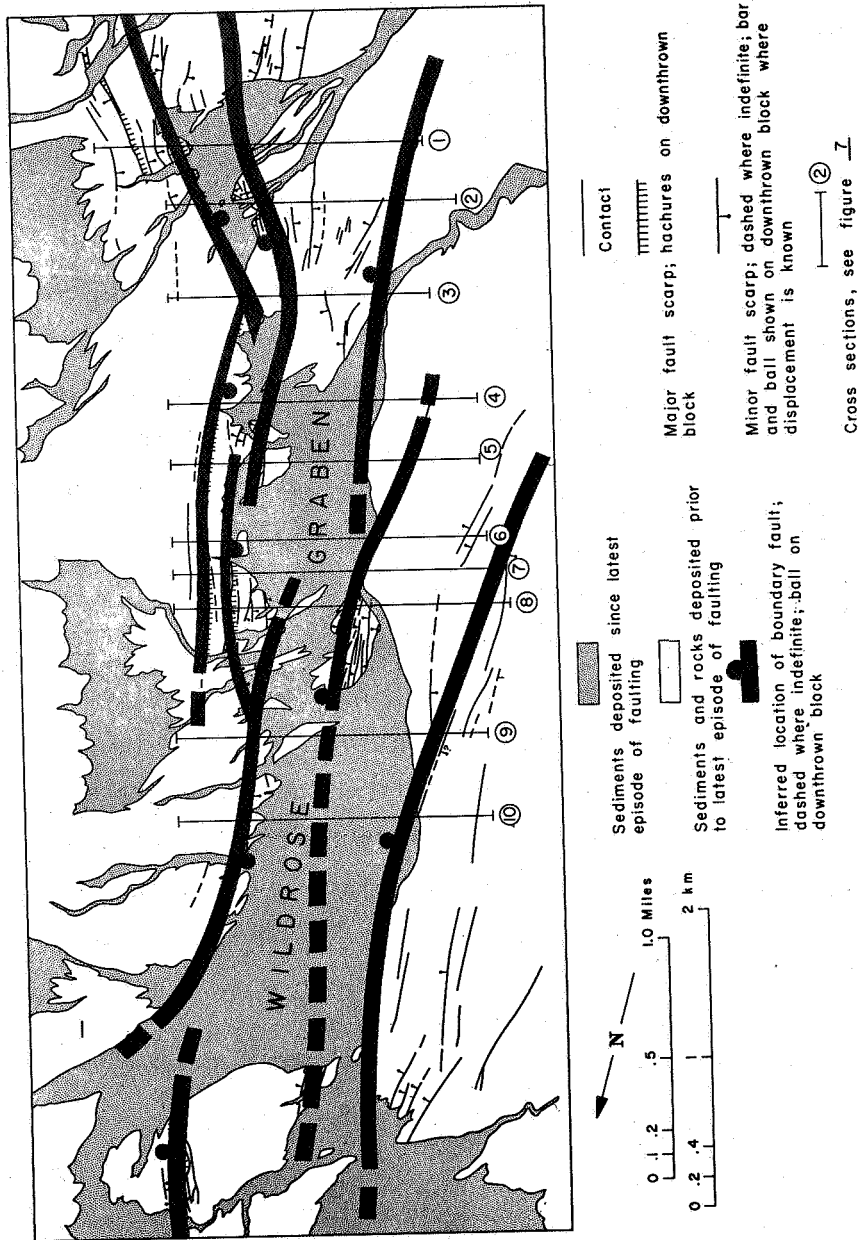


Figure 1 -Photogeologic map of Wildrose graben, Pamint Valley, Calif Base from uncorrected aerial photo. GS-CQ7-83.



Figure 2.--Oblique aerial photograph of Wilprose graben. View toward south, Panmint Range on left.



**Figure 3. --Oblique aerial photograph of Wildrose graben. View toward north.**

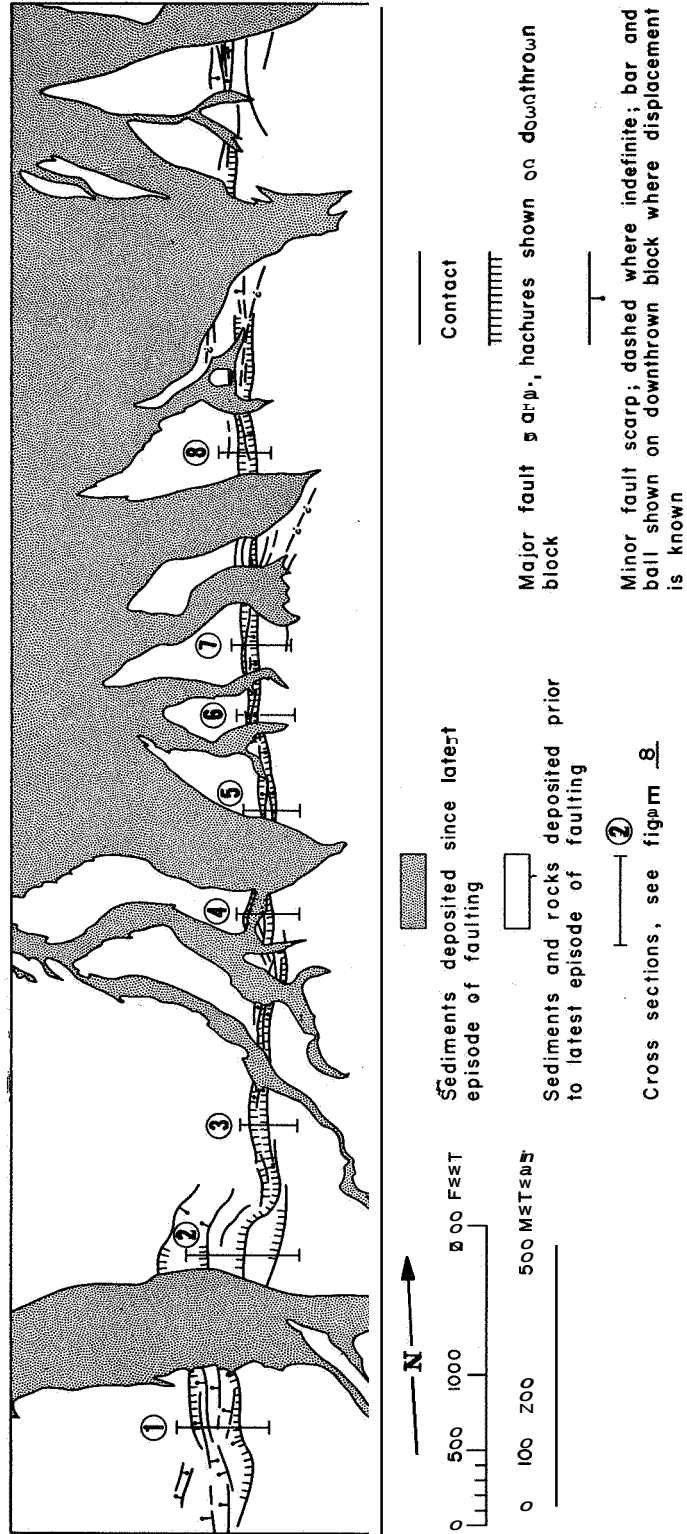


Figure 4.--Photogeologic map of Slate Range graben, Searles Valley, Calif. Base from uncorrected aerial photo. 184 (Pacific Air Industries).

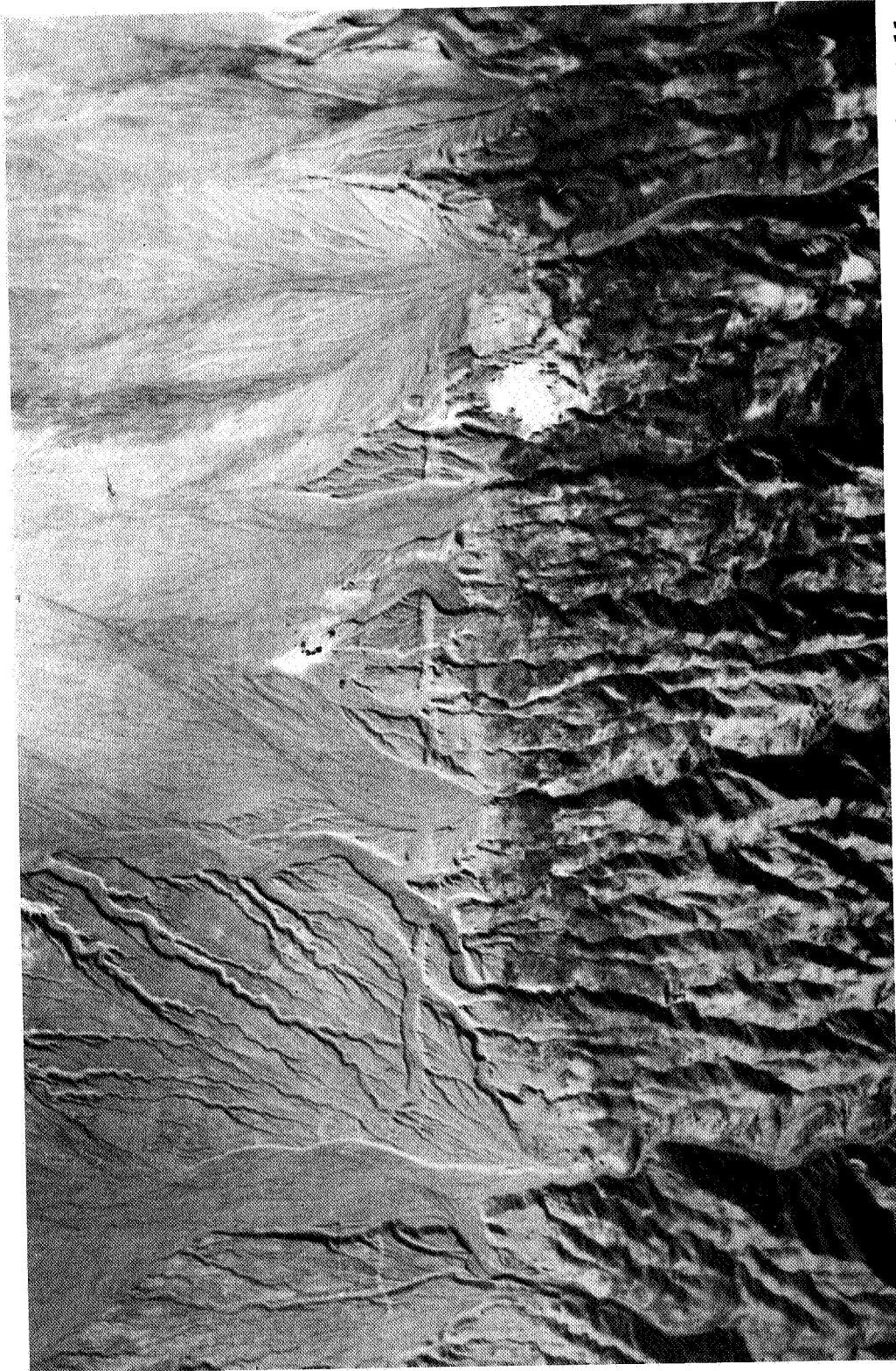


Figure 5.--Vertical aerial photograph of Slate Range graben. Slate Range at bottom and Searles Valley at top. North is to right; width of area shown is about 4 km. Photograph by Pacific Air Industries.



**Figure 6.** --Oblique aerial photograph of Slate Range graben. View toward south. Single-lane road in lower right corner gives scale.

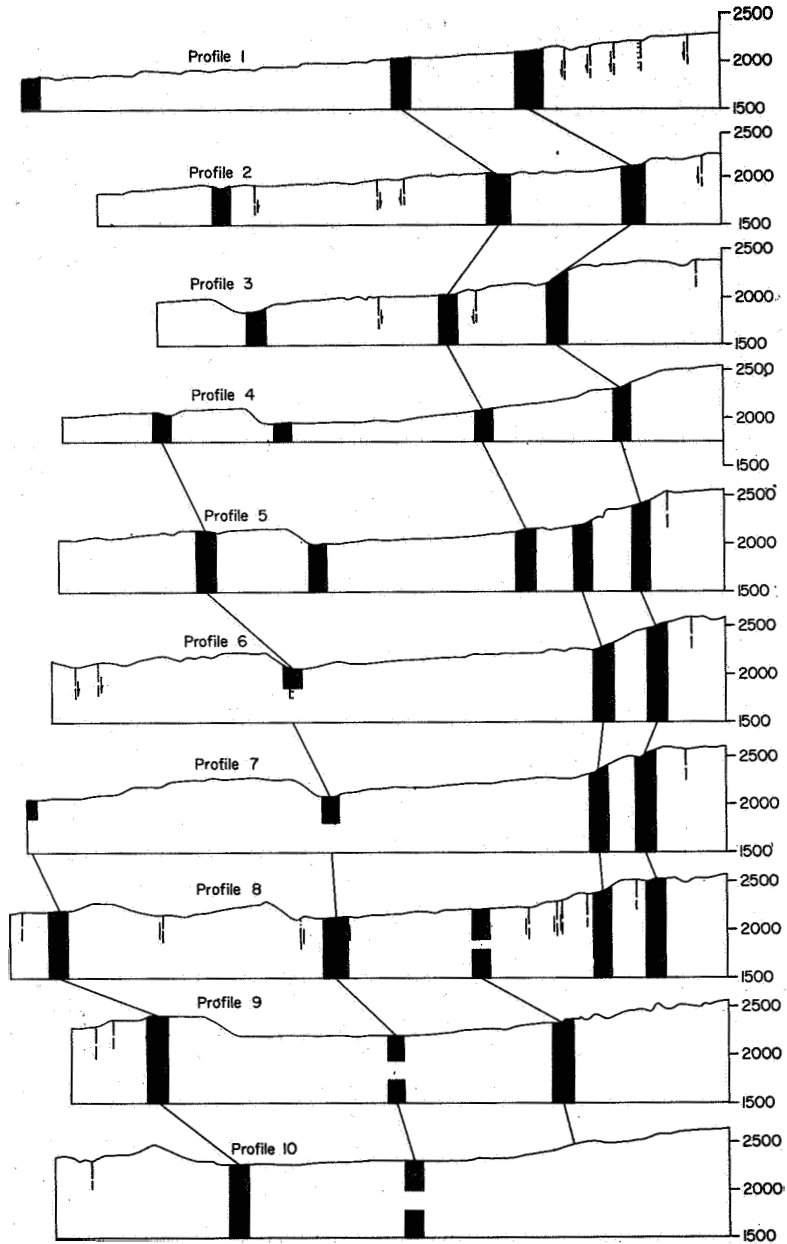


Figure 7.--Topographic cross sections across Wildrose graben, Panamint Valley, Calif. Faults from figure 1; dips arbitrarily **shown** vertical. Horizontal and vertical scale: 1 in. = 500 ft; vertical accuracy =  $\pm 5$  ft.

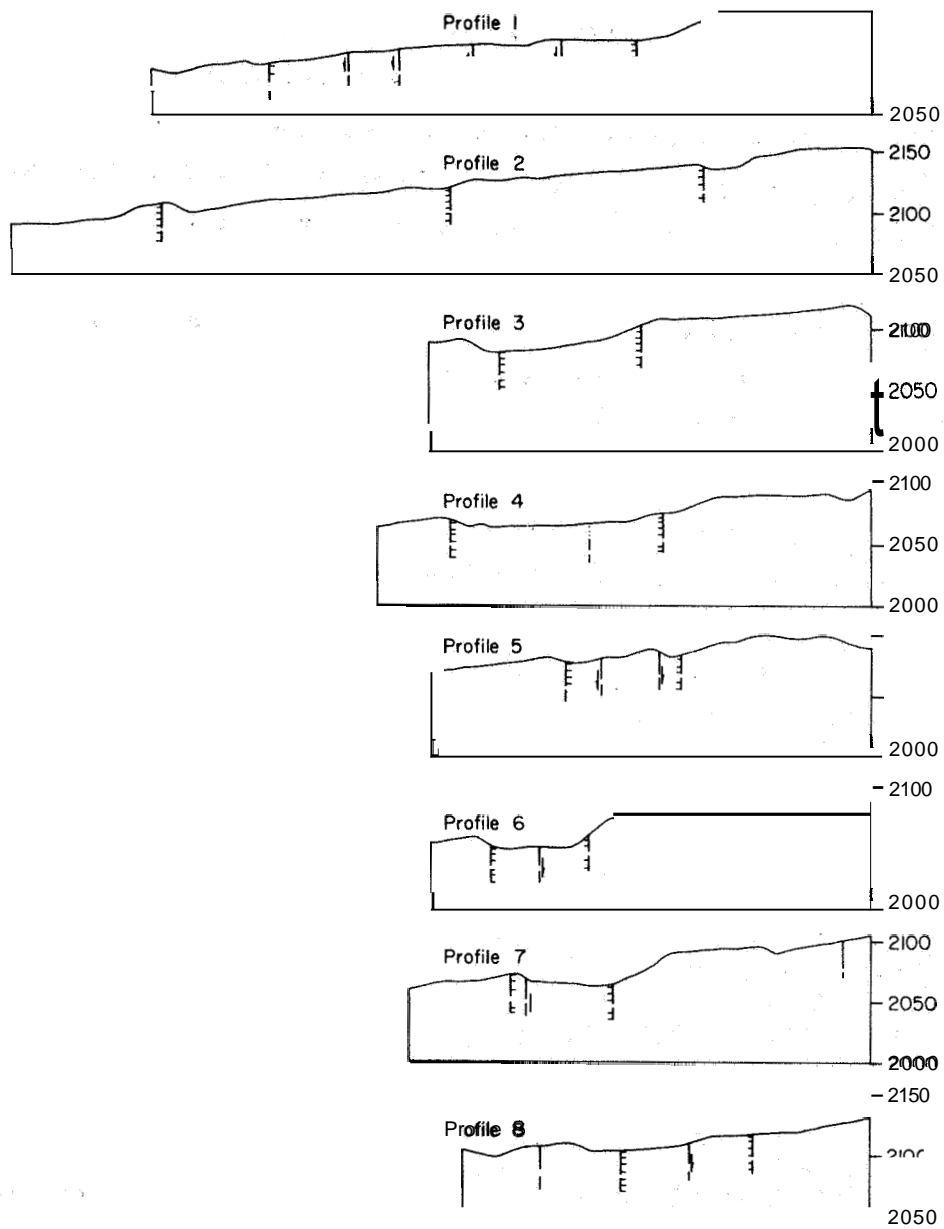


Figure 8.--Topographic cross sections across Slate Range graben, Searles Valley, Calif. Faults from fig. 4; dips arbitrarily shown vertical. Horizontal and vertical scale: 1 in. = 50 ft; vertical accuracy =  $\pm 2$  ft.

The two grabens chosen for study are typical of this type of feature. The faults that formed them are approximately parallel and are of about the same age. The grabens formed when displacements on these faults isolated elongate central blocks and dropped them down relative to their two sides. The maps of exposed faults, however, require some study to relate the indicated fault pattern to this idealized model. This is especially true of the map of the Wildrose graben because most of the downdropped block and long segments of the boundary faults are covered by the sheet of postfaulting alluvium that filled the depression (figs, 2, 3). The positions of those boundary faults have been inferred on the basis of exposed geology and are shown on the map (fig. 1) by wide stippled bands.

Approximate dimensions and dimension ratios of these terrestrial grabens follow. The lengths and widths are taken from the photogeologic maps (figs. 1, 4); the depths are approximated from the cross sections (figs. 7, 8).

	<u>Wildrose graben</u>	<u>Slate Range graben</u>
Length (km)	7	3.3
Width (m)	1,000	30
Depth (m)	70	5
<u>Length</u> Width	7	110
<u>Length</u> Depth	100	660
<u>Width</u> Depth	14	6

The lengths, width, and depths shown above differ by factors of 2, 33, and 14, respectively. The two ratios relating length to width and depth are also notably different. The width-to-depth ratios, however, are more similar. These ratios would have been even closer if tectonic depth had been used for the Wildrose graben; the depth of that graben is measurable only to the surface of younger alluvium, not to the top of the downthrown block, so it is less than the tectonic relief.

In addition to the width-to-depth ratios, other similarities between these terrestrial grabens can be noted. In detail, the boundary faults are sinuous (figs. 1, 4, 6), but the overall trends of the grabens appear nearly straight (fig. 5). The boundary faults are not continuous single fractures but a series of nearly aligned, overlapping en echelon fractures; the direction of en echelon overlap on both walls of both grabens is generally to the left. Between and outside of these boundary faults are numerous subparallel or branching faults, most of which have similar displacements. Both grabens appear simplest and clearest in their middle segments, and most complex and obscure near their ends.

The maps, as well as the dimension data, also point out several differences between the two grabens. The maps show that the major and minor faults on both sides of the Slate Range graben are of about equal length. The en echelon faults overlap, but the overlap distance is small compared with lengths of those faults. The major bounding faults along the west side of the Wildrose graben appear to be slightly longer than those along the east side, possibly because the section of faulted gravels on the east side is thinner. The boundary faults of this graben also tend to overlap each other to a greater extent. The dimensions and, as previously noted, two of the three dimension ratios of the two grabens are also notably different.

#### LUNAR RILLES RIMA ARIADAEUS AND RIMA HYPATIA

Fault systems are shown on the maps of the lunar rilles Rima Ariadaeus (fig. 9) and Rima Hypatia I and II (fig. 10) on the basis of the assumption that the linear scarps visible on photographs are faults. Rima Ariadaeus was studied on Lick Observatory photographs ECD-36 (fig. 11) and ECD-15, which provide stereoscopic effects when viewed together. Rima Hypatia was studied on photographs taken by Ranger VIII (fig. 12). Study of these photographs suggests that the average depth of Rima Ariadaeus is similar to that of the crater Ariadaeus BA, listed on the Agrippa quadrangle

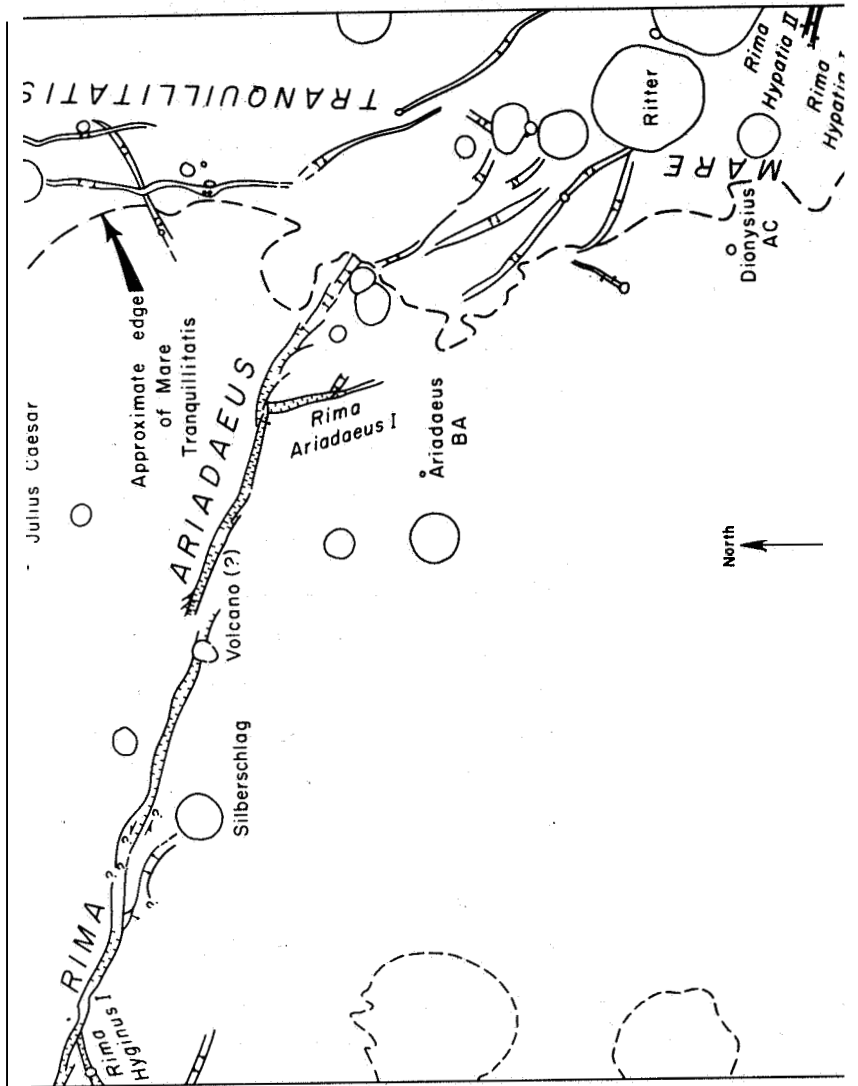


Figure 9 - Photogeologic map of inferred fault systems of Rima Ariadaeus. See fig. 1 for explanation; arrows on fault show relative horizontal movement.

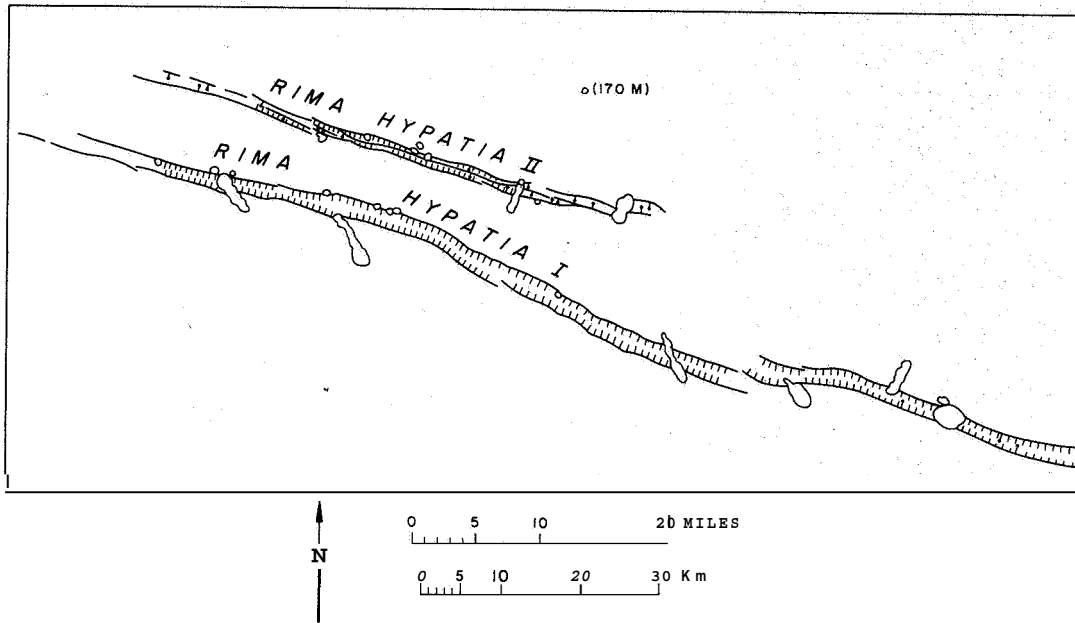


Figure 10.--Photogeologic map of inferred fault systems of Rima Hypatia I and II. See fig. 1 for explanation. Base from Sabine Ranger chart (RLC 7) by USAF ACIC.

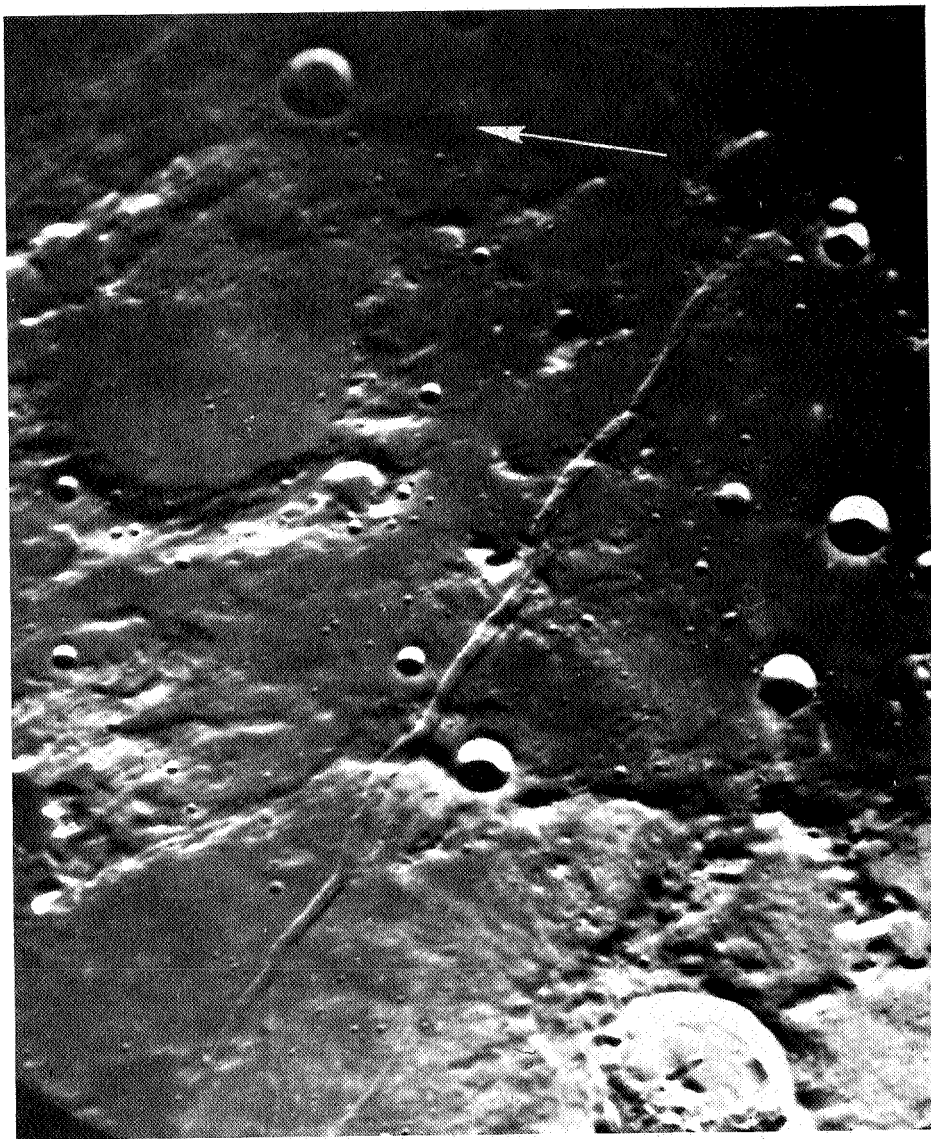


Figure 11.--Photograph of Riga Ariadaeus (Lick Observatory photo. ECD-36). Lunar north indicated by arrow.

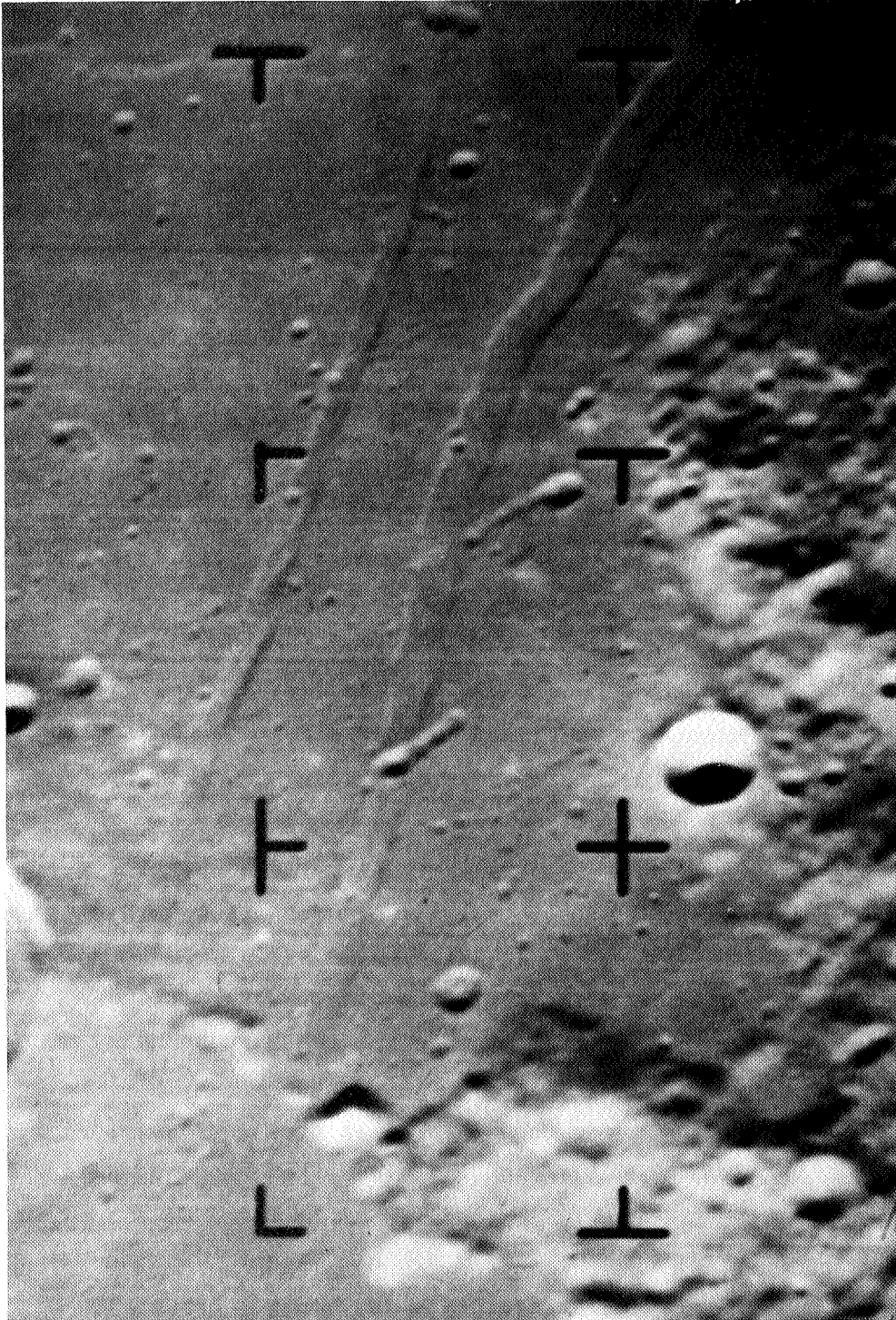


Figure 12.- Ranger VIII photograph of Rima Hypatia I and II (Jet Propulsion Lab., 1966, frame B 38).  
Lunar north at top

as about 490 meters, and that the depths of Rima Hypatia I and II are similar to that of an unnamed crater on the map of the Sabine area, listed as about 170 meters.

The scarps bounding Rima Ariadaeus vary in height depending on the terrane they cross; in smooth areas they tend to be highest and steepest, whereas in areas of ridges and mountains they tend to be lower and more irregular. This may be due to differences in the coherence of the rocks forming each type of topography; if so, the older rocks of the mountainous areas should have a low coherence and would tend to crumble or form landslides, whereas the younger rocks of the smooth areas should have a high coherence that permits them to stand as steep slopes. Rima Hypatia I and II are entirely in smooth mare material, and the height of the scarps is nearly constant over much of their lengths.

Dips on the boundary faults are probably nearly vertical. Rima Ariadaeus does not widen where the faults cross highlands; it would if the faults dipped inward. If any dip is indicated on these faults, it is southward on both inasmuch as there are several places where both faults curve northward crossing a ridge.

Displacements of the boundary faults are apparently dip slip. Some vertical displacement is obviously required, and, with one exception, relations show that lateral displacement is either not indicated or not possible. The exception is in the part of Rima Ariadaeus just north of the crater Silberschlag, where a ridge appears to be offset left laterally along the southern boundary fault.

Rima Ariadaeus is younger than the rilles that surround it. The fractures bounding Rima Ariadaeus displace those forming Rima Ariadaeus I and Rima Hyginus I; curiously, though, the displaced northward extensions of these features are not visible,<sup>1</sup> so the possibility arises that Rima Ariadaeus is the younger expression

---

<sup>1</sup>A faint lineation that could be the northern projection of Rima Ariadaeus I is visible along the east edge of the crater Julius Caesar, but this feature has not been noted in the intervening 65 km between the north edge of Rima Ariadaeus and the crater.

of an older crustal discontinuity which limited the original northern extent of Rima Ariadaeus I and Rima Hyginus I. Rima Ariadaeus may be older than the material in Mare Tranquillitatis inasmuch as scarps cannot be traced into the mare area. Rima Hypatia I and II lie in and are apparently younger than Mare Tranquillitatis material. These features could have existed prior to deposition of a thin layer, but the boundary scarps appear fairly sharp on the Ranger VIII photographs and burial by such material seems unlikely.

A related feature of possible importance is shown on the map of Rima Ariadaeus (fig. 9) as a "volcano(?)." It consists of a crater in the top of a mound that is not visibly cut by the scarps bounding Rima Ariadaeus. Both the crater and mound are thus younger than the scarps. The mound is domelike, thus differing from the raised rims that surround impact craters. The crater appears to be directly above the base of the scarp that has been interpreted as a fault. These physical forms and age relations suggest that the feature is a volcanic dome and crater formed when lava rose through a conduit that followed the line of weakness caused by the fault.

Estimates of the dimensions and their ratios of these lunar features follow. All data are approximate. Data for Rima Ariadaeus are computed for the full length of the feature (a) and for the individual segment east of long 14° E. (b). Data for Rima Hypatia I are listed for the full length (a) and west half (b).

	<u>Rima Ariadaeus</u>		<u>Rima Hypatia I</u>		<u>Rima Hypatia II</u>
	(a)	(b)	(a)	(b)	
Length (km)	260	110	170	90	65
Width (m)	3,000	3,000	2,100	2,100	1,200
Depth (m)	500	500	170	170	170
<u>Length</u> <u>Width</u>	87	37	80	43	54
<u>Length</u> <u>Depth</u>	520	220	1,000	530	380
<u>Width</u> <u>Depth</u>	6	6	12	12	7

## COMPARISON OF TERRESTRIAL AND LUNAR FEATURES

The physical dimensions of the terrestrial grabens described here are generally much less than those of the lunar features being considered. Their lengths and depths provide the greatest contrasts. The contrast between the width of the Slate Range graben and the lunar rilles is also great, but the width of the Wildrose graben is similar to that of Rima Hypatia II.

The ratios of these dimensions are also mostly very different. Of the ratios that relate length to width and depth, though, the values for lunar features mostly fall between those for terrestrial grabens. With respect to these ratios, at least, the Slate Range graben is somewhat more analogous to the lunar rilles than is the other graben. The width-to-depth ratios for all the features being compared, however, are strikingly similar; the ratios for terrestrial grabens range from 6 to 14, and the comparable ratios for lunar features range from 6 to 12.

The scarps of the terrestrial grabens reflect the patterns of boundary faults, and the similar scarps bounding the lunar features are inferred to have the same significance. The pattern associated with the Slate Range graben is more similar to the lunar examples, and that graben is again considered a closer analog. The maps show those faults to be generally discontinuous and slightly overlapping in an en echelon pattern. In most, the en echelon overlap is on the left. Associated with both grabens are subsidiary faults that branch from or are parallel to the main faults.

The overall patterns of the Slate Range graben and the lunar features are also similar; they are sinuous in detail but straight in overall trend, and their walls tend to remain equidistant regardless of trend.

## ORIGIN OF TERRESTRIAL AND LUNAR FEATURES

The terrestrial and lunar features described herein are probably all due to extension of the crust, although the fundamental cause of that extension--the tectonic origin--is undoubtedly very different in each case.

The Slate Range and Wildrose grabens probably resulted from tensional stresses that created high-angle normal faults during extension of the crust. The Slate Range graben is apparently the result of tension created by normal displacement along an underlying fault that dips about  $25^\circ$  W. (Smith and others, 1967). The displacements appear to have only dip-slip components and one period of activity. There is no evidence of strike-slip faulting on this or related faults.

The geology of the Wildrose graben is broadly similar to that of the Slate Range graben, but detailed geologic maps are available only for areas to the north (Hall and Stephens, 1962) and east (Lanphere, 1962). No evidence of strike-slip displacement was noted among the graben faults, but stress related to right-lateral faulting along the nearby Panamint Valley fault zone may have been responsible for the graben's existence; in other parts of California, short and relatively wide grabens are present in the blocks adjacent to large strike-slip faults, and the Wildrose graben might be an example of this type.

The lunar features Rima Ariadaeus and Rimae Hypatia I and II seem best explained as analogs of terrestrial grabens. The dimensions and proportions are mostly different, but the width-to-depth ratios and details of construction are strikingly similar. Tectonic extension of a linear zone of the lunar crust, accompanied by the creation of parallel faults and downfaulting of a middle block thus seems likely.

A deep-seated tectonic origin for these features seems necessary because the alternatives lack supporting evidence. Near-surface tension due to local compaction of the lunar crust is unlikely because the scale of the rilles is large, their trends are linear, and their distribution is unrelated to areas thought most likely to be undergoing compaction. Surface extension due to lateral displacement along nearby faults should probably be eliminated as a possible cause because of the lack of lunar features that

are in any way similar to terrestrial faults having such displacement. No other alternatives seem available. The conclusion is thus reached that Rima Ariadaeus and Rima Hypatia I and II are grabens, and that deep-seated tectonic forces are operative on the Moon.

The postulating of such forces on the Moon has major implications. One is that tectonic tremors--moonquakes--would be almost inevitable (though perhaps widely spaced in time). Another is that there exists some internal mechanism for the sporadic creation of stress. The existence of lunar grabens of different age, extent, and orientation suggests that this stress is the product of a migrating tectonic framework. These all imply a mobile subcrustal zone, and this, in turn, encourages speculation regarding increasing downward temperatures, a mobile core, and magnetic fields.

Grabens of these magnitudes on the lunar surface provide excellent areas for future geologic fieldwork. The bounding scarps, if not covered with talus, expose sections of the crust several hundred meters thick. Stratigraphic relations of the material making up ridges and smoother areas along Rima Ariadaeus could be determined, and the volcano(?) might be investigated as part of the same study. The layering and stratigraphic makeup of Mare Tranquillitatis could be investigated along Rima Hypatia I and II. All three grabens are narrow enough so that major stratigraphic units and relations could be verified by observations of the opposite walls, and experience in terrestrial stratigraphy shows that sites permitting such verification provide significantly better data than those allowing only spot observations.

#### REFERENCES CITED

- Hall, W. E. , and Stephens, H. G., 1962, Preliminary geologic map of the Panamint Butte quadrangle, Inyo County, California: *U.S. Geol. Survey Mineral Inv. Field Studies Map MF-251*, scale 1:48,000.

- Jennings, C. W., 1958, Geologic map of California, Olaf P. Jenkins ed., Death Valley sheet: California Div. Mines, scale 1:250,000.
- Jet Propulsion Laboratory, California Institute of Technology, 1966, Ranger VIII photographs of the Moon, cameras "A," "B," and "P": Natl. Aeronautics and Space Adm Spec. Pub. 111.
- Lanphere, M. A., 1962, pt. I, Geology of the Wildrose area, Panamint Range, California; pt. II, Geochronologic studies in the Death Valley-Mojave Desert region, California: California Inst. Technology, Pasadena, Ph. D. thesis, 171 p.
- Maxson, J. H., 1950, Physiographic features of the Panamint Range, California: Geol. Soc. America Bull., v. 61, p. 99-114.
- Smith, G. I., Troxel, B. W., Gray, C. H., Jr., and van Huene, Roland, 1967, Geologic reconnaissance of the Slate Range, San Bernardino and Inyo Counties, California: California Div. Mines and Geology Spec. Rept. (in press).



Ranger photographs clearly show, however, that planar surfaces on crater walls and rims and on hills and ridges are very rare. Rather, the surfaces are structured and uneven. This suggests that post-depositional events disrupt the smoothing process of small particle bombardment. The photographs reveal a variety of surface forms which, while explainable in part by particle erosion, require a disturbing force competent to displace masses of material of probable low cohesion over low-angle slopes. Many features disclosed by Ranger resemble forms that on Earth are produced by slump, creep of particulate debris, and landsliding.

The most logical recurrent perturbing mechanism that can be hypothesized to produce certain of the features of lunar surface fine structure is seismicity. As an agent of landscape modification, seismicity may be as important as particulate erosion in moving and redistributing lunar surface materials. It is emphasized that seismic activity is called upon here to produce only the forms and textures on the surface that are indicative of recurring instability on an otherwise apparently stable configuration.

#### SOURCES AND NATURE OF LUNAR SEISMICITY

Little can be said of the amount and nature of seismicity originating from within the Moon except to speculate a probability of seismic history. If moonquakes are analogous with earthquakes, their effects on lunar landforms would include settling, compaction, landslips, and fracturing. In a very general way one would expect the sources of lunar endogenous seismicity to be tectonism, volcanism, and, perhaps, plutonism.

Although little can be stated with confidence regarding the endogenous seismicity of the Moon, the evidence for seismic energy sources related to cratering phenomena is unequivocal. Part of the kinetic energy involved in producing a crater by impact is transmitted beyond the zone of fracturing as a seismic pulse.

#### Energy Considerations

The magnitude of seismicity from an impact and the effects of

that seismicity are dependent upon a number of variables. Principal among these are the nature of the material impacted and its structural arrangement and the depth of penetration and dynamics of the impacting object. In terms of the propagation of seismic energies and in terms of the influence of seismicity in modifying the lunar surface, the state of aggregation and densities of the uppermost 500 meters of lunar crust are the most important factors.

The energy involved in development of a lunar impact crater slightly larger than 1 km is on the order of  $10^{23}$  ergs. Shoemaker (1959) calculated that the energy needed to form Meteor Crater in Arizona was on the order of  $6 \times 10^{22}$  ergs. As a scale for comparison, the Alaskan earthquake of March 27, 1964, released  $3 \times 10^{24}$  ergs of seismic energy (Press and Jackson, 1965). The profound and widespread effects of this quake have been well documented. During an earthquake, a significant fraction of the total energy is liberated as seismicity. During an impact, only a small fraction of the total energy is liberated as seismic pulses,

Although the analogy is not exact, the data from nuclear explosions provide a useful scale to which impacts can be related. In a review of seismic wave propagation, Mickey (1964) emphasized that the percentage of source energy of nuclear explosions that is converted to seismic energy is very small and ranges, for the examples cited, from about 0.3 to 0.02. The factor for the Sedan shot (a yield of  $1 \times 10^5$  metric tons) was 0.08 percent. Variables which influence the efficiency include the size of the yield, the depth of burial, and the geological environment. With increasing yield and greater depths of burial, an increased percentage of energy is transmitted seismically. Mickey has tabulated percentages for three yields as follows: 10 kt, 0.34 percent; 100 kt, 1.67 percent; and 1,000 kt, 6.67 percent.

As another example, Carder and Cloud (1959) have analyzed the seismic effects from the deeply buried Rainier nuclear explosion. They determined that only 10 percent of the estimated source energy ( $7.2 \times 10^{19}$  ergs) was converted to seismic energy. This was

sufficient energy, however, to produce an earthquake of magnitude 4 at a distance of 2 miles from the detonation.

#### Magnitude and Intensity of Seismicity.

The surface and near-surface effects of seismicity are probably the most important lunar landform modifiers. Thus, magnitude (energy) of an impact-derived earthquake must be distinguished from its intensity or effects. As a very general rule, a high-energy event produces a greater surface modification than a low-energy event, but there are exceptions as pointed out by Richter (1958, p. 354).

A convenient scale for equating energy (E) to magnitude (M) is the Gutenberg-Richter relationship,  $\log E = 11.8 + 1.5M$ . A cratering event of  $10^{23}$  ergs and a "seismic efficiency" of  $10^{-3}$  to  $10^{-4}$  would give rise to an earthquake of 4.1 to 5.5 magnitude.

In a review of quake-produced ground phenomena, Neumann (1954, p. 15) has attempted to make a tentative correlation of the Gutenberg-Richter magnitude numbers with the intensity numbers of the MM (Modified Mercalli) system. For magnitudes of 4, 5, and 6, the corresponding intensity numbers are 4.5, 6.2, and 7.8, respectively. MM intensities of 7 and 8 are representative of relatively severe surface disturbances and are characterized by considerable damage of poorly built structures, caving along sand and gravel banks, and cracks in wet ground and on steep slopes. There is general correlation of intensities with horizontal accelerations (expressed as fractions of g). For intensities of 7 and 8, these are about 0.06 g and 0.15 g, respectively, from Richter's expression:

$$\log a \text{ (cm per sec}^2\text{)} = \frac{I}{3} - \frac{1}{2} \text{ (1958, p. 140).}$$

The ground motions of an earthquake are produced by vibration of the basement rocks which in turn produces motion in overlying strata. In studying several earthquakes, Neumann found that surface effects are occasionally noticeable and pronounced for distances of 100 miles with only minor diminution of intensity and that

surface-wave energies diminish as  $R^{-1}$ , whereas body-wave energies decrease as  $R^{-2}$ .

The nature of the materials overlying the basement profoundly influences the extent of propagation of surface waves. Furthermore, low-intensity basement effects can be transmitted to lighter and less-consolidated overburden with considerable magnification of intensity. Neumann found, from a study of the April 13, 1949, Puget Sound earthquake, that the intensities recorded on the lighter cover rocks are nearly four numbers greater than the intensities measured on bedrock (granite or equivalent). (See fig. 1.)

The properties of the medium in which the shock originates have a critical effect on the extent of propagation of seismic energy. Seismic waves are rather quickly damped in weak materials. Shallow earthquakes such as those resulting from an impact are likely to originate in weak materials. Very large impacting objects or objects moving at high velocities may penetrate to hard rocks of a possible lunar "basement".

#### Summary

The presence of craters on the lunar surface indicates the existence of a source of recurrent seismic energy. The energy needed to form a 1-km impact crater is slightly less than  $10^{23}$  ergs. On the basis of extrapolating from nuclear explosions such an event would result in release of  $10^{19}$  to  $10^{20}$  ergs of seismic energy, equivalent to an earthquake of magnitude 4.1-5.5. Such an earthquake could result in widespread surface disturbances and bring about failure of debris-cumposed slopes, cracking, and caving.

#### NATURE OF LUNAR SURFACE MATERIALS

Critical to an evaluation of seismic influences upon lunar landforms is the character of materials making up the lunar surface and their possible thicknesses as well as their grain size and degree of aggregation. The engineering experiments carried aboard Surveyor I (Natl. Aeronautics and Space Adm., 1966) have provided

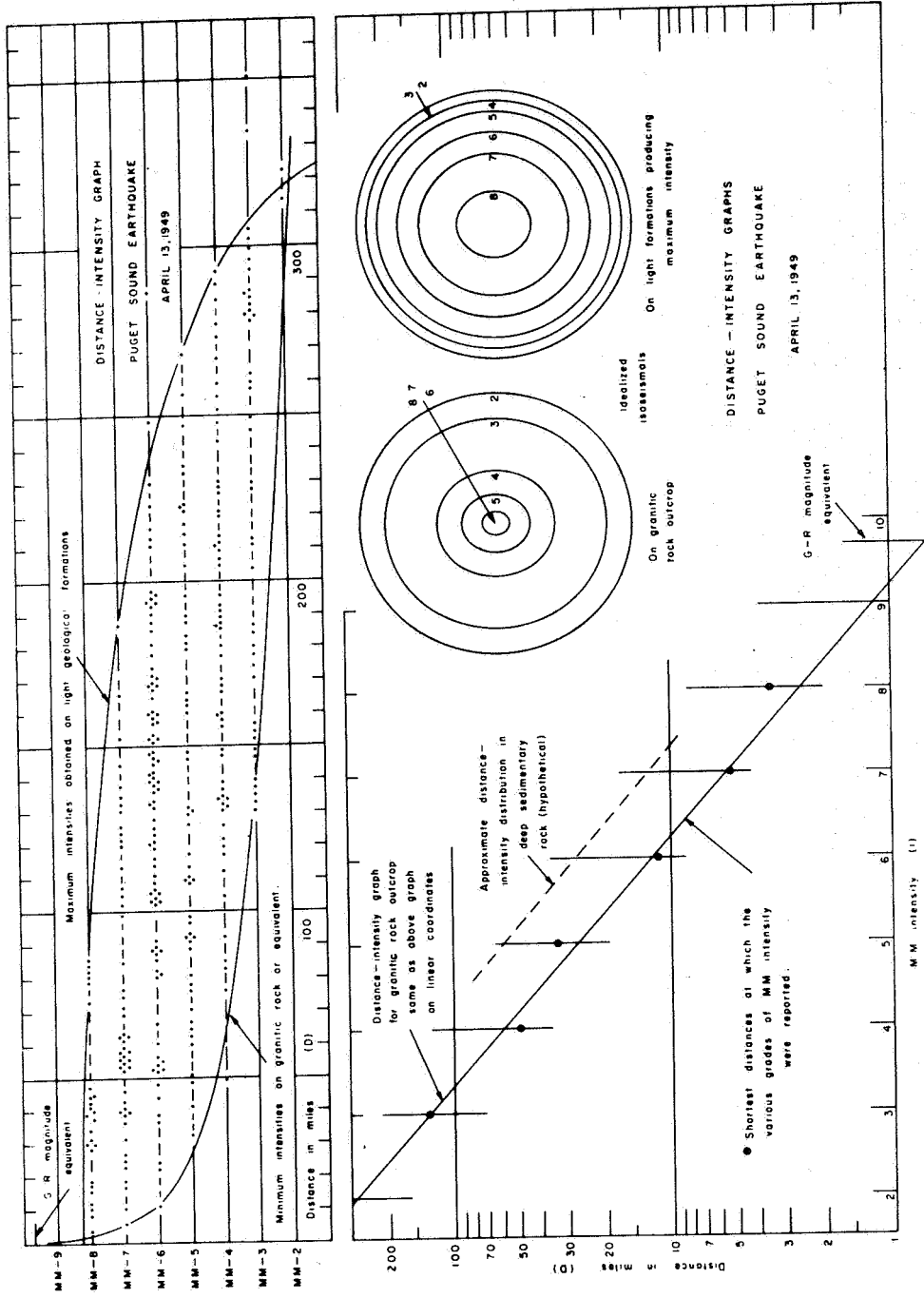


Figure 1.--Distance-intensity graphs for Puget Sound earthquake of April 3, 1949, showing influence of type of geological formation (from Neumann, 1954, fig. 2). Abbreviations: MM, Modified Mercalli scale; G-R, Gutenberg-Richter scale.

some data on bearing strength and soil properties. The report suggests alternative interpretations of the data, but the properties of the soil are consistent with material having an internal angle of friction of  $30^{\circ}$ - $40^{\circ}$ , a cohesion ranging from 1- to  $4 \times 10^3$  dynes per  $\text{cm}^2$ , and a density of 1.5 gm per  $\text{cm}^3$ . These properties are analogous to those of common terrestrial soils. Alternatively, the Surveyor data are consistent with a soil profile consisting of a shallow (2 cm) layer of cohesionless material overlying a comparatively strong subsurface with  $7 \times 10^5$  dynes per  $\text{cm}^2$  cohesion.

The recent literature abounds with discussions related to the nature of lunar surface processes and the nature and properties of lunar soils. Much of the pre-Surveyor thought was presented by Salisbury and Glaser (1964). In considering the effects of seismicity, the nature of the static stability of lunar slopes must be evaluated. Halajian (1964) summarized much of the data related to lunar slope behavior, and noted that for a frictional soil on the Moon, the angle of repose will approximate angles of repose for similar materials on Earth. However, if surface-to-volume ratios of the soil particles increase, a corresponding increase of van der Waals forces will result in considerably steeper slopes. Consideration of many aspects of the problem led Halajian to conclude that with moderate values of cohesion, lunar slopes will have a greater angle of repose than those on Earth.

Consideration of regional geological factors is also necessary in evaluating effects of lunar seismicity. The lunar stratigraphic column was established partly on the basis of recognition of regional ejecta blankets around Mare Imbrium and other large mare-filled basins. The ejecta blankets are interpreted to be sedimentlike deposits derived from the basins and spread around the basins by the basin-forming event. These materials have blanketed subjacent topographic forms and consist of unconsolidated fragments of rock and dust particles deposited in chaotic assemblages (see Shoemaker and Hackman, 1962; Eggleton, 1964).

SURFACE SEISMIC EFFECTS ON EARTH  
AND THEIR RELATIONSHIPS TO THE MOON

Over the past half-century, surface seismic effects have been rather well documented and are summarized by Richter (1958). Although earthquake shocks produce a great variety of phenomena on Earth, the absence of a hydrosphere and atmosphere on the Moon limits the types of effects that shaking would produce. For this reason, only the phenomena of compaction, slope failure or landslides, and debris creep will be examined.

Compaction

Evidence from the Alaskan earthquake of 1964 indicates that compaction of alluvium was common, particularly at Whittier (Kachadorian, 1965, p. 15) where compaction on the order of a few feet was measured. Coulter and Migliaccio (1966, p. 18) described evidence of compaction of unconsolidated sands at Valdez. Hansen (1965, p. 27-29) described cracking at Anchorage that resulted from differential compaction.

In a general discussion concerning effects of earthquakes on earth dams, Terzaghi (1950, p. 90) suggested that fills are stabilized through compaction produced by shaking. Terzaghi and Peck (1948, p. 528-529) have shown and emphasized the importance of natural or artificial shaking in effecting compaction of unconsolidated granular material. The Compaction of sand, for example, is many times greater under a vibrating or pulsating load than under static loading and reaches a maximum at certain natural resonant frequencies that are functions of properties of the material.

Lunar case

In connection with experimental studies evaluating sonic velocities and shear strengths of possible lunar materials, Osgood and Green (1966, p. 552) have shown the effect of vibration frequency on packing of basaltic ash and suggested that resonant frequency may be closely dependent upon grain size. In view of the Surveyor I evidence that lunar surface materials are particulate,

the effects of shaking are of potential importance to any consideration of the state of aggregation and strength of the surface.

### Slope Failure and Landslides

The importance of the stability of manmade structures and modified terrestrial landforms has given rise to a considerable research effort relating earthquakes to slope and structural stabilities. The problems of slope stabilities and slope stabilization are extremely complicated; numerous variables must be considered. Generally speaking, an earthquake produces an acceleration that increases shear stress in a slope or bank. If the shear stress is increased so that it exceeds shear strength, failure takes place. MM intensity of 7, corresponding to the first signs of caving of banks, is manifested by horizontal accelerations of 0.06 g, approximately.

Stability of a slope is directly related to the state of aggregation and grain size of the particles which comprise it. Terzaghi (1950, p. 90) has noted that materials most sensitive to stability angles are "slightly cemented grain aggregates such as loess and submerged or partly submerged loose sand." He further noted (p. 90) that "The destructive effect of earthquakes on slightly cemented grain aggregates . . . . seems to be chiefly due to the rapid vibratory movement of the particles with reference to each other . . . ."

The response of an earth bank to acceleration varies with its height and strength. Idriss and Seed (1966) have calculated response as a function of these two parameters (figs. 2, 3).

Seed and Goodman (1964) and Goodman and Seed (1965) have defined a parameter of slope stability, yield acceleration,  $k_y$ , expressed as a fraction of g, which is "the acceleration at which sliding will begin to occur" (1965, p. 3-6). The acceleration is related to:  $\phi$ , the angle of internal friction;  $\alpha$ , the slope angle;  $s_i$ , the shear strength intercept at 0 normal pressure;  $s_e$ , equivalent shear resistance; d, depth of critical sliding surface; p,

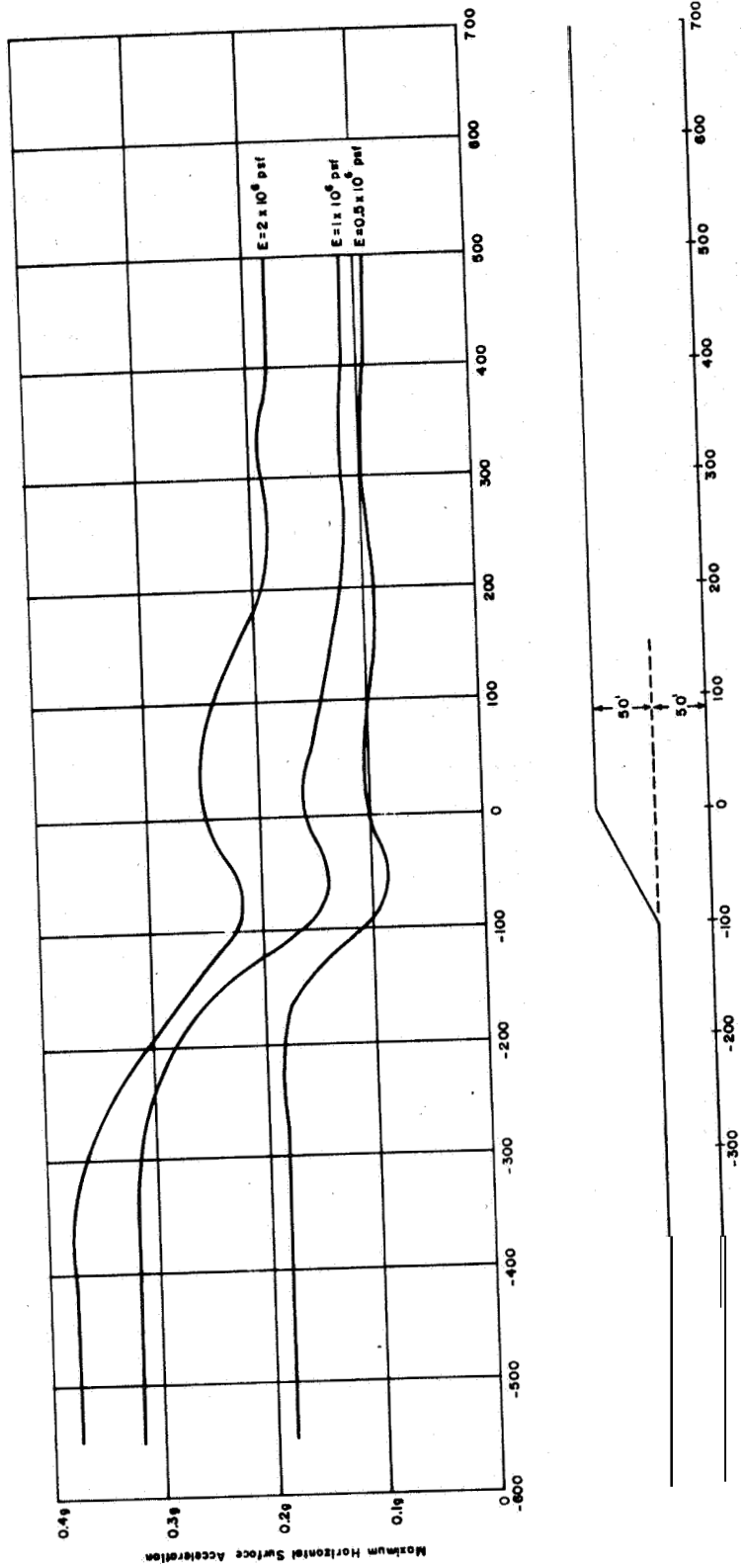


Figure Z -- Influence of material characteristics on response of earth banks (from Idriss and Seed, 1966, fig. 14).

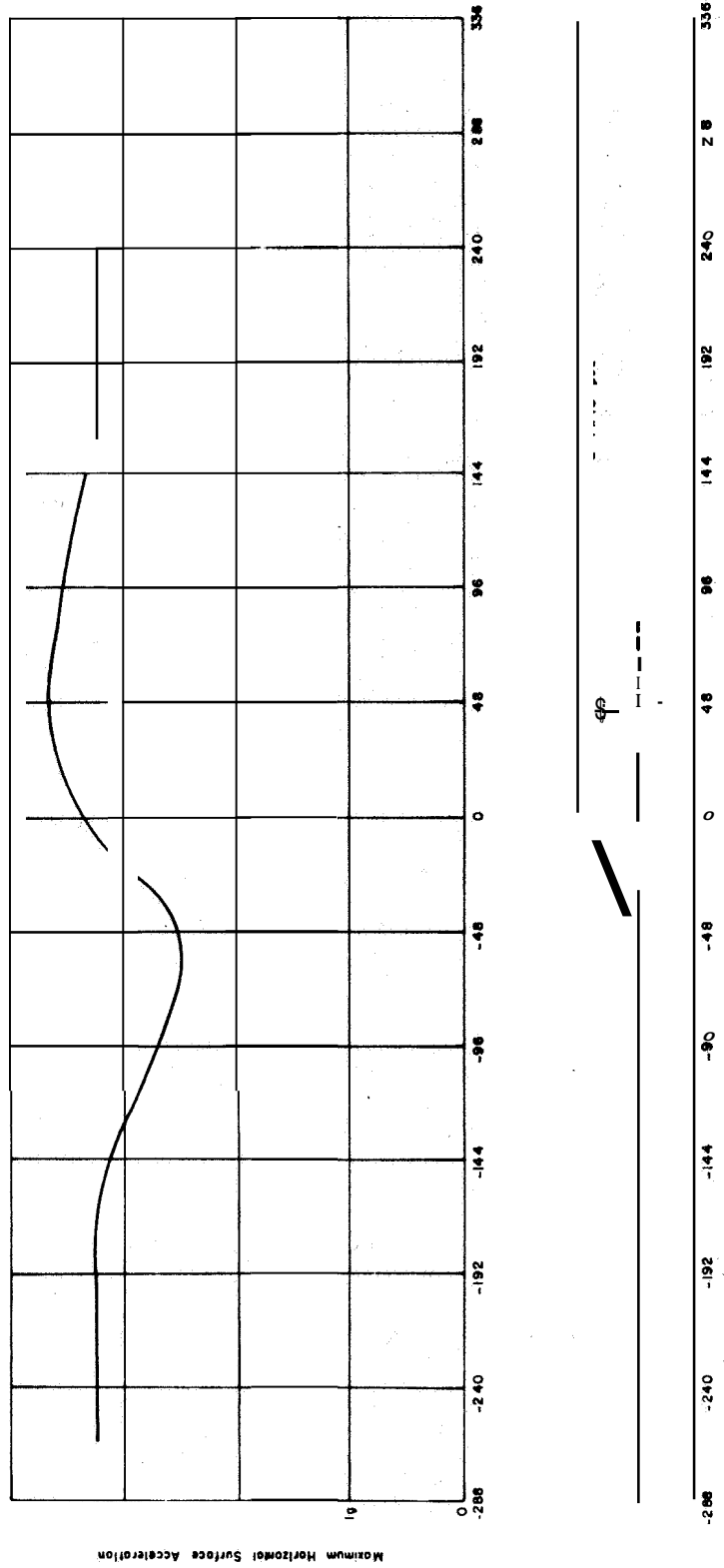


Figure 3.--Maximum horizontal ground-surface accelerations for 24-foot-high earth bank (from Idriss and See $\omega$ , 1966, fig. 15).

soil density; and  $g$ , acceleration of gravity, through the following expression:

$$k_Y = \tan (\phi - \alpha) + \frac{s_i + s_e}{dpg (\cos \alpha + \sin \alpha \tan \phi)} \quad (1)$$

The second term of this expression evaluates the effect of the toe and the shear strength intercept at 0 normal pressure.

#### Lunar case

Using a value of  $35''$  for  $\phi$ , suggested from the results of the Surveyor I experiments, values of  $k_Y$  can be obtained for several slope angles. Using inclinations of slope of  $5^\circ$ ,  $10^\circ$ ,  $20^\circ$ , and  $30^\circ$ , and ignoring the effect of the toe and shear strength, yield accelerations of  $0.577 g$ ,  $0.466 g$ ,  $0.268 g$ , and  $0.087 g$  are indicated. In the absence of any means to approximate  $s_i$  or  $s_e$ , the second term in equation 1 has not been evaluated, but it may be of considerable significance.

#### Debris Creep

Low-intensity seismicity may induce minor movement of particulate material. On Earth, owing to comparatively rapid erosion, the effects of intermittent seismicity would scarcely be observed and it would be difficult to separate those particles moved "seismically" from those moved by atmospheric erosional processes unless direct observations were possible. However, intensities as low as MM II or III may possibly cause minor movement.

#### Lunar case

In the absence of an environment such as Earth's, which produces rapid modification, low-intensity seismic effects acting over a long period of time may contribute to smoothing and destruction of slopes. Seismicity may be significant in enhancing slow down-slope creep of particulate debris.

## EVIDENCE OF LUNAR SEISMIC EFFECTS

Crater forms and the texture of slopes shown by Ranger photographs are strongly suggestive, by terrestrial analogy, of modification by slumping, creep, and differential compaction. Tree-bark-like patterns in the three large depressions near the center of Ranger IX B-camera frame 87 were noted by Kuiper and others (1966, p. 138) and had previously been described as resembling the original surfaces of terrestrial lava flows (Kuiper, 1965, p. 55). However they are also similar to debris-creep patterns that form on terrestrial material and in this report are considered to result from slumping and down-slope movement of particulate materials.

Surface textures on the hills making up the lower part of the eastern wall of Alphonsus, as disclosed by high-contrast reproduction of Ranger IX photographs, are typical of the pattern produced by either differential compaction, slumping, or landsliding. Any one or a combination of these processes can be triggered and produced by seismic energy. A typical pattern, and one resembling the pattern of benches and scarps seen in Alphonsus, is that developed on Government Hill, Anchorage, Alaska, after the earthquake of 1964 (fig. 4).

Schmitt (in Shoemaker, 1966, p. 328) has recognized slumping on the north rim of a crater wall shown in the southeast corner of Ranger VIII B-camera frame 90.

### SUMMARY

In view of the energies released by impact cratering, it is highly probable that seismic activity occurs on the Moon. This exogenous source supplements an unknown amount of seismic energy derived from within the Moon. On the basis of comparison with terrestrial processes, seismic activity should be sufficient to produce many of the morphological features and modifications shown in Ranger and Surveyor I photographs. Seismic activity may be a major modifying agent, although not necessarily the dominant one, and together with erosion by particles, may produce many of the features observed on the lunar surface.

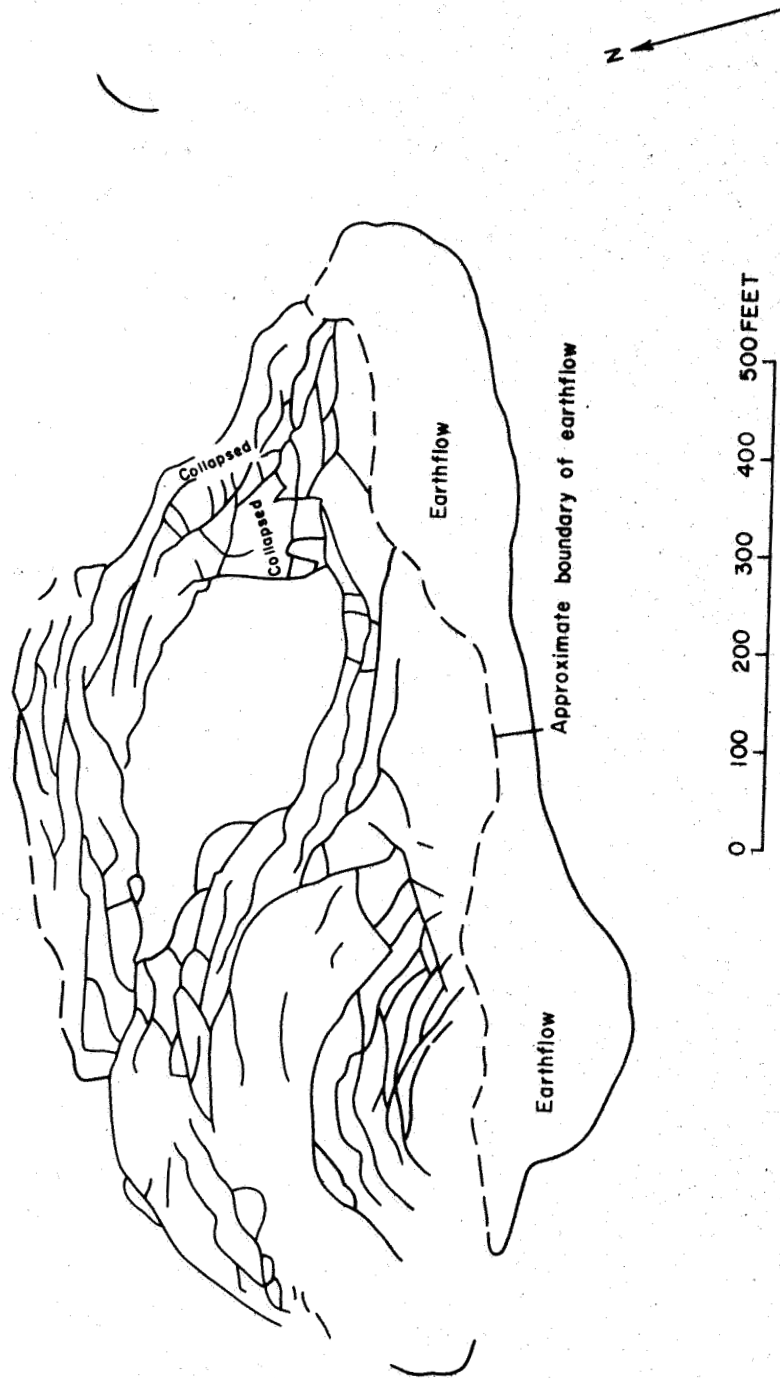


Figure 4.--Fault pattern in Government Hill slide, Anchorage, Alaska. Many small fractures have been omitted. (Simplified from Hansen, 1965, fig. 38.)

Of potential significance, but as yet undeterminable, is the effect of shaking upon compaction of lunar surface materials. Sufficient terrestrial examples exist to suggest that lunar materials, possibly volcanic ash or impact-derived rock fragments, could have become consolidated by seismic activity and that some of the fine structure revealed on slopes could be the result of differential compaction, slumping, and subsidence.

#### REFERENCES CITED

- Carder, D. S. , and Cloud, W. K., 1959 , Surface motion from large underground explosions: Jour. Geophys. Research, v. 64, no. 10, p. 1471-1487.
- Coulter, H. W., and Migliaccio, R. R., 1966, Effects of the earthquake of March 27, 1964 at Valdez, Alaska: U.S. Geol. Survey Prof. Paper 542-C, 36 p.
- Eggleton, R. E., 1964, Preliminary geology of the Rhipaeus quadrangle of the moon and definition of the Fra Mauro formation, in Astrogeol. Studies Ann. Prog. Rept., pt. A: U.S. Geol. Survey open-file report, p. 42-61.
- Goodman, R. E., and Seed, H. B., 1965, Displacement of slopes in cohesionless materials during earthquakes: California Univ. Soil Mechanics and Bituminous Materials Research Lab., Berkeley, 26 p.
- Halajian, J. D. , 1964, Gravity effects on soil behavior, in Salisbury, J. W., and Glaser, P. E., eds.; The lunar surface layer: London, Academic Press, p. 67-91.
- Hansen, W. R. , 1965, Effects of the earthquake of March 27, 1964 at Anchorage, Alaska: U.S. Geol. Survey Prof. Paper 542-A, 68 p.
- Idriss, I. M., and Seed, H. B. , 1966, The response of earth banks during earthquakes: California Univ. Soil Mechanics and Bituminous Materials Research Lab., Berkeley, 42 p.
- Kachadoorian, Reuben, 1965, Effects of the earthquake of March 27, 1964 at Whittier, Alaska: U.S. Geol. Survey Prof. Paper 542-B, 21 p.

- Kuiper, G. P., 1965, Interpretation of Ranger VII records, in Ranger VII, pt. 2, Experimenters' analyses and interpretations: Jet Propulsion Lab. Tech. Rept. 32-700, Pasadena, p. 9-73.
- Kuiper, G. P., Strum, R. G., and Le Poole, R. S., 1966, Interpretation of the Ranger records, in Ranger VIII and IX, pt. 2, Experimenters' analyses and interpretations: Jet Propulsion Lab. Tech. Rept. 32-800, Pasadena, p. 35-248.
- Mickey, W. V., 1964, Seismic wave propagation: **AEC** Tech. Inf. Doc. 7695, p. 181-194.
- Natl. Aeronautics and Space Adm., 1966, Surveyor I, A preliminary report: **NASA** Spec. Pub. 126, 39 p.
- Neumann, Frank, 1954, Earthquake intensity and related ground motion: Washington Univ. Press, Seattle, 77 p.
- Osgood, J. H., and Green, Jack, 1966, Sonic velocity and penetrability of simulated lunar rock dust: *Geophysics*, v. 31, p. 536-561.
- Press, Frank, and Johnson, David, 1965, Alaskan earthquake, 27 March 1964; Vertical extent of faulting and elastic strain energy release: *Science*, v. 147, p. 867-868.
- Richter, C. F., 1958, Elementary seismology: San Francisco, W. H. Freeman, 768 p.
- Salisbury, J. W., and Glaser P. E., eds., 1964, The lunar surface layer: London, Academic Press, 532 p.
- Seed, H. B., and Goodman, R. E., 1964, Earthquake stability of cohesionless soils: *Jour. Soil Mech.*, **ASCE** SM6, v. 90, p. 43-73.
- Shoemaker, E. M., 1959, Impact mechanics at Meteor Crater, Arizona: **U.S.** Geol. Survey open-file report, 55 p.
- \_\_\_\_\_ 1965, Preliminary analysis of the fine structure of the lunar surface in Mare Cognitum, in Ranger VII, pt. 2, Experimenters' analyses and interpretations: Jet Propulsion Lab. Tech. Rept. 32-700, Pasadena, p. 75-134.

- Shoemaker, E. M., 1966, Progress in the analysis of the fine structure and geology of the lunar surface from the Ranger VIII and IX photographs, in Ranger VIII and IX, pt. 2, Experimenters' analyses and interpretations: Jet Propulsion Lab. Tech. Rept. 32-800, Pasadena, p. 249-337.
- Shoemaker, E. M., and Hackman, R. J., 1962, Stratigraphic basis for a lunar time scale, in Kopal, Zdenek, and Mikhailov, Z. K., eds., The Moon--Symposium 14 of the I.A.U. : London, Academic Press, p. 289-300.
- Terzaghi, Karl, 1950, Mechanism of landslides, in Paige, S., chm., Application of geology to engineering practice (Berkeley volume): Geol. Soc. America, p. 84-121.
- Terzaghi, Karl, and Peck, R. B., 1948, Soil mechanics in engineering practice: New York, John Wiley, 566 p.

N67-21944

PRELIMINARY REPORT ON THE  
GEOLOGY OF THE PLATO QUADRANGLE OF THE MOON

By J. W. M'Gonigle and D. L. Schleicher

INTRODUCTION

The Plato quadrangle, in the north-central part of the Moon (lat  $48''-64''$  N., long  $10^\circ$  E.  $-20''$  W.) , includes the northern part of Mare Imbrium and part of Mare Frigoris. The maria there are separated by a strip of upland that includes the crater Plato, the Montes Alpes, and the Vallis Alpes. Rising from Mare Imbrium are isolated masses of terra material--Montes Recti and Montes Teneriffe. W. Bond and other polygonal depressions occur on an upland surface north of Mare Frigoris. The age of the units in the quadrangle probably ranges from pre-Imbrian through Copernican; the great bulk of visible material is probably Imbrian. The more widespread and important morphological units are shown in figure 1.

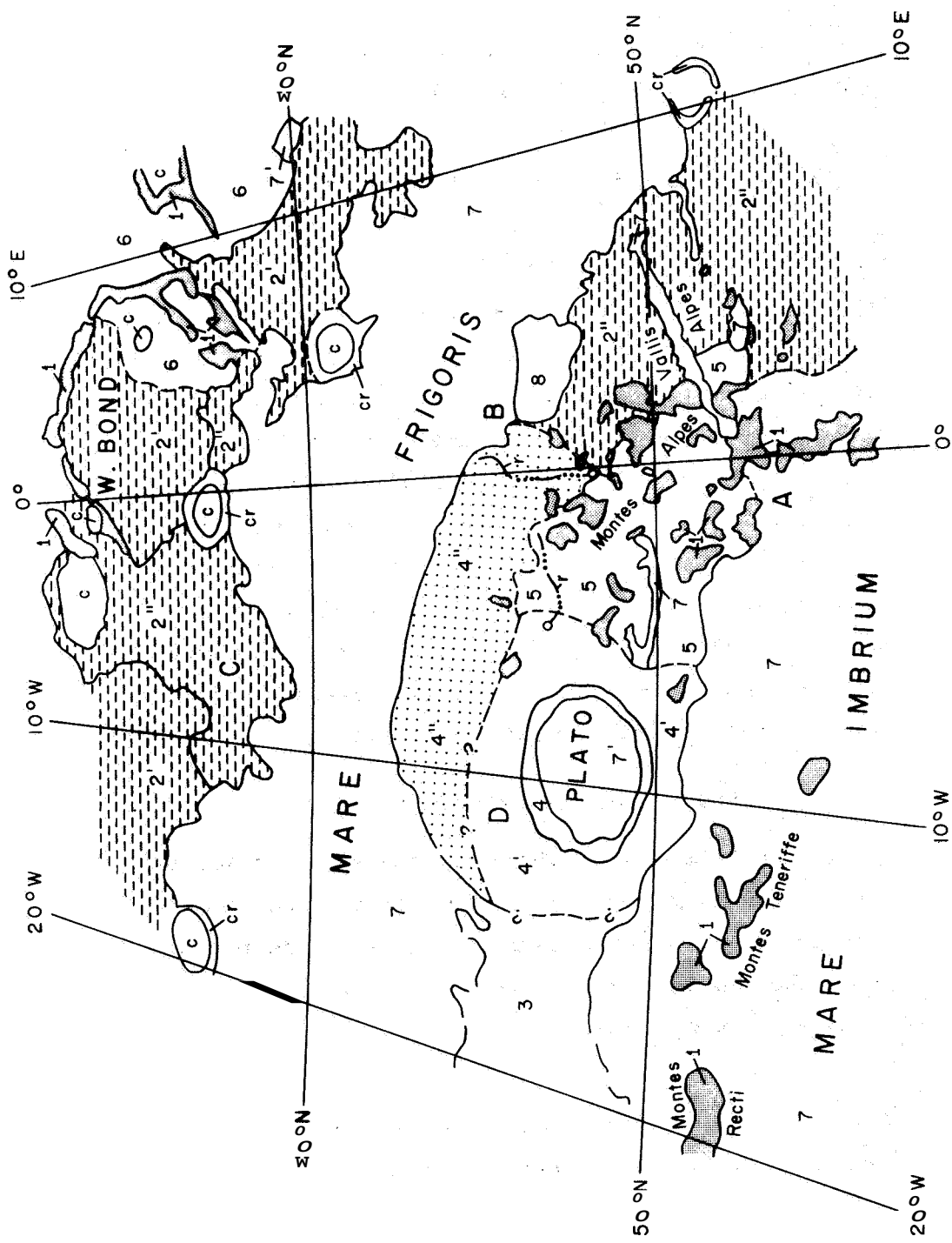
8 copies  
P 105-114  
RS  
2/10/60

DESCRIPTION OF ROCK UNITS

Many of the units mapped in the Plato quadrangle resemble units that have been mapped and given stratigraphic names elsewhere. We prefer a system of numerical designation instead of names to avoid the implication that our units are correlative with the units as mapped by others.

Unit 1

Pre-Imbrian or pre-mare Imbrian rocks, many of which are probably upfaulted blocks of old terra material, make up unit 1. They form mountainous areas with high albedo and include the Montes Alpes, Montes Teneriffe, and Montes Recti, as well as the rims of W. Bond and other polygonal depressions. Their intricate topography and steep slopes suggest bedrock exposed at the surface or mantled by a thin covering of younger materials.



SCALE 1:4,100,000 (approximate)

EXPLANATION

<p>8</p> <p>Dark mare-like material; appears to emanate from a dark-halo crater</p>	<p>4</p> <p>Well material of Plato crater</p>
<p>7'</p> <p>Mare-like material filling lows in the terra</p>	<p>Heavily eroded surface</p>
<p>7</p> <p>Mare material of Mare Imbrium and Mare Frigoris</p>	<p>2</p> <p>Hummocky terrain. 2"; strongly lineated, 2'; moderately lineated</p>
<p>6</p> <p>Ray-covered plains-forming unit of the northern uplands</p>	<p>1</p> <p>Pre-Imbrian or early Imbrian rocks, locally mantled by younger rocks</p>
<p>5</p> <p>Plains-forming unit</p>	<p>c</p> <p>Crater materials undivided</p>
<p>4"</p> <p>Pitted facies of Plato ejecta</p>	<p>cr</p> <p>Crater rim materials undivided</p>
<p>4'</p> <p>Hummocky ejecta from Plato crater</p>	<p>6'</p> <p>Sinuuous rill</p>

-----?-----  
 Contact  
 Dashed where approximately located, queried where uncertain

Figure 1 -Generalized geology of the Plato area.

### Unit 2

Unit 2 consists of hummocky terrain near the Vallis Alpes. The unit has a moderate albedo and is characterized by many low hills and ridges, generally 1 to 5 km across. Unit 2' includes possibly correlative hummocky terrain north of Mare Frigoris; it differs from Unit 2 proper in that it has many faint northeast- and northwest-trending lineations. A subdivision of Unit 2', labeled 2'' in figure 1, occurs only on the uplands north of Mare Frigoris. It is distinguished from Unit 2' by the presence of much larger hills and ridges, and of stronger northeast- and northwest-trending lineations that probably reflect structures in a buried topography.

### Unit 3

Unit 3 is a heavily cratered surface with low relief. The area is so greatly embayed by the basin fillings of Mare Frigoris and Mare Imbrium that it appears to be "awash" with mare material. The heavy cratering may be due to impacts of material ejected from Sinus Iridum and Plato.

### Unit 4

Units 4, 4', and 4'' are related to the crater Plato. Unit 4, the inner slumped wall material of Plato, has a moderately high albedo. Unit 4' is hummocky terrain that is probably ejecta from Plato; it apparently grades into Unit 4'', a pitted facies of the ejecta. Unit 4'' appears to mantle part of the hummocky Unit 2 northwest of the Vallis Alpes. The albedo of Unit 4' is fairly low, yet not as low as that of typical mare materials. The albedo of Unit 4'' is slightly higher, about the same as that of Unit 2. The formation of Plato and deposition of its ejecta were probably Imbrian events that postdated Unit 2.

### Unit 5

Unit 5 has a moderate albedo and occurs east of Plato. It is somewhat rough, although smoother than Units 2 or 4''. The

unit seemingly mantles and subdues underlying topography. It may cover parts of Unit 2 near the southwestern end of the Vallis Alpes and probably covers part of Unit 4". The unit apparently thins westward over Unit 4'. Locally, Unit 5 may lightly mantle some of the smaller blocks of the Montes Alpes, as the edges of these blocks appear rounded.

#### Unit 6

Unit 6 is a plains-forming deposit that is locally ray covered. It occurs throughout much of the northeast uplands and extends far beyond the Plato quadrangle. In the uplands the unit fills polygonal depressions; it has many of the physical attributes of Unit 5 in that it apparently mantles underlying topography. It has a moderate albedo, but it is more extensively cratered than Unit 5. The designation of only one plains-forming deposit in this region may be erroneous, but we have been unable to discern criteria for subdividing it.

#### Unit 7

This unit includes the materials that fill Mare Imbrium and Mare Frigoris. Relief is very low although there are scattered linear ridges and broad low domes in the maria. The general albedo of Unit 7 is very low, the lowest of any unit in the Plato quadrangle; minor local albedo changes possibly reflect differences in the type and age of the basin-filling materials. At Location A, next to the Montes Alpes, the mare materials have a higher albedo and are rather more heavily cratered than the mare surface directly to the west. We interpret this lighter material as an older deposit that is overlain by the younger, darker mare filling to the west. Similarly, at Location B, north of the Montes Alpes, the mare materials have a higher albedo than most of the materials elsewhere on the surface of Mare Frigoris and probably represent an older deposit. Unit 7' is marelike material that fills lows in the terrae, most conspicuously in such places as the floor of Plato and the bottom of the Vallis Alpes. This unit almost certainly is roughly correlative with the rest of the mare material.

## Unit 8

Unit 8 consists of marelike materials that appear to have emanated from various dark-halo craters in Mare Frigoris. Unit 8 appears to be younger than all adjacent parts of Unit 7. This relationship is particularly clear near Location B; there, distinct fault scarps border a northwest-trending graben in the older part of Unit 7 and are apparently buried where the graben passes through Unit 8.

### AGE RELATION OF UNIT 2

Material of the Fra Mauro Formation may be present in the Plato quadrangle. In the quadrangles in which it has been described (Eggleton, 1964, Rhipaeus Mountains quadrangle; Wilhelms, 1965, Julius Caesar and Mare Vaporum quadrangles) the formation is distributed circumferentially about the Imbrium basin. Hummocky topography near the basin becomes progressively lineated and then smoother outward from the edge of the basin. The Fra Mauro has been interpreted as a blanket of debris ejected from the Imbrium basin by an impact that formed the basin. In the Plato quadrangle the hummocky terrain (Unit 2) near the Vallis Alpes may be a depositional unit wherein many of the hummocks are either low hills or older terrain mantled by a younger deposit or clots of thick ejecta; the unit may represent the Fra Mauro Formation locally covered by the plains-forming Unit 5, and by ejecta from Plato (Units 4' and 4''). The similar hummocky terrain north of Mare Frigoris (Units 2' and 2'') may be a lineated facies of the Fra Mauro Formation. We feel, however, that there is no positive evidence within the quadrangle to confirm the hypothesis that these three units (2, 2', 2'') represent ejecta from the Imbrium basin. As explained below, we doubt that the lineations in the hummocky terrain north of Mare Frigoris resulted from the deposition of the units; we suggest that they may have been formed subsequently.

### STRUCTURE

Lineaments (shallow grooves) and probable faults in the Plato quadrangle have two major trends: northwest and northeast. These features are especially conspicuous along the edge of individual

blocks of the Montes Alpes, along the sides of the Vallis Alpes, and along the southeast side of the W. Bond depression.

In this quadrangle, structures radial to the Imbrium basin are not demonstrably the result of a major impact. Hartmann (1963) cited two features as elements of Imbrian sculpture: 1) a N. 20°-25° E. structural trend at Location C and 2) the Vallis Alpes (which trends N. 50° E.). We find, however, that very few of the bounding faults are parallel in trend to the Vallis Alpes; rather, the N. 20°-25° E. trend and other directional sets predominate in the faulted sides of the Vallis Alpes and in faults bounding it. Moreover, the N. 20°-25° E. trend does not appear to be any more prevalent or important than a N. 40°-50° W. trend of faults and lineaments throughout the quadrangle. We think that these two trends coincide with the lunar grid structure shown on maps compiled by Strom (1964). The fact that one of the trends is locally radial to Mare Imbrium seems largely coincidental. A major impact would almost certainly have reactivated preexisting structures that happened to be radial to the basin, but we have found no clear evidence of radial fractures formed by an impact.

The consistency of fault trends in the individual blocks of the Montes Alpes and the coincidence of these trends with faults and lineations throughout the quadrangle indicate fairly clearly that the blocks are not haphazardly strewn ejecta from the Imbrium basin but have resulted from regional tectonic activity. Similar reasoning suggests that the Vallis Alpes was dropped down along faults following regional patterns.

The hummocky terrain of Unit 2" is strongly lineated around Location C in a roughly rectangular area of higher elevation than adjacent territory. Similarly trending lineations are also expressed at Location D, in Unit 4' on the northwest side of Plato. If these lineations were lineated facies of the Fra Mauro Formation the lineations at Location D would subsequently have been obliterated by the ejecta from Plato. Similarly, ejecta from Plato would probably have obliterated earlier lineations parallel to the lunar grid, since the ejecta appear to have almost completely covered

)

huge blocks of the Montes Alpes at a distance of roughly one crater radius. Since the lineations are expressed in depositional materials in both Areas C and D they are tentatively interpreted as structural lineations due to regional tectonic activity subsequent to the formation of Plato.

#### GEOLOGIC HISTORY

The sequence of Imbrian and later events in the Plato quadrangle appears to have been as follows:

1. Formation of the Imbrium basin, possibly with concomitant formation of the low area now occupied by Mare Frigoris. The mountainous uplands of Unit 1 are probably pre-Imbrian surfaces. The Montes Recti and Montes Teneriffe appear to have been structurally uplifted at this time; alternatively they may be enormous blocks of ejecta from the Imbrium basin. The polygonal depressions north of Mare Frigoris were probably formed by block faulting about this same time. The heavily cratered surface of Unit 3 may represent a pre-Imbrian lowland; alternatively, it may be a facies of the Fra Mauro Formation, that was also formed at this time.
2. Deposition of the hummocky Units 2, 2' and 2". These units are marginally inundated by mare material (Unit 7) and must therefore be Imbrian or older. If they are indeed the Fra Mauro Formation, they are earliest Imbrian in age. We suggest, however, that at least some parts of the units may well represent a pre-Imbrian terra topography.
3. Uplift of the Montes Alpes. The exact time of uplift of the Alpes--whether it preceded or followed the deposition of the hummocky Unit 2--is difficult to determine. However, the Alpes do not seem to be inundated by Unit 2 and thus may have been uplifted after it was deposited.
4. Formation of Plato by impact and the deposition of ejecta (Units 4' and 4"). The formation of Sinus Iridum by impact probably preceded the formation of Plato but may have occurred

about this time. Ejecta from both Plato and Sinus Iridum caused secondary cratering of Unit 3.

5. Deposition of the plains-forming Unit 5, locally overlying Plato ejecta and hummocky terrain (Unit 2).
6. Formation of the Vallis Alpes by down-faulting. The plains-forming Unit 5 occurs on either side of the valley but apparently does not mantle its steep sharp-edged slopes. On this basis we suggest that the Vallis Alpes was formed after the deposition of Unit 5. It is almost certainly younger than Unit 2.
7. Deposition of the mare basin filling (Unit 7), which is probably made up of subunits of several different ages. Deposition of interior marelike filling (Unit 7') probably took place at about the same time.
8. Deposition of dark marelike material (Unit 8) about dark-halo craters. No direct evidence of the age of Unit 8 has been obtained yet; but since similar dark-halo crater deposits on Mare Frigoris apparently cover rays on the mare material (Unit 7), the implication is that Unit 8 may be of Copernican age.

The place of the upland plains-forming material of Unit 6 in the geologic history is not clear; it is probably younger than the hummocky terrain of Unit 2', which it appears to mantle locally.

#### REFERENCES

- Eggleton, R. E., 1964, Preliminary geology of the Rhipaeus quadrangle of the Moon and definition of the Fra Mauro Formation, in Astrogeologic Studies Ann. Prog. Rept. , Aug. 1962-July 1963, pt. A: U.S. Geol. Survey open-file report, p. 46-63.
- Hartmann, W. K. , 1963, Radial structures surrounding lunar basins, I; the Imbrium System: Arizona Univ. Lunar and Planetary Lab. Commun. , v. 2, no. 24, p. 1-16.

Strom, R. G., 1964, Tectonic map of the Moon: Arizona Univ. Lunar and Planetary Lab. Commun., v. 2, no. 39.

Wilhelms, D. E., 1965, Fra Mauro and Cayley Formations in the Mare Vaporum and Julius Caesar quadrangles, ~~in~~ Astrogeologic Studies Ann. Prog. Rept., July 1964-July 1965, pt. A: U.S. Geol. Survey open-file report, p. 13-28.

100003  
N67-31945

PRELIMINARY GEOLOGIC SUMMARY OF THE CASSINI QUADRANGLE  
OF THE MOON

By Norman J. Page

INTRODUCTION

The Cassini quadrangle, lat 32"-48" N. , long 10" E. -14° W. , contains three physiographic provinces: the northeastern sector of Mare Imbrium, the Montes Caucasus, and the southwestern part of the Montes Alpes (fig. 1). This report briefly describes the stratigraphic relations and structural features of the quadrangle, emphasizing those that differ from previously described lunar relations and features.

STRATIGRAPHY

Most stratigraphic units mapped in the Cassini quadrangle have been previously recognized and described in nearby quadrangles (Shoemaker, 1962; Hackman, 1963, 1964; Carr, 1964; and M'Gonigle and Schleicher, Plato report, this volume). The pre-Imbrian, Imbrian, Eratosthenian, and Copernican Systems occur in the quadrangle.

Fra Mauro Formation.--The hummocky facies of the Fra Mauro Formation (Ifh) occurs extensively in the eastern part of the quadrangle, between the Montes Alpes and the Montes Caucasus, and forms most of the numerous isolated hills that stand above the generally level terrain in this region. The material of the hilly areas is designated Fra Mauro because it resembles the unit as defined in the type area (Eggleton, 1964) and because of its analogous structural position with respect to the Imbrium basin.



Scale 1:7,500,000

.....

Major basin structure

—————

Graben

Dotted where inferred

—•—

Fault

-----

Lineament interpreted

as a fault

Figure 1. --Imbrium basin structure. A-A', inner ring of islands; B-B', ring representing Apennine bench structural block and its inferred continuation to the frontal scarp of Montes Alpes; C-C', frontal scarp of Montes Apenninus and continuation to Montes Caucasus. Structure largely after Hartmann and Kuiper (1962). Base modified from Lunar Earthside Hemisphere mosaic (LEM-1), USAF-ACIG.

Eggleton and several others regard the Fra Mauro as a blanket of impact ejecta from the Imbrium basin, but the present topography may be largely the product of structural deformation contemporaneous with or later than the formation of the basin. Material covering the eastern slopes of the Montes Alpes around Mont Blanc has been tentatively assigned to the smooth facies of the Fra Mauro Formation (**Ifs?**) since it does not form the low hills that characterize the hummocky facies. This material is probably part of the regional blanket around Mare Imbrium, but its surface texture has been smoothed by downslope postdepositional movement. The smooth Fra Mauro mapped here is therefore not exactly analogous to the smooth Fra Mauro of the type area, which has a smooth texture even on level terrain. In the type area the smooth texture is probably a depositional feature, whereas in the Montes Alpes the smoothness apparently results from postdepositional movement. Downslope movement of the Fra Mauro in the Montes Alpes may have resulted in thinning of the unit to such an extent that pre-Imbrian material crops out locally on steep slopes.

Apennine Bench Formation.--In the Montes Alpes and Montes Caucasus, material with a smooth (locally rolling) surface fills low areas between hills of Fra Mauro and has been assigned to the Apennine Bench Formation because of its appearance and stratigraphic relation to the type occurrence of that formation (Hackman, 1964). The Apennine Bench Formation embays the Fra Mauro in the Cassini quadrangle as well as in the type area, and is therefore younger.

#### **SPECIAL FEATURES**

Cassini crater rim material. --Materials that may consist of stratified volcanics derived from local fissures resulting from the impact that formed the Imbrian crater Cassini occupy a crude semicircular band north, east, and south of the crater. Their albedo is moderate to low; their surface, smooth and rolling.

Alternatively, these materials could represent moderately sorted ejecta from the crater.

Irregular crater.--An unusually large (10 km greatest dimension) irregularly shaped crater occurs north of the crater Aristillus and directly west of Piton. Elongate northwest-southeast, it could be a large secondary crater but is more likely volcanic.

Dark materials.--Dark, very young material, younger than Copernican slope material, occurs in three localities in the Cassini quadrangle. The albedo is lower than that of the mare material. In the Copernican crater Aristillus the dark material has no visible topographic relief of its own. It covers an elongate area extending east-west from crater floor up over the Copernican slope materials on the crater walls and across the rim to the edge of the crater rim material. The relation with ray material is unclear at that locality. Similar dark material occurs on the pre-Imbrian "island" Piton, from the highest point down onto the mare. There, the material appears to be younger than ray material. An egg-shaped spot of dark material occurs on the mare-covered floor of the Imbrian crater Cassini. This material is also superposed on ray material. The dark materials in all three places are interpreted as a thin covering of young volcanics.

#### STRUCTURE

Mare ridges, linear scarps and depressions (lineaments), and faults make up the structural pattern in the Cassini quadrangle. Most mare ridges trend northwest-southeast, but a northeast-southwest trending element is also present. On the terra, two sets of lineaments and faults are present: elements of one set strike N. 25"-60" E. and elements of the other strike N. 25"-45" W.

The continuity of broad ringlike concentric structures in and surrounding the Imbrium basin is interrupted by a trough between the Montes Alpes and Montes Caucasus (fig. 1). This low area is 125-150 km wide, and trends about N. 30° E. Narrow grabenlike structures (rilles), faults, and lineaments occur within it, and generally parallel the trend of the trough. These structural features provide evidence of the manner in which the major structures to the north and south of the trough are related. The principal hypotheses are: (1) The Montes Alpes are part of the same structural ring as the Montes Apenninus and Caucasus; (2) the Montes Alpes are a continuation of the rugged terrain next to Archimedes on the Apennine bench (suggested by Hartmann and Kuiper, 1962). The crests of the Caucasus and Alpes are not aligned; the first hypothesis therefore implies a large lateral displacement of the mountain rings along a transcurrent fault (Fielder, 1965, p. 107). However, the displacement on most of the faults in the trough appears to have been vertical, and there is little evidence of strike-slip displacement. The largest visible strike-slip displacement on a northeast-southwest trending fault is about 3-4 km, far less than required for strike-slip separation of the ridge crests of the two mountain ranges. Therefore, of the two hypotheses, the second is considered to be in best accord with the evidence.

#### REFERENCES

- Carr, M. H. , 1964, The geology of the Timocharis quadrangle, in Astrogeologic Studies Ann. Prog. Rept. , Aug. 1962-July 1963, pt. A: U.S. Geol. Survey open-file report, p. 9-23.
- Eggleton, R. E., 1964, Preliminary geology of the Rhipaeus quadrangle of the Moon and definition of the Fra Mauro Formation, in Astrogeologic Studies Ann. Prog. Rept., Aug. 1962-July 1963, pt. A: U. S. Geol. Survey open-file report , p. 46-63.

- Fielder, Gilbert, 1965, Lunar geology: London, Lutterworth Press, 184 p.
- Hackman, R. J., 1963, Stratigraphy and structure of the Apennine region of the Moon, in Astrogeologic Studies Ann. Prog. Rept., Aug. 1961-Aug. 1962, pt. A: U.S. Geol. Survey open-file report, p. 2-10.
- \_\_\_\_\_ 1964, Stratigraphy and structure of the Montes Apenninus quadrangle of the Moon, in Astrogeologic Studies Ann. Prog. Rept., Aug. 1962-July 1963, pt. A: U.S. Geol. Survey open-file report, p. 1-8.
- Hartmann, W. K., and Kuiper, G. P., 1962, Concentric structures surrounding lunar basins: Arizona Univ. Lunar and Planetary Lab. Commun., v: 1, no. 12-13, p. 51-66.
- Shoemaker, E. M., 1962, Interpretation of lunar craters, in Kopal, Zdenek, ed., Physics and astronomy of the Moon: London, Academic Press, p. 283-359.

N67-31946

Issue 3

3 PROBABLE IGNEOUS RELATIONS IN THE  
FLOOR OF THE CRATER J. HERSCHEL

By G. E. Ulrich<sup>0</sup>

8 2009 P 230 132  
RS 5100

INTRODUCTION

An area of very low albedo containing three craters, a steep dome, and a Y-shaped rille occurs along the eastern boundary of the crater J. Herschel (lat 62° N., long 42" W.) The area is irregular in outline, approximately 20 km east-west and 50 km north-south (fig. 1). It is of interest because structural relations and resemblance to terrestrial volcanic landforms suggest that several features in it are volcanic. These features were studied during mapping of the J. Herschel quadrangle at a scale of 1:1,000,000. Lick-Herbig photographs ECD-66 and ECD-77, Pic du Midi 43-inch reflector photograph 55, and visual observations with the U.S. Geological Survey 30-inch reflector, Flagstaff, Ariz., provided most of the information presented here.

MORPHOLOGY OF FEATURES

Figure 2 shows the area of interest within the crater J. Herschel. The three dark-halo craters are very low rimmed depressions with rounded inner edges. They lie within a smooth dark blanketing deposit and range in diameter from 3 to 5 km. The southern pair of craters occur within terrain that is gently convex upward. The blanketing deposit, which is formed by the coalescing dark halos of the three craters, appears to subdue the walls of the associated craters and rille; its contact with adjacent higher albedo units is gradational.

The Y-shaped rille trends northward from the southeast crater for a distance of about 20 km and branches into two forks at about

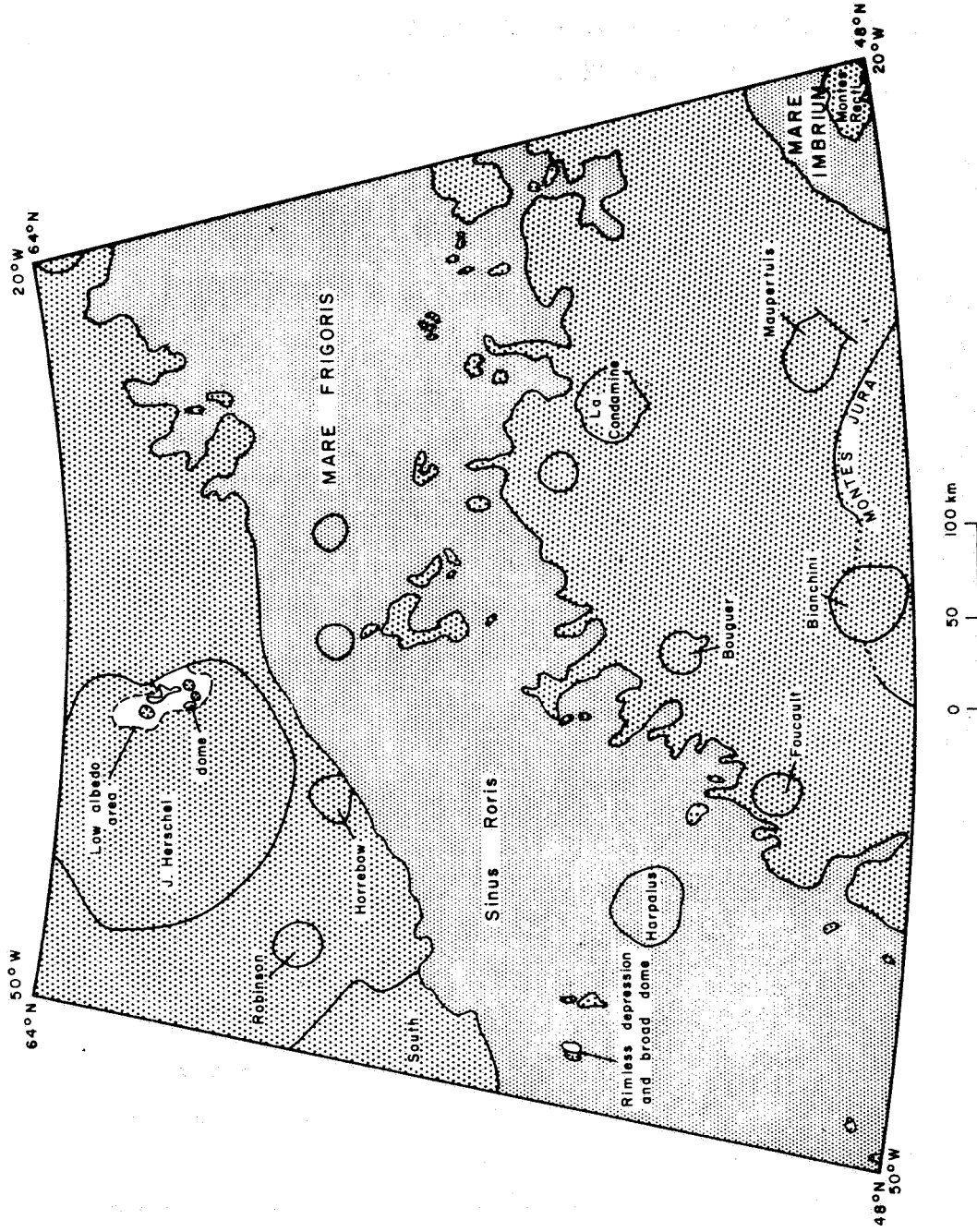


Figure 1 --J Herschel quadrangle. Heavy stipple indicates terra and light stipple indicates mare. No pattern in area of interest.

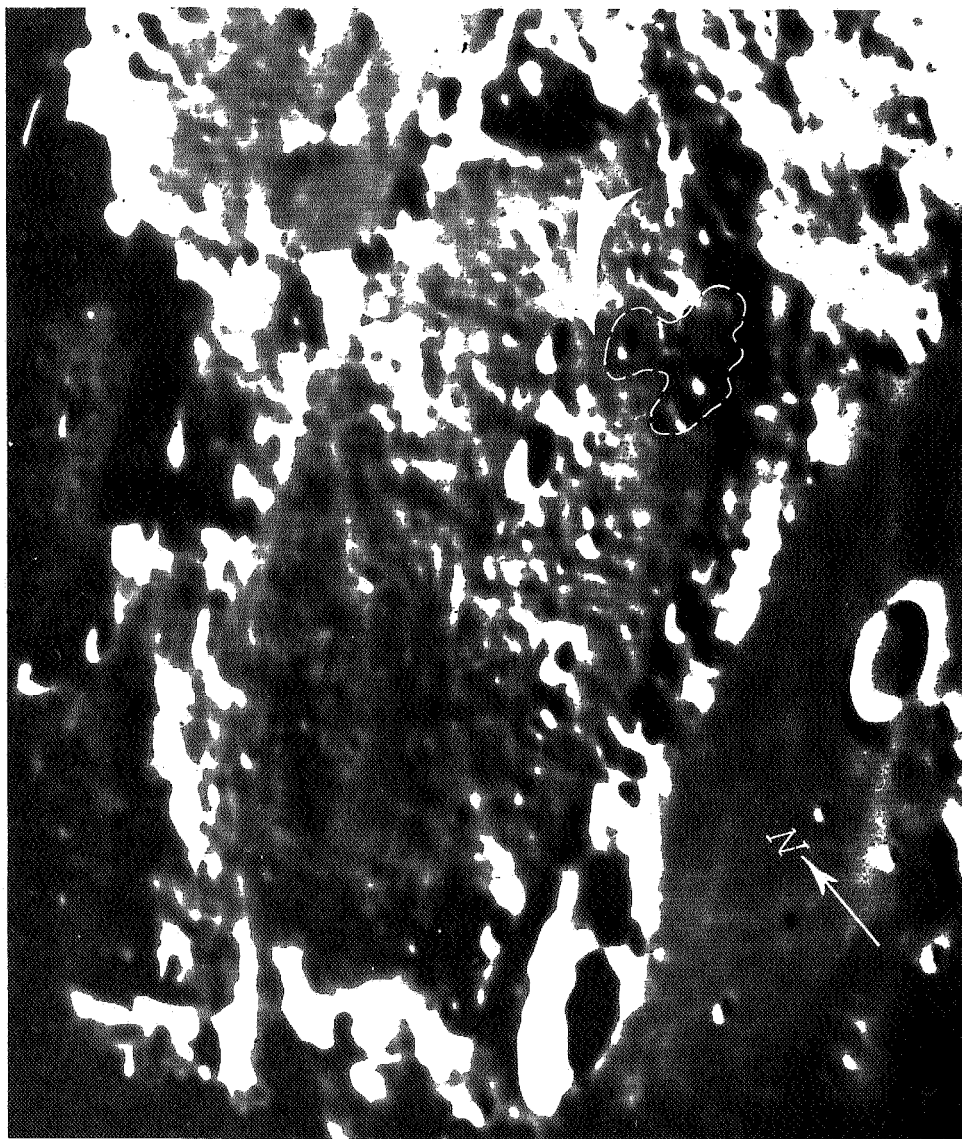


Figure 2 -- Crater J. Herschel, showing probable volcanic complex near east edge of crater floor. (Un-  
rectified; photo by C. H. Herbig at Lick Observatory.)

half this distance. From the best resolution available (about 1 km), it is not certain whether the rille intersects the crater wall. The rille may terminate or become subdued beyond recognition 1 or 2 km from the crater's edge. The rille is entirely within the low-albedo area, but the area between the branches of the "Y" has a higher albedo.

The dome adjacent to the southwestern crater is about 4 km in diameter and over 1 km in height. It is convex upward over most of its slope, although its base is probably concave. The occurrence of this relatively steep-sided hill within the low-albedo area and its proximity to a dark-halo crater suggest a possible genetic relationship. A similar association of steep hill and adjoining depression occurs in Sinus Roris on the west edge of the J. Herschel quadrangle, although the depression there lacks a dark halo.

#### GEOLOGIC INTERPRETATION

The features described above are similar to other lunar features interpreted as volcanic, as well as to known terrestrial volcanic features.

A dark blanketing unit in the form of a halo surrounding rimless depressions or low-rimmed craters has been interpreted as dark volcanic ejecta around Langrenus C (Wilhelms and others, 1965) and in the crater Alphonsus (Masursky, 1964, p. 130; Kuiper and others, 1966, p. 134; Carr, 1966, p. 275; McCauley, 1966, p. 317). The dark-halo craters on the floor of Alphonsus (fig. 3) average about 2 km in diameter and have dark rims approximately 6 km across. The dark rim material seems to partially fill rilles adjoining the dark-halo craters. The craters and rilles are clearly related genetically.

The rimless depressions and low-rimmed craters on the Moon may have terrestrial counterparts in small collapse calderas such as those found in the Pinacate volcanic field of northwestern Sonora, Mexico. Figure 4 is an oblique aerial view of Elegante Crater, which is 1.6 km in diameter and 240 meters deep, and has

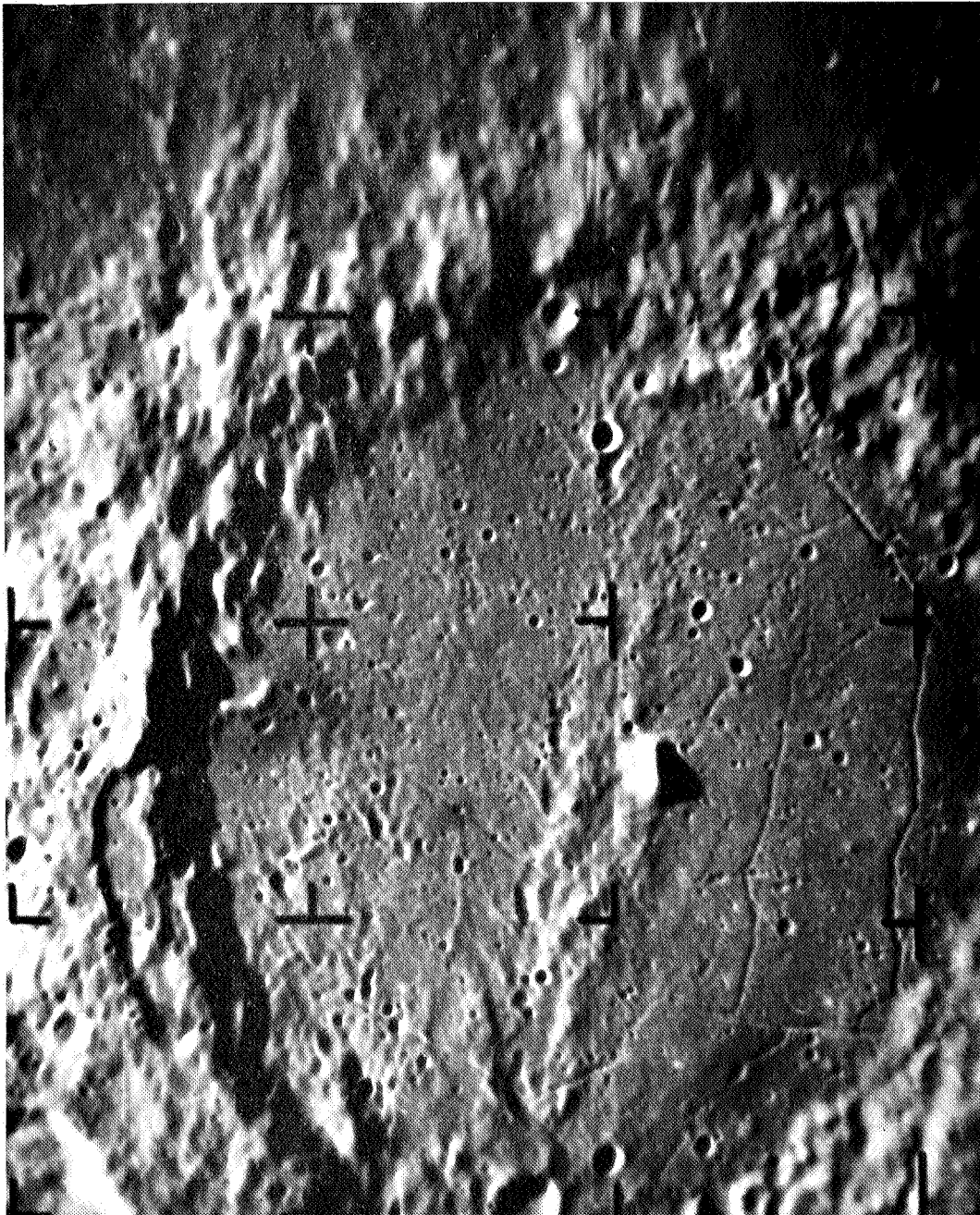


**Figure 3.--Crater Alphonsus, showing dark-halo craters. Craters in east (right) are associated with rilles. (Ranger IX frame A44, Jet Propulsion Lab., 1966.)**



.Figure 4. --Elegante Crater, Pinacate volcanic field, Sonora, Mexico,  
Note **low** slopes of tuff rim overlying sequence of basalt flows  
exposed in steep wall **and small** amount of rim material compared  
to size of crater. Prominence on far rim is part of a cinder  
cone cleaved by the collapse and partly covered by tuff rim.

a narrow rim of stratified tuff-breccia averaging 45 meters in thickness (Jahns, 1959, p. 170-171). The narrow tuff rims and the steep inner walls of the Pinacate craters indicate that the volume of pyroclastic material ejected was small compared with the size of the craters. The lack of dark-halo material around some low-rimmed craters in areas such as western Sinus Roris may be due to ejection of similarly small volumes of pyroclastic material. Alternatively, these and similar lunar craters may be more closely analogous to another type of terrestrial crater which is rimless and volcanic in origin, the pit craters on broad basaltic domes (Wentworth and MacDonald, 1954, p. 17-21). These craters are as much as 1.1 km in diameter near the summit of Mauna Loa and have vertical walls. They are formed entirely by collapse due to withdrawal of underlying magma, and no pyroclastic phase is present.

Conversely, a proportional increase in pyroclastic ejecta might produce dark-halo craters such as those in the craters J. Herschel and Alphonsus, where extensive aprons of low-albedo material, blanketing effect on surrounding topography, and rounded inner edges of the craters may indicate that the volume of pyroclastic material is large compared with crater-floor subsidence. The common terrestrial cinder cone with its small summit crater is largely pyroclastic and constructional in nature, and collapse is negligible or absent; in the Pinacate craters, both pyroclastic eruption and collapse have occurred, with collapse predominating. The low smooth-rimmed dark-halo craters in J. Herschel and Alphonsus are perhaps intermediate between the cinder cone and Pinacate-type crater.

The dome in J. Herschel could be a large cinder cone; it seems to be truncated by the adjoining crater as is the smaller cone next to Elegante Crater (fig. 4). Alternatively, the J. Herschel dome could be of intrusive origin or it could be nonigneous. The hill adjacent to the depression in western Sinus Roris can be interpreted either as an "island" of terra material or as a volcanic dome.

Rittman has classified volcanic structures on the basis of increasing viscosity and quantity of magma produced (1962, p. 114). The quantity of pyroclastic material around the J. Herschel craters, the form of the craters, and the association with a dome suggest that the volcanism is of the intermediate, viscous type in Rittman's classification.

A final argument for volcanic processes within the low-albedo area of J. Herschel stems from the location of the presumed volcanic features. They are all near the edge of the main crater floor (figs. 1, 2) and closely associated with a rille. Figure 3 shows a similar relation, in Alphonsus, of rilles and dark-halo craters at the east edge of the crater floor. The rilles are roughly marginal and concentric to the crater wall, suggesting structural control related, secondarily at least, to the formation of the crater floor. It follows that the locations of the craters are also structurally controlled, and their formation must result from processes related to subsurface lunar structure. The rilles may be the surface expression of fractures that served as conduits along which magma moved to the surface, erupting finally as pyroclastic material.

The fact that J. Herschel is near the Moon's limb and has a complexly covered floor prevents a detailed telescopic resolution of marginal fracture systems, especially near the low-albedo area. Refined mapping of the structural relations of this region will have to await observation from future Lunar Orbiters.

#### CONCLUSIONS

The combination of (1) low-rimmed craters with rounded rim crests and dark, coalescing halos which blanket surrounding topography, (2) a rille trending away from one of the craters, and (3) a steep-sided dome near the edge of the floor of crater J. Herschel is similar to that found on the floor of Alphonsus and in terrestrial volcanic fields. The dark-halo craters are analogous to some terrestrial craters which fit into a gradational series of volcanic

depressions and form an intermediate class between cratered cinder cones and rimless collapse craters. The rille probably reflects structural control of at least one of the dark-halo craters marginal to the floor of J. Herschel. The dome adjacent to another of the craters is interpreted as a blanketed cinder cone or a steep-sided intrusive body. Thus the volcanic, and possibly intrusive, features are believed to be related to each other and to structural features near the edge of the crater floor.

#### REFERENCES CITED

- Carr, M. H. , 1966, The structure and texture of the floor of Alphonsus, in Ranger VIII and IX, pt. 2, Experimenters' analyses and interpretations: Jet Propulsion Lab. Tech. Rept. 32-800, Pasadena, p. 270-284.
- Jahns, R. H. , 1959, Collapse depressions of the Pinacate volcanic field, Sonora, Mexico, in Arizona Geol. Soc. Guidebook 11: Arizona Geol. Soc. Digest, 2d Ann. , p. 165-184.
- Jet Propulsion Laboratory, California Institute of Technology, 1966, Ranger IX photographs of the Moon, cameras "A," "B," and "P": Natl. Aeronautics and Space Adm. Spec. Rept. 112.
- Kuiper, G. P. , Strom, R. G. , and LePoole, R. S. , 1966, Interpretation of Ranger records, in Ranger VIII and IX, pt. 2, Experimenters' analyses and interpretations: Jet Propulsion Lab. Tech. Rept. 32-800, Pasadena, p. 35-248.
- Masursky, Harold, 1964, A preliminary report on the role of isostatic rebound in the geologic development of the lunar crater Ptolemaeus, in Astrogeologic Studies Ann. Prog. Rept. , July 1963-July 1964, pt. A: U.S. Geol. Survey open-file report, p. 102-134.
- McCauley, J. F., 1966, Intermediate-scale geologic map of a part of the floor of Alphonsus, in Ranger VIII and IX, pt. 2, Experimenters' analyses and interpretations: Jet Propulsion Lab Tech. Rept. 32-800, Pasadena, p. 313-319.

- Wilhelms, D. E. , Masursky, Harold, Binder, A. B. , and Ryan, J. D. ,  
1965, Preliminary geologic mapping of the easternmost part  
of the lunar equatorial belt, in Astrogeologic Studies Ann.  
Prog. Rept. , July 1964-July 1965, pt. A: U.S. Geol. Survey  
open-file report, p. 45-53.
- Rittman, A., 1962, Volcanoes and their activity: New York, Inter-  
science Publishers, 305 p.
- Wentworth, C. K. , and MacDonald, G. A., 1953, Structures and forms  
of basaltic rocks in Hawaii: U.S. Geol. Survey Bulletin 994,  
98 p. [1954].

N67-31947

3 STRUCTURE OF THE TRIESNECKER-HIPPARCHUS REGION

By T. W. Offield

Basin P 133 153

INTRODUCTION

More than 800 linear structures, including straight segments of curved lineaments, have been identified and measured in the Triesnecker-Hipparchus region (figs. 1-3) near the center of the earthside hemisphere of the Moon. The most common features are straight valleys between nearly linear ridges and the bases of straight escarpments. Other lineaments include rilles, chain craters, mare ridges, and polygonal crater rims. This paper describes the structural pattern observed and defines and interprets probable relationships of the local lineaments to distant mare basins, to a suggested lunar grid, and to other regional structures,

Measured lineaments range in length from about 5 to 250 km. They have been arbitrarily classified on the basis of length as an index of their importance. First-order lineaments are more than 50 km long, second-order lineaments are 25 to 50 km long, and third-order lineaments are less than 25 km long. Some aligned features of second- and third-order lengths have been judged to make up a somewhat discontinuous first-order lineament and were treated as such for purposes of analysis.

The lineaments were identified on earth-based photographs and by telescopic observation. Many photographs were studied, but the most useful were Lick Observatory ECD 63 and 85, Lick Moore-Chappell of October 26, 1937, and an unpublished photograph by Catalina Station (Lunar and Planetary Lab., Univ. Ariz.). Structures were plotted on 1:500,000 shaded-relief maps of the Triesnecker (AIC 59C) and Hipparchus (AIC 77B) quadrangles prepared by USAF ACIC.

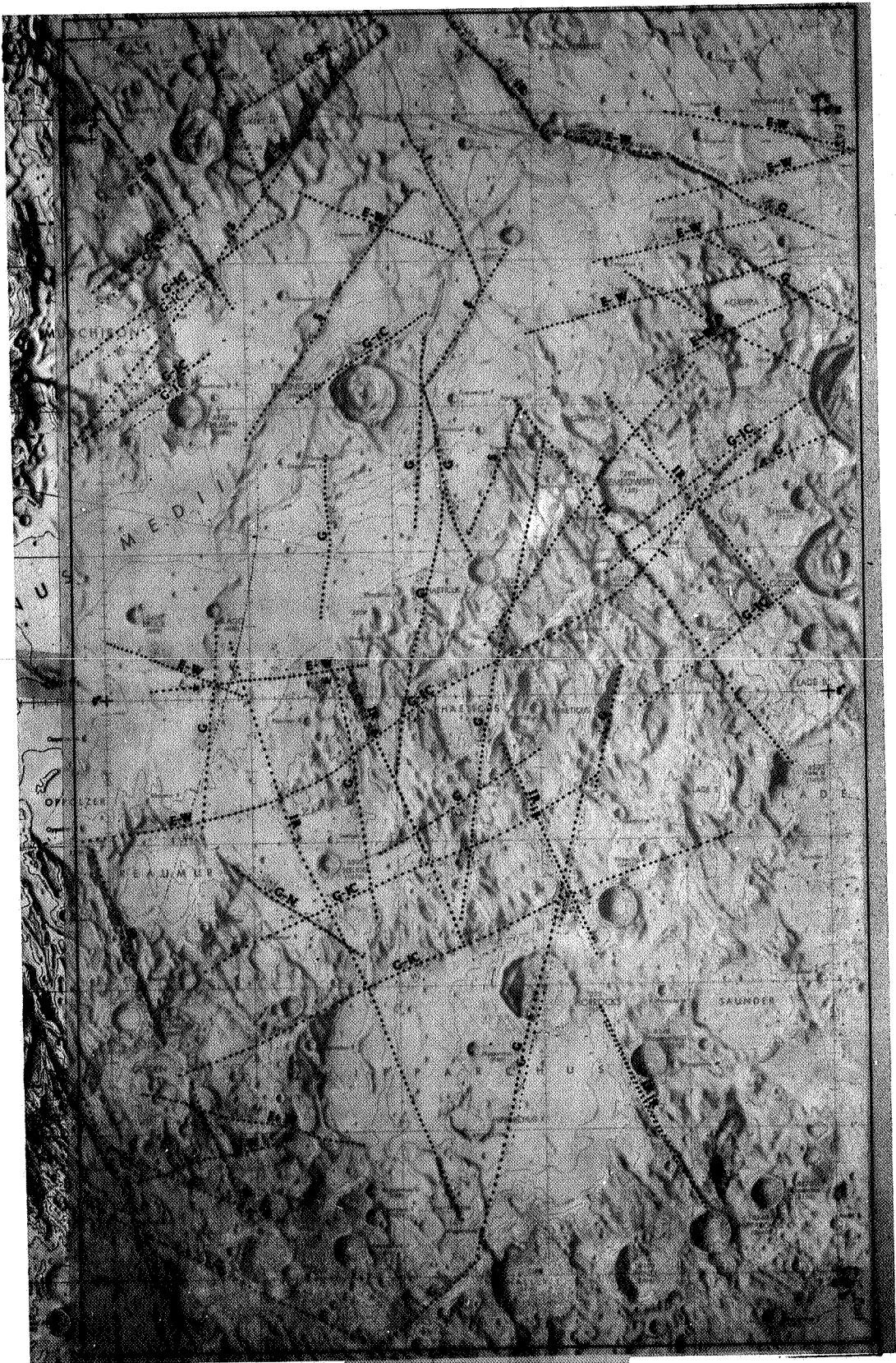


Figure 1.--First-order lineaments of the Triesnecker-Hipparchus region. G: N, NE, and NW elements of possible lunar grid; IR: Imbrian radials; IC: Imbrian concentric structures; S: Serenitatis radials; N: possible Nectaris radial; E-W: system spanning N. 65"-90" E. and N. 65"-90" W. ; ? : lineaments not part of previously reported systems; ambiguities are indicated by more than one designation. Base charts are LAC 59 (north of 0" lat) and 77 (south of 0° lat).

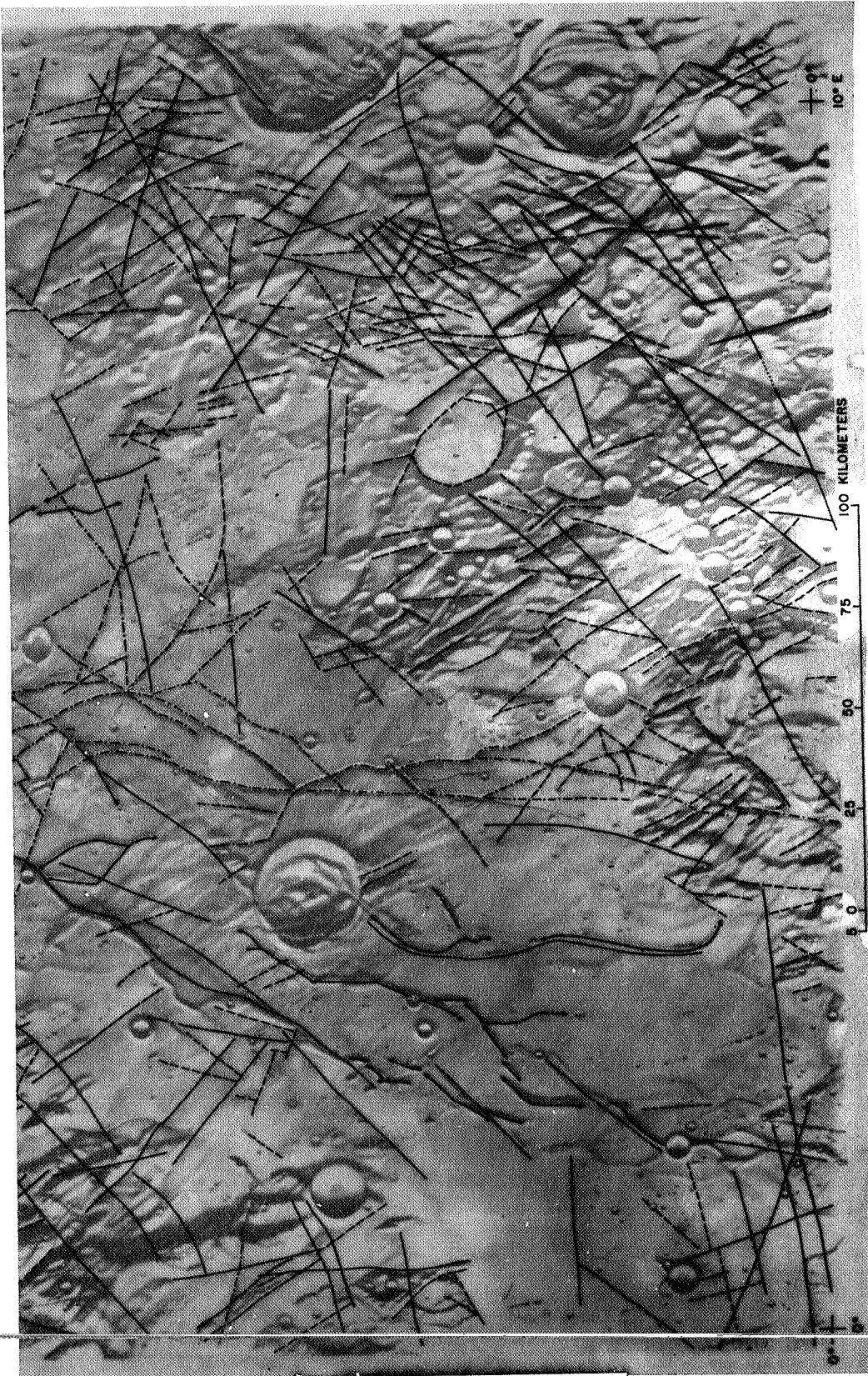


Figure 2.--Lineaments of the Triesnecker quadrangle (AIC 59C). Symbols: Rille, dash-dot line; second-order lineament, solid line (includes lines longer than 50 km, but which are irregular enough to have been measured in shorter segments); third-order lineament, dashed line; ridge, solid line with arrow showing tapering end.

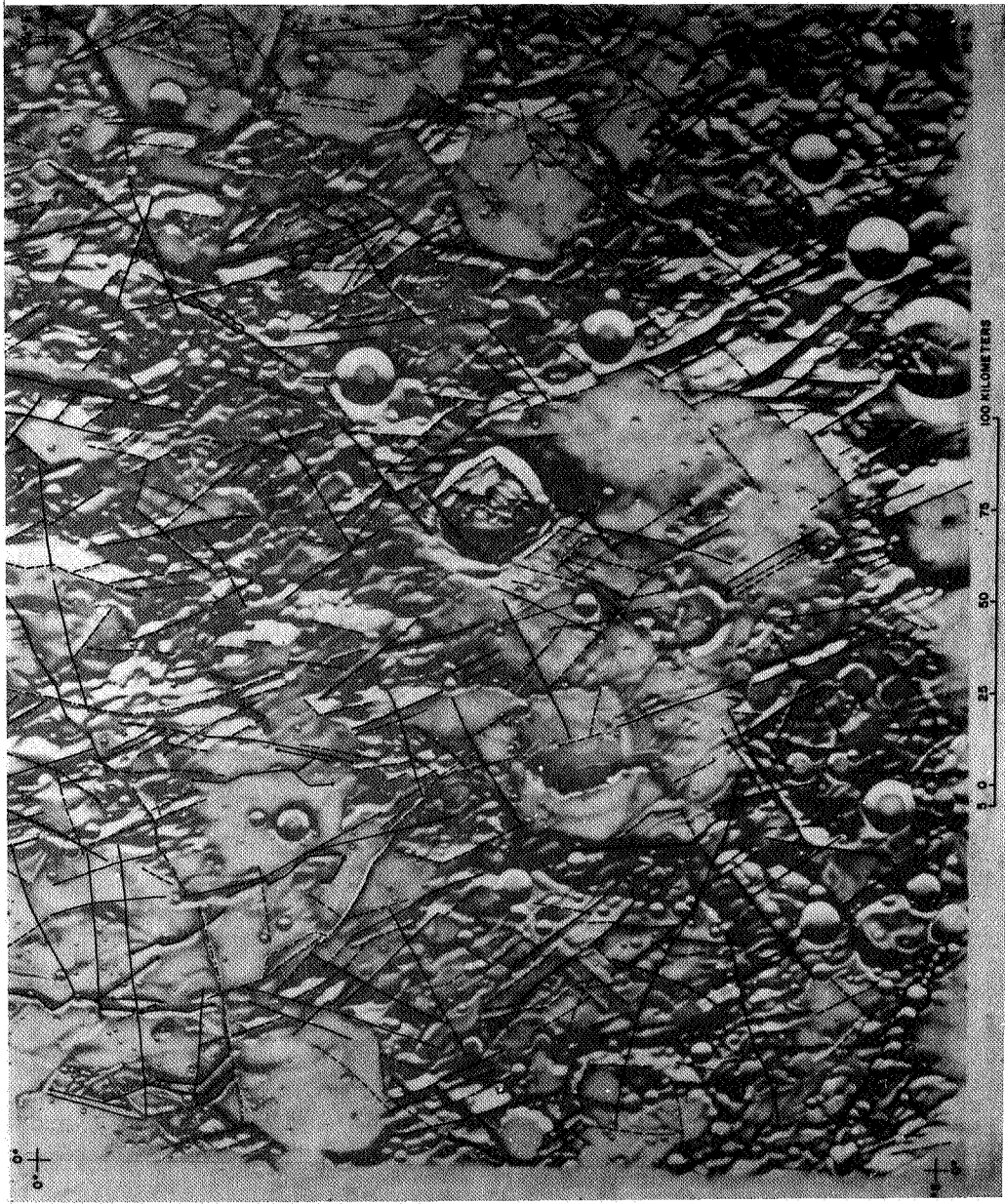


Figure 3.--Lineaments of the Xipharcus quadrangle (AIC 77B). Symbols: Rills, dash-dot line; shorter lineament, solid line (includes lines longer than 50 km, but which are irregular enough to have their measurement in shorter segments); third-order lineament, dash-dot line; rills, solid line with arrow showing tapered ends; chain crater, .

## REGIONAL SETTING

The broad structural pattern in the Triesnecker-Hipparchus region probably is a product of the event which formed the Mare Imbrium basin (Wilhelms, 1964). Sinus Medii and the Hipparchus-Saunders-Lade belt of low terrain are believed to be parts of essentially synclinal arcuate troughs concentric with the Imbrium basin. The intervening uplands and those northwest of Sinus Medii are interpreted to be anticlinal belts belonging to the circum-Imbrium pattern. Lineaments radial to the Imbrium basin are prominent in the region.

In nearby areas, an older pattern of broad highs and lows probably concentric to Mare Serenitatis was noted by Baldwin (1963, p. 320) and Wilhelms (1964, p. 12). Such concentric features have not been specifically identified in the present study, but several large lineaments radial to Serenitatis have been recognized. Other structures possibly related to the Tranquillitatis and Nectaris basins add further complexity to the regional pattern.

## DISTRIBUTION OF LINEAMENTS

The chief problem in interpreting plots of lineaments is separating those belonging to the radial and concentric systems of the mare basins from those belonging to a lunar grid of structures unrelated to basins.

Strom (1964) presented an excellent survey of lunar structure based on his plotting of about 10,000 lineaments within 60° of the center of the earthside hemisphere. For comparison with the present study, Strom's results are shown in part in figure 4; in orthographic projection, the main peaks are at N. 15°-25° E., N. 45°-65° E., N. 5°-15° W., N. 25° W., and N. 45°-65° W. Small concentrations are centered at N. 75° E. and N. 75° W. Strom ascribed the pronounced N. 25° W. peak south of the equator to lineaments radial to the Imbrium basin, but this explanation would apply to no more than half of his sample area and would not hold at all for the peak at the

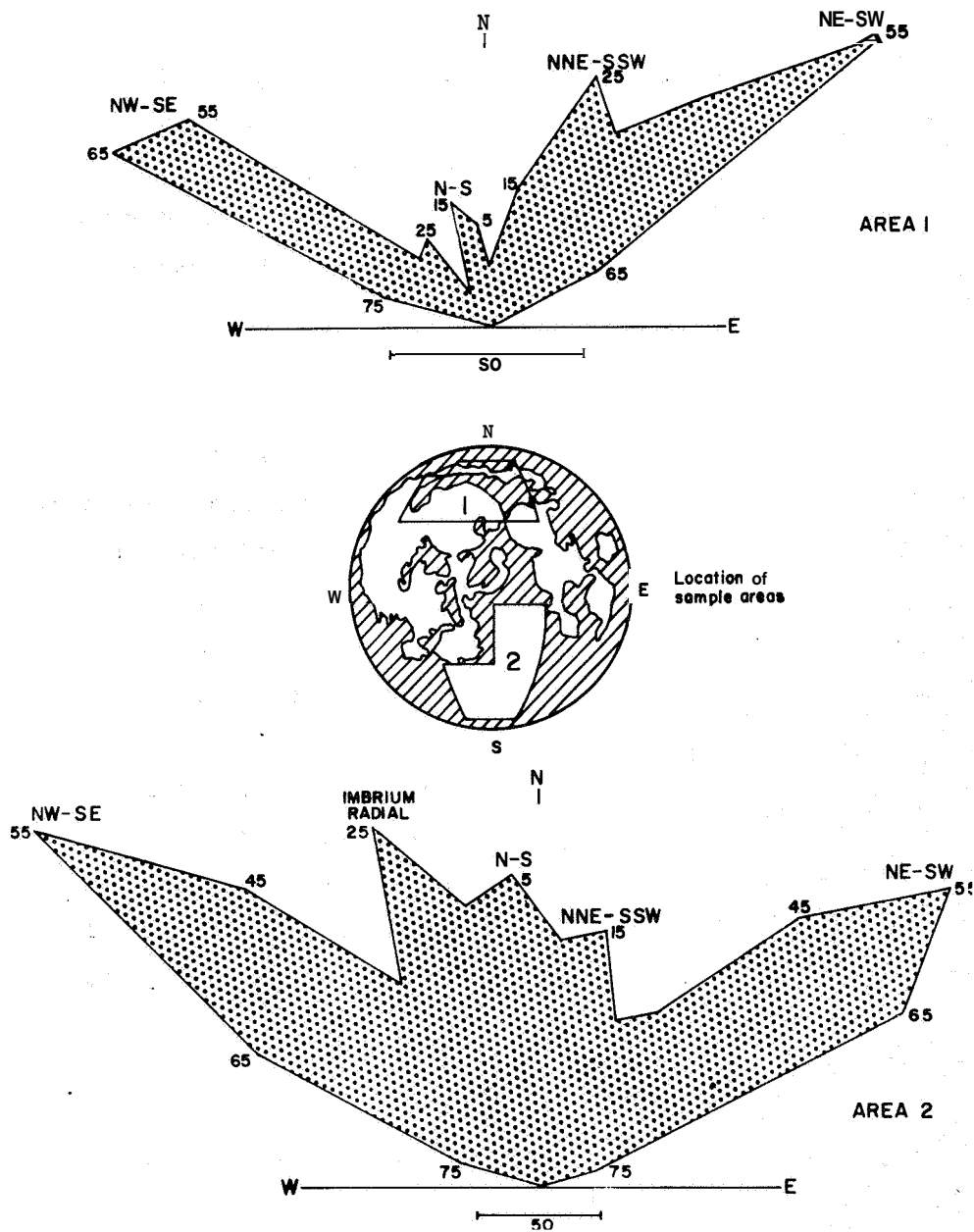


Figure 4. --Azimuth frequency of lineaments (orthographic projection) in two large sample areas (after Strom, 1964, figs. 1, 2).

same azimuth in his northern sample. He considered that the other concentrations of lineaments are not radial to basins and make up a pervasive lunar tectonic grid. Fielder (1963) also made an extensive lineament study, independently of Strom.

Measurements were made on a rectified base in the present study, so in comparing the data with figure 4, Strom's apparent azimuth angles should be decreased slightly; those near north are approximately correct, but distortion in azimuth angles between 45° and 75° from north probably averages 5° to 10° in the sample areas.

For the Triesnecker-Hipparchus region, figures 5 and 6 show the azimuth frequency of linear segments of rilles, mare ridges, and crater rims, and of structural lines considered here to be faults. First-, second-, and third-order lineaments are distinguished.

Mare ridges, linear crater rims, and some rilles and probable faults constitute third-order lineaments. The ridge, rille, and rim trends are well dispersed (fig. 6), but fault trends are distinctly concentrated, and it is these which may be compared with the peaks in Strom's diagram.

The pattern of third-order faults (fig. 6) is grossly similar to that of the longer faults (fig. 5). However, since many of the third-order structures may be lines of adjustment resulting from movement on first- and second-order lineaments, the pattern of the longer faults is considered to be more significant in analyzing lineament distribution.

#### Basin-Radial Structures

Figure 5, showing lineaments 25 km and longer, has a large northeast double peak, two smaller peaks slightly east and west of north, and a strong northwest peak in azimuth frequency. To interpret this diagram several ambiguities must be considered. For example, many lineaments in the Triesnecker-Hipparchus region appear to be geometrically radial or concentric to the Imbrium, Serenitatis, Tranquillitatis, and possibly Nectaris basins. Although the geometric

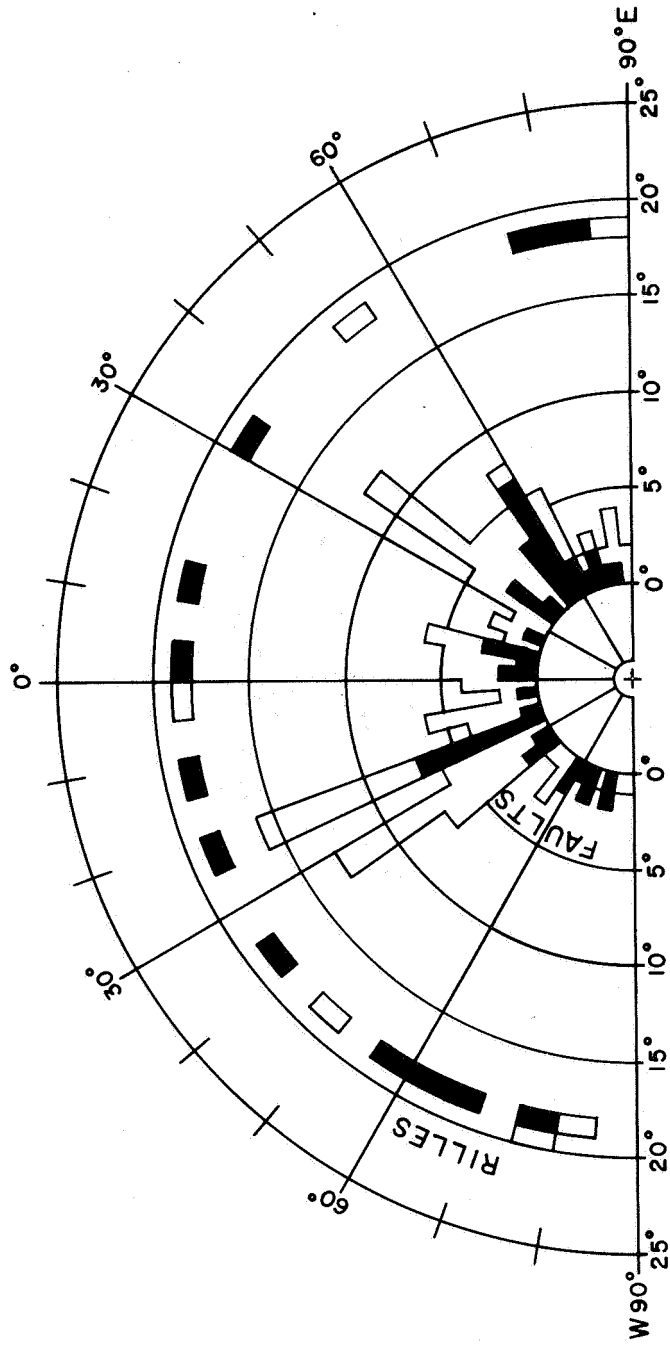
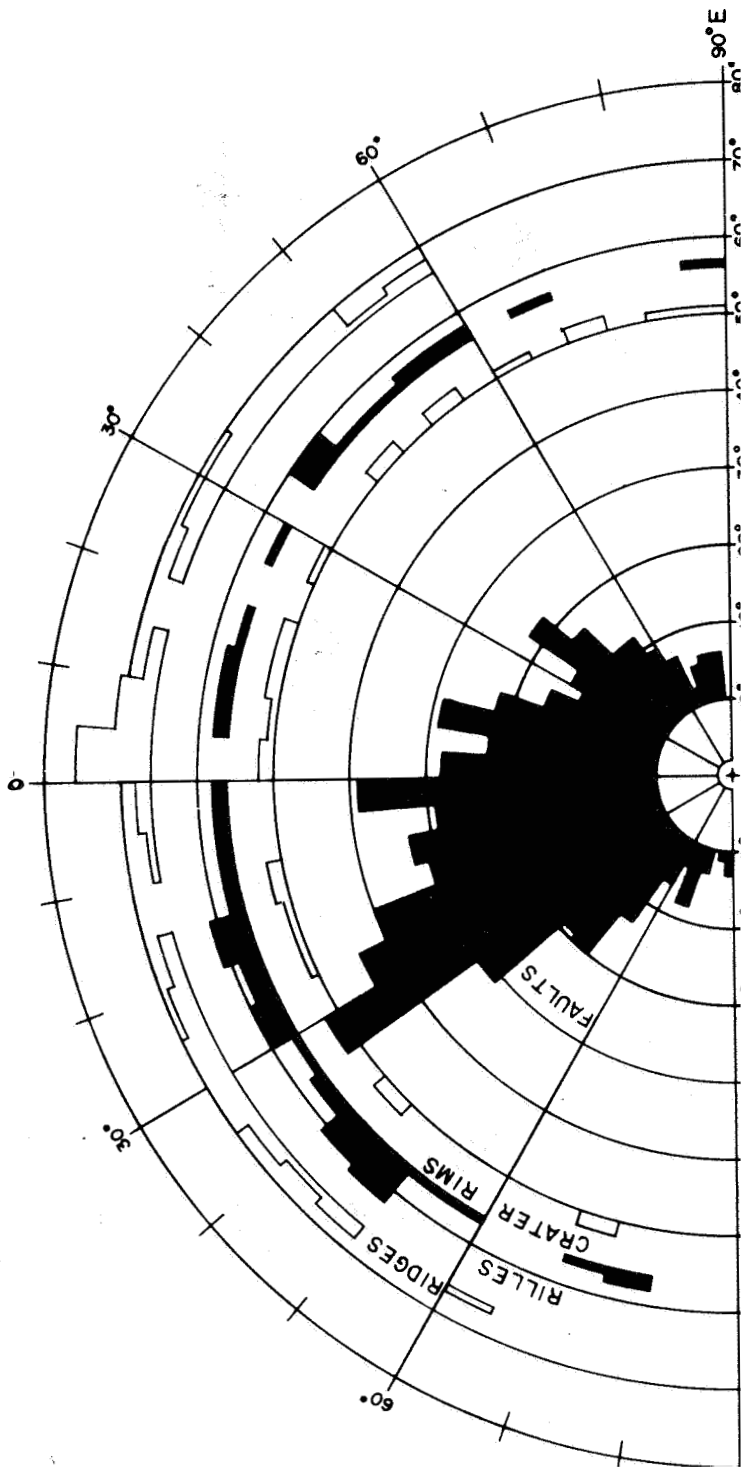


Figure 5. --Azimuth frequency of first-order (black) and second-order lineaments.



3

Figure 6. --Azimuth frequency of third-order lineaments.

relationship is not sufficiently marked to prove that the lineaments are genetically related to the basins, the possibility that they are must be considered in any attempt to identify a lunar grid of structures unrelated to basins.

In the region studied, the most prominent apparently radial structures are those which converge on the Imbrium basin. These radial lineaments fan across the region, changing in trend from N. 20° W. in the southwest corner of the region to N. 44° W. in the northeast corner. Figure 5 shows a strong peak in the N. 20°-40° W. sector. However, the azimuths of many of the lineaments in the sector do not match that of the part of the radial fan in which they occur, so only 21 of the 45 faults and rilles in the N. 20°-45° W. sector are clearly radial to Imbrium. Similarly, possible Serenitatis radials would be found in the N. 23°-42° E. sector. In figure 5, this sector is part of a double peak, but only 10 of the 29 lineaments of that sector can be considered clearly radial to Serenitatis.

Possible Nectaris radials would be found in the N. 40°-60° W. sector. Strom (1964, map 2) identified lineaments in the floor of Hipparchus as Nectaris radials, but this identification seems doubtful as the lineaments are 10°-20° off true radial azimuths.

Structures radial to Tranquillitatis would occur in the N. 55°-90° E. sector. The walls of the Hipparchus-Lade trough and rather nebulous large lineaments near Ukert and Chladni have the right azimuths to be Tranquillitatis radials.

#### Basin-Concentric Structures

Lineaments concentric to Imbrium would vary in trend across the area from N. 46° E. to N. 70° E. In that sector, 15 to 29 first- and second-order lineaments are approximately normal to Imbrian radials. These include the walls of the Hipparchus-Lade trough, noted above as also being geometrically radial to Tranquillitatis. This ambiguity of Imbrian concentrics and Tranquillitatis radials is intriguing; the explanation may well be that where older Tranquillitatis

structures were oriented properly, they were rejuvenated and enhanced when the younger Imbrian structures formed.

With one or two possible exceptions, no lineaments concentric to Serenitatis or Tranquillitatis were identified in the region; however, closer to the basins, outside the region, probable concentric structures can be seen.

#### Lunar Grid

In trying to assess the reality of a lunar grid of structures unrelated to basins, the relatively unambiguous Imbrian and Serenitatis radials can be removed from the distribution shown in figure 5 on the basis that they do not coincide with any previously recognized pervasive lunar grid elements. This has been done in figure 7, and peaks still remain at N. 30"-35" W. and N. 35°-40° E. These peaks are not seen in Strom's larger samples, although they might be obscured because of angular distortion and his choice of 10" intervals for plotting. Other concentrations appear at N. 10"-25" W. and N. 0"-15" E. and are believed to represent elements of at least a local tectonic grid because structures geometrically related to mare basins do not occur in these azimuth sectors.

Ambiguity is unavoidable, however, in the sectors 40"-60" or 65" east and west of north, which Strom (1964) and Fielder (1963) found to be the directions of dominant elements of a lunar grid. These sectors in the Triesnecker-Hipparchus region include possible Nectaris radials and probable Imbrian concentric structures (in part coincident with possible Tranquillitatis radials). The ambiguous lineaments which geometrically can be assigned to more than one "system" are indicated separately in figure 7.

The possible Nectaris radials are few and of doubtful relationship and can be included with the true nonradial lineaments without much affecting the distribution pattern. However, if probable Imbrium concentric lineaments are removed from the distribution (fig. 7), the northeast and northwest grid systems of Strom and Fielder are not evident. The distribution of lineaments is uniformly

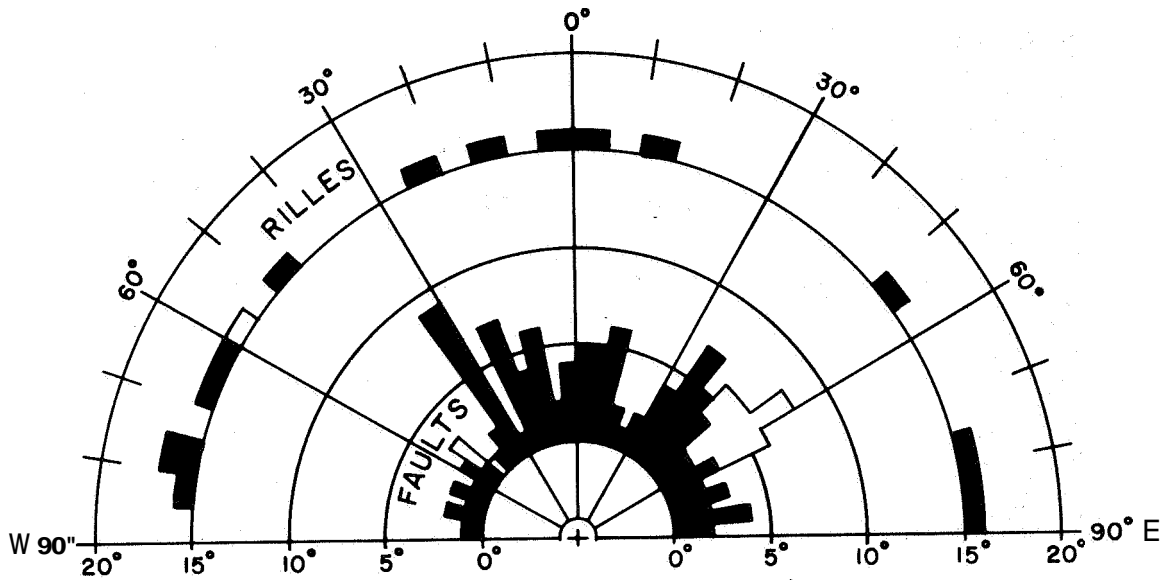


Figure 7.--Azimuth frequency of first- and second-order lineaments, excluding Imbrian and Serenitatis radials. Probable Imbrian concentric structures (NE) and possible Nectaris radials (NW) indicated separately (not black).

low in the sectors N. 50"-90" E. and N. 35"-90" W. If the Imbrian concentric lineaments are not removed, on the assumption that they simply are rejuvenated elements of an older grid, that grid is very asymmetric in the Triesnecker-Hipparchus region; therefore, some true Imbrian concentrics are probably present. The problem will be considered further in the section on interpretation.

The spread of lineaments between N. 15" E. and N. 25" W. in figure 7 is essentially continuous but may be considered to peak at N. 0°-15° E. and N. 25" W. These concentrations of lineaments might be called north-northeast and north-northwest systems. If they are systems and are not merely chance peaks in a random distribution, they are not the same systems as Strom's N-S and NNE-SSW systems, and they are not symmetric with respect to north.

Several prominent lineaments, notably the Ariadaeus, Hyginus, and Oppolzer rilles, and faults parallel to them, are oriented rather symmetrically with respect to east. First-order lineaments in the sectors N. 65"-90" E. and N. 65"-90" W. are identified as an "east-west" system in figure 1. This would correspond to the weak "system D" of the lunar grid recognized by Fielder (1963). In the Triesnecker-Hipparchus region, 27 first- and second-order lineaments are in this grouping, compared with 29 (or 44 if probable Imbrian concentric structures are included) in the presumed lunar grid sectors N. 40"-65" E. and N. 40"-65" W., so they represent a grouping of considerable importance.

Some third-order lineaments may have formed as lines of adjustment during movement on longer lineaments and thus could have nonsystematic orientations. The similarity of azimuth-frequency patterns in figures 6 and 7, however, suggests that, in general, third-order lineaments are not randomly distributed and that Imbrian structures and possible "systems" of lineaments oriented within 40" of north very much dominate the structure of the area at all scales so far observed.

## NATURE OF LINEAMENTS

With the exception of ridges and crater rims, all the lineaments drawn in the region are interpreted as faults. Most of these are lines across which there is a change in topographic relief, presumed to indicate vertical movement on the faults. Some of these features are single lines, as at the base of escarpments which surround the plains-filled floors of craters such as Hipparchus or along the borders of Sinus Medii. Others are subtle linear breaks in slope which probably represent small vertical offsets. Some are clearly double lines which define grabens, as with rilles and some of the more prominent Imbrian radial structures. Many are narrow linear valleys which cut older crater rims or upland units; these commonly seem to be single lines but are almost certainly very narrow grabens. All faults observed are believed to have moderate to steep dips ( $60^\circ$  or more).

Possible lateral offset on lineaments was recognized in only three places. A north-trending fault seems to offset the Hyginus rille a very small amount. The northeast wall of Hipparchus appears to be very slightly offset along two or three northeast-trending lineaments. An elongate crater east of Hipparchus G may be offset along a northeast-trending fault. All these faults appear to have left-lateral slip.

The most conspicuous lineaments in the area are the rilles Rimae Hyginus, Ariadaens, and Triesnecker. These cut the floor of Sinus Medii and the plains northeast of it and are linear steep-sided grabens, most of which are broad enough to have rather flat floors. Small craters commonly occur along the rilles and at rille intersections.

The position of most of the Triesnecker rilles roughly coincides with the crest of a broad swell which separates a broad low area on the east from a partly faulted trough on the west that is about one-fourth the width of the entire Sinus Medii trough and is west and north of the crater Triesnecker. Rima Triesnecker III

extends northwest from the crest of the swell, along the contour of a regional sag centered at the crater Hyginus. The rilles, which generally follow the swell throughout its length, branch at acute angles or are en echelon; they variously cut and are cut by a few rilles that cross the swell. Many of the linear segments of the rilles and ridges which cross the faulted western trough match in trend older structures radial to basins or elements of a presumed lunar grid. The general pattern is one of tension cracks, prefigured in part by older lineaments, which formed in part approximately radial and circumferential to the Hyginus sag, in part marginal to the deepest part of the faulted western trough, and also along the length of the swell. Probably the whole rille system is the product of a single episode of irregular subsidence and upwarp of the floor of Sinus Medii. Regional tension is indicated by the fact that some rilles propagated well beyond the main area of rille formation.

The few chain craters present in the area generally parallel regional structural directions but do not seem to follow any specific one.

The narrow ridges in the floor of Sinus Medii and in the low area east of Oppolzer and Reamur generally are made up of short linear segments. The azimuths of these segments are within 65° of north and are slightly concentrated at N. 0°-10° E. (fig. 6). The overall trend of the ridges is parallel to, or an extension of, the boundary faults of the faulted trough west of Triesnecker, suggesting that the surface features are either fault ridges or were formed by accumulation of volcanic material along tension cracks.

In the Triesnecker-Hipparchus region, polygonal crater rims reflect local structural trends and show little concentration in azimuth (fig. 6). The rims of some Copernican craters are cut by faults; thus even some of the youngest craters have been modified by tectonic activity. In general, the older the crater, the more polygonal the rim and the more battered the walls, indicating

progressive modification of crater shape with time. Much of the polygonal shape of many craters, however, is almost certainly original, due to prefiguring by older structure as the craters formed. Triesnecker, Agrippa, and Godin are good examples of noncircular young craters.

#### RELATIVE AGES OF LINEAMENTS

A lineament generally is younger than a lineament or stratigraphic unit that it transects (one exception would be the development of two faults abutting opposite sides of an older fault). But rejuvenation of an old structural line commonly reverses the age relations that existed before the rejuvenation. Reversals of age relations among members of any two possible systems of lineaments (lunar grid, basin radials, etc.) are common throughout the Triesnecker-Hipparchus region.

From study of relations among lineaments alone, it is not clear whether the systems have developed continuously or whether local rejuvenation has obscured an older general sequence of structural development. Some clarification is obtained if the relation of lineaments to stratigraphic units is considered; in this way, some systems are seen to be predominantly younger than others.

Several stratigraphic units are useful in specific areas in determining relative ages of lineaments, especially the widespread Cayley Formation and Copernican crater ejecta deposits. The Cayley Formation is a plains-forming, probably volcanic, unit which covers about half of the Sinus Medii trough and most adjoining low areas and fills many old craters and troughs. It fills troughs bounded by Imbrian radial and concentric structures and occupies breaches in old crater walls cut by Imbrian radials.

Nearly all systems contain some lineaments that are older than the Cayley and some that are younger. The Imbrian radial system is predominantly older, but some radials cut the Cayley and it is not known if this is the result of rejuvenation. The N. 0"-15"

E. and east-west systems contain the most lineaments that are predominantly younger than the Cayley. The N. 0"-15" E. system includes 13 first- and second-order lineaments which can be dated relative to the Cayley; 11 of these cut the Cayley and 2 are older. Of 21 east-west first- and second-order lineaments which are in contact with the Cayley, 18 cut the unit and 3 have equivocal relationships. Among third-order post-Cayley lineaments, those in the N. 0°-15° E., N. 10°-25° W., and east-west systems are the most abundant. For many systems the sample is too small to determine whether the system is predominantly older or younger.

In the area studied it seems clear therefore that the N. 0"-15" E. and east-west systems have been the most active since the deposition of the Cayley Formation. As some elements of the N. 0°-15° E. system are cut by Imbrian radials, it is inferred that the N. 0"-15" E. system developed continuously, increasing in relative importance in this area in post-Cayley time. A few pre-Imbrian east-west structures were noted, but many more east-west structures were post-Cayley, suggesting that most of the east-west system is really younger than the Cayley rather than selectively rejuvenated more than other systems.

Most structures in the area that contact Copernican crater ejecta appear to be mantled by it. Rare post-Copernican structures, quite possibly resulting from reactivation of older lineaments, include two faults in the grid sector N. 40°-65° W., two faults in the east-west sector which cut dark material younger than rays, and a fault in the grid sector N. 40"-65" E. which cuts the rim of the Copernican crater Agrippa.

#### ORIGIN OF LINEAMENT PATTERN

Many first- and second-order lineaments in the Triesnecker-Hipparchus region are geometrically radial and concentric to the Mare Imbrium basin and radial to the Mare Serenitatis basin. These largely control the detailed outline of Sinus Medii and appear to

have prefigured part of the younger Triesnecker rille system. Imbrian concentric structures coincide in part with lineaments radial to the Mare Tranquillitatis basin. A few lineaments may be radial to Mare Nectaris. If all these structures are removed from consideration (fig. 7), the pattern of the remaining lineaments presumably is unrelated to basins and can be examined for elements of a possible lunar grid.

The distribution of lineaments in the Triesnecker-Hipparchus region is different than that found by Strom (1964) and Fielder (1963) in much larger sample areas. They found the strongest grid systems in the N. 40"-60" E. and N. 40"-60" W. sectors. These widespread lineament systems are scarcely represented in the Triesnecker-Hipparchus region, unless part of the Imbrian radial and concentric structures are considered to have been prefigured by the northwest and northeast systems of an older grid. Strom's map 7 and rectified plates of other upland areas in the equatorial belt also show a general lack of development there of these grid systems that are so prominent in the southern and northern uplands. The concentration at N. 0"-15" E. in figure 7 is probably the north-south system of Strom and system C of Fielder. The additional peaks in figure 7 (N. 30"-50" E., N. 10°-25° W., N. 30"-35" W.) do not correspond to lineament systems evident in the larger samples.

Strom and Fielder regard the northeast and northwest systems as forming a right-angle Moon-wide system bisected by a north-south system. This configuration is not present in the Triesnecker-Hipparchus region. One possibility is that the peaks at N. 30"-50" E. and N. 30"-35" W. in the Triesnecker-Hipparchus region mark a lunar grid more acute than elsewhere, bisected by the N. 0"-15" E. system of lineaments. By this explanation the northeast and northwest systems of a grid would consist of structural planes developed approximately symmetrically (or locally asymmetrically) about a north-south axis. This configuration would be typical if north-south compressive forces had been active; a cone of shear planes would be bisected by a system of tensional features

parallel to the compressive axis. This is the explanation invoked by Strom (1964, p. 213). Considering this compressional model for the Triesnecker-Hipparchus region, the acute angle of the grid there would indicate shear of a brittle body (in Strom's Moon-wide sample the generally obtuse angle indicates shear of a ductile body). If a shear system is envisioned, the peak at N. 10°-25° W. in figure 7 of this report might represent a preferred orientation of second-order shears (Moody and Hill, 1956).

One important difficulty with this explanation is that lineaments trending northeast and northwest should be shears, yet only four or five display possible lateral offset. All other lineaments show apparent vertical offset, suggestive of tensional stress. Rilles--obvious tensional features--are not oriented exclusively north, although figure 7 does show them to be absent in the primary shear directions required by the explanation. Moreover, the apparent left-lateral offsets noted on two faults trending northeast are in the right direction for the proposed shear system.

Another difficulty is that structures in the sectors 65°-90° east and west, at large angles to the proposed compressive axis, should be compressional but instead are obviously tensional. The large rilles are linked to local upwarp and subsidence in large part, but regional tension is suggested by the fact that some of them extend far beyond the focus of local warping. Age relationships, however, suggest that this "system" of tensional structures is younger than most other lineaments. It is possible, then, that this system was produced by relatively late regional tension which also resulted in some of the vertical offsets seen on faults of older systems. Such regional stress might be effectively independent of possible Moon-wide stresses.

The difficulties with invoking regional north-south compression apply equally to east-west compression. An alternative is to invoke only vertical tectonics in an environment of regional tension, but it is then difficult to explain the development of systems of lineaments and their observed patterns.

Perhaps the clearest point that can be made is simply that the lineament pattern in the Triesnecker-Hipparchus region is different than that shown in larger samples, and Strom's maps suggest that structure of the entire equatorial belt may be different than that of other regions of the Moon. Local structural influences which probably changed with time are perhaps more important than has been supposed and should be investigated carefully in all regions. A presumed lunar grid needs further systematic study.

#### REFERENCES

- Baldwin, R. B. , 1963, The measure of the Moon: Univ. of Chicago Press, 488 p.
- Fielder, G. , 1963, Lunar tectonics: Geol. Soc. London Quart. Jour. , v. 119, p. 65-94.
- Moody, J. D., and Hill, M. J., 1956, Wrench-fault tectonics: Geol. Soc. *Am.* Bull. , v. 67, p. 1207-1246.
- Strom, R. G. , 1964, Analysis of lunar lineaments, I: Tectonic maps of the Moon: Arizona Univ. Lunar and Planetary Lab. Commun. , v. 2, no. 39, p. 205-216.
- Wilhelms, D. E., 1964, Major structural features of the Mare Vaporum quadrangle, in Astrogeologic Studies Ann. Prog. Rept. , July 1963-July 1964, pt. A: U.S. Geol. Survey open-file report, p. 1-15.



### SECTION III

## LUNAR AND PLANETARY PHYSICS



N67-31948

100 e  
3 THE THEORY OF RADIATIVE  
TRANSFER IN THE LUNAR SURFACE

By Robert L. Wildey

The earlier attempts to explain infrared observations of the temperature variations of the lunar surface in terms of heat flow analysis (Wesselink, 1948; Jaeger, 1953) consisted in the solution of the one-dimensional heat diffusion equation, expressible as

$$\frac{\partial}{\partial z} \left[ \kappa \frac{\partial T}{\partial z} \right] = c\rho \frac{\partial T}{\partial t} \quad (1)$$

with the specific heat, density, and thermal conductivity as constants, subject to the boundary condition at the surface imposed by solar insolation

$$(1-A) F_{\odot} H(\cos \omega t) \cos \omega t = \left| \sigma T^4 - \kappa \frac{\partial T}{\partial z} \right|_{z=0} \quad (2)$$

in which an infrared emissivity of unity and a constant specific insolation are assumed. The unit step function, used to represent zero insolation between sunset and sunrise, is  $H(X)$ , and  $A$  is the Bond albedo of the moon. The sun is treated as a point source during lunation heating and cooling. The manner of treating the sun altitude,  $\omega t$ , in the equation implies that the solution is for a lunar point at which the sun passes through the zenith during the course of the given lunation. Jaeger's treatment was an extension of sophistication over Wesselink's in that two-layer cases of multiple values of  $\rho c K$  were considered,

More recently, consideration has been given to the fact that the high porosity of the lunar surface implies a physical significance to the transfer of energy by radiation between the elements of matter composing the surface. Reasoning from a geometric model

of a porous medium, Watson (1964) has concluded that radiative transfer, when incorporated into conductivity, leads to an additive term in the conductivity proportional to the cube of the temperature. This may be derived somewhat more generally by starting from two of the classical equations of stellar interiors (e. g., Schwarzschild, 1958, p. 96).

$$\frac{dL}{dr} = r^{-2} \rho \epsilon \quad (3)$$

$$L_r = - \frac{16\pi}{3} \left[ \frac{\sigma r^2}{\rho \kappa} \right] \frac{\partial T^4}{\partial r} \quad (4)$$

We may consider equations 3 and 4 as describing a system which is locally plane parallel. If we thus maintain  $r$  constant in equation 4, and replace  $dr$  by  $-dz$ , the two equations combine to yield

$$\frac{\partial}{\partial z} \left[ \frac{16\sigma T^3}{3\rho\kappa} \frac{\partial T}{\partial z} \right] = - \rho \epsilon \quad (5)$$

If  $\epsilon$ , the rate of energy generation per gram, is made equal to  $-c \frac{\partial T}{\partial t}$ , so that cooling, through the thermal capacity, is the only source of energy generation; and if we set

$$K = \frac{16\sigma T^3}{3\rho\kappa} \quad (6)$$

then equation 5 becomes identical with equation 1. Equation 5 is merely a statement of the divergence of radiative flux. Equation 1, as it stands, could represent a statement of the divergence of the conductive flux (with constant conductivity). Since the total flux is merely the sum of radiative and conductive terms, it is clear from the addition of equations 1 and 5 that the overall process is describable by equation 1, with the following expression for the combined conductivity

$$K = K_c + \left[ \frac{16\sigma}{3\rho\kappa} \right] T^3 \quad (7)$$

Thus  $K_c$  is the ordinary heat conductivity of the lunar material independent of microtopographic expression, and  $\kappa$  is the Rosseland mean (e. g., Aller, 1953) of the effective opacity of the lunar surface material as a porous medium. For absorbing and reradiating elements (grains, fibrils, etc.) consisting of particulate matter, we expect  $\kappa_\nu$  to be wavelength independent, and probably independent of depth.

It is important to note that the validity of the treatment in which equations 1, 2, and 7 are solved simultaneously rests on the validity of the assumption, from the theory of stellar interiors, that the radiation field is nearly isotropic. Because this is not the case near the boundary of the lunar surface, we conclude that a more correct analogy of the problem is that which can be derived for the theory of stellar atmospheres. It is noted that the need for improvement of the theory of the heat flow of the lunar surface is independently founded on its failure to correctly predict recent infrared observations of lunar nighttime cooling (Murray and Wildey, 1964; Wildey, Murray, and Westphal, 1967), even when temperature-dependent conductivity and two-layered models are used (Watson, 1964).

Consider the lunar surface as a plane parallel medium. The fundamental equation of radiative transfer (Chandrasekhar, 1950) must be satisfied, as it describes only the existence of radiative emission and absorption processes, except when the source function is specified. Furthermore, if the medium elements are considered as small absorbing and emitting black bodies, then local thermodynamic equilibrium and Kirchoff's law will apply. Assuming a wavelength independent opacity for reasons cited above, we can write the wavelength-integrated equation of transfer

$$\mu \frac{\partial I}{\partial \tau} = I - \frac{\sigma}{\pi} T^4 \quad (8)$$

where the usual variable definitions prevail (Woolley and Stibbs,

1953; Münch, 1960). In addition, the usual radiative boundary conditions must hold. The peculiarity of the present case is the dependence of the specific intensity on time.

$$I = I(\tau, t, \mu)$$

$$I(0, t, \mu) = 0, \quad -1 < \mu < 0, \quad \text{all } t \quad (9)$$

What is finally needed is a statement of overall energy continuity. Consider a vertical column in the lunar surface of unit cross-sectional area located at depth  $\tau$  and of thickness  $d\tau$ . Although the dimensioned variable,  $z$ , could be used, optical depth has been used as a matter of convenience. Write separately the radiative and conductive fluxes as  $F_r$  and  $F_c$ . Any non-zero differential of these combined fluxes across the column must be made up from the solar energy absorbed in the column and the changing of temperature acting through the thermal capacity of the medium. This is expressible as

$$dF_r + dF_c + F_0 e^{-\eta\tau/\cos \omega t} H(\cos \omega t) d\tau - c' \frac{\partial T}{\partial t} d\tau = 0 \quad (10)$$

A modified specific heat has been introduced. It is a bulk heat capacity per unit volume in which two dimensions are geometric and the third is a unit optical thickness. Hence

$$c' = \frac{\partial^2 E}{\partial A \partial \tau} = \frac{\partial^2 E}{\partial m} \cdot \frac{\partial m}{\partial A \partial z} \cdot \frac{\partial z}{\partial \tau} = c/\kappa \quad (11)$$

where  $E$  is energy per degree,  $A$  is area, and  $m$  is mass.

The radiative absorption term is explainable as follows. The solar flux at the lunar surface is  $F_0$ . Its attenuation factor at depth  $\tau$  and sun angle  $\omega t$  is  $\exp[-\eta\tau/\cos \omega t]$ , where  $\tau$  is still the optical depth due to pure absorption and is considered the same for sunlight as for lunar thermal radiation, and  $\eta$  is the ratio of the sum of the mass absorption coefficient and the scattering coefficient to the absorption coefficient alone. Inasmuch as only first order scattering is being considered, which should be a good approximation for a body of as low an

albedo as the moon's, we must have

$$\left( \int_0^{\infty} e^{-\tau} d\tau \right) / \left( \int_0^{\infty} e^{-\eta\tau} d\tau \right) = 1-A = \eta \quad (12)$$

The effective cross-sectional area of the attenuated solar flux which passes into the column is  $\cos \omega t$ . The optical thickness of the column to a beam of radiation from the solar direction is  $d\tau/\cos \omega t$ , hence the fraction of the threading radiative power that is absorbed.

We may replace the differential for the conductive flux by the term from the ordinary heat diffusion equation, substituting a  $K'$  defined as  $\kappa\rho k$ . The differential of radiative flux may be obtained in the classical way by integrating both sides of equation 8 over all directions, taking the cosine of the angle to the local normal,  $\mu$ , to the right of the partial derivative sign. When the results of these operations are substituted into equation 10, one obtains the following integro-differential (partial) equation

$$K' \frac{\partial^2 T}{\partial \tau^2} - c' \frac{\partial T}{\partial t} - 4\sigma T^4 + 2\pi \int_{-1}^{+1} Id\mu = -F_0 e^{-\eta\tau/\cos \omega t} H(\cos \omega t) \quad (13)$$

Equations 8, 9, and 13 constitute the complete system whose solution prescribes the behavior of the infrared radiation recorded on earth. The predicted observation becomes, however, the left-hand-side of

$$I_4(o, t, \mu) = \int_0^{\infty} B_{8-14}(T) e^{-\tau/\mu} d\tau/\mu \quad (14)$$

where  $\mu$  refers to the observing angle,  $B_{8-14}(T)$  is the Planck function integrated from 8 to 14 microns, and  $T$  is a function of  $\tau$  and  $t$  as provided by solution of equations 8, 9, and 13.

At the present time, the most satisfactory technique of solution appears to lie in the application of Chandrasekhar's method of discrete directional beams in Gaussian quadrature, so

that the integro-differential equation will be replaced by a large number of simultaneous partial differential equations. Solution of equations 8, 9, and 13 for various values of  $K'$  and  $C'$  will be discussed in a later report.

#### REFERENCES

- Aller, L. H. , 1953, The atmospheres of the sun and stars: New York, Ronald Press Co., p. 219.
- Chandrasekhar, S., 1950, Radiative transfer: London, Oxford at the Clarendon Press (repr. 1960, Dover Pubs. , New York) , chs. 1, 11.
- Jaeger, J. C., 1953, The surface temperature of the moon: Australian Jour. Physics, v. 6, p. 10-21.
- Münch, G. , 1960, The theory of model stellar atmospheres, in Greenstein, J. L. , ed. , Stellar atmospheres: Chicago, Univ. Chicago Press, p. 1-6.
- Murray, B. C., and Wildey, R. L. , 1964, Surface temperature variations during the lunar nighttime: Astrophys. Jour., v. 139, p. 734-750.
- Schwarzschild, M., 1958, Structure and evolution of the stars: Princeton, Princeton Univ. Press, p. 96.
- Watson, Kenneth, 1964, I. The thermal conductivity measurements of selected silicate powders in vacuum from 150° K to 350° K. 11. An interpretation of the moon's eclipse and lunation cooling as observed through the earth's atmosphere from 8-14  $\mu$ : California Inst. Technology, Pasadena, Calif. , Ph. D. thesis.
- Wesselink, A. J. , 1948, Heat conductivity and the nature of the lunar surface: Netherlands Astron. Inst. Bull. , v. 10, p. 351-363.
- Wildey, R. L. , Murray, B. C. , and Westphal, J. A. , 1967, Photometric reconnaissance of the moon's disk during lunar nighttime at  $\lambda$  100,000Å: Jour. Geophys. Research (in prep.).
- Woolley, R. v. d. R., and Stibbs, D. W. N. , 1953, The outer layers of a star: London, Oxford at the Clarendon Press, p. 2.

1 same 3

N67-31949

3 MAXIMUM POLARIZATION VALUES OF  
SOME LUNAR GEOLOGIC UNITS

By N. J. Trask

and P 3 7 RS

The U.S. Geological Survey is continuing its program of measuring the degree of polarization of moonlight in order to describe as completely as possible some of the widespread and significant lunar geologic units that have been mapped on the basis of observations from earth. Measurements discussed in this report were made with a Lyot fringe polarimeter mounted on the 12-inch refractor at Lick Observatory. The methods and scope of the study have been discussed previously (Wilhelms and Trask, 1965).

Data obtained since publication of the last annual report are given in table 1. The values of maximum percentage polarization were obtained by taking several readings on each point near quarter moon, when maximum occurs, over a period of 2 to 4 months. As with the previous report, some values for points in darkness when maximum polarization occurs have been obtained by extrapolating values obtained before quarter moon along a smooth curve parallel to the curves for other units for which the maximums are established. Values obtained this way are indicated in table 1.

The data accumulated in the 2 years since this program began enable the following generalizations: (1) Bright rays and the bright floors of some craters have the lowest values of maximum polarization--from 3.5 to 6.0 percent; (2) maximum polarization values of light terra plains-forming materials, such as the Cayley Formation, range from 5.0 to 6.5 percent; (3) maximum polarization values of regional units surrounding some circular mare basins,

Table 1.--Location, description, and maximum polarization of some geologic units

Region	ACIC chart	Center of region	Geologic unit	Maximum polarization (percent)
39-3	Aristarchus	A, -46" 40' β, +24° 40'	Dark rim material of Aristarchus	10.9
42-7	Mare Serenitatis	λ, +24° 30' β, +24° 10'	Procellarum Group (Ipm2) in central Mare Serenitatis	12.2
43-2	Macrobius	A, +30° 40' β, +26° 30'	Procellarum Group (Ipm4) in Le Monnier	10.5
56-1	Hevelius	λ, -54" 20' β, +12° 00'	Marius Group	13.9
56-2	--do--	λ, -63" 50' β, +10° 30'	Cavalerius Formation or Pro- cellarum Group, dark (Ipm4)	13.0
56-4	--do--	A, -58" 50' β, +8" 30'	Reiner Gamma Formation	7.8
62-1	Mare Undarum	λ, +56° 50' β, +13° 40'	Procellarum Group in Mare Crisium	10.7
74-2	Grimaldi	A, -50" 20' β, -13° 40'	Procellarum Group, dark (Ipm4 on floor of Billy)	11.9
74-4	--do--	A, -59" 50' β, -2° 40'	Procellarum Group, dark (Ipm4)	13.3
75-2	Letronne	λ, -43" 40' β, -2° 30'	Procellarum Group (Surveyor I landing site)	15.2
76-3	Montes Riphaeus	A, -24" 40' β, -15" 30'	Vitello Formation or coarse hummocky material	*7.1
76-4	--do--	A, -19" 10' β, -14" 30'	Fra Mauro Formation (smooth facies)	*8.3
76-5	--do--	A, -17" 40' β, -5° 30'	Fra Mauro Formation, type locality	*7.6
78-3	Theophilus	λ, +15° 50' β, -11° 00'	Kant plateau-forming material	5.2
79-1	Colombo	A, +36° 20' β, -0° 30'	Censorinus Formation	6.2
79-2	--do--	A, +41° 30' β, -5° 40'	Dark mare material near Gutenberg (CEmd)	8.8
79-3	--do--	A, +46° 30' β, -2" 40'	Procellarum Group near Messier (Ipm)	11.8
80-1	Langrenus	λ, +60° 00' β, -8" 00'	Floor of Langrenus	4.7
80-2	--do--	λ, +58° 50' β, -6" 20'	Dark halo crater material on rim of Langrenus	8.4
93-3	Mare Humorum	A, -44" 30' β, -27" 00'	Doppelmayr Formation	11.5
93-4	--do--	A, -34° 40' β, -30" 30'	Vitello Formation, type locality	1.4
93-5	--do--	A, -38" 00' β, -23" 00'	Procellarum Group (Ipm3)	12.5
94-6	Pitatus	A, -28° 30' β, -17° 00'	Procellarum Group (Ipm4) near Lubiniezky	"11.9
96-1	Rupes Altai	A, +29° 00' β, -23" 00'	Tycho ray	5.5

"Value of maximum polarization obtained by extrapolating curves from low phase angles to phase angles near quarter moon, when maximum polarization occurs.

such as the Fra Mauro Formation around the Imbrium basin, range from 6.0 to 8.5 percent; and (4) maximum polarization values of dark mare materials of the Procellarum Group and local dark covering materials younger than the Procellarum, such as the Doppelmayer Formation, are the highest and cover the greatest range--9.0 to 15.0 percent.) The more interesting results are among this last group. Although maximum polarization is generally inversely related to albedo (Hapke, 1966), materials with the highest polarization values may depart from this relationship in detail. The mare material of 74-2 appears very dark and uniform,  $P_{\max} = 11.9$  percent; it is similar in all respects to material of 74-1, described in the last annual report. At 75-2, the landing site of Surveyor I, the albedo of the mare material is apparently about the same or slightly higher than that of 74-2 or 74-1, but  $P_{\max} = 15.2$  percent, much higher than for 74-1 or 74-2. Similarly, maximum polarization of the dark mare material of 43-2, on the margin of the Serenitatis basin, is apparently lower than that of the mare material with higher albedo at 42-7, closer to the center of the basin. This discussion is based on visual estimates of the albedos from full-moon photographs; precise measurements of the albedos should be available soon.

The maximum polarization of a unit is dependent on both albedo and grain size. Hapke (1966) showed that for natural terrestrial materials it increases with increasing grain size, and he suggested that the low maximum polarization of the moon as a whole indicates that the grain size of lunar materials peaks somewhere between 1 and 10  $\mu$ . High values measured for some areas of the moon could therefore be due to above-average grain size. High-resolution photographs returned by Lunar Orbiter II show that in some areas blocks as much as several meters in diameter are relatively abundant, and in other areas such blocks are absent. None of the photographs cover areas for which polarization has been measured, however, nor is it certain that the resolution of the Orbiter photographs is sufficient to detect the grain sizes that

might contribute to variations in **maximum** polarization. Another unit for which an especially high value has been measured is the Marius Group on the western edge of Oceanus Procellarum (table 1). McCauley (1967) interpreted this unit as a relatively young volcanic complex with intercalated flows and ash deposits surrounding a large number of volcanic domes; the unit could have above-average grain size because of relative youth.

A brief investigation of the crater Dawes (long  $+26^{\circ} 20'$ , lat  $+17^{\circ} 10'$ ) was carried out because this feature is one of the strongest thermal anomalies discovered by Shorthill and Saari (1965) during the eclipse of December 1964. As far as could be determined, the polarization of Dawes is not anomalous; the albedo and **maximum** polarization of the rim of the crater are almost the same as that of the surrounding mare material.

A puzzling aspect of the measurements made during this study has been a tendency for all values of positive polarization to change very markedly from month to month. For example, virtually all values obtained in September 1966 were from 10 to **13** percent higher than values for the same points in August 1966. Gehrels, Coffeen, and Owings (1964) reported that the positive polarization for a point in Mare Crisium fluctuated 12 percent between 1959 and 1963. Although of the same order, the fluctuations noted above seem especially rapid. Attempts to explain them by such processes as lunar luminescence would be premature until their reality has been probed further by additional measurements with the Lyot instrument and with a photoelectric polarimeter later to be installed on the U.S. Geological Survey telescope near Flagstaff, Ariz.

#### References

- Gehrels, Thomas, Coffeen, T. , and Owings, D. , 1964, Wavelength dependence of polarization, 111--The lunar surface: *Astron. Jour.* , v. 69, no. 10, p. 826-852.

- Hapke, B. W., 1966, Optical properties of the Moon's surface, & Hess, W. N. , Menzel, D. H. , and O'Keefe, J. A. , eds., The nature of the lunar surface: **IAU-NASA** Symposium, 1965, Proc., Baltimore, The Johns Hopkins Press, p. 141-154.
- McCauley, J. F., 1967, Geologic map of the Hevelius region of the Moon: **U.S.** Geol. Survey Misc. Geol. Inv. Map 1-491.
- Shorthill, R. W., and Saari, J. M., 1965, The non-uniform cooling of the eclipsed Moon: a listing of thirty prominent anomalies: Science. v. 150, p. 210.
- Wilhelms, D. E., and Trask, N. J. , 1965, Polarization properties of some lunar geologic units, in Lunar and planetary investigations, pt. A of Astrogeologic Studies Ann. Prog. Rept. , July 1964-July 1965: **U. S.** Geol. Survey open-file rept. , p. 63-80.

1 same<sup>3</sup> N67-31950

2 SPATIAL FILTERING OF  
ASTRONOMICAL PHOTOGRAPHS

By<sup>6</sup> Robert L. Wildey

Sp 169-181  
RS  
same

It has been known for ~~some~~ time that use of Huygen's principle to find out how the distribution of electric vector in the image plane relates to the distribution of electric vector in the aperture of the preceding lens leads to the fortuitous mathematical conclusion that one is the two-dimensional Fourier transform of the other, if scales are properly chosen. For the last several years, many in industry have applied this fact and corollary phenomena in solving optical problems. However, Fourier transform techniques have almost never been applied to problems of astronomical imagery.

As a linear system, an optical train is susceptible to very elegant and rigorous treatment of the problem, for example, of the preservation of sufficient object integrity for image recognition, by the use of the concept of the transfer function. The "sine wave response" is nearly equivalent terminology. By multiplying the Fourier transform of the object brightness distribution by the transfer function of the optics, the Fourier transform of the image is obtained. If a photographic record is kept and the plate resolution is of ~~some~~ consequence, then the overall transfer function is merely the above transfer function multiplied by the individual transfer function of the photographic emulsion. Finally, an inverse transform of the result provides the image. A recent review of the fundamental theory has been provided by Smith (1963). A more direct application of the Fourier transform pair relationship in optical systems is the use of a photograph itself for

diffraction of a plane wave of light. If the photograph is placed immediately in front of a lens, then the Fourier transform of the picture itself is obtained in the focal plane of the lens. Thus, at this point in the train, the fine detail of the picture, which is determined by high spatial frequencies, is represented by light far from the optic axis, whereas the broader variations in photographic density are represented by light close to the optic axis. By placing, at this point on the optic axis, a filter whose transmission varies with its position in the focal plane of the lens, and then inverting the transform simply by placing a similar lens, now used as a "collimator", farther down the optic axis, and photographing the light immediately behind the second lens, a wide variety of picture manipulation is possible. To a degree, seeing compensation is possible in this way. This technique has already been applied to seismic records (Dobrin, Ingalls, and Long, 1965).

An earlier report (Wildey, 1966) described in detail how an optical system can be constructed which alters the relative harmonic coefficients in the Fourier series representation of an image brightness distribution, as discussed above. One of the functions which can be performed by this spatial filtering of an image is the removal of television scan lines. Because it involves pure low-pass filtering, this is one of the simplest functions, as can be shown from figure 1. The following argument is sufficiently general that the columns on the right in figure 1 may or may not abut one another, so that dark intervals may or may not exist in the picture. The height of each column when they abut represents the average over a local neighborhood one column space wide. Therefore, all the Fourier components of the original picture on the left whose average value over a distance equal to one column space (television line interval) is zero, will not be passed through the video channel. This corresponds to a zero-valued transfer function for spatial wavelengths equal to the television line interval, or higher harmonies thereof. Of course, from the appearance of the right-hand picture we conclude that Fourier components of such frequencies

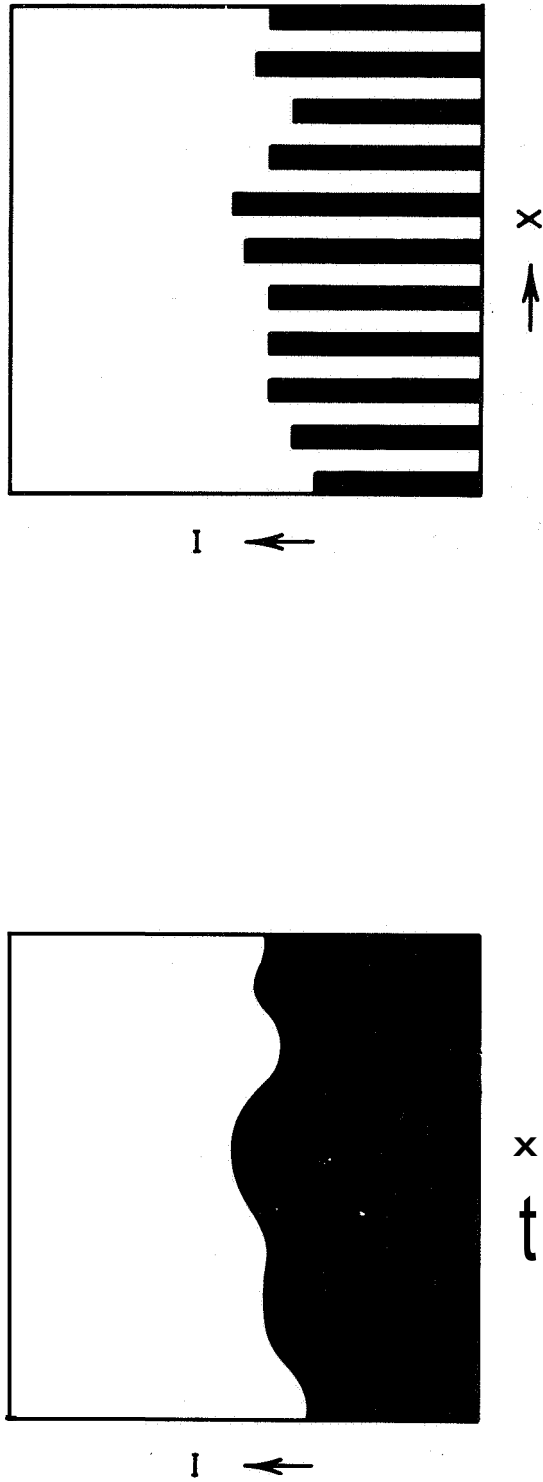


Figure 1.--The curve on the left represents a one-dimensional picture. The ordinate is proportional to image brightness and the abscissa is picture position. The right-hand columnar display is the result of passage of the left-hand picture through a video channel.

are truly present in the output, but from the foregoing we infer that these frequencies contain only distortion and no real picture information. Therefore their complete removal through the use of a low-pass filter (in an optical system--a circular knife edge) is justified because true image detail is not sacrificed.

In practice, it is better to cut-off at a spatial wavelength twice as long as the television line interval. The prudence of this operation emerges from the following reasoning. What will be the representation of a sinusoidal picture component whose wavelength is equal to twice the line interval? The answer is ambiguous. It depends on their relative phases. For a phase difference of zero, the result is an alternating periodic height difference in the columns on the right in figure 1, with a frequency equal to the frequency of the real sinusoid of the picture. The phase of the picture sinusoid can be changed by  $\pi/2$ , however, and the response in the output will become zero. For shifts of other values, intermediate amplitudes at the same spatial frequency are produced. For intermediate frequencies between the TV line frequency and one-half the TV line frequency, a beat frequency appears in the output. This can be seen in figure 2, which shows the average value of the sine wave over the hatched intervals, representing fully abutting scan lines. In the interval shown, the sine wave crests five times, there are seven television lines, and the periodicity of the line strength variation has two crests. Two is a beat between five and seven. Similar difficulties beset the higher harmonics of these spatial frequencies. This is an aliasing error well known in time-division telemetry systems. Inasmuch as the components in this frequency category undergo such thorough intermodulation distortion, they are better left out of any reconstituted image.

The above result, together with even more severe aliasing effects, can be derived more elegantly and more rigorously in the case of television line widths sufficiently narrow as to lead to the asymptotic expressibility of the video picture as the product

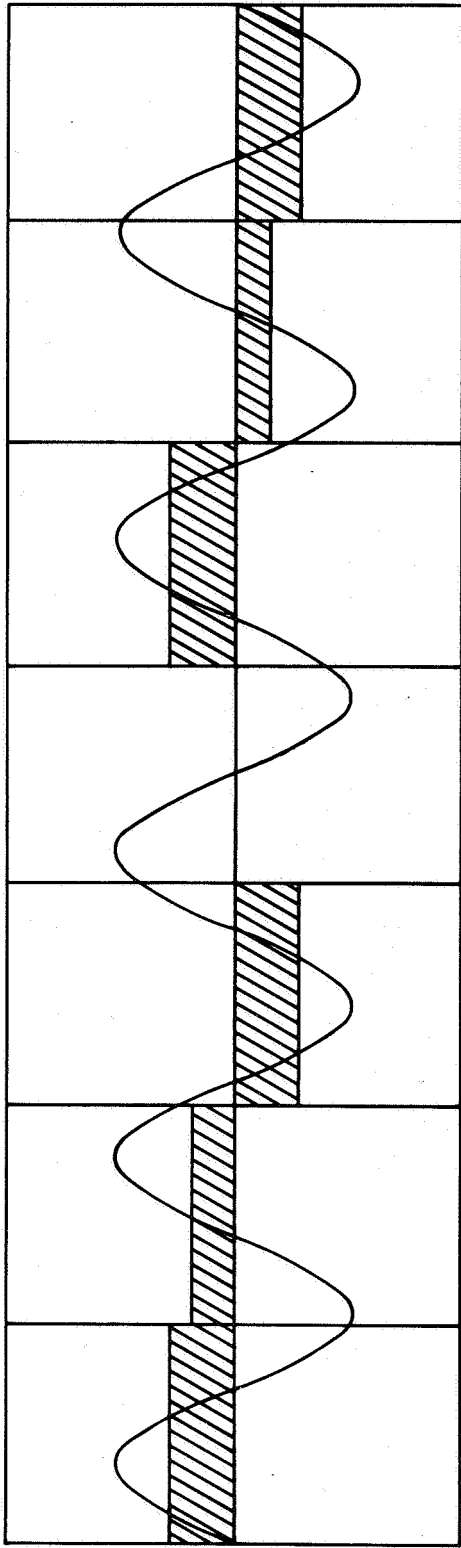


Figure 2.--A sinusoidal distribution in picture brightness is shown together with the mathematical result of passage through a channel which periodically averages the picture information without blank interval. The periodicity of the resulting signal is a beat between the information frequency and the processing frequency.

of two functions.

$$f(x) = \sum_{n=0}^m R_n \cos \left[ \frac{2 \pi n x}{l} \right]$$

Here we have represented the focal plane image as  $f(x)$ . The video's spatial response function, which has a periodicity repeating at intervals in  $x$  of  $n l$ , where  $l$  is the TV line interval, is shown as a Fourier series. The expression is correct only if  $f(x)$  varies negligibly over an interval in  $x$  equal to the TV line thickness.

We now recall the fact that the Fourier transform of the product of two functions is the convolution of the individual Fourier transforms of each function separately. Let  $F(w)$  be the Fourier transform of  $f(x)$ . Then the Fourier transform of the video picture is

$$\int_{-\infty}^{\infty} f(w-w') \sum_{n=0}^{\infty} R_n \delta \left[ w' - \frac{2 \pi n}{l} \right] d w'$$

or

$$\sum_{n=0}^{\infty} F \left[ w - \frac{2 \pi n}{l} \right] R_n$$

We thus see that whereas the spatial frequency spectrum of the focal plane image may be anything which falls to zero at a frequency whose wavelength equals the TV line thickness (a much higher frequency than that corresponding to the TV line interval), the spectrum of the result obtained after passage through a video channel is this same primary spectrum, centered on the origin, and, in addition, reproduced an infinite number of times centered on the fundamental and all the higher harmonics of the spectrum of the TV spatial response function. Therefore, unless the primary image spectrum,  $F(w)$ , goes to zero before reaching one-half the frequency corresponding to the TV line interval, it will overlap with its convolution at the fundamental of the line frequency. If we were to insert a knife edge to eliminate the higher frequencies, what would be left would not be the pure spectrum of the primary image at all, but something insidiously contaminated all the way down

to the d-c level. In spatially filtering photographs, pictorial defects and photometric errors cannot be avoided unless the transfer function of the TV camera lens cuts off at a space wavelength at least twice as large as the TV line interval.

Granting the above, space filtering can be performed without difficulty. In practice, an additional problem exists. In order to obtain a Fourier transform of a photographic image it is necessary to form a planar distribution in the amplitude of electric vector, at a lens aperture, which is proportional to the image intensity for corresponding spatial positions (or is a known monotonic function thereof, as in photographic density). This can be done by using a transparent reproduction of the image to attenuate a plane wavefront immediately in front of a lens. It is important to distinguish between a plane wavefront and true coherent light. In the former, the relative phase of the electric vector over the wavefront is a pseudorandom variable where the correlation length for phase in the plane of the wavefront is extremely minute compared to the lens aperture. For light to be coherent, all that is required is that some surface exist in space, not necessarily a plane, at time  $t_1$ , where the electric vectors are oscillating in phase, and that this surface will propagate to form another surface at time  $t_2$  without the development of phase differences. A star is a good example of a source of a highly incoherent plane waveform of light. It is extremely close to being a point source at infinity (hence, its spherical wavefront is locally planar), and yet the emission of photons from its vast photosphere is a highly random phenomenon. The laser, through proper spatial filtering, becomes the best current source of a coherent plane wave. The process of stimulated emission is one in which photons collect additional photons from atoms in a highly ordered manner. The coherence<sup>1</sup> of laser light is unnecessary to optical picture processing; however, the laser is by far the best source of high radiant power in plane waveform. In fact, the

---

<sup>1</sup>See note, p. 181.

coherence of the light is a disadvantage, which fact may be derived in the following way.

Let  $\mathbf{I}_A(\mathbf{x})$  be the electric vector amplitude distribution in the focal plane. From linear systems analysis we may express the relationship:

$$D(\mathbf{x}) = \mathbf{I}_A(\mathbf{x})$$

where  $D(\mathbf{x})$  is a linear operation. Using coherent light, the optical system is linear in amplitude, and, in particular, we have:

$$D(\mathbf{x}) = \tilde{A}(\mathbf{x}) = \mathbf{I}_A(\mathbf{x})$$

where  $A(\mathbf{x})$  is the amplitude distribution in the superseding aperture stop, and the tilde ( $\sim$ ) denotes "the Fourier transform of". Now, for a point source in object space,  $A(\mathbf{x})$  is constant everywhere in the aperture and zero outside.  $\mathbf{I}_A(\mathbf{x})$  is furthermore the spread function for that point source, so that we have, by definition, for the transfer function for coherent light:

$$T_A(W) = \tilde{\mathbf{I}_A(X)} = \tilde{A(X)} = A(W)$$

In the case of incoherent light, the optical system is linear in intensity, or the square of the amplitude, hence

$$\begin{aligned} I_I(X) &= D^2(X) \\ T_I(W) &= \tilde{I(X)} \\ &= \tilde{D^2(X)} \\ &= \widetilde{(A(x))^2} \\ &= \tilde{A(x)} * \tilde{A(x)} \\ &= A(W) * A(W) \end{aligned}$$

Here the asterisk denotes convolution rather than multiplication. Thus, at zero spatial frequencies, both coherent and incoherent transfer functions agree. The attenuation at higher frequencies for incoherent light is represented by the size of the overlapping area as the aperture is moved on itself along a spatial frequency axis ( $W = \frac{X}{\lambda}$ ), where  $X$  is the physical dimension (in focal lengths) and  $\lambda$  is the wavelength of light. Thus, the transfer functions have the same high frequency cutoff, but whereas the incoherent transfer function attenuates approximately linearly to zero, the coherent transfer function is constant with a discontinuous cutoff. It may be objected that there are no discontinuities in nature. The answer to this is that the discontinuity is smoothed to the degree allowed by the residual incoherence of the light. The discontinuity is real enough with regard to the problems it creates. Because of Gibb's phenomenon, a truncated Fourier series representing a sharply varying function will "ring". Inasmuch as the effect of the transfer function for coherent light of a lens is to truncate the Fourier series representing the amplitude distribution in image space, any sharp edge in the image will be reproduced with a ringing effect. In addition, any sharp imperfection, such as a lens bubble or certain types of emulsion defects, will also produce rings. The effect is similar to the appearance of a small piece of wood floating on placid water compared with the appearance of the object freshly dropped on the water and thus surrounded by a radially symmetric wake of attenuating periodic wave crests.

In order to alleviate this problem in presently used systems, the United Geophysical Corporation was asked to build an auxiliary device which destroys the coherence of the laser light while preserving its plane waveform.

The device consists of a Dove prism mounted in a cylinder and rotated by an oblique feed of compressed air (fig. 3). A stationary beam entering one end of the prism emerges from the other end with a rotational velocity twice that of the prism.

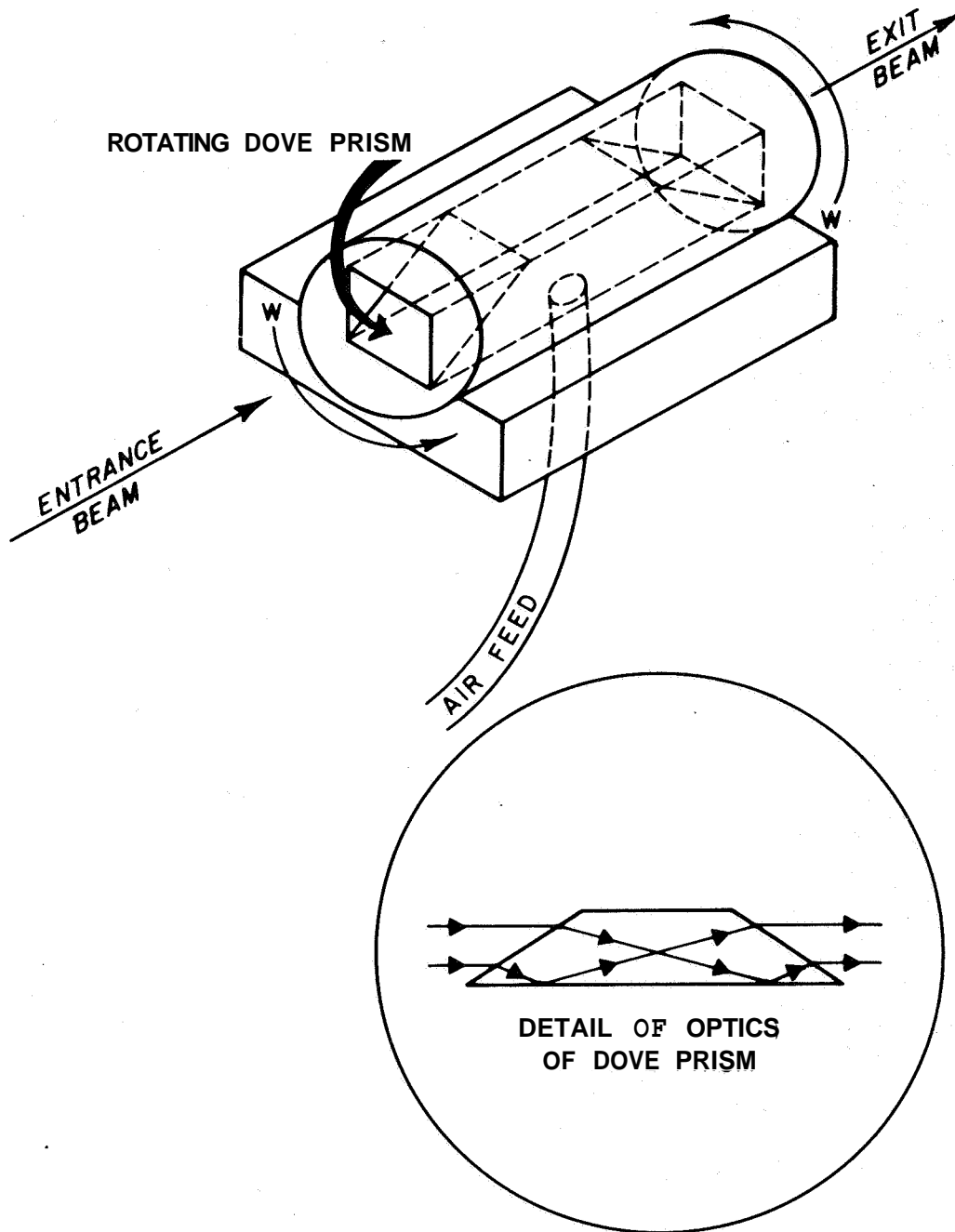


Figure 3.--The Dove prism shown rotates many times over the photographic exposure period used to capture the image of the processed photograph. The result is the partial destruction of the coherence of the traversing light beam.

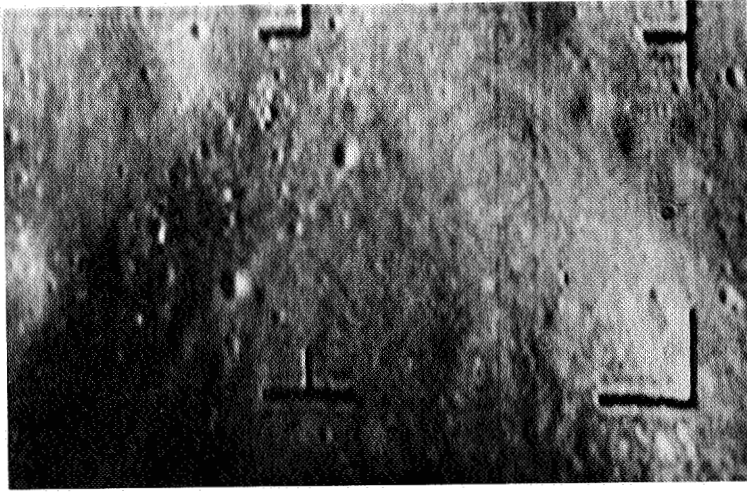
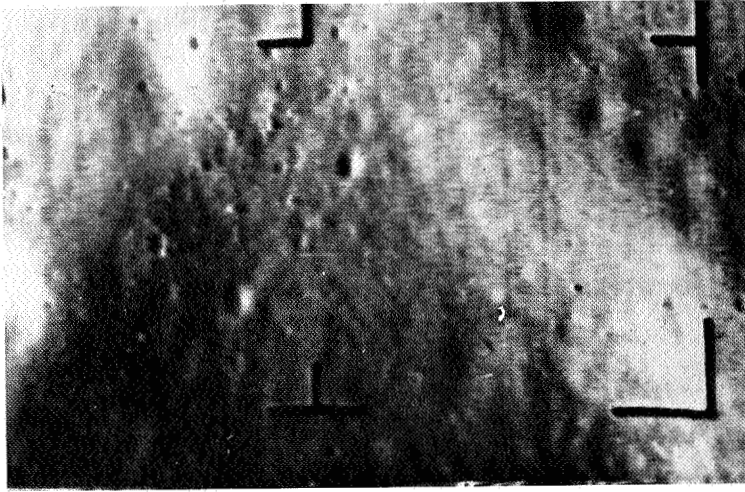
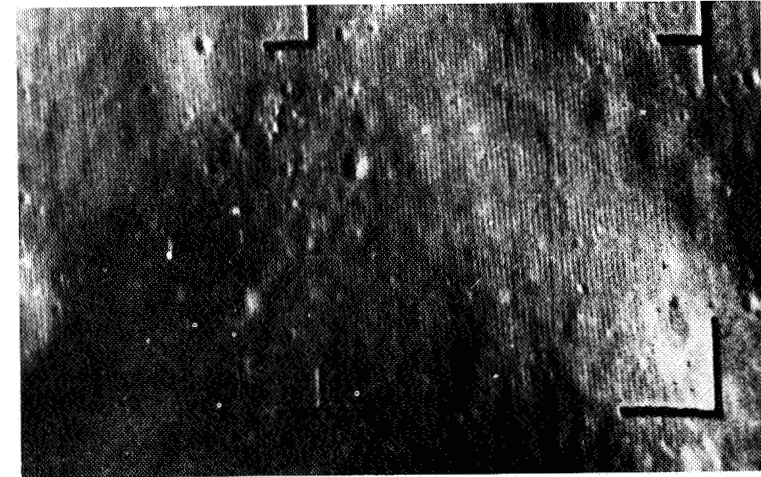


Figure 4.--On left, a specimen of video imagery from Ranger 7; on the right, the results of spatially filtering out the television lines, in which process the spatial frequency spectrum is obtained by diffracting a coherent plane wave with the original Ranger photograph. Note ringing at edges of fiducial marks. Radially symmetric ringing results from lens bubbles and dust specks. Center photograph shows result of processing with a fairly incoherent plane wave obtained by placing a rotating D e prism between the coherent beam and the Ranger photograph. The imperfections are removed.

The device destroys the coherence of the light for time intervals of the order of many prism revolutions or longer because 1) the optical figure of the prism is not perfect and 2) the rotational motion of the device is not smooth to the extent of being without positional perturbations of the order of a fraction of the wavelength of light or larger. The perturbations considered above do not constitute a severe departure from plane waveform, however. The optical system thus continues to operate as it should, except that all lenses have transfer functions without discontinuities so that the Fourier series representations of the images have higher harmonics attenuating to zero even after truncation and thus do not show ringing.

An example of the success with which the device destroys coherence, and thus facilitates the application of spatial filtering to astronomical photographs, is shown in figure 4.

#### Acknowledgments

The construction of the rotating Dove prism was supervised by Mr. Otto Shoenberg. The author is indebted for discussions of this problem to Dr. 's Milton Dobrin, Tom Skinner, and especially Robert Leighton, who, as far as the author is aware, originally conceived of the applicability of a rotating Dove prism in spatial filtering of imagery.

#### **REFERENCES**

- Dobrin, M. B., Ingalls, A. L., and Long, J. A., 1965, Velocity and frequency filtering of seismic data using laser light: *Geophysics*, v. 30, p. 1144.
- Smith, F. D., 1963, Optical image evaluation and the transfer function: *Applied Optics*, v. 2, p. 335.
- Willey, R. L., 1966, Laser scan filtering technique, in *Lunar Orbiter--Image analysis studies report: U.S. Geol. Survey open-file report*, p. 137-142.

NOTE.--It must be remembered that when the diaphragm in the Fourier transform plane removes high spatial frequencies, it does not simply block rays of light but diffracts waves of light. Neglecting aberrations, it is mathematically equivalent to view the action of a simple iris in the mutual focal plane of two collimators of sufficient size--in determining the relationship between the light distributions in the two collimated light beams immediately beyond the two collimating lenses--as equivalent to the action of but one lens in establishing the relationship between light distributions in its image plane and object plane. Thus from the foregoing analysis the diaphragm in the Fourier transform plane can only be viewed to block high spatial frequencies in this simple way when coherent light is used. When totally incoherent light is used, the iris acts as a lens with an incoherent transfer function. If the function cutoff is placed so as to remove the TV lines, the action is equivalent to what would have been obtained in a much less sophisticated way by using a photographic enlarger whose copy lens was stopped down to the required size. The removal is thus accomplished at the expense of degrading information. It is therefore apparent that the destruction of coherence by the rotating Dove prism entails the retention of a high degree of partial coherence, so that the transfer function of the iris is flat out to the highest picture information frequency and then falls smoothly to zero without the undesirable discontinuity.

*same 5*  
N67-31951

APPLICATION OF MOIRÉ PATTERNS  
TO LUNAR MAPPING

By David Cummings and H. A. Pohn *8*

*same p 183 187*  
*R!*

INTRODUCTION

A moiré pattern is the figure produced by superposition, with slight offset or rotation, of two or more repetitive patterns. The patterns used to form the moiré are commonly printed on transparent overlays or screens and may consist of parallel lines, concentric circles, or any other geometrically consistent pattern. Analysis of apparently random patterns can be carried out with the aid of the moiré technique. A screen with a linear repetitive pattern is superimposed on the object being analyzed and is rotated. In certain screen positions, elements of the seemingly random pattern that have a periodicity or preferred orientation are enhanced while other elements are suppressed. The technique therefore facilitates recognition of preferred patterns hidden in a complex background.

Moiré patterns have been used in crystallography to determine imperfections in the lattice, and in refractametry to determine refractive indices, as well as in other fields for other analytical purposes. Moiré patterns have been described by Oster and Nishijima (1963), Nishijima and Oster (1964), and Oster, Wasserman, Zwerling (1964).

This paper focuses attention on the use of moiré patterns in the study of lineaments on lunar photographs. The superposed screen does not produce repetitive elements that are not already present in the photographs. It enables rapid determination of whether or not lineaments are present, and if present, what their

orientations are. Quantitative analysis of lineaments in photographs may be accomplished through use of the theoretical model of Oster, Wasserman, and Zwerling (1964). Such an analysis, however, is not the purpose of this paper.

#### SCREENS AND TECHNIQUE

Two types of screens were used in the examination of lunar photographs: a line screen and a dot screen. The line screen had 26 lines per cm; the width of each line was 0.52 mm. The dot screen consisted of aligned dots, about 52 per cm; spaces between the dots were equal to the size of the dots.

Lineaments are enhanced only when there are certain spatial relationships between photograph, screen, and eye. The relative positions of these three may be determined by trial and error simply by varying the distances between them. The proper distance between screen and photograph depends on four factors: spacing of lineaments on the photograph, spacing of lines on the screen, width of screen lines, and distance between eye and photograph. The proper relationship can be obtained in a manner similar to that described by Minnaert (1954). In our analyses, the distance between screen and photograph ranged from 10 cm to 1 meter.

Rotation of the line screen enhanced photograph lineaments having different orientations when the line screen was properly aligned with respect to the photograph lineaments. Rotating the screen presents all lineament orientations quickly and with little strain to the observer.

The dot screen was used in the same manner as the line screen, but instead of enhancing one set of lineaments at a time it enhanced several because the dots on the screen created "sets of lines" with different orientations. The dot screen, because it brings out the several orientations of lineaments, is even more convenient to use than the line screen. Rotation of the dot screen affects the moiré pattern only slightly because as one set of lines moves from proper alignment, another set is moved into the same orientation. The dot

screen produces spurious image effects such as a fine rectangular grid, which should not be confused with actual lineaments. Rotating the grid causes these spurious images to rotate in the same direction, whereas the actual lineaments retain their orientations.

#### APPLICATION OF MOIRÉ PATTERNS TO LUNAR PHOTOGRAPH INTERPRETATION

Moiré patterns produced by superposed screens have been used to analyze photographs of certain parts of the southern lunar highlands region which are covered by several plains-forming units: a smooth unit, a pitted unit, and a sculptured-plains unit (fig. 1). Weakly developed lineaments can be detected without moiré screens in some parts of the plains-forming units on high-quality continuous-tone photographs of the area. When a line screen is superposed on the top photograph in figure 1, a linear moiré pattern appears (middle photo.) on the sculptured-plains unit but not on the other units. The authors interpret the linear features of the sculptured-plains unit as having been produced by deformation. The pitted unit does not show the linear moiré pattern, and the interpretation is that the pits (craters) are not structurally controlled.

The dot screen was also superposed on the photograph, and several lineament orientations became apparent (fig. 1, bottom photo.). Use of the dot screen on other photographs has revealed that apparently circular craters show slightly polygonal outlines (T. Offield, oral commun.).

When screens are used on photographs in which the image is comprised of a series of lines (Lunar Orbiter or Ranger photos.), these lines will produce moiré patterns. These moiré patterns are easily distinguished from moiré patterns that reflect lunar surface features.

#### CONCLUSIONS

Moiré patterns produced by screens can be used for easy and rapid examination of lunar photographs to determine the presence of subtle lineaments. The advantage of this method is apparent where many photographs must be examined in a relatively short period

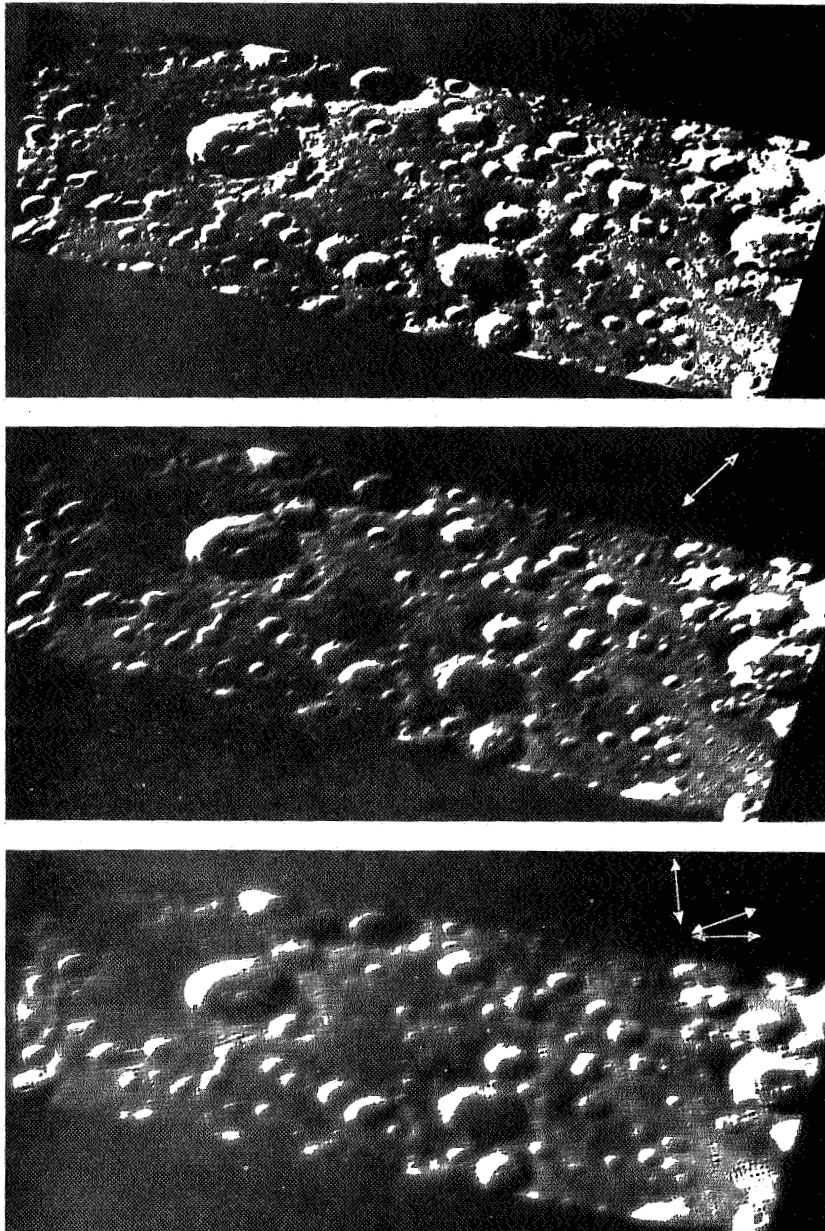


Figure 1.-- Enhancement of lineaments by superposition of transparent screens. Top, Photograph (Lick Observatory L-31, portion) without overlay. Middle, Line screen superposed on photograph. The orientation of the line screen enhances a family of lineaments parallel to the direction of the arrow. Bottom, Dot screen superposed on photograph. Several families of lineaments can be seen parallel to the direction of the arrows.

of time. The technique, of course, can also be used for interpretation of terrestrial photographs.

#### REFERENCES

- Minnaert, M., 1954, *The nature of light and color in the open air*: New York, Dover Pubs., Inc. , 362 p.
- Nishijima, Yasunori, and Oster, Gerald, 1964, Moire' patterns--their application to refractive index and refractive index gradient measurements: *Optical Soc. America Jour.* , v. 54, no. 1, p. 1-5.
- Oster, Gerald, and Nishijima, Yasunori, 1963, Moiré patterns: *Sci. Am.*, v. 208, no. 5, p. 54-63.
- Oster, Gerald, Wasserman, Mark, and Zwerling, Craig, 1964, Theoretical interpretation of moiré patterns: *Optical Soc. America Jour.*, v. 54, no. 2, p. 169-175.

10/2/67

**N67-31952**

THE PROCESSING OF  
PHOTOCLINOMETRIC DATA

8 wref 189 19 RS  
same

By Alexander J. Swartz

The U.S. Geological Survey is currently developing an improved system for processing photoclinometric data. The primary goal of this system is to maximize the ratio of work done by the computer relative to manual reduction.

Photoclinometry is a technique for determining one component of terrain slope (in the phase plane) as a function of the variation of the lunar surface brightness in an area of constant albedo (van Diggelen, 1951; Watson, 1967). As an applied scientific domain, photoclinometry has been utilized in the reduction of Lunar Orbiter data and the selection of Project Apollo landing sites. Slope data can be obtained along lines passing through a point at the lunar surface which is the intersection of a line through the Sun and spacecraft (lens nodal shadow point). The photoclinometric technique, though partially degenerate in the topographic degrees of freedom, theoretically can provide quantitative topographic information from high-resolution photographs lacking the overlap needed for stereoscopic viewing.

Rapid processing techniques are required to handle the large amounts of data available. There have been two approaches to the problem thus far. The first, recently made operational at the National Aeronautics and Space Administration's Manned Spacecraft Center, uses the analog tape of the spacecraft telemetry detections as a data source. The second, implemented jointly by Langley Research Center and the U.S. Geological Survey, obtains data by photometric scanning of the reconstructed photographs along phase lines. The main drawback to the first method is that data must be transferred from the analog magnetic tape to the digital format

required by the computer. The recorded analog data rate is about eight times the digital conversion rate.

An advantage of the second approach is that density data are obtained directly along the phase plane intersection with the surface rather than along consecutive raster scan lines of the photograph. The data subset for a given photoclinometric reduction comes from the one-dimensional subspace of the picture (as a two-dimensional space) that is thus obtained. Because the picture raster lines are arbitrarily oriented, it is difficult to sort all the two-dimensional density data of the raster scan lines from the analog data tape. The present technique therefore reduces the amount of data processing required by an order of magnitude.

In addition to these advantages, the second method can be applied to original photographs returned from future manned lunar missions. In this report, all subsequent references to photoclinometric data processing will be to the second method.

The system being developed by the U.S. Geological Survey represents an improvement in the second method. The system's contributions involve more efficient data-handling procedures.

Various data are placed along the edge of each framelet for the purpose of calibration. One of the most important of these "edge data" items is the grayscale. The grayscale gives a quantitative measure of the photographic response of the particular segment of the film containing the associated framelet. Using this piece of edge data, the H and D curve (density vs. log exposure) is developed entirely on the computer.

The following method is used: A scan is made of the grayscale using the Joyce-Loebl Microdensitometer and Beckman-Whitley Isodensitracer combination (IDT). The density values are digitized and stored on magnetic tape. The digitizing apparatus attached to the isodensitracer maps the continuous analog density acquired from the film into a sequence of numbers, each of which correspond to one of 168 discrete density intervals. When the section of the tape containing the entire grayscale scan is read into the computer,

the machine ascertains the number of grayscale data points falling in each of the 168 discrete density intervals. A histogram is formed of the frequency distribution of the film data density that is characteristic of the grayscale. Nine discrete exposure steps in the original calibration are provided by the grayscale. Ideally therefore, the resulting histogram should have nine peaks. The machine next selects the densities corresponding to these peaks. The mesh of the histogram is sufficiently fine that spurious peaks, arising solely from the random error of the photographic grain, may appear in this step. These peaks are eliminable by certain of their properties, such as improbably close agreement in density or improbably high frequency of the minima separating them. Under such circumstances, the desired density value is represented by two peaks. This problem is solved by comparing the above histogram with histograms constructed with broader mesh.

The result of the above procedure is a noise-filtered set of density-exposure pairs which constitute the empirical density-log exposure relationship. A least-squares fit is then made, permitting the nine density values to be mapped into the nine known exposure values. These exposure values are an integral part of the preflight calibration of the Lunar Orbiter camera. A third-degree polynomial is fitted which provides the requisite inflection point. The empirical function best suited to this fitting procedure requires further study, but a third-degree polynomial provides a practice function for program debugging. Beyond this, all mapping of image density information into normalized brightness is encompassed by the data processing procedure.

Data are fed into the program in two sets: the picture parameters and the actual point densities. The picture parameters are used to calculate the transformation matrix and the image coordinates of the lens nodal shadow point. The individual point densities are mapped into normalized brightnesses, which in turn are mapped into individual point slopes (Watson, 1967). The second mapping entails the use of a resident photometric function with a table look-up procedure.

At the present time no corrections have been attempted for the ostensible periodic errors encountered in the photographs. However, the subroutine structure of the program will permit the introduction of a periodic compensating subroutine at a later date. These systematic errors, however, must be minimized if consistently meaningful results are to be obtained from photogrammetry.

The reduced data (object space coordinates, point slopes, normalized brightness, phase angle, brightness longitude and brightness latitude) are put on magnetic tape to facilitate further processing. In addition to the development of a series of slope-profile (partial topographic) solutions, such data can be used in conjunction with photogrammetry to study the regional high-resolution light-scattering properties of the Moon.

The primary programming difficulties thus far have stemmed from the differences in the isodensitracer magnetic tape output format and the input format required by the FORTRAN computer language. These difficulties are irresolvable purely in the context of FORTRAN. Solutions were sought among the capabilities of PL/I, but without success. The most promising method seems to be a combined assembly-language--FORTRAN program. This is however a machine-oriented solution, dependent on the assembly language associated with the particular computer and therefore lacks the flexibility desired.

The main contribution of the system being developed by the U.S. Geological Survey will be, in addition to the data-handling improvements mentioned above, the use of a table look-up procedure in mapping via the photometric function. The photometric function resides in on-line storage as a matrix whose columns represent constant phase angles and whose rows represent constant normalized brightnesses. The elements are the corresponding brightness longitudes. This layout provides the most efficient computer access to the photometric function.

The manipulation of data by technical personnel has been the point of breakdown in the efficiency of second-method systems used

to date, notably the Langley Research Center program. The system being developed should move the stricture in efficiency to its logical place in the procedure: the speed limitations of the isodensitracer apparatus itself.

A device called a Programmed Light Source (Information International, Inc.) is available for spatial microphotometry. In sampling a given area, it reduces by two orders of magnitude the scanning time required by the device currently employed (IDT). However, at its current stage of development, it fails to meet some of the specifications for accuracy required for a meaningful analysis of data. In the near future, the device should be developed to the point that it can fulfill the requirements. Its operation may provide a data rate competitive with magnetic tape input, so that eventually it could be developed into a regular on-line density input device. This last improvement would reduce the overall data processing time by an additional order of magnitude.

The author is grateful for the extensive programing assistance rendered to date by Mr. Jay Ridgely, U.S. Geological Survey.

#### REFERENCES

- Diggelen, J. van, 1951, A photometric investigation of the slopes and the heights of the ranges of hills in the maria of the Moon: Netherlands Astron. Inst. Bull. , v. 11, no. 423, p. 283-289.
- Watson, Kenneth, 1967, Photoclinometry from spacecraft images: U.S. Geol. Survey Prof. Paper 599-B (in press).

N67-31953

THE NGCTURNAL HEAT SOURCES  
OF THE SURFACE OF THE MOON

By Robert L. Wildey

1967  
209 RS  
2000

SUMMARY

A map of the thermal surface brightness of lunar regions darkward of the sunset terminator, together with a positional chart of a large number of nighttime hotspots, has recently been made by telescopic reconnaissance in the 8-14  $\mu$  region. Nine additional thermal anomalies and a morphological analysis of the signal properties of these anomalies are presented here. The extraction of information by this process has been carried to the limit allowed by system noise. Attempts to regain the cooling curves of anomalies themselves provide information suggestive that the anomalies are not all volcanic, a fact previously suspected but never observed directly. In addition it may be concluded that two categories of anomalies are present on the Moon's dark side, not including "false" anomalies of the "delayed sunset" type in which surface prominences are illuminated for some time after sunset on the surrounding lowlands.

INTRODUCTION

Early mapping of the thermal emission of the full Moon by Geoffrion, Korner, and Sinton (1960) disclosed no peculiar selenographic variations beyond the small amounts to be expected by the known variations in the absorptivity to solar radiation. Later it was discovered by Shorthill, Borough, and Conley (1960) that Tycho cooled much more slowly during a lunar eclipse. Still later, when recently developed photoconductors could be applied to the much more difficult problem of measuring thermal radiation from the much colder surface of the Moon during lunar nighttime,

hotspots were also found, one of which coincided with Tycho (Murray and Wildey, 1964). Since that time such thermal anomalies have been mapped over both the face of the eclipsed Moon by Saari and Shorthill (1965) and the lunar nighttime surface by Wildey, Murray, and Westphal (1967). Determination of selenographic coincidences in the two collections of hotspots, thus observed is difficult because of the greater uncertainty in the locations of anomalies of the lunar nighttime. The infrared signal from the telescope environment is small enough compared with the signal from the eclipsed Moon that the photometer can be rapidly and accurately moved along a precise raster in the focal plane, using a precision two-dimensional engine, while the telescope tracks a fixed lunar point. During lunar night, the infrared signal from the Moon is so small that the slightest movement of the photometer in the focal plane produces a change in the net background radiation--even with complex baffling systems--that overwhelms the signal (Wildey, 1966). It is the pointing of the telescope itself, which is of inferior accuracy, augmented by various techniques of providing periodic lunar ground control (Wildey and others, 1967; Wildey, 1964), that must be monitored for the retrieval of selenographic positions. Nevertheless, it may be reasonably concluded that many, but not all, of the nighttime hotspots are also eclipse hotspots.

Two explanations for the nocturnal hotspots are a priori conceivable: 1) they are magmatic in origin and therefore intrinsic heat sources, 2) they result from the slower cooling of relatively more efficient solar heat reservoirs. (The aforementioned reservoirs are visualized as concentrations of more consolidated lunar material--material with relatively high thermal conductivity). A third explanation, which makes the effect spurious in the sense that the hotspots are unrelated to crustal conditions, is that a spot may be a surface prominence and therefore illuminated for some time after sunset on the surrounding lowlands. The writer has observed such isolated spots of illumination and later, when

the entire terrain was dark, found strong infrared anomalies. Because this is largely a delayed sunset effect, it produces strong hotspots near the terminator but very weak ones well into the dark part. Such hotspots are often further eliminable through examination of lunar topographic maps. It is clear from eclipse geometry that this explanation is only admissible for nighttime hotspots. Hotspots of the third type probably do not significantly affect the data discussed herein.

True hotspots have been previously supposed to represent anomalies of heat conductivity. There are four reasons for this conclusion: 1) The hotspot prototype, Tycho, is a radar back-scattering anomaly suggestive of boulders of the order of a meter across (Pettengill and Henry, 1962); 2) a search for hotspots in the vicinity of Tycho when near the morning terminator was unsuccessful (Murray and Wildey, 1964) though perhaps not exhaustive (hence suggesting a lack of the constancy to be expected of intrinsic heat sources); 3) the geologic superposition and high normal albedo of Tycho (Wildey and Pohn, 1964; Pohn and Wildey, in prep.) suggest that it is young and relatively unexposed to the disintegrative forces of cosmic erosion; and 4) the actual eclipse cooling curve observed by Sinton (1960) is compatible with a theoretical cooling curve for a simple material of appropriate heat conductivity without sources or sinks. The crucial evidence provided by the cooling curve of a nighttime anomaly has never been published and to do so reliably would be very difficult. What has not been eliminated by previous work is the possibility that two kinds of anomalies exist. This possibility is strengthened by the evidence of lunar vulcanism detected in Lunar Orbiter photographs.

#### OBSERVATIONS

The hotspots of the supplementary collection presented in this paper (table 1) were observed in precisely the same manner as those in the main collection reported by Wildey and others (1967) ;

Table 1.--Supplementary tabulation Of the nocturnal hotspots of the Moon

Note	Local date (1964)	$\lambda^\circ$	$\alpha^\circ$	H/W	W/R	$\Delta I/I$	$\Delta I(10^{-4})$	$\lambda-\lambda_c$
1	Aug. 30	58E	29S	1.0	1.5	1.60	11.0	60.7
2	30	21E	20s	-1.0	1.0	.15	4.0	23.7
3	29	17E	1s	1.0	1.0	.10	5.6	7.5
4	29	33E	2N	.5	2.0	.30	8.0	23.5
5	29	36E	1N	1.0	4.0	.60	13.0	26.5
6	29	43E	3N	.5	2.0	.40	5.7	33.5
7	28	35E	10N	.4	2.5	.10	4.3	13.3
8	29	42E	7N	1.0	1.5	.40	6.0	32.5
9	28	59E	4N	.3	3.0	.50	6.5	37.3
10	29	26E	10N	4.0	3.0	.80	30.0	16.5
11	30	11E	28N	2.0	1.0	.38	16.0	13.7
12	29	25E	22N	.8	3.5	.30	12.0	15.5
13	28	29E	23N	.5	1.5	.05	2.8	7.3
14	28	39E	25N	1.0	1.0	.10	3.5	17.3
15	28	44E	26N	.5	2.0	.20	5.8	22.3
16	28	18E	31N	2.0	1.0	.10	3.7	3.7
17	29	38E	53N	.7	2.0	.50	17.0	18.5
18	30	10E	53N	4-8	1-2	1.20	52.0	12.7
19	28	13E	54N	1.0	1.0	.10	8.3	8.3
20	30	4E	58N	2.0	1.0	.20	17.3	-17.3
21	29	49E	54N	1.0	1.0	.20	2.4	39.5
22	28	73E	53N	.6	1.3	.40	3.4	51.3

NOTES

1. Signal reproduces, with definite structure, central dip about 15 percent fainter than peak. Crater Snellius, highlands.
2. Reproduces; appears to be a genuine cool spot, but marginally small. May be relative dip in very broad and shallow hotspot. On Altai Scarp, uplands-transitional.
3. Lack of signal reproducibility may often be due to slight track irreproducibility. Between small fresh appearing halo crater Theon Senior and much larger crater Delambre, highlands.
4. Not pronounced, not reproduced. Appears to be highland peninsula projecting in Mare Tranquillitatis. Positional errors are large enough to allow association with crater Maskelyne.
5. Definite signal structure, lower shoulder on east. A small bay of Mare Tranquillitatis, maria.
6. Not pronounced not reproduced. Crater Secchi, maria. Limb of moon definite signal drop this scan.
7. Reproduces; signal is broad and flat topped with peak twice as high on west end. Plain maria with a few very tiny craters scattered in vicinity.
8. Not on scan reversal. In mountain chain of highland isthmus between Tranquillitatis and Fecunditatis.
9. Reproduces; signal rise is very broad, continuous through saddle with immediately preceding sharper hotspot, has real "relative" cold spot just west of center, though not an "absolute" cold spot. Infrared corresponds nicely with extension of upland mountains into Mare Fecunditatis, with mare bay corresponding to relative cold spot.
10. Reproduces; definite structure--cooler shoulder on west. In Mare Tranquillitatis, association with small crater of proximity less than positional uncertainty is possible.
11. Reproduces; definite cooler western shoulder. Bland open maria. Bright (visible) spot Linné 2° SE. Nothing else available for possible correlation.
12. Reproduces; signal spike is broad with gently sloping sides. Part of the rille in Mare Serenitatis.
13. Reproduces; signal shows gentle east shoulder. In Mare Serenitatis, corresponds to crossing of straight bright (visible) band (crater ray?) running south from mountain at tip of Le Monnier's archipelago.
14. Reproduces; rugged uplands.
15. Reproduces; broad, flat-topped signal. May be associated with sharp-bordered darker region in upland.
16. Reproduces; very close to terminator. Anomaly was close to terminator but not really illuminated. The negative longitude from terminator results from a combination of small placement error and, larger, libration of the terminator. The latter effect was not large these nights, is zero in the statistical average, and the labor of correcting for it was not exercised. There are several very small bright spots and bright halo craters scattered in this region of Mare Serenitatis.
17. Reproduces; very broad, shallow. Highland isthmus between Mare Frigoris and mare-filled crater Endymion.
18. Reproduces; cool west-side shoulder. Mare Frigoris, bright-halo crater within 1°.
19. Reproduces; not really illuminated. Tall mountain peak--very possibly delayed-sunset type of anomaly.
20. Reproduces; not really illuminated, libration of terminator makes polar anomalies poor subjects for analysis. Reduced position is in open maria (Frigoris) but very close to crater (fairly large) Archytas.
21. Not on scan reversal. Cratered uplands west of Endymion.
22. Reproduces. Dark area in highlands near limb.

the total observed is now 119. The instrumental limitations have been detailed elsewhere (Wildey, 1966). The new hotspots are fainter than most of the others (Wildey and others, 1967). Each was observed twice, except where noted otherwise. All the previously tabulated hotspots (Wildey and others, 1967) were observed twice. Some of the entries were previously presented but are reproduced here because they have signal structure. The structure, not previously described, is detailed in the footnotes. The value of the photometer's spatial resolution is 45 km at the subearth point. The accuracy in location of hotspots is within about 90 km. A computerized system for position recovery showed a repeatability in telescope pointing of nominally 30' of selenodetic arc (Wildey, 1964) over a several-hour period when the telescope was newly installed; however, during the succeeding year the repeatability deteriorated and the system was abandoned. In its place, monitor photographs of the position of the photometer aperture on the Moon's bright side were used for time-location fixes at the beginning of each drift of the telescope onto the night side. Position location on the night side then follows in each drift by extrapolation of the one-to-one correspondence between time and selenographic coordinates that is thereby established.

I in table 1 represents true surface brightness--alternatively termed specific intensity or luminance. Its absolute units are watts per  $\text{cm}^2$  per steradian/ $\Delta\lambda$ , and it is directly proportional to the photometer signal in the case of an extended object. The unit of **AI** used in column 8 is the thermal surface brightness of a water-ice blackbody.  $\Delta I/I$  is the ratio of peak brightness (hence signal voltage) excess of an anomaly to the brightness (or signal voltage) of the surrounding region. H/W is the ratio of the height of the heat spike on the recorder trace to its width, W/R is the ratio of the width of the signal spike to instrumental resolution, and  $\lambda - \lambda_t$  indicates time-since-sunset ( $\lambda_t$  is the average longitude of the lunar terminator) but is inaccurate in the regions of extreme latitude.

## ANALYSIS

As much information as possible regarding the cooling curves of hotspots should be extracted, bearing in mind that the accuracy of the data is limited by procedural shortcomings. The hotspots tabulated in this and the previous paper (Willey and others, 1967) were observed on 3 consecutive nights. Many of the anomalies are close enough together that they may be manifestations of the same agent observed on 2 separate nights. In making this assumption in order to obtain the brightness changes of hotspots, one obtains a new collection of data in which the signal-to-noise ratio is greatly reduced. The primary noise associated with any such comparison is not the photometer noise exhibited on the primary data traces. It arises from an aliasing error associated with the inexactness of the interidentifications. The associated signals are not likely to have emanated from identical areas of the features emitting anomalously, and some anomalies are associated which are not, in fact, due to the same lunar feature. Even though the resulting noise is much higher, there is no reason why it should not be random, allowing some information to be reliably extracted.

The brightness excesses for associated anomalies are represented in figure 1 by vectors. The positions of the two ends of each vector represent the brightness excesses on 2 separate nights. The system noise is obviously very high. Some of the vectors even indicate brightness increases, probably unreal. The figure does, nevertheless, show that the hotspots, as an entire system, do decay in thermal brightness with time after sunset. If all the hotspots were volcanoes, heat excesses they represent should approach a constant value in time shortly after detectability was achieved.

"Normal" cooling curves eventually flatten with time, but only after brightness has been greatly reduced by cooling. Although a variable bolometric correction has been neglected, it also should approach a constant value for the case of an intrinsic heat source. We therefore conclude that this is positive evidence that many of

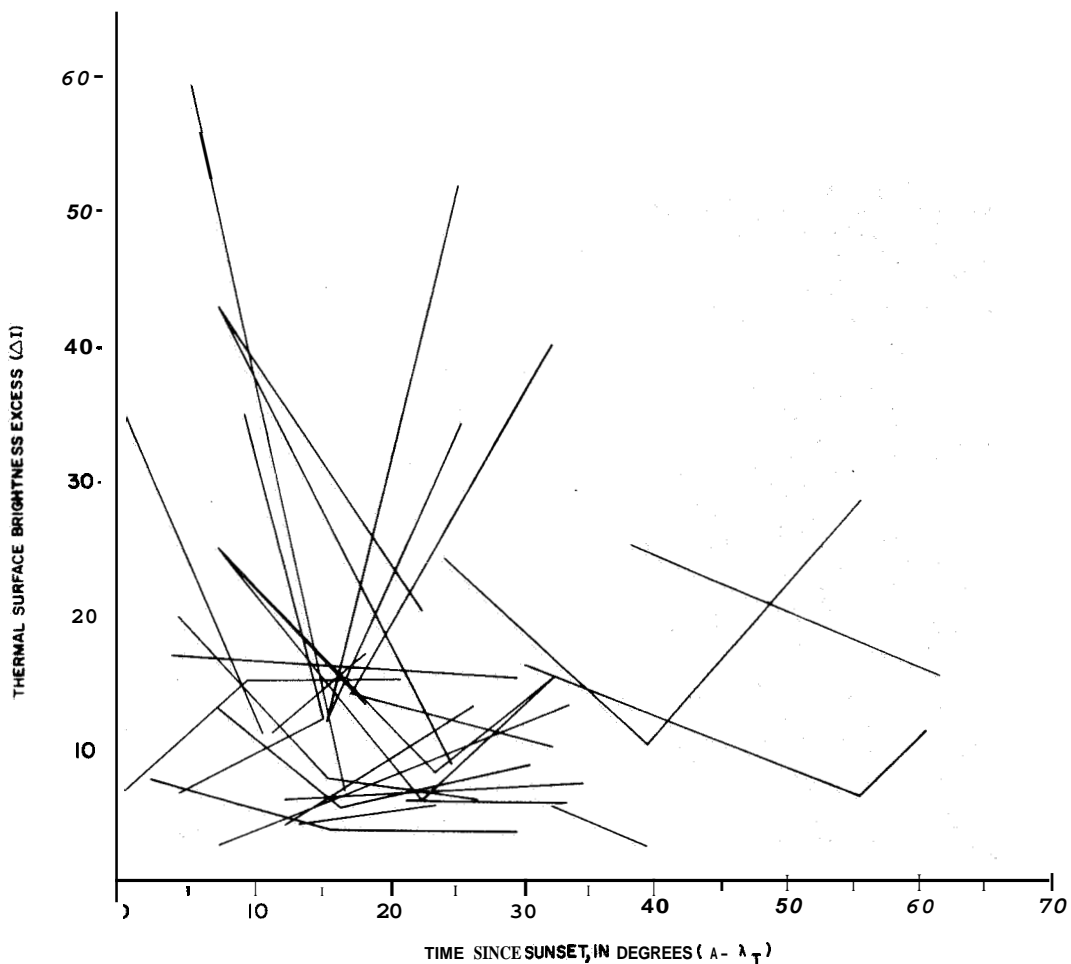


Figure 1.--Vectors representing changes in observed brightness excess (wavelength 8-14 $\mu$ ) for hotspots assumed to be reobserved on later nights. The unit of specific intensity is the surface brightness of a 273" K blackbody. For very close hotspots observed the same night (closer than absolute position uncertainty), all positionally possible associations for other nights are allowed.

the hotspots are not volcanoes or near-surface magma chambers.

The data can be further utilized to determine differences between the average cooling curves of the hotspots and the cooling curve of the "normal" lunar surface (Wildey and others, 1967). The latter is very reliable because it comes from a brightness versus longitude observation rather than the observation of true temporal variations. It should be remembered that the average curve for hotspots may represent a composite of various classes of thermal phenomena. In the averaging the noise level will be reduced in the resulting diagram. Unfortunately, sacrifice of homogeneity in the amalgamation cannot be avoided. Because the magnitudes of the vectors in figure 1 depend upon whether the anomalous region completely fills the focal plane aperture, differences in  $\ln AI$  must be considered, rather than differences in  $AI$  itself. The vectors in figure 1 were thus transformed and the resulting slopes were averaged every 2" in longitude. They are plotted as the points in figure 2. The points represent a plot of the differentiation of the average cooling curve for hotspots, somewhat poorly resolved (that is, the incremental mesh is about 10"). The solid curve in figure 2 has been obtained for comparison from the cooling curve of the normal lunar surface in the following way: At every 2" in longitude the difference in  $\ln I$  5" to either side has been divided by 10" and the result plotted in figure 2. The effects of different bolometric corrections for the 8-14  $\mu$  excesses as compared with the local "normal" lunar background radiation are again neglected, but they cannot explain the magnitude of the following features: (a) The curve for hotspots is far from being merely a phase-shifted version of the normal curve, and therefore few of the hotspots are the delayed sunset type. (b) The curve for hotspots is generally less negative, showing that they are cooling more slowly than the normal terrain over the entire range of observation. (c) The delay in the point of inflection of the cooling curve for hotspots (in figure 2--the initial minimum),

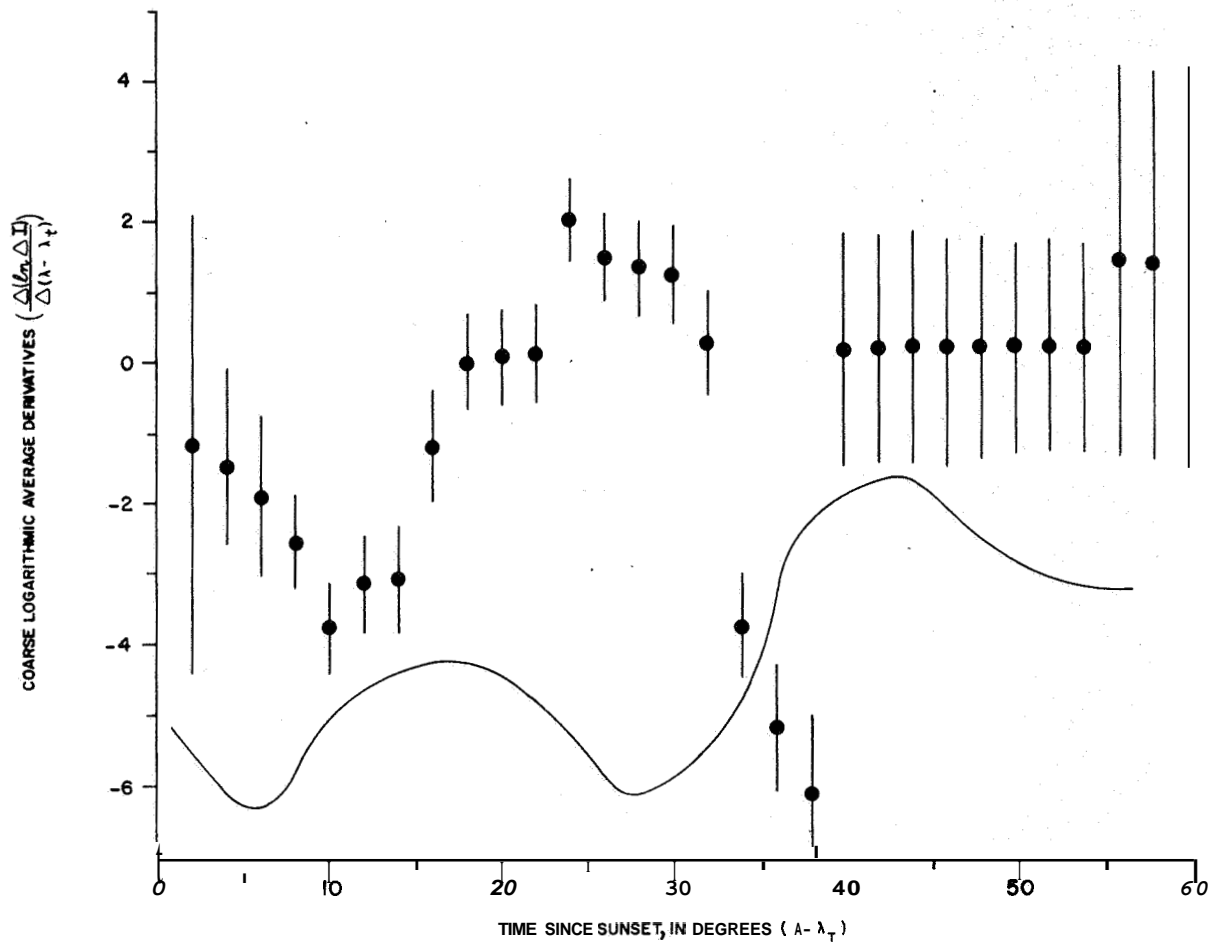


Figure 2.--Averaged derivatives  $\Delta(\ln\Delta I)/\Delta(\lambda-\lambda_t)$  corresponding to averaged slopes of vectors in figure 2 for every 2" in longitude. Vertical bars represent formal probable errors computed by assuming that each vector is statistically independent of all others. Of course the data points computed do not possess resulting errors that are completely independent of the errors of adjacent data points. The curve corresponds to the cooling after sunset for the normal lunar surface, appropriately converted to the natural logarithm of  $8-14\mu$  brightness and differentiated with appropriate coarse increments as described in the text.

as compared with the normal curve, would be expected if only the heat conductivity were increased, whereas a medium of the same conductivity containing a heat source would have an earlier inflection, if anything, as the heat source began to produce an artificial lessening of the normal cooling; however, a phase delay in the inflection point is a conceivable property of the curve representing the phenomenological mixture. These conclusions, which stem from wide-range general characteristics of the plot, are reasonably sound. Certainly a detailed comparison of the points and the curve in figure 2 is unwarranted by data reliability, especially at large values of  $\lambda - \lambda_t$ .

In an attempt to associate possible morphological features of the signal from infrared anomalies with the nature of terrain, they have been divided up on the basis of the physiography into four classes: (1) What appear to be craters in highlands, (2) craters in maria, (3) what appear to be mountainous regions of a more "normal" (earthlike) character or old rugged uplands where superposition is not easily delineable and in which no dominant single object is noted, and (4) open maria where no visible features appear to be responsible for the anomaly. The width-to-resolution ratio has been chosen as one infrared feature to be so associated, and the infrared excess as another. They are plotted as dots and crosses, respectively, in figure 3.

Of the four classes of terrain present where the anomalies were discovered, no distinctions with regard to  $W/R$  and  $\Delta I/I$  are exhibited with the sole exception that anomalies in open maria tend to be larger. The largest few are also the clearest cases of truly open maria where a small bright halo crater is not uncomfortably nearby just at about the limits of positional accuracy.

In figure 4 this approach is carried to a three-dimensional classification in which width-to-resolution is plotted against relative infrared excess. **For** the third dimension of terrain classification we have used three morphological groupings: (1) Anomalies

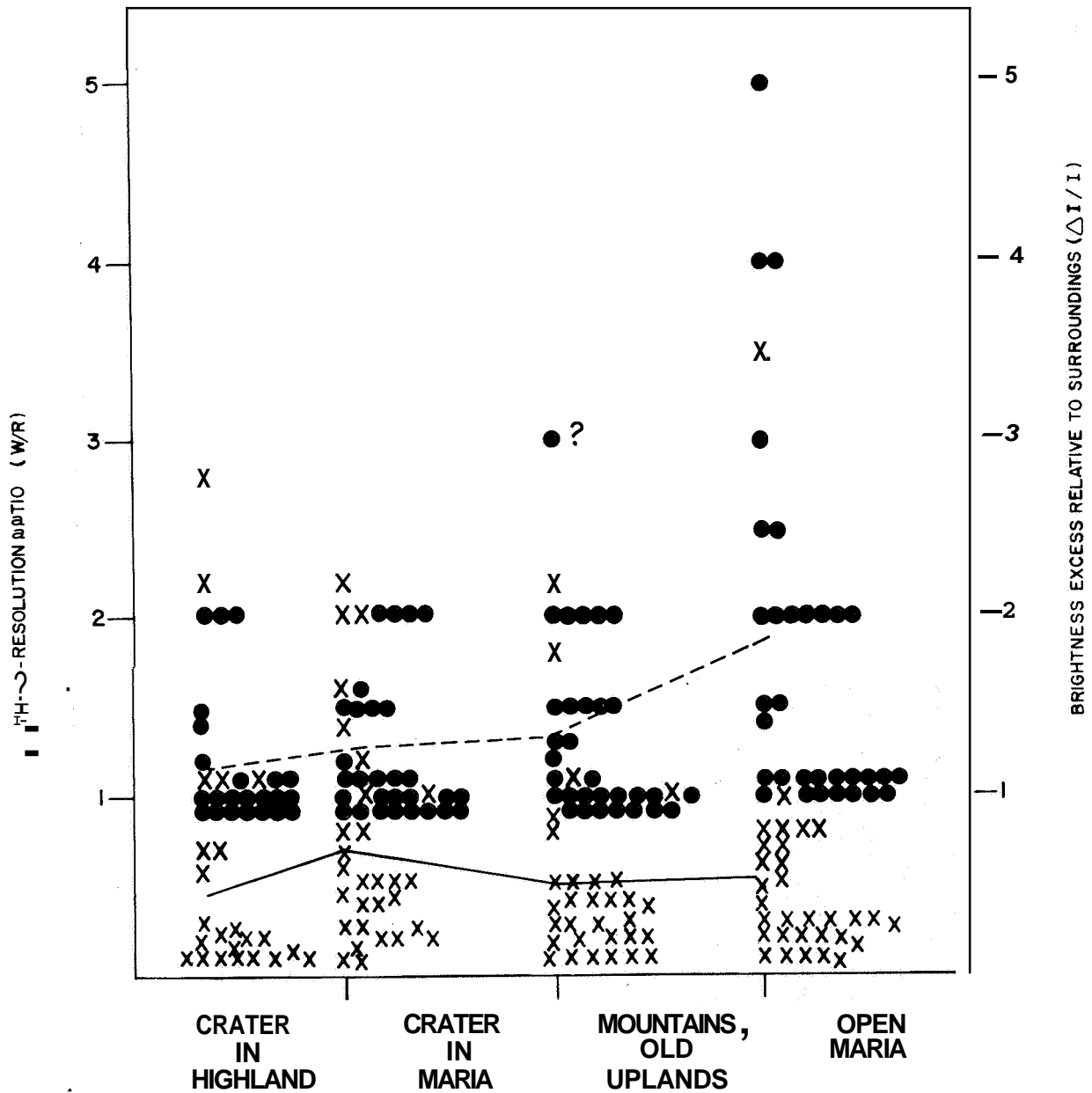


Figure 3.--Width-to-resolution ratio of signal trace of a lunar hotspot (dots) and relative 8-14μ brightness excess (crosses) versus terrain classification for all nighttime anomalies. Variation of average is represented by dashed line (for ΔI/I) and solid line (for W/R).

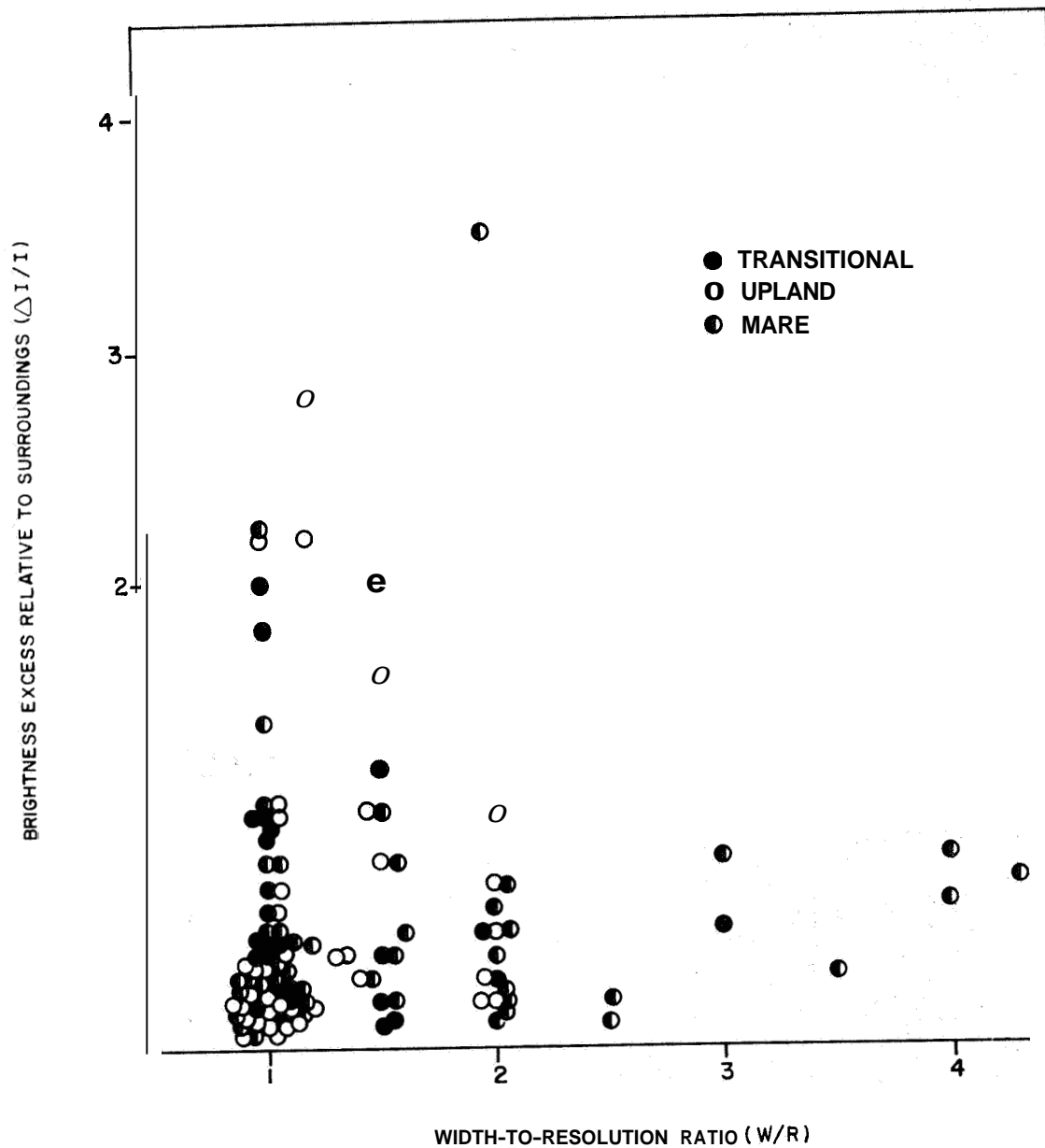


Figure 4. --Width-to-resolution ratio versus relative infrared excess brightness for all nighttime anomalies. Those on maria are represented by half-filled circles while those on uplands and in transitional regions are plotted as open and filled circles, respectively. Note apparent forbidden region.

in maria, (2) those on uplands, and (3) those in the transition region (within a resolution of a maria border). The greater discriminating power of this plot expands upon the dichotomy emerging in figure 3. A general trend appears to be that an extensive anomaly will not be very strong and a strong anomaly will not be very extensive, as indicated by what appears to be a forbidden region in figure 4. Of the three types which populate the diagram, all seem to be uniformly represented except that by far the largest eight only include one transitional case. The very large clumping of points at the limits of detectability (the represented spread is larger than it should be in order that all points could be plotted in a page-size illustration) indicates that only a fraction of the size distribution of the anomalies is found above the photometer resolution. Otherwise it is necessary to explain why such a sharp cutoff exists, and why it coincides with photometer resolution.

A final important feature of this morphological approach is the actual fractional division of hotspots in the last three categories. About 25 of the hotspots observed occur in the maria and about 35 in the uplands, while the category "transitional" totals nearly 60. The concentration in the third class is all the more impressive considering the fraction of the lunar disk covered by the three classes.

#### CONCLUSIONS

While figures 1 and 2 show that the Moon's nocturnal hotspots do not consist exclusively of intrinsic heat sources, figure 4 shows that there are at least two phenomenological types of hotspots. In one class we have very small, but intensely hot features, whereas the other class, whose warmth is never but a small fraction of that of the first class, may be as much as a few hundred kilometers in size. Any attempt to integrate these classes under a single physical cause must provide the peculiar evolutionary connection which explains the forbidden region of figure 4. It seems

more simple to explain them as a collection both of magmatic heat sources and regions of more highly consolidated rock, or perhaps conductivity anomalies on the whole, part of which arise from the exposure and fusion resulting from impact and the balance from magma solidified too recently to have reached the steady state conductivity which cosmic agents of erosion, transport, and sedimentation produce. To further substantiate this explanation, it is noted that the somewhat higher concentration of hotspots near mare borders cannot arise purely through the production of fused surface materials and exposure of subsurface rock through meteoric impact without an agent of selective disintegration of the consolidated material thus formed that is especially weak near mare borders. Certainly the original distribution of impact will not favor mare borders. That we should therefore expect an internal origin for this concentration is compatible with the recent discovery by Middlehurst (1966) that the various types of lunar transient phenomena which have been recorded over the last 300 years tend to concentrate along mare borders.

#### REFERENCES

- Geoffrion, A., Korner, M., and Sinton, W. M., 1960, Mapping the daytime lunar temperature: Lowell Observatory Bull. 5, p. 1.
- Middlehurst, B. M., 1966, An analysis of lunar events [abs.]: Am. Geophys. Union Trans., v. 47, p. 150.
- \_\_\_\_\_, 1966, Transient changes on the Moon: Observatory, v. 86, p. 239.
- Murray, B. C., and Wildey, R. L., 1964, Surface temperature variations during the lunar nighttime: Astrophys. Jour., v. 139, p. 734.
- Pettengill, G. H., and Henry, J. C., 1962, Enhancement of radar reflectivity associated with the lunar crater Tycho: Jour. Geophys. Research, v. 67, p. 4881.

- Pohn, H. A., and Wildey, R. L., A photoelectric-photographic map of the normal albedo of the Moon: U.S. Geol. Survey Misc. Geol. Inv. Map (in prep.).
- Saari, J. M., and Shorthill, R. W., 1965, Infrared observations of the lunar eclipse of December 1964: *Nature*, v. 205, p. 964.
- Shorthill, R. W., Borough, H. C., and Conley, J. M., 1960, Enhanced lunar thermal radiation during a lunar eclipse: *Astron. Soc. Pacific Pubs.*, v. 72, p. 481.
- Sinton, W. M., 1960, Eclipse cooling of Tycho: *Lowell Observatory Bull.* 5, p. 25.
- Wildey, R. L., 1964, A computer program for the transformation of lunar observations from celestial to selenographic coordinates: *Icarus*, v. 3, p. 136.
- \_\_\_\_\_ 1966, Far-infrared stellar astronomy: *Internat. Astron. Union Symposium* 24, p. 267.
- \_\_\_\_\_ 1966, Ten micron stellar flux measurements--synopsis and diagnosis: *Zeitschr. für Astrophysik*, v. 64, p. 32.
- Wildey, R. L., Murray, B. C., and Westphal, J. A., 1967, Reconnaissance of infrared emission from the lunar nighttime surface: *Jour. Geophys. Research*, v. 72 (in press).
- Wildey, R. L., and Pohn, H. A., 1964, Detailed photoelectric photometry of the Moon: *Astron. Jour.*, v. 69, p. 619.

12/15/53  
A PHOTOELECTRIC-PHOTOGRAPHIC MAP  
OF THE NORMAL ALBEDO OF THE MOON

N67-31954

By Howard A. Pohn and Robert L. Wildey

INTRODUCTION

The two basic principles of superposition and intersection are as fundamental to lunar geologic mapping as they are to terrestrial mapping. There are, in addition to these two concepts, many secondary criteria which are useful to the terrestrial mapper, the most familiar being topographic expression and rock color. Although variation in topographic expression is a mapping tool applicable to both Earth and Moon, the Moon lacks the diversity of colors found in terrestrial rocks (at least at astronomical resolution). The Moon does, however, exhibit a wide variation in its surface brightness.

While variation in reflective brightness is an important characteristic of surficial appearance during all phases of the Moon, it is inseparable from topographic expression except when the phase angle is close to zero, i.e., at full Moon. At that time, when no shadows are visible from Earth, the distribution of reflectivity appears to express real variations in the composition or surface characteristics of the lunar surface materials. The parameter commonly used to express the diffuse reflectivity of the full Moon is the normal albedo, which is the brightness of the lunar surface divided by the brightness of a Lambert surface when observer and illuminator are located along the same normal vector. Because the reflectivity of the Moon appears to be independent of the incident and emergent angles at zero phase angle (at least for terrestrial observations), one may equate the measured geometric albedo at zero phase angle with the normal albedo, even though their formal definitions do not coincide except at the sub-Earth point (see note 1, p. 232).

Although normal albedo can be measured on a full-Moon photograph, the density measured on the plate can only be used to specify isophotic charts of unknown and variable contour interval unless it is calibrated to absolute measurements external to the plate (see note 2, p. 233). Even this is not possible unless care is taken to ensure uniformity of exposure, emulsion sensitivity, and development.

Most early lunar photometric observations were purely photographic (Minnaert, 1961). The advantage of a photographic plate is the simultaneous observation of all image elements in the brightness distribution of a celestial body. On the other hand, the photoelectric technique, while it can only record **one image** element at a time, produces a recorded signal which is linear in specific intensity, extremely precise, and highly stable, as well as easily calibrated to absolute units. Unfortunately, individual resolution elements of the picture must be recorded consecutively by some form of spatial scanning. This is time consuming and can also lead, under certain conditions, to spurious brightness variations in the image because of the fluctuation in time of the atmospheric transmission.<sup>1</sup> Clearly, one solution to the problem of obtaining reliable photometric measurements of the entire full-Moon disk is to utilize a photoelectrically calibrated photograph.

Several problems are inherent in obtaining reliable photoelectric and photographic data on the full Moon. As regards the photoelectric information, the sky must be absolutely cloud free and the minimum lunar phase must be small (1.5" - 2.0"). Atmospheric transmission difficulties necessitate that this minimum phase be at a time when the Moon is at an elevation of 30" or more above

---

<sup>1</sup>Of course the atmospheric transmission must change because the zenith angle of the Moon is changing. What is really referred to here is a fluctuation in the value of the atmospheric extinction coefficient.

the local **horizon.**<sup>2</sup> Furthermore it is desirable, but not necessary, for the astronomical seeing to be reasonably good.

Although the photoelectric equipment requirements are no longer difficult to meet, the necessary control of photographic parameters requires innovations still in the development stage.<sup>3</sup> There are two techniques which may be used to ensure uniform exposures. The first employs a moderately fast emulsion coupled with a highly uniform motion of the shutter across the focal plane. The second employs a slow emulsion, hence relaxed shutter tolerances (e.g., even a hand-pulled slide), coupled, however, with very precise guiding of the telescope. The latter technique has been employed in the present study.

Regarding the requirement for uniform development, there are several techniques to be considered. In one of the oldest the plate is inserted flush with the bottom surface of a square tray, The tray rotates about an axis normal to its bottom surface. **This** axis in turn is caused to precess about the local vertical of the Earth, with which it makes an angle of about 10". Another technique involves the periodic bursting of nitrogen gas into a developing solution in which the plates are vertically mounted. Although many plates can be processed simultaneously, it has been the authors' experience that the uniformity of development in this technique is inadequate. Probably the slowest but most uniform technique of development is one in which a very fine fiber brush, constrained to pass at a fixed depth in the emulsion, spreads the developer back and forth across the emulsion. Brush development has been employed in the present study.

---

<sup>2</sup>The atmospheric transmission, from an information-theoretical point of view, is a source of nonstationary noise. The fluctuation of atmospheric extinction is neither random nor predictable for practical observing durations. Consequently the larger the extinction correction, the larger the error of its determination. The practical limit for 1 percent accuracy is about 30°.

<sup>3</sup>**This** limitation is with regard to the aspect of improving the speed and cost of competing techniques. The ability to actually meet these requirements, given unlimited resources, has existed for some time.

Uniformity of emulsion sensitivity is usually obtainable. Occasionally, however, one of us (Wildey) has found that a single shipment of Eastman-Kodak 5 x 7-in. spectroscopic plates has had spatial responsivity variations leading to systematic discrepancies amounting to 0.10 magnitude in stellar photometry. This phenomenon should always, therefore, be monitored in some way. It has not presented a problem in the present study.

#### THE OBSERVATIONS

On the night of June 2-3, 1966, a 45-second exposure was taken at the folded prime focus of the 61-in. astrometric telescope of the U.S. Naval Observatory's Flagstaff Station. Harold Ables of that institution exposed and processed the plate. The phase angle at the time of the exposure (07<sup>h</sup>07<sup>m</sup>05<sup>s</sup> u. t.) was 1.52°. The emulsion employed was Eastman Kodak 649 F and was preceded in the focal plane by a Schott GG 14 filter of 2.0 mm thickness. Although the spectral response of the filter plus emulsion does not exactly correspond to the photoelectric visual band, the small magnitude of lunar surface color variation precludes any need for correction. The plate was brush developed for 6 minutes in U. F. G. developer diluted one to one with water, thus ensuring highly uniform development. The preparation of the original emulsion by Eastman Kodak appears to have been highly uniform. The overall uniformity is well represented by the scatter in the calibration curves of the present investigation because of the wide distribution of calibration over the lunar surface.

The photoelectric photometer designated by the authors employs an RCA IP 21 photomultiplier in combination with a Wratten 8 filter to produce a close first approximation to the visual bandpass used in the Johnson UBV system (Johnson and Morgan, 1953). The blue bandpass employed a filter consisting of 1.3 mm of Schott GG 13 and 0.7 mm of Schott BG 12. The ultraviolet filter used was a Corning 9863. The focal plane diaphragm transmits a circular beam of light 2.64" of arc in diameter corresponding to a spot 4.8 km

across at the center of the lunar disk. The photoelectric observations were collected about 15 miles away from the Naval Observatory, at about the same elevation, using the 30-inch reflector of the U.S. Geological Survey observatory at Anderson Mesa, Ariz. Although the seeing was only fair, the seeing tremor disk was much smaller than the aperture size of the diaphragm utilized in the photometer. The photographic data were reduced on the Joyce-Loebl microphotometer--Beckman and Whitley Isodensitracer (IDT) combination using a square aperture 0.173 mm on a side. The area of the Moon thus measured on the photographic plate was equal to the lunar area responsible for the light flux admitted to the photomultiplier at the telescope.

The interval between scan centers on the plate was 75  $\mu$  and provided an overlap between successive scans of 57 percent. The calibration wedge used in the IDT had a dynamic range of 0 to 2.4 in optical density with step increments of 0.1195.

#### ABSOLUTE CALIBRATION

Of the four photoelectric scans taken on the night of June 2-3, one scan in the Southern Highlands was rejected on the basis of the difficulty of precise location, and a second scan taken centrally on the disk was rejected owing to the necessity of a large atmospheric extinction correction. The two remaining scans were located in the vicinity of the equator and at approximately lat 25" N. and were taken immediately preceding and immediately following the epoch of the photographic plate. Scanning time was approximately 25 minutes, and these two scans were taken from limb to limb. In order to ensure coverage of the extremes of brightness of the lunar disk, single points in Aristarchus, Tycho, and Le Monnier were also measured.

The photographic plate was positioned on the IDT (operating in the scan mode) to reproduce exactly the scans which were obtained by the photoelectric photometer (fig. 1).

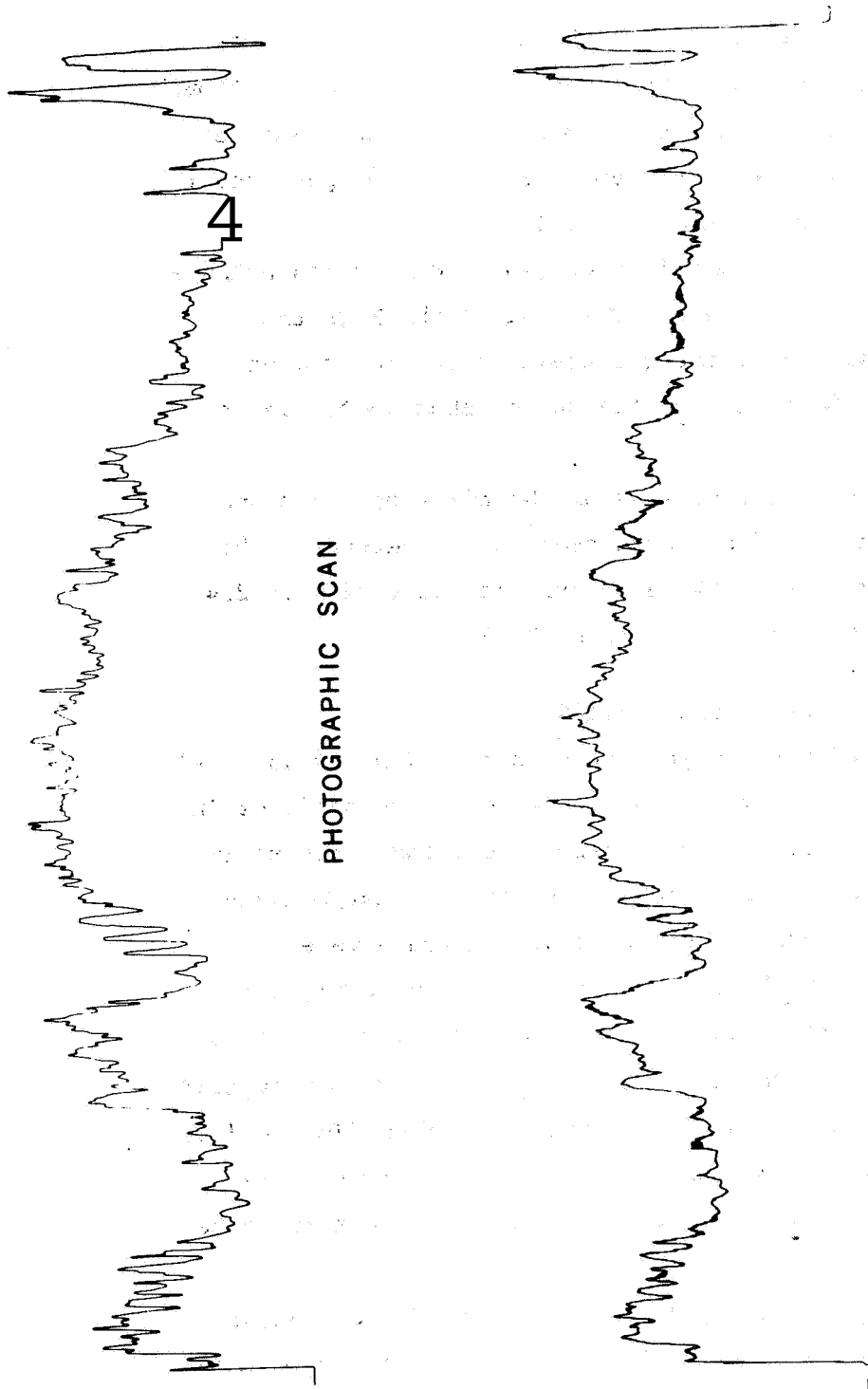


Figure 1.--A comparison of signal traces adjusted to the same scale of abscissa. The track across the Moon is the same. Lower curve: amplified photoelectric voltage on the same scale as are recorded the flux voltages of standard stars. Upper curve: continuous record of density of the simultaneously recorded photographic plate on the same scale as is coded by the Joyce-Loebl--Beckman and Whitley Hso0ensitracer.

Determination of normal albedo from photoelectric signal proceeds in three steps: (1) Correction of the photometry for differences in spectral response and power scale between the operational system of the telescope-photometer (after correcting for atmospheric extinction) and an intermediate standard system, in this case, the Johnson-Morgan UBV system (see App. A). (2) Conversion of the intermediate V magnitude to a wavelength-averaged absolute specific intensity or surface brightness and a corresponding effective wavelength (see note 3, p. 233). (3) Determination of the normal specific intensity of a Lambertian scattering surface at the same distance from the Sun on the basis of published absolute solar photometry (App. B).

A small correction (0.05 magnitude), obtained from the brightness versus phase curves at small angles (Willey and Pohn, 1964), has been applied to extrapolate magnitudes to zero phase angle. Within about 5" of zero phase angle, no variation in size of the extrapolation can be observed to correlate with class of lunar feature, and the waxing and waning branches of the brightness versus phase curves coincide. This indicates the degeneracy of the photometric function in all its geometric degrees of freedom except phase angle, due to the smallness of the phase angle. This is of course essential to the labeling of the full-Moon photograph with values of normal albedo, because the phase angle is the only geometric degree of freedom in the photometric function which is reasonably constant over the entire Moon.

The ordinate of the photoelectric trace is linear in the number of photons received per second and thus linear in specific intensity and in normal albedo. The zero point on the trace is determined by the signal of the adjacent sky (negligible compared to the Moon). The hypothetical full-scale signal of the yellow trace, together with a blue signal obtained from the previously measured ratio, can therefore be reduced to obtain, in sequence, a V magnitude, a specific intensity, and a normal albedo for a full-scale deflection.

By obtaining absolute spectral radiometry on any one of the UBV standard stars, or any nonvariable star whose V magnitude and B-V color index will at some time be determined by photoelectric measurement, an absolute calibration of the entire UBV system can be determined. Such data have been collected by Willstrop (1960). The resulting calibration has been determined by Wildey and Murray (1963). This calibration has been assumed in this preliminary report but will be refined later. The resulting blanket correction is unlikely to exceed 5 percent.

The distance from the Sun to the Earth-Moon system for the epoch of the observations is obtained from the ephemeris. A hypothetical Lambert scattering surface has a specific intensity under normal illumination which is completely specified by the properties of (1) total reflection, (2) a specific intensity constant over all positive directions and zero over all negative directions, and (3) a known apparent V magnitude for the Sun (Stebbins and Kron, 1957). An observational normal albedo is obtained by dividing the observed specific intensity by the Lambert surface specific intensity.

The photographic and photoelectric records are compared in figure 1. The maximums and minimums of the curves obtained from the photographic and photoelectric scans were intercompared, and a calibration curve was constructed using the density values from the photographic plate and the absolute albedo values obtained from the photoelectric photometry (fig. 2). Several values near the limb were rejected owing to the more severe effects of the differences in lunar libration between the time of the photographic exposure and the times of the photoelectric measurements. The point plot for the calibration curve shows the maximum possible random error since the extremes of the signal traces are most likely to be subject to errors due to astronomical seeing and positional inaccuracy. The scatter about the calibration curve implies a nominal error of about  $\pm 1$  percent.

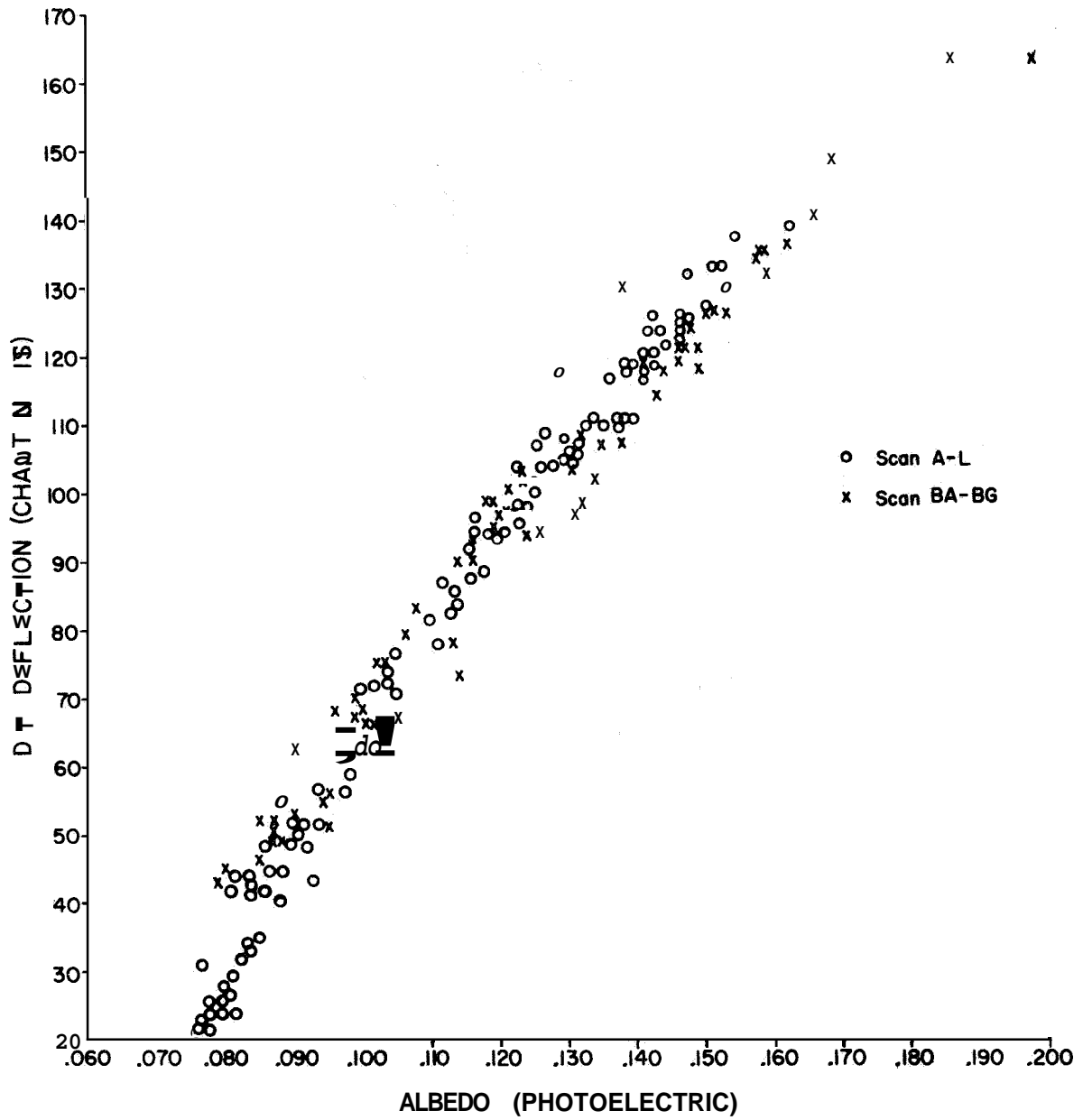


Figure 2.--Calibration plot of points of the Moon measured simultaneously by photoelectric photometry and photography. Corresponding maximums and minimums of the photoelectric and photographic spatial scans are used.

## THE ABSOLUTE ALBEDO MAP

One major departure from standard procedures of mapping has been used in constructing the map (enclosed in map supplement). A brief explanation of this departure will enable the reader to better utilize the data. The contour intervals of the full Moon are constant in photographic density but not in albedo (see fig. 2). This is an unavoidable limitation in the present operation of the IDT. Despite this, the authors felt that the labeling of contours by albedo would be more practical than the imprinting of optical density, which would require frequent reference to the calibration curve.

In order for the albedo map to be used to maximum advantage, it must be understood that the quantization interval of the IDT is not sufficiently small to permit an adequate linear interpolation between contours in all cases. The photograph of the plate itself (fig. 3) should therefore be used as an "interpolation formula". As an example of an associated problem, the contour lines do not necessarily correspond to geologic contacts. The IDT shifts operational mode at predetermined equal increments. Therefore, if the machine is set to change mode at density increments corresponding, at a certain level, to 5 percent variation in surface brightness, a geologic contact corresponding to a 3 percent brightness change, at that level, may or may not show on the tracing. An example is shown in figure 4. The area measured is in Mare Serenitatis. In figure 4A, the setting of the zero point of the machine fortuitously correlated the mode switch with the border of dark materials which surround Mare Serenitatis (fig. 5). In figure 4B, the zero point was shifted slightly and the contour lines no longer have geologic significance in this region.

A second source of confusion results from areas with extremely steep brightness gradients. When the machine reaches an area of large change in brightness over an interval which is small with respect. to the aperture. it is forced by the finite speed of the

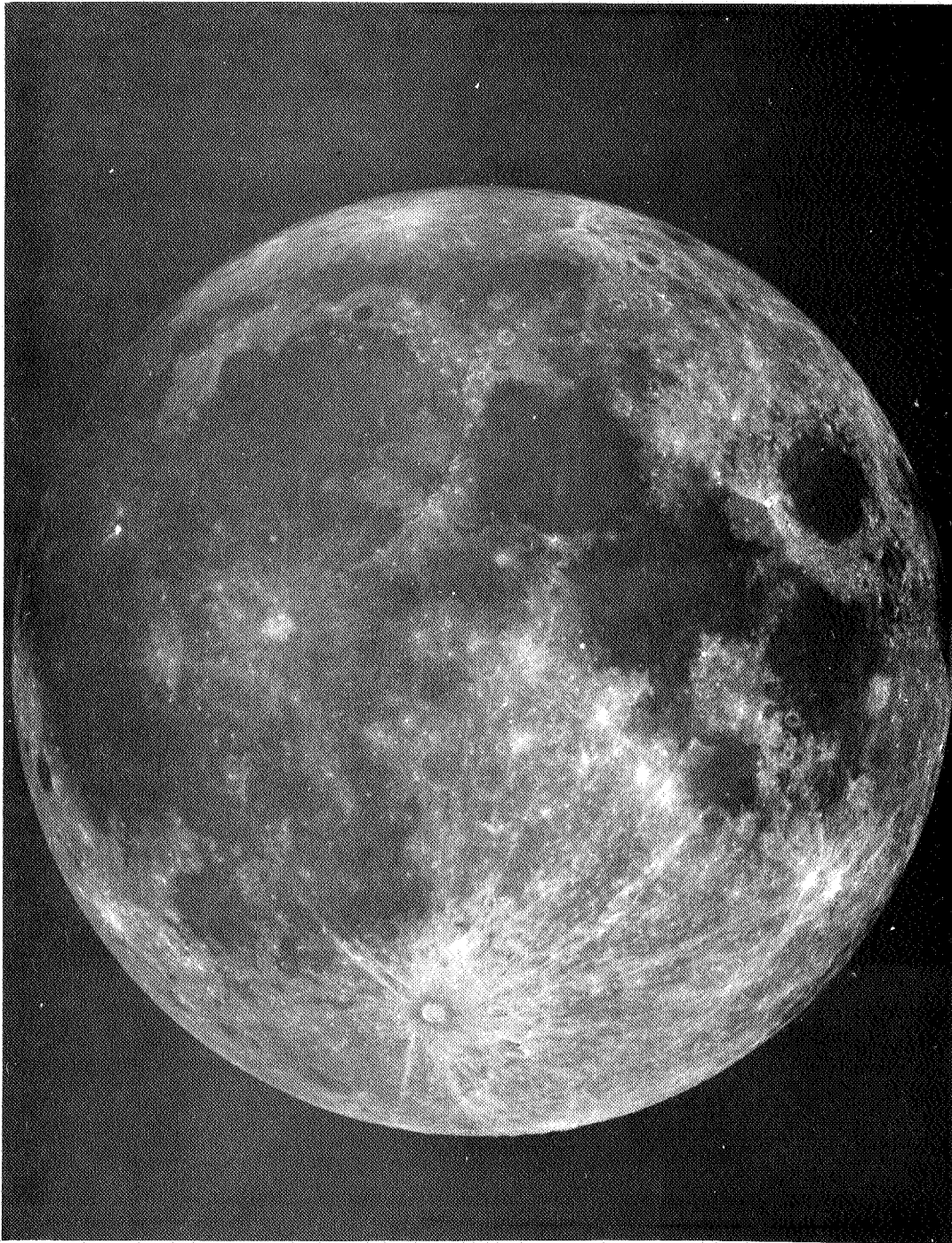
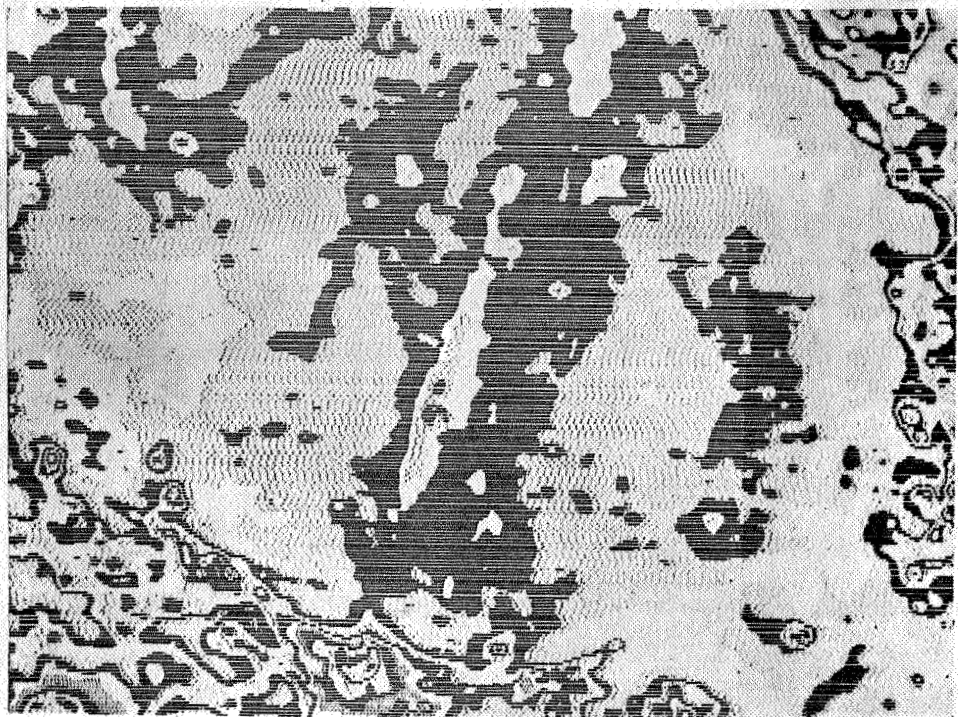
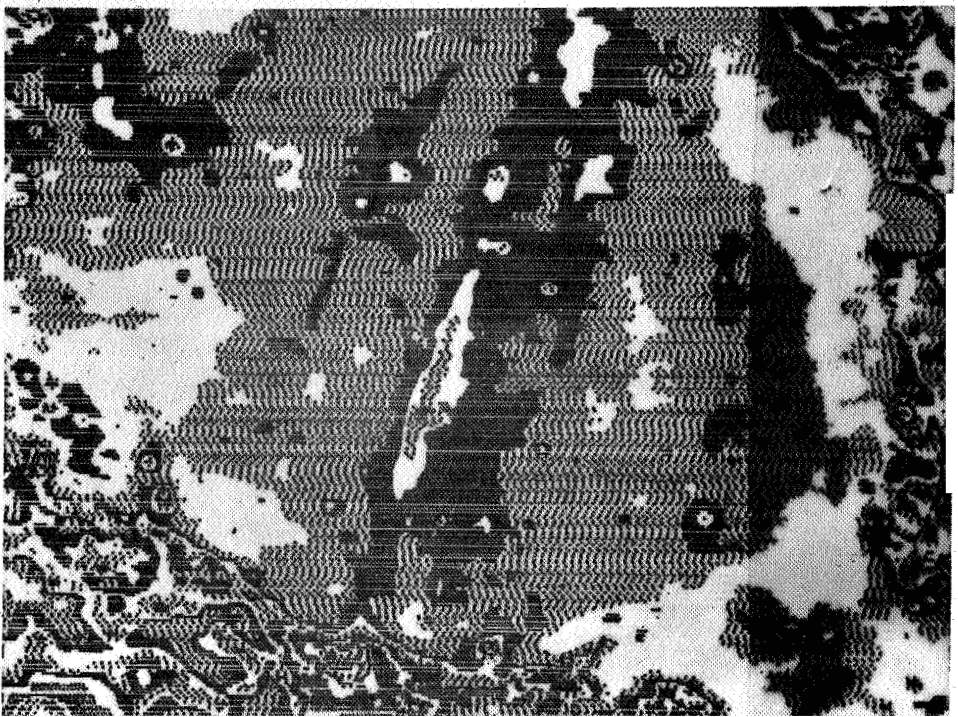


**Figure 3.--Reproduction of the photographic plate used in the present lunar photometry. Where linear interpolation between contours of the absolute albedo map is inadequate, this photograph may be used by eye for higher order interpolation.**



A



B

Figure 4.--Isodensitracings made from figure 3.

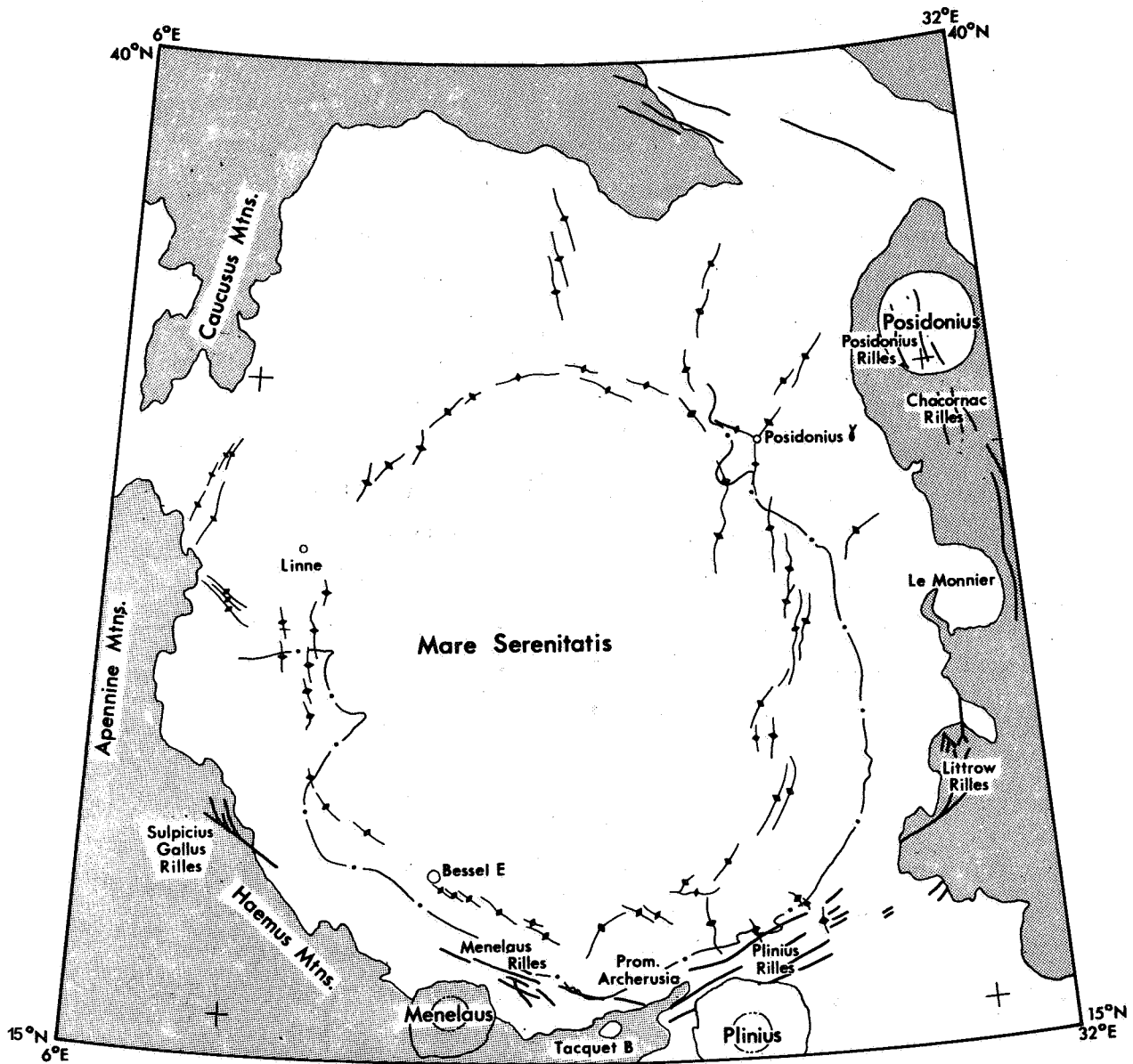


Figure 5.--Sketch of Mare Serenitatis showing extent of dark mare unit (dash and dot symbol). Stipple indicates terra. Ticks near lower right- and left-hand corners indicate corners of geologic map of region (Carr, 1966). Scale 1:5,000,000.

plate carriage to change modes as rapidly as it can. Therefore, the contours in a small bright spot will tend to assume a symmetrical shape even if the spot is, in reality, asymmetrical.

In summary, the map presented in this report is the first reliable map of the absolute normal albedo of the Moon, in which real-time photoelectric calibration is utilized, and for which the necessary uniformity in plate parameters is known.

The map is considered preliminary for two reasons: (1) The absolute scale of normal albedo may undergo a blanket correction factor of the order of a few percent difference from the present data owing to a refinement in absolute calibration presently under study. This will not disturb any albedo read from the map, considered as a ratio to the albedo read at some other arbitrary point on the map. (2) The brightness gradients of very small bright lunar features, such as some bright halo craters, are too steep to have been followed by the IDT, and the peak values indicated are too low by an uncertain amount. The authors are preparing a larger scale map to which these reservations will not apply.

#### ACKNOWLEDGMENTS

While many individuals were involved in the collection and reduction of the data, the authors would particularly like to express appreciation to Harold Ables, of the U.S. Naval Observatory, who took the responsibility of obtaining and processing the plates, Gerald Kron, Director, for permitting use of the 61-inch telescope for this purpose, and Jim Wooldridge of the U.S. Geological Survey who supervised the plate reduction on the Joyce-Loeb 1 Isodensitracer.

## APPENDIX A

### THE THEORY OF ASTRONOMICAL PHOTOMETRY **AND** SYSTEMS OF STELLAR MAGNITUDES **AND** COLORS

Normally, the establishment of standards of celestial photometry is based upon the measurement, over a period of time during which equipment response parameters can be kept constant, **of a** collection of stars of constant luminosity. The photometric investigation of other objects (undertaken at arbitrarily later times), when coordinated with the measurement of some **of** these standard stars on the same nights, can then be rendered on a highly homogeneous photometric system. Extremely accurate comparison with other objects measured in the same way is possible because corrections can be made not only for 1) the nightly deviation of the average atmospheric extinction from the secular average used in the reductions, and **2)** the uncertainty in the bolometric responsivity of a given photometer, but also for **3)** small color deviations in the spectral response characteristics of a given photometer from those of the original photometer used to establish the collection of standard stars. In order to do this, the photometry must be at least two-color (*i. e.*, in two different wavelength bands).

The reduced form of stellar photometry is on a logarithmic scale. The flux measurement is given as a "magnitude," and the colorimetry (a magnitude difference) is a "color index." The unit, or zero point of the magnitude system, is essentially arbitrary though it stems ultimately from the naked-eye observations by Aristarchus of Samos, whose brightest stars were "stars of the first magnitude." Although the original reason for a logarithmic scale is physiological, a more scientific rationale can now be developed for its preservation.

Consider the monochromatic radiation of a blackbody at four different wavelengths. Let us then define four monochromatic magnitudes as follows:

$$m_j = -2.5 \log \left[ \frac{5}{\lambda_j} \frac{hc/\lambda_j}{kT} \right] \quad 1)$$

The expression on the right is the Planck function multiplied by a convenient constant which need not concern us since the zero point of the  $m_j$  magnitude is arbitrary, needing only to be preserved after once being chosen.

For stellar temperatures and the wavelengths of ordinary photometry, Wien's approximation holds, hence:

$$m_j = 12.5 \log I_j + (2.5 \log e) \frac{hc}{\lambda_j kT}$$

Color indices are, for a given T:

$$m_i - m_j = 12.5 \log \left( \frac{\lambda_j^i}{\lambda_i^j} \right) + \left[ 2.5 \frac{hc}{k} \log e \right] \frac{1}{T} \left( \frac{1}{\lambda_i} - \frac{1}{\lambda_j} \right)$$

By writing down the foregoing equation for  $i, j, = 1, 2$  and again for  $i, j = 3, 4$ , one can readily solve simultaneously for the following relationship:

$$m_1 - m_2 = \left( \frac{\frac{1}{\lambda_1} - \frac{1}{\lambda_2}}{\frac{1}{\lambda_3} - \frac{1}{\lambda_4}} \right) (m_3 - m_4) + 12.5 \left[ \log \left( \frac{\lambda_1}{\lambda_2} \right) - \left( \frac{\frac{1}{\lambda_1} - \frac{1}{\lambda_2}}{\frac{1}{\lambda_3} - \frac{1}{\lambda_4}} \right) \log \left( \frac{\lambda_3}{\lambda_4} \right) \right]$$

The important feature of this equation is that it does not contain T. It is therefore a canonical equation of blackbody photometry

which is the same for any four spectral measurements of a black-body regardless of its temperature.

Suppose we now have a photoelectric chart deflection,  $d_y$ , at relative amplifier gain  $G_Y$  expressed in magnitudes rather than decibels. Let the subscript refer to a particular radiation wavelength band,  $y$  for yellow and  $b$  for blue, and presume that the observations have been corrected for atmospheric extinction. Let there be a standard magnitude-color system (in practice the Johnson BV system was used) called  $B$  and  $V$ . From the foregoing equation the following formulas must be valid:

$$V = (-2.5 \log d_Y + G_Y) + A (2.5 \log \frac{d_y}{d_b} - G_y + G_b) + C$$

$$B - V = D (2.5 \log \frac{d_y}{d_b} + G_l) + E$$

These equations are called the color equations or the transformation equations from the natural magnitude-color system of the telescope-photometer to the BV system. On a given night one obtains the observed parameters in the above equations for all objects measured. Among these are the standard stars for which  $V$  and  $B-V$  are also known. The constant coefficients and additive constants  $A$ ,  $C$ ,  $D$ , and  $E$  in the color equations can therefore be determined by a least-square fit to the data. The transformation is then used to reduce the photometry to the BV system.

Of course a star is not exactly a blackbody because of its complicated opacity and radiative equilibrium, and there is a gradual variation with wavelength of the Moon's reflectivity. Our photometry is rather broad-band and not monochromatic. However, if response variations with the wavelength for  $V$  and  $y$  (and  $B$  and  $b$ ) do not differ by more than the commercial tolerances for a filter and a photoemissive surface of the same type as was originally used to establish the BV system, these effects will produce errors much less than 1 percent. This is true even when the color corrections themselves are in a range of as high as

10 to 15 percent. A useful check on the photometry is the closeness of D to unity and of A to zero.

It should also be made clear that although the V magnitude can be defined in the following way:

$$V = -2.5 \log \left( \frac{\int_0^{\infty} F_{\lambda} R_{\lambda} d\lambda}{\int_0^{\infty} R_{\lambda} d\lambda} \right) + \text{const.},$$

where  $F_{\lambda}$  is the stellar flux and  $R_{\lambda}$  is the spectral response of the V system, spectrophotometric control can be maintained indefinitely by the use of the color equations without ever knowing anything about  $R_{\lambda}$ . Indeed, the precision is superior to what would be obtained by ordinary laboratory techniques for measuring and correcting for  $R_{\lambda}$  using a nominal spectral shape for  $F_{\lambda}$  and evaluating integrals.

The photoelectric observations which calibrate the albedo map of the present investigation employed 10 BV standard stars measured before, during, and after the lunar photoelectric observations. Actually, a photoelectric ultraviolet color was also measured, the overall system being the Johnson-Morgan UBV system.

The ensuing calibration of the photography, according to the technique discussed in the text, implicitly assumes that in the connection between the spectral bands of photoelectric V and 649F + GG14, there is no color term (i.e., in the connection between the BV system and a photoelectric system for which the blue response is spectrometrically identical with B and the yellow response is identical with 649F + GG14, the coefficient A is zero). The color equation shows that this will not lead to error even if the assumption is poorly founded if the Moon does not show a large dispersion in color-index. This appears to be the case. Although Eastman Kodak emulsion 103a-D + 2.0 mm of Schott GG11 filter has a spectral response almost identical with that of V, this spectroscopic emulsion is very grainy and is also too fast for a photometric exposure by our presently operational technique.

## APPENDIX B

### THE THEORY OF LAMBERT SCATTERING AND THE ABSOLUTE CALIBRATION OF NORMAL ALBEDO

Given a V magnitude corresponding to full scale on a photoelectric trace from which points for the plate calibration are taken, the normal albedo to which it corresponds must be determined. This is done in two steps. First, determine the absolute specific intensity (defined in note 3, p.233) that would be exhibited by a Lambert scattering surface when placed at the distance from the Sun corresponding to the epoch of the observations. Then, convert the V magnitude to an absolute specific intensity.

A Lambert surface is the ideal diffuse reflecting surface which absorbs no light and shines with a specific intensity constant over all directions. In order for the surface brightness thus defined to be consistent with the first laws of thermodynamics, it must be proportional to the cosine of the angle of incidence of the illuminator. For considerations of the normal albedo, the desired geometry requires that  $\cos i = i$ .

Let the solar flux in the V band be  $F_V$  at the position in space occupied by the Earth-Moon system. Then the energy striking the Lambert surface in a unit area per unit time is  $F_V$ . Let the specific intensity in the V band exhibited by the surface be  $I_{VL}$ . In a given direction,  $\theta$  (polar),  $\varphi$  (azimuth), with respect to the local normal, the total area perpendicular to this direction through which the beams passing in this direction will have come from the unit area, is  $\cos \theta$ . Thus the radiant (V band) power per unit solid angle in this direction that comes from the unit area of Lambert surface is  $I_{VL} \cos \theta$ . The total V band power that is leaving the surface is obtained by integrating over the half space of solid angle above the surface. Equating this to the power arriving per unit area:

$$F_V = \int_0^{\frac{\pi}{2}} \int_0^{2\pi} (L_{VL} \cos \theta) \sin \theta \, d\theta \, d\phi$$

Because the surface is Lambertian,  $L_V$  can be taken outside the integral and we obtain

$$41, \quad \bar{F}_V = \frac{F_V}{\pi} \quad (\text{Power in the band per unit area per steradian})$$

Stebbins and Kron (1957) have measured the apparent V magnitude of the Sun. Willstrop (1960) has measured the absolute value of  $F_\lambda$  (watts per A per  $\text{cm}^2$ ) for 100 A bandwidths at various points in the solar spectrum. This is sufficiently wide as to effectively smooth the Fraunhofer lines, and sufficiently narrow as to be a reasonable mesh for a numerical integration over the V spectral response function. We can thus write

$$V_\odot = -2.5 \log F_V + \text{const.}$$

$$\frac{\int_0^{\infty} F_\lambda R_\lambda \, d\lambda}{\int_0^{\infty} R_\lambda \, d\lambda}$$

Carrying out the integration in the second equation using Willstrop's data and Johnson's (1955) tabulation of the V response function, one then solves for the constant in the first equation.  $F_V$  is thus evaluated.

The V magnitude corresponding to the lunar photoelectric observational scale of this study is also translatable into a flux using the foregoing two equations. The calibration of  $F_V$  thus provided is independent of color; however, the effective wavelength of the lunar  $F_V$  is somewhat longer because the Moon is redder than the Sun. Normalization of values to the same monochromatic wavelength has not been done but leads to a small change at worst. There is also no a priori reason why a monochromatic evaluation will be more meaningful than one corresponding to a broad band. The  $F_V$  for the Moon can be changed to a

specific intensity by dividing it by the solid angle of the celestial sphere imaged within the focal plane aperture. This is because the area of integration of specific intensity, while it can be chosen anywhere along the light beam, will be common to both the stellar and the lunar measurement if it is chosen at the telescope entrance pupil. With the solid angle chosen as above, one accounts for 1) all the lunar light that is responsible for the photoelectric signal, and 2) the entire stellar image. Hence the rationale for the above conversion to specific intensity.

With both the Lambertian and the observed lunar specific intensities evaluated as above, the normal albedo in the Johnson V band is evaluated according to definition by dividing the latter by the former.

#### REFERENCES

- Carr, M. H. , 1966, Geologic map of the Mare Serenitatis region of the Moon: U.S. Geol. Survey Misc. Geol. Inv. Map 1-489.
- Johnson, H. L., 1955, Spectral responses of a precisely transformable two-color system which excludes the Balmer jump: *Astrophys. Annales*, v. 18, p. 292-295.
- Johnson, H. L. , and Morgan, W. W. , 1953, Photometry of 290 stars in three colors: *Astrophys. Jour.* , v. 117, p. 313-323.
- Minnaert, M. , 1961, Photometry of the Moon, ch. 7 of Kuiper, G. P. , ed. , *Planets and satellites*: Univ. Chicago Press.
- Stebbins, J. , and Kron, G. K. , 1957, Six color photometry of the sun: *Astrophys. Jour.*, v. 126, p. 266-283.
- Willey, R. L. , and Murray, B. C. , 1963, Ten micron stellar photometry--First results and future prospects : *Colloque Internat. d' Astrophys. tenu a l'Univ. de Liege*, 24-6 juin 1963, v. 26, p. 460-468.
- Willey, R. L. , and Pohn, H. A. , 1964, Detailed photoelectric photometry of the Moon: *Astron. Jour.*, v. 69, p. 619-634.
- Willstrop, R. V., 1960, Absolute measures of stellar radiation: *Royal Astron. Soc. Monthly Notices*, v. 121, p. 17-26.

## NOTES

1.--In other words, the brightness exhibited by the lunar surface when observer and illuminator lie along the same direction (idealistically avoiding eclipse), is the same whether the lunar surface is oriented perpendicular to the line of sight or oriented in any other arbitrary way. Of course we must bar natural discontinuities. Therefore, the abrupt transition to zero brightness at an observing angle of  $90^\circ$ , beyond which forward scattering into an opaque medium would be indicated, must be smoothed to some extent. The map resulting from the present study shows no obvious limb darkening with the possible exception of the extreme proximity to the limb. This constitutes one of the observational bases for the assumption that the photometric function of the Moon has a value, at zero phase angle, which is independent of all other geometric degrees of freedom. The test is partly vitiated by the fact that the Moon is not a body of uniform absorptivity.

There is an additional observational basis for the above assumption. It is a fact, previously observed photoelectrically by the authors, that the brightness versus phase curves of a collection of 25 lunar features of various types and locations, possess waxing and waning branches which coincide asymptotically near zero phase angle, regardless of location on the Moon. The meaning of this is that for two small and equivalent phase angles (up to about 5") taken before and after full Moon, the value of the photometric function is the same even though changes in the values of the angle of incidence and the angle of observation may be as much as several degrees. This is, of course, a direct test of the assumption that the Moon's zero phase albedo is equivalent to its normal albedo. Unfortunately, the geometric limitations imposed by the Moon's synchronous rotation and the Earth-based nature of the observations do not permit a test of this type in which the changes in observing and incident angles are a large fraction of their possible range.

A third basis derives from the fact that previous studies have shown that the Moon's photometric function depends predominantly, if not wholly, upon phase angle and brightness longitude, over the general range of variables. From the geometrical definition of brightness longitude, it can be easily shown that it is mathematically indeterminate at zero phase angle. Hence the implication that it must approach zero influence in this neighborhood.

It thus appears that the assumption of the equivalence of normal albedo and zero phase albedo rests upon a great deal of evidence. It is not fair to say, however, that the precision (over all the ranges of the variables involved) with which the assumption has been tested has been equal to the fundamental precision of the observational photometry. There appears to be a fundamental limitation to such a test ever being applied by the techniques of ground-based astronomy. Should practical consequences of the fact ever become significant, the authors wish to point out the reservation that the present study has

produced a rigorous map of zero-phase geometric albedo whose approximation to a map of normal albedo is better than we can now measure,

2.--This reservation arises from two sources. First of all, if the H and D curve is not obtained in any way whatsoever, contours of equal density will be isophotes whose relative brightnesses will be unknown and also variable as one goes from higher to lower densities, inasmuch as there is not a linear relationship between density and brightness. If the H and D curve is obtained from the imprint of a wedge or a spot photometer, one will obtain relative brightnesses devoid of systematic errors only if (1) the exposure times used in the lunar and calibration photography are the same to within approximately 50 percent and (2) the radiative energy distributions of the Moon and the calibration source agree to within a few tens of percent. The imprinting process must also be known to be devoid of errors. Finally, absolute calibration by purely photographic means requires an absolutely standard comparison source whose image is processed in a rigorously equivalent manner. If errors due to atmospheric transmission fluctuation are avoided, the standard should be extraterrestrial, preferably near the Moon. In general, if the spectral energy distributions are not exactly the same, the spectral responsivity of the emulsion must be known.

3.--Specific intensity is the most general parameter associated with a radiation field. It is the one from which all others (e.g., mean intensity, flux, radiation pressure) are derivable, and it is defined in the following way: Consider a truncated cone where the apex angle of the fully extended cone defines a solid angle and the truncating cap defines an area. Measure the radiative power for all photons which pass first through the truncating cap and then through the base of the cone. Divide by the product of the area of the cap and the solid angle of the cone. In the limit as the cone angle approaches zero, the quantity so defined is the specific intensity. It is characterized by a direction and has the units of watts per square centimeter (of area normal to the direction) per steradian (of solid angle surrounding the direction) per unit wavelength (if not bolometric). If not bolometric, it may be truly monochromatic or an average associated with some broad spectral response function. In the latter case, it can be associated with an effective wavelength. At least two kinds of effective wavelength can be defined, the most meaningful of which is probably

$$\lambda_e = \frac{\int_0^{\infty} \lambda I_{\lambda} R_{\lambda} d\lambda}{\int_0^{\infty} I_{\lambda} R_{\lambda} d\lambda}$$

$\lambda$  = wavelength  
 $I_{\lambda}$  = specific intensity  
 $R_{\lambda}$  = spectral response of photometer

The effective wavelength for the present observations is approximately 5540 A.

That the number of photons per second registered by the photometer is directly proportional to specific intensity may be realized **as** follows: The power originates in an area of lunar surface encircled by the aperture in the focal plane diaphragm. **If** the direction remains fixed, the projection of this area onto a plane perpendicular to the line of sight also remains fixed. Furthermore, the photons originating in this area are constrained to be those contained within the solid angle subtended at the Moon by the telescope objective. If the Earth-Moon distance is changed, the diminution of solid angle is exactly compensated by the increase in the geographic area of the Moon being measured. The signal will thus remain unchanged if resolution is not a consideration, in which case the solid angle and the area considered are small enough to be considered as mathematical differentials.' Their product, which would be divided into the signal, is thus a constant. Hence the signal is proportional to specific intensity.

SECTION IV  
SUMMARY OF TELESCOPIC  
LUNAR STRATIGRAPHY



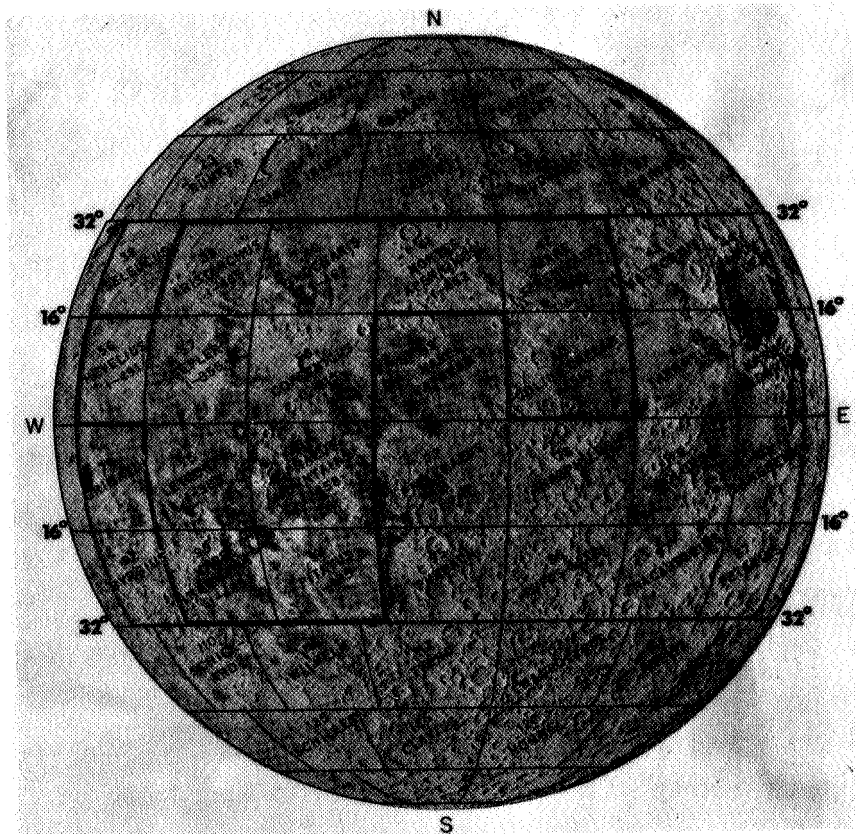


Figure 1.--Index map showing status of mapping at the 1:1,000,000 scale as of mid-1966. Preliminary maps were completed of the area outlined by medium-weight line (lat 32° N.-32° S. , long 70° E.-70° W.). Maps of the area defined by heavy line were published or in press, and their revised, rather than preliminary, stratigraphy is discussed in this report. Number above quadrangle name refers to USAF-ACIC lunar base chart (LAC series); number below refers to published geologic map.

Figure 2 (opposite).--Photomosaic of part of the lunar earthside hemisphere showing areas covered by illustrations in this report, and major features (as well as all features mentioned in the text). Base modified from LEM-1A (2d ed. , Nov. 1962, pub. by the Aeronautical Chart and Inf. Center, U.S. Air Force).





reconnaissance. Mapping techniques developed as a result of this effort are applicable with refinement to Lunar Orbiter photography, and maps made by remote techniques will continue to be the framework within which lunar geologic knowledge expands. Furthermore, spacecraft designers and mission planners need Earth-based data and results of reconnaissance studies in order to choose targets and develop mission strategies. This Earth-based regional reconnaissance has provided a basis for such planning and for advanced studies through identification of some of the fundamental lunar stratigraphic units.

#### APPLICATION OF STRATIGRAPHIC PRINCIPLES TO THE MOON

Geologists studying the Moon have performed much useful preparatory work because they have been able to recognize and map units by applying stratigraphic methods used on Earth. These methods are based on the concept that the Earth's crust is neither homogeneous nor heterogeneous but comprises rock units of different composition, origin, age, and postdepositional history. Geologic mapping consists of recognizing these units and delimiting their surface or subsurface extent. The objective of mapping is an understanding of the crust--how and when its rocks formed and how and when they were emplaced. Lunar geologic maps, therefore, show those units believed most effective (at the map scale used) for summarizing and conveying knowledge of the structure, history, and formative processes of the lunar crust.<sup>1</sup>

Geologic units are of several conceptual types. The basic practical mapping units are rock-stratigraphic units, material subdivisions of the crust which are distinguished, delimited, and defined solely on the basis of lithologic properties. Derivative from rock-stratigraphic units and defined in terms of actual rock

---

<sup>1</sup>The term "crust" here means the upper parts of a planet accessible to direct study, and usage of the term does not imply that we know or believe that the Moon is differentiated into distinct layers.

sections (in current practice) are time-stratigraphic units, planet-wide material units which include all rocks formed in a specific interval of time. A third kind of unit is the geologic-time unit, a nonmaterial unit defined in terms of time-stratigraphic units.

These three types have been confused both in terrestrial and lunar geology, but at least recently distinctions among them have been clarified (Cohee, 1962). The distinctions are particularly important in mapping the Moon; units shown on a map should be objective rock-stratigraphic units mapped by criteria which other geologists can recognize and not derivative time-stratigraphic or other interpretive units that represent opinions regarding origin, age, or role in geologic history. Objective units can be combined and divided and age assignments changed with new data and interpretations, whereas strictly interpretive units must be remapped.

#### Lunar Surface Units and Rock-Stratigraphic Units

The basic lunar units which correspond conceptually to terrestrial rock-stratigraphic units are surface areas which have a limited range of physical properties that can be observed and measured by visual telescopic observation, study of photographs, or instrumental measurements on the telescopic image or on photographs. These properties are observed under different angles of Sun illumination (compare figs. 3 and 11). Gross morphology and surface texture are best revealed by shadows cast by a low Sun (fig. 3). Albedo, a property of the uppermost surface layer, is best seen under high illumination when no shadows are cast (near full Moon) (fig. 11).

Although surface units defined by such properties are objective and reproducible, some interpretation inescapably enters into the choice of defining properties. Boundaries drawn to delimit the various high- and low-illumination properties do not naturally coincide to define unique units. Since the purpose of subdividing the surface is to distinguish the underlying rock units, the surface properties generally chosen to delimit units are those considered most likely to reflect the underlying geology. Of all the

properties now observable, topography is the best choice. Lateral uniformity of topography or regular lateral gradation probably reflect horizontally layered rock units or discrete nonlayered units of uniform lithology. Most terrestrial rock-stratigraphic units are of this type. Recognition of such units is the first step in analyzing the geology and must precede any interpretation.

Properties of the uppermost surface materials may also reflect underlying lithology, as the properties of many terrestrial soils are related to the composition of the underlying bedrock. The correlation may be only indirect, as it is also with many soils, because external processes such as impact cratering, mass wasting, and radiation subsequently may alter the original properties. The lunar surface properties that have been studied to date include albedo, albedo in nonvisual wavelengths (infrared, radar, microwave), color, polarization, and infrared emissivity at eclipse.

After units believed to represent three-dimensional rock bodies are recognized, defined, and mapped, the lunar geologist is faced with the problem of interpreting the origin of units through knowledge of terrestrial materials and processes and through experiments. Because of the limitations of this approach, only tentative interpretations of lunar units can be made now. For example, many large lunar craters are certainly of impact origin, and many craters and other units are surely of volcanic origin, but most materials cannot be classified confidently either way at present. Therefore, interpretations of origin are strictly separated on lunar geologic maps from physical characteristics used to define units.

Arrangement of units in order of relative age is basic to all stratigraphic work and the concept of relative age is the most important and distinctive contribution of the geologist to lunar studies. The application of stratigraphic principles to the lunar surface rests on the reasonable postulate that principles of superposition of strata and transection of faults, contacts, and



Figure 3 --Craters Copernicus (center), 90 km in diameter, and Eratosthenes (upper right), 60 km in diameter; Carpathian Mountains (Middle) above Copernicus and Alpine Mountains above Eratosthenes. Both mountain ranges are part of the high terra surrounding Mare Imbrium. Mountains are embayed by mare material and are older than the mare material. Rim and ray material of Copernicus exhibit radial symmetry and are younger than the mare material. North is at top and east at right in this and all ensuing photographs (Internat Astron. Union convention, 1961). Geologic map of most of this area is the Copernicus quadrangle by Schmitt, Trask, and Shoemaker (in press); a strip across the top of the area is in the Timocharis quadrangle mapped by Carr (1965b). This unpublished photograph (1196) was taken with the 61-in. reflector at Catalina Observatory, University of Arizona Lunar and Planetary Laboratory. Enslung photographs taken with this telescope, all of which are unpublished, are cited by number and the words "Catalina Observatory."

other linear features apply to the Moon as well as the Earth. Because these relations are geometric, we can learn something of the history of the Moon--or the Earth--from photographs and without contact with rocks. In an undeformed depositional sequence of rocks, the young rocks lie upon the old ones; intrusive rocks are younger than the rocks they transect; rocks cut by faults are older than the faults. These relations are revealed in the areal pattern of the units and the geometry of their contacts. A young unit appears to lap upon or embay an older unit; the contact of a young unit cuts across the contact between two older units. Relative ages are also determined by secondary and less objective means such as density of superimposed craters, and apparent freshness of units. Because cratering and mass wasting are continuing processes, older units are more densely cratered than younger ones and subdued-rim craters are generally older than sharp-rim craters in the same size category. Determinations of relative ages of lunar units are probably about as reliable as interpretations of surface units in terms of subsurface units, and more reliable than interpretations of origins.

Two examples will show how rock-stratigraphic units are recognized on the Moon and how superposition and transection relations between them are deduced. The first examples are the units which make up the maria. The characteristics which, taken together, distinguish the maria from other lunar surface areas are smooth flat topography and low albedo. Surfaces with these characteristics extend laterally for great distances on the lunar surface. In many places the surfaces terminate abruptly against the rugged chiefly lighter terra and continue into the intervening valleys (fig. 3). The most reasonable interpretation of this map pattern is that the surfaces are formed by material in flat-lying beds emplaced in a generally fluid state and that the mare material is younger than the terra it embays.<sup>2</sup>

---

<sup>2</sup>The term terra, the antonym to mare, includes light plains and both light and dark rugged terrain, but not individual craters.

A second important class of lunar rock-stratigraphic units-- identifiable as such at least in young craters such as Copernicus (fig. 3)--are crater rim materials (defined as all material from the rim crest outward that has positive relief). The morphology of rim material is generally uniform in belts surrounding the crater and is regularly gradational outward. Near the rim crest it forms a high ring, and its surface is randomly hummocky or has a branching pattern with convex-outward arcs; farther out the rim material is characterized by radial ridges and grooves and is topographically lower. The radially symmetric pattern of rim material around the crater indicates that the formation of the rim material is related to the formation of the crater, and that the material probably consists of ejecta, either impact or volcanic, from the crater.<sup>3</sup> The rim material must have been deposited as a layer or layers upon earlier rocks. The age of these layered rocks relative to other materials can be deduced from their map pattern. Where the rim material is younger, it is arrayed around the crater in an unbroken roughly circular pattern with a fringed or lobate boundary, and the concentric morphologic belts or facies are uninterrupted. Where the rim material is older, its circular map pattern is interrupted by the younger materials, and parts of one or more of the rim facies may be missing at the surface. The pattern of the Archimedes rim material illustrates both relations (fig. 4). On the Apennine bench it is complete like that of Copernicus, so it is superimposed on the material of the bench and is younger; however, parts of the rim are covered by mare material, and Archimedes is therefore older than the mare surface. This age relation is confirmed by the obvious filling of the crater by mare material. Additional evidence for the ages of craters relative to adjacent material is provided by satellitic craters--small elongate or composite craters which surround large craters

---

<sup>3</sup>The rim material of a crater formed by impact consists of debris ejected simultaneously with formation of the crater; the ejecta from a caldera is volcanic and comes to the surface before and during collapse; ejection from a maar occurs sporadically over a period of time.

and probably formed nearly simultaneously with the large crater, whatever their origin.<sup>4</sup> The satellitic craters of Copernicus are visible on the surrounding mare surface and thus younger than the mare material; those of Archimedes are obliterated by the mare material and thus older than the mare.

Local stratigraphic columns can be constructed by such reasoning with little recourse to genetic interpretations. Extending the second example above, a fairly detailed history has been worked out in the Archimedes area (fig. 4B) (Hackman, 1964, 66; Shoemaker, 1964). The oldest recognizable material is the rugged terra of the Apennine Mountains ("Apennines" on fig. 2), stratigraphically complex material whose surface unit is the Fra Mauro Formation (If). Following in succession are: the smooth flat material of the bench (Apennine Bench Formation, Iab), the material of Archimedes (Ic), and the mare material (Ipm). Next youngest are two craters (Aristillus and Autolycus, unit Cc) which, like Copernicus, clearly overlie the mare material. Much of the history of the entire Imbrium basin (fig. 5) was deduced from the stratigraphic relations of these units in the Archimedes area. These relations show, for example, that at least some of the material filling the Imbrium basin is considerably younger than the basin itself. (All units in this area are discussed further in later pages.)

#### Morphologic Units

Many, possibly most, lunar rock-stratigraphic units, rather than being single lithologic units, are more nearly comparable in scale and complexity with an assemblage of rocks that would occupy a geologic province on Earth and would be designated as a "complex"; for example, the early Tertiary volcanic complex of the Basin and

---

<sup>4</sup>The writer and most of his colleagues believe satellitic craters form by impact of material ejected as the result of other, larger impacts (see especially Shoemaker, 1962). Thus, they are secondary craters. However, stratigraphic meaning of the superposition relations is the same under any interpretation provided the satellitic craters formed at about the same time as the parent craters.

Range province. Many units probably represent intricately overlapping and interfingering beds of various volcanic materials, blankets of local and far-flung impact ejecta, and erosional debris.

Where a unit is believed too complex to be designated as a single rock-stratigraphic unit, it is classed as a morphologic unit. Some areas are mapped as morphologic units whose visible properties apparently are caused by structural, erosional, impact, or other processes which have obscured original stratigraphic relations. For example, much of the lunar terrae consist of an intricate mosaic of topographic forms--hills, pits, various undulating surfaces, etc. Morphologic units here are given such designations as coarse hummocky material, regional pitted material, ridge material, and so forth.

Some morphologic units are primarily structural units. From the Moon, the Colorado Plateau or one of the ranges of the Basin and Range province might be mapped as a unit. Comparable lunar structural units which are commonly mapped as morphologic and not rock-stratigraphic units are the inner basin, shelf, and concentric troughs and high arcs of mare basins (figs. 5, 7, 8).

#### Time-Stratigraphic Units

Local sections of rock-stratigraphic units such as those of the Archimedes area are correlated by means of widespread rock-stratigraphic units or by second-order assumptions such as that the density of superposed craters is related to the age of the underlying bedrock. A lunar stratigraphic column has been built up of rock-stratigraphic and morphologic units and like the terrestrial column has been divided into time-stratigraphic (time-rock) units for convenience in summarizing geologic history (table 1) (Shoemaker, 1962, p. 344-351; Shoemaker and Hackman, 1962). Following terrestrial convention, the major time-stratigraphic units are designated systems and their subdivisions, series. The corresponding geologic-time units are periods and epochs, respectively. The

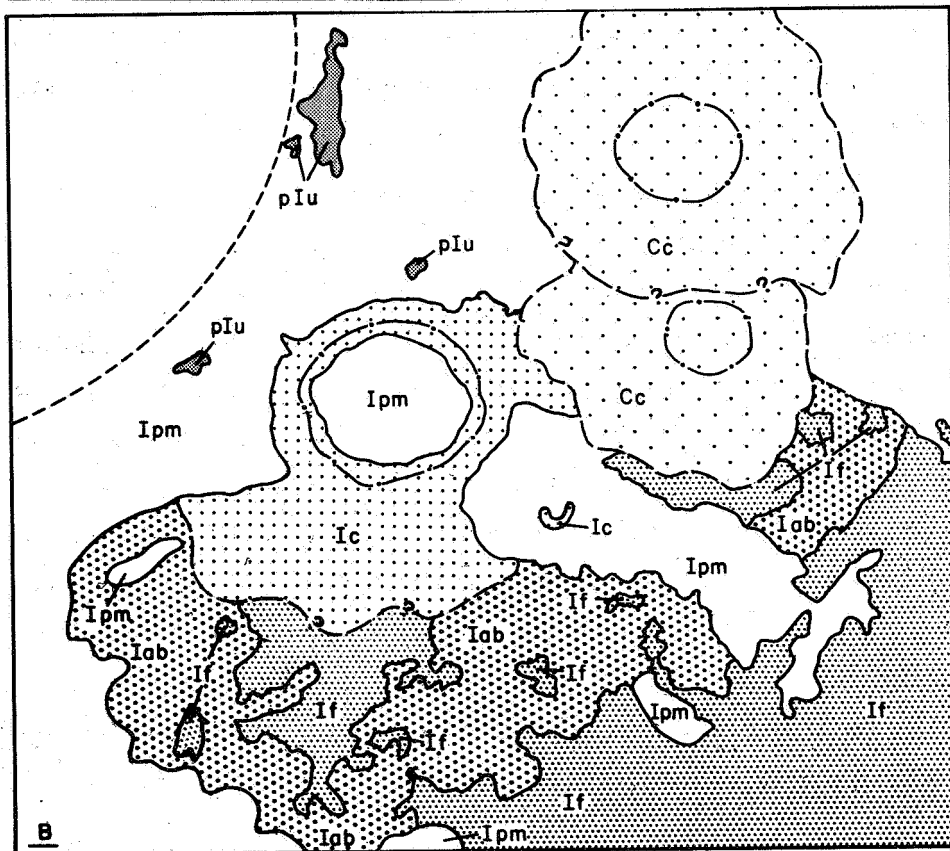
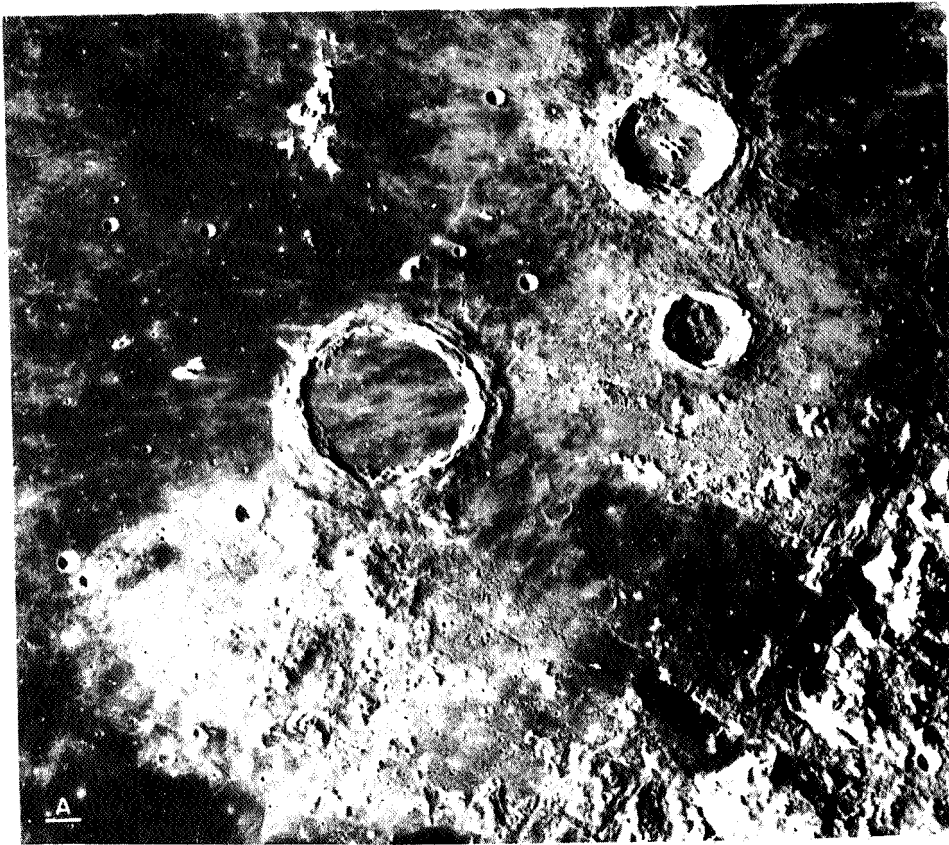
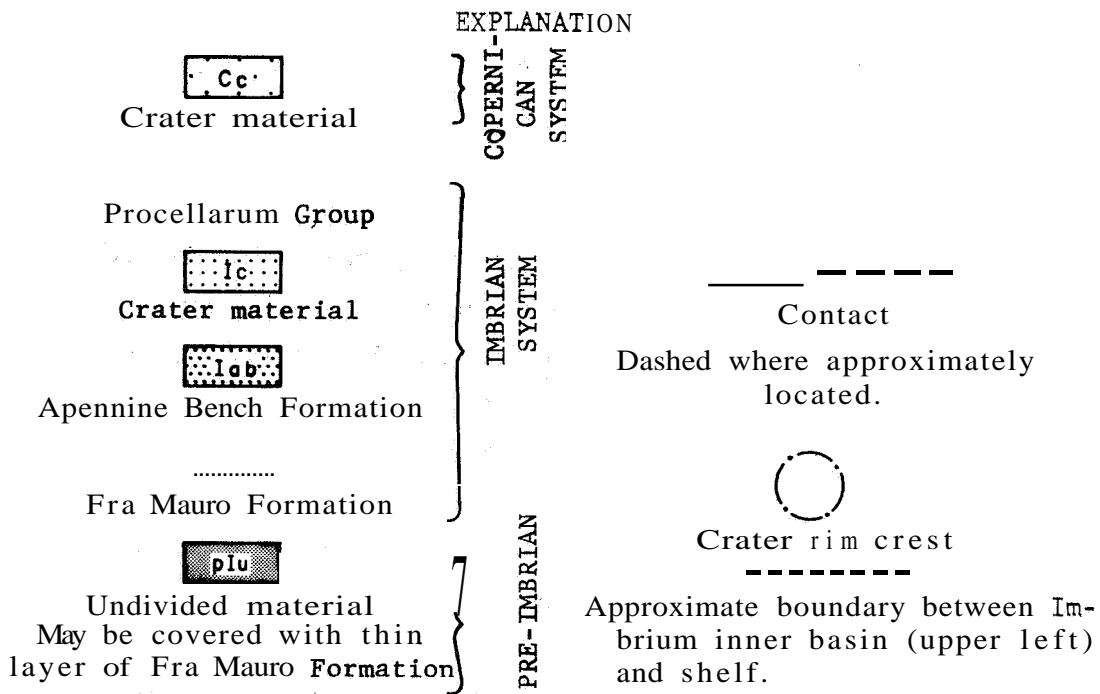


Figure 4A.--Largest crater is Archimedes, 80 km in diameter; rugged terrain in lower right corner is Apennine Mountains (Montes Apenninus); dark mare between Archimedes and Apennines is Palus Putredinis; remainder of mare is part of Mare Imbrium; light terrain south of Archimedes is the Apennine bench (informal name). Archimedes is younger than the bench but older than the mare material. This photograph (L-35) was taken with the 120-in. reflector, Lick Observatory, by G. H. Herbig.

Figure 4B.--Geologic sketch map of area in figure 4A (after Hackman, 1966). Boundary between shelf and high arc surrounding Imbrium basin is approximately at contact between main mass of Fra Mauro Formation in Apennine Mountains and the two units Iab and Ipm.



three systems recognized at present, from oldest to youngest, are the Imbrian, Eratosthenian, and Copernican (one fewer than proposed by Shoemaker and Hackman, who included a Procellarian System). Materials older than the Imbrian System are not yet assigned to systems and are designated simply as pre-Imbrian. The Imbrian System has been divided into two series, the Apenninian and Archimedian (Shoemaker and others, 1962). These series have been used on some maps but have never been formally proposed.

The Imbrian System is the only time-stratigraphic unit so far defined by type sections of rock units, and unfortunately the original definition is now in doubt. The defining units are the Fra Mauro Formation at the base and Procellarum Group at the top; both are widespread and moderately uniform, but the designation of the Fra Mauro as a rock-stratigraphic unit is controversial and the age of the Procellarum may vary enough from area to area to prohibit exact regional correlations. For the Eratosthenian and Copernican Systems, an assumption of age based on physical characteristics is the basis for system assignment. Many rayed craters are known to be younger than nonrayed craters; rayed craters are therefore placed in the Copernican System and nonrayed craters on the maria in the Eratosthenian. However, some nonrayed or dark-rayed craters are known to be younger than some bright-rayed craters. Lunar time-stratigraphic units therefore express only approximate correlations and the approximate position of separated units in lunar geologic history as a whole. They will be retained for this purpose on reconnaissance maps at a scale of 1:1,000,000 or smaller, but on all larger scale maps will be dropped and replaced by purely rock-stratigraphic sections until rigorous Moon-wide correlations are made from spacecraft photographs and surface radiometric dates.

#### Map Units and Symbols

A map unit may represent one or several rock-stratigraphic, morphologic, or time-stratigraphic units, depending on the scale and purpose of the map. A lunar map unit commonly represents

several occurrences of like materials each of which formed at a different time but within a certain interval of time. Each individual occurrence of such material is regarded as a formation, as it would be terrestrially, but all are given the same name because it is not convenient at scales of 1:1,000,000 or less to give each a separate name. The symbol for a lunar map unit, like a terrestrial one, consists on an abbreviation of the system to which it is assigned (capital letter) and an abbreviation of the formal or informal name (lowercase letters). Where the age is unknown, only the abbreviated formal or informal name is used.

#### Portrayal of Superposed Units

In some areas where the surface unit is thin, the subjacent unit can be recognized and mapped on the basis of its characteristic morphology. Buried units that can be recognized are shown by symbols in parentheses and by dotted contacts drawn at the limit of observed topographic expression (not at the inferred or projected limits). Generally the unit shown in color as the surface unit is the youngest unit which contributes significantly to the topography, although opinions differ about which unit should be stressed. The choice of surface unit depends largely on the scale of mapping. At telescopic resolution, the rim material of an old crater of the Southern Highlands is easily recognized as a morphologic unit and on maps at 1:1,000,000 scale it is the unit mapped. But spacecraft photographs show such a rim to have a mantled appearance, and on larger scale maps based on these photographs various mantling materials may be the units mapped, with the rim unit shown underlying them.

#### THE LUNAR STRATIGRAPHIC COLUMN

The remainder of this paper is a systematic review of lunar stratigraphic units which have appeared on 1:1,000,000-scale maps, grouped into time-rock units as they are on the maps. The first part of the discussion, devoted to units of pre-Imbrian and Imbrian age, will concentrate on areally extensive units associated with

mare basins. The second part, devoted to units of Imbrian and (or) Eratosthenian, Eratosthenian, and Copernican age, will include discussions of local materials *of* probable volcanic origin that generally formed later than the main basin filling. Crater materials, the dominant kind of lunar materials, will be discussed in all sections since craters have formed in all lunar geologic-time periods.

#### General Observations

Mare basins are, by definition, very large circular depressions hundreds of kilometers in diameter that are at least partly filled with mare material. The formation of a mare basin is a major event which largely obliterates evidence of earlier events in its vicinity and initiates a new stratigraphic succession.

The time of formation of each of the basins relative to one another has been estimated by freshness of structures surrounding the basins and density of superposed craters. The sequence of basins., from oldest to youngest, is approximately as follows: Fecunditatis, Serenitatis, Nectaris, Humorum, Crisium, Imbrium, Orientale. The last two are Imbrian in age; the Imbrian Period began with the formation of the Imbrium basin. Other features, such as Nubium and Tranquillitatis, whose circular form is less clear may also be mare basins, but each possibly consists of two or more coalescing but separately formed basins. Oceanus Procellarum is an irregular generally depressed mare-covered area, and if any basins are present they are obscured by the mare material.

The stratigraphic sequence in each basin is grossly similar to the sequence established in the Archimedes area for the Imbrium basin, though the units vary in age from basin to basin (table 1). At the base of each local section are the material and structural units believed to have formed before the basin, followed by those formed contemporaneously with it. Structural units formed contemporaneously with the basin include the rugged, cratered terra in several concentric raised arcs and scarps surrounding the basin (figs. 5, 7, 8). They may be formed only of uplifted prebasin

bedrock, or may be overlain by a deposit of debris ejected from the basin during its formation. Deposits which have been interpreted as ejecta are found around five basins: Imbrium, Orientale, Humorum, Nectaris, and Fecunditatis (in order of decreasing confidence in interpretation).

Two kinds of units that are younger than the circumbasin materials are light plains-forming materials and crater materials. The light plains-forming materials fill troughs between the raised arcs and cover the shelves of the basins (figs. 4, 5, 7). In the Archimedes area of the Imbrium basin, the plains-forming materials are older than the crater Archimedes, but in most areas there is a complex overlapping sequence of plains-forming and crater materials.

Next younger in all basins, covering part of the lighter plains-formers in the troughs and shelves and filling the inner basin, is widespread dark plains-forming mare material. This rock-stratigraphic unit, the Procellarum Group, was originally thought to be approximately the same age in all basins but more and more exceptions to this are being found. Lastly, crater materials and other materials of the Eratosthenian and Copernican Systems overlie the Procellarum Group in all basins.

Craters--young and old, large and small--are obviously the dominant features everywhere on the Moon. Many topographic features are recognized as parts of craters after allowance is made for faulting and partial burial.

Craters that are round or equidimensionally polygonal and have raised rims are normally assigned to systems. Craters older than the Fra Mauro Formation are pre-Imbrian. Craters younger than Fra Mauro but older than the Procellarum Group are Imbrian. Nonrayed craters on the Procellarum Group are Eratosthenian. All bright-rayed craters are Copernican. Many craters whose stratigraphic relations are not directly determinable must for the present be dated subjectively by apparent freshness. There seems to be an age progression from the very fresh craters like Copernicus with high sharp rims, deep floors, and well-developed hummocky and

Table 1.--Composite lunar stratigraphic columnar section showing rock-stratigraphic and morphologic units discussed in text. Units are arranged according to the mare basin they are nearest, but many units are not genetically related to the basins; units not near a basin are listed under terra. Units believed to have formed contemporaneously with each basin are shown in narrow horizontal boxes (for example, If, a rock-stratigraphic unit, and plkr, a morphologic or structural unit); the relative positions of these boxes therefore indicate the relative time of formation of the basins. In the column for each basin below unit Ipm, crater materials are shown in the left-hand subcolumn and plains-forming and other materials in the right-hand subcolumn. Satellitic crater materials (for example, Gsc) are not shown separately; they have the same position as primary crater units (in this example, Cc).

SYSTEMS	ROCK-STRATIGRAPHIC AND MORPHOLOGIC UNITS																		
	West					East													
COPERNICAN	Orientale		Humorum		Imbrium			Serenitatis		Nectaris		Fecunditatis		Crisium		terra			
	Cs	Cc	Cs	Cc	Cs	Cc	Cs	Cc	Cs	Cc	Cs	Cc	Cs	Cc	Cs	Cc	Cs	Cc	
ERATOSTHENIAN	Ec	Ec	Eld	Ec	Els	Ec	Em	Et	Elh	Ec	Ec	Elp	Ec	Ec	Ec	Ea	Eic		
	Ipm	Ipm	Ipm	Ipm	Ipm	Ipm	Ipm	Ipm	Ipm	Ipm	Ipm	Ipm	Ipm	Ipm	Ipm	Ipm	Ipm	Ipm	Ipm
IMBRIAN	lk	lp	lp	lp	lc	lc	lca (ln,lp)	lab											
	Ico and lh	Iplc	Iplg	Iplp (Iplhb)	Ic	Ic	Ic	Iab											
PRE-IMBRIAN	Iplc	Iplu	Iplu	Iplu	Iplu	Iplu	Iplu	Iplu	Iplu	Iplu	Iplu	Iplu	Iplu	Iplu	Iplu	Iplu	Iplu	Iplu	Iplu
	Iplc	Iplu	Iplu	Iplu	Iplu	Iplu	Iplu	Iplu	Iplu	Iplu	Iplu	Iplu	Iplu	Iplu	Iplu	Iplu	Iplu	Iplu	Iplu

EXPLANATION OF SYMBOLS USED IN TABLE 1

[Numbers in parentheses refer to pages on which principal descriptions of units are given.]

Crater units younger than Procellarum Group

Cc Crater material (light-rayed) (285) Ccd, dark-halo crater material (285) has same stratigraphic position

Ec Crater material (28) Miscellaneous units younger than Procellarum Group

Cs Slope material (287)  
Cca Cavalerius Formation (291)  
Cre Reiner Gamma Formation (293)  
Cnd Dark mare material (287)  
Csr Sinuous rille material (294)  
Ch Cobra Head Formation (294)  
Ct Theophilus Formation (291)

E<sub>3</sub> Vallis Schrötteri Formation (294)  
Em Marius Group (294)  
Emd Dark mare material (291)  
Et Tacquet Formation (293)  
Ea Apollonius Formation (291)

Units partly contemporaneous with Procellarum Group

E<sub>2</sub> Crater material (281)  
E<sub>1</sub> Doppelmayer Formation (282)  
E<sub>3</sub> Sulpicius Gallus Formation (282)  
E<sub>4</sub> Harbinger Formation (283)  
E<sub>5</sub> Petavius Formation (291)  
I d Diophantus Formation (273)  
Ipmd? Dark mare material (278) may be younger than Procellarum Group

Procellarum Group

Ipm Mare material (276)  
[Ipd, dome material (279)  
Ipr, rough-dome material (279)  
Ipsc, cone-crater material (279)  
Iph hummocky material  
These units also belong to the Procellarum Group (279) but may be younger than most of the mare material.]

Crater units younger than the basins but older than the Procellarum Group  
Ik Krüger Group (275)  
Ic Crater material (272) [Archimedes Group]

Ip<sub>1c</sub> Crater material (265)  
Ip<sub>1g</sub> Gassendi Group (267)  
Ip<sub>1f</sub> Fracastorius Group (267)  
Ip<sub>1y</sub> Yerkes Group (267)

Plains-forming and other noncrater units younger than the basins but older than Procellarum Group

Ip Plains-forming material (271)  
Ica Cayley Formation (271)  
Iab Apennine Bench Formation (271)  
Iaz Anzout Formation (275)  
Ip<sub>1p</sub> Plains-forming material (266)  
Ip<sub>1pp</sub> Fitted Plains Formation (267)

Units contemporaneous with formation of basins

Ico Cordillera Formation (274)  
Ih Hevelius Formation (274)  
If Fra Mauro Formation (268)  
Ip<sub>1kr</sub> Crisium rim material (263)  
Ip<sub>1v</sub> Vitello Formation (263)  
Ip<sub>1py</sub> Pyrenees Formation (264)  
Ip<sub>1ce</sub> Censorinus Formation (264)  
Ip<sub>1r</sub> Regional material (264)  
Ip<sub>1se</sub> Secchi Formation (264)

Units older than the basins

Ip<sub>1c</sub> Crater material (265)  
Ip<sub>1u</sub> Undivided material (not discussed)  
Ip<sub>1c</sub> Crater material (260)  
Ip<sub>1u</sub> Undivided material (257)  
Ip<sub>1rh</sub> Ridge and hill material (263)

The following symbols, shown in parentheses in the table, appear on preliminary maps only and are superseded by symbols shown above them:

In, Ip Plains-forming material (271)  
Inb Nectaris Bench Formation (266)  
Iso Sommi Formation (266)  
Ip<sub>1hb</sub> Humorum Bench Formation (266)  
Ip<sub>1b</sub> Bond Formation (266)

radial rim-material facies to subdued craters, like many in the Southern Highlands, with low rounded rims, shallow broad floors, and little detectable rim material except for a narrow rim. Craters dated only by freshness are placed in three broad categories: pre-Imbrian, pre-Imbrian or Imbrian, and Imbrian or Eratosthenian. These designations overlap, probably enough so that they are not much in error. In any case, they are useful conventions to discriminate morphologic subtypes of round or equidimensionally polygonal craters.

Most craters that are not round or high rimmed, other than satellitic craters, are not assigned to systems. They include irregular high-rimmed craters, low-rimmed round or slightly elongate craters, and craters alined in chains or along rilles. Round or irregular depressions are commonly mapped by depression symbols or by the interpretive convention of arcuate faults and not as geologic units. Most round or equidimensionally polygonal craters that have raised rims, and their satellitic craters, are believed to be of impact origin, whereas most other craters are believed to be of internal origin.

#### Pre-Imbrian Units

Materials older than the basal unit of the Imbrian System, the Fra Mauro Formation, are complex and have been divided mainly into morphologic units, though a few formal rock-stratigraphic units have been recognized and interpreted as depositional units. Chief among pre-Imbrian units are raised arcs concentric with mare basins, complex terrain units in interbasin areas, and crater materials. Materials are recognized as pre-Imbrian in age in several ways. Near the Imbrium basin, pre-Imbrian materials are identified either directly, in areas where they appear to be buried by the Fra Mauro Formation, or indirectly, in areas where they are cut by structures known as Imbrian sculpture believed largely contemporaneous with the Fra Mauro. Farther from the Imbrium basin, regional materials are inferred to be pre-Imbrian where the density

of superimposed craters is greater than on the Fra Mauro, and craters are inferred to be pre-Imbrian if their relief is much more subdued than that of known Imbrian craters or if they are overlapped by pre-Imbrian regional materials.

The Imbrium basin, like all mare basins, is surrounded by several concentric belts of alternately raised and depressed terrain (fig. 5). In the center is an island-free inner basin approximately 650 km in diameter surrounded by a ring of islands (Straight Range, Mons Pico, Spitzbergen, La Hire, the hill-like promontories at the cusps of Sinus Iridum, etc.). Next outward is the low shelf, including the Apennine bench. Outside the shelf is the most prominent topographic ring, composed of rugged arcuate mountain ranges named the Carpathians, Apennines, Caucasus, and Alps in different areas. The subsurface material of the rugged ring is by definition pre-Imbrian, because the surface material except for a few apparent pre-Imbrian System. This pre-Imbrian material is no doubt a complex assemblage of rocks and has been mapped by most workers merely as pre-Imbrian undifferentiated (pIu, table 1).

Pre-Imbrian undifferentiated is, loosely considered, a rock-stratigraphic unit, but the ring surrounding the Imbrium basin probably owes its present form to structural deformation, probably at the time of formation of the basin. Under the impact hypothesis, the Apennine Mountains and the rest of the ring were uplifted by shock waves from the impact and immediately covered by the Fra Mauro Formation, the ejecta from the impact.

Many rocks near the Imbrium basin are transected by Imbrian sculpture, a system of scarps, ridges, and troughs radial to the center of the basin (fig. 6) (Gilbert, 1893; Hartmann, 1963).<sup>5</sup>

---

<sup>5</sup>Gilbert and several later authors believed the troughs and ridges to have been "sculptured" by flying debris from the Imbrian impact, but the morphology of the so-called sculpture can easily be explained as a series of fault horsts and grabens, and faulting is the preferable mechanical explanation. Sculpture remains a convenient term for the set of features radial to the Imbrium basin. Similar sculpture is present around other basins (Hartmann, 1964).

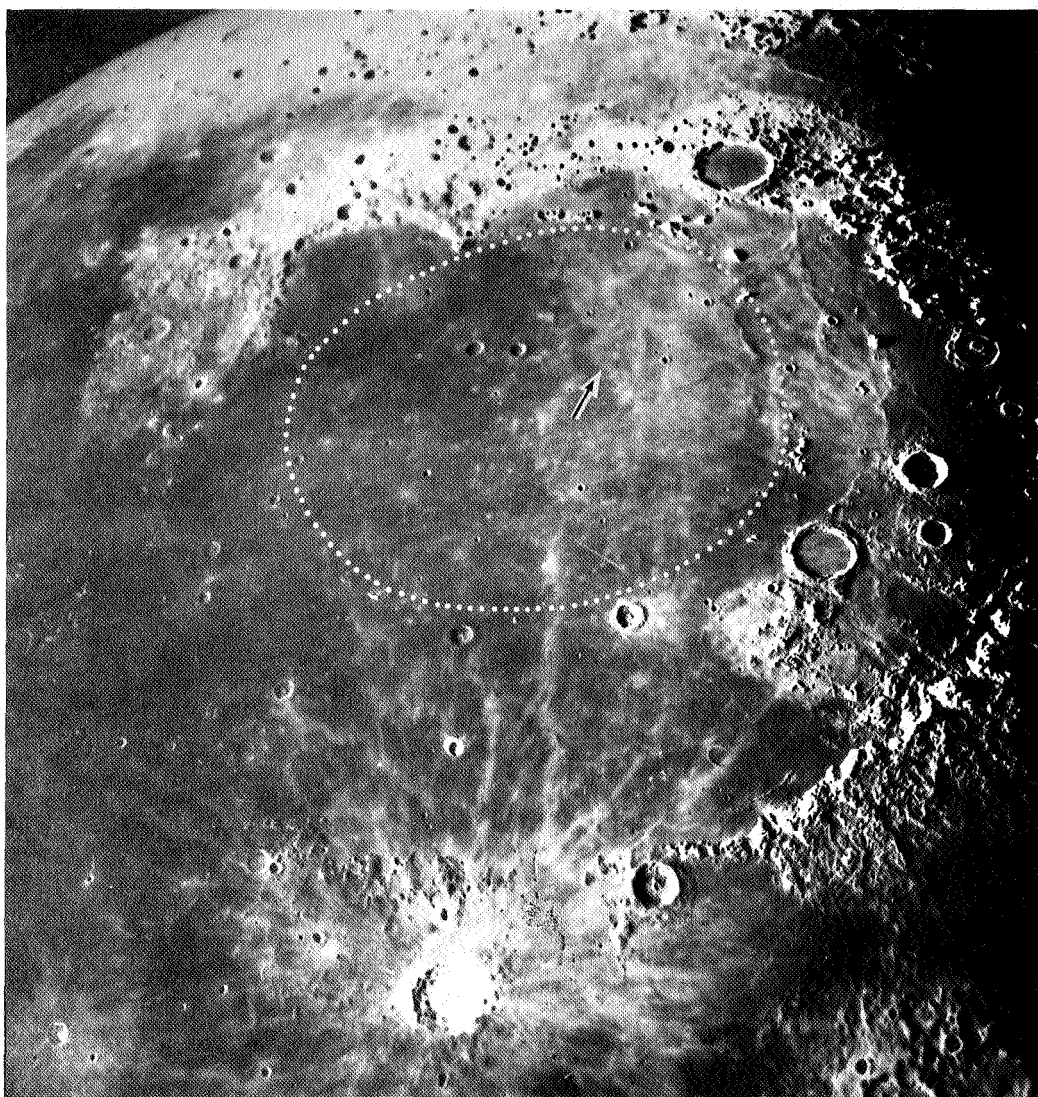


Figure 5.--Mare Imbrium. Frontal scarps of Apennine Mountains and other ranges (see fig. 2) enclose **main** Imbrium basin. Ring of dots outlines approximately the inner basin, about 650 km in diameter. Apennine bench (see fig. 4) is part of shelf between inner basin and main scarp. Elongate maria at top of picture are in troughs concentric with the basin. Note lobate contacts between mare units of different albedo (arrow). See rectified photographs of basin in Hartmann and Kuiper (1962). This unpublished photograph was taken with the 100-in. reflector, Mt. Wilson Observatory.

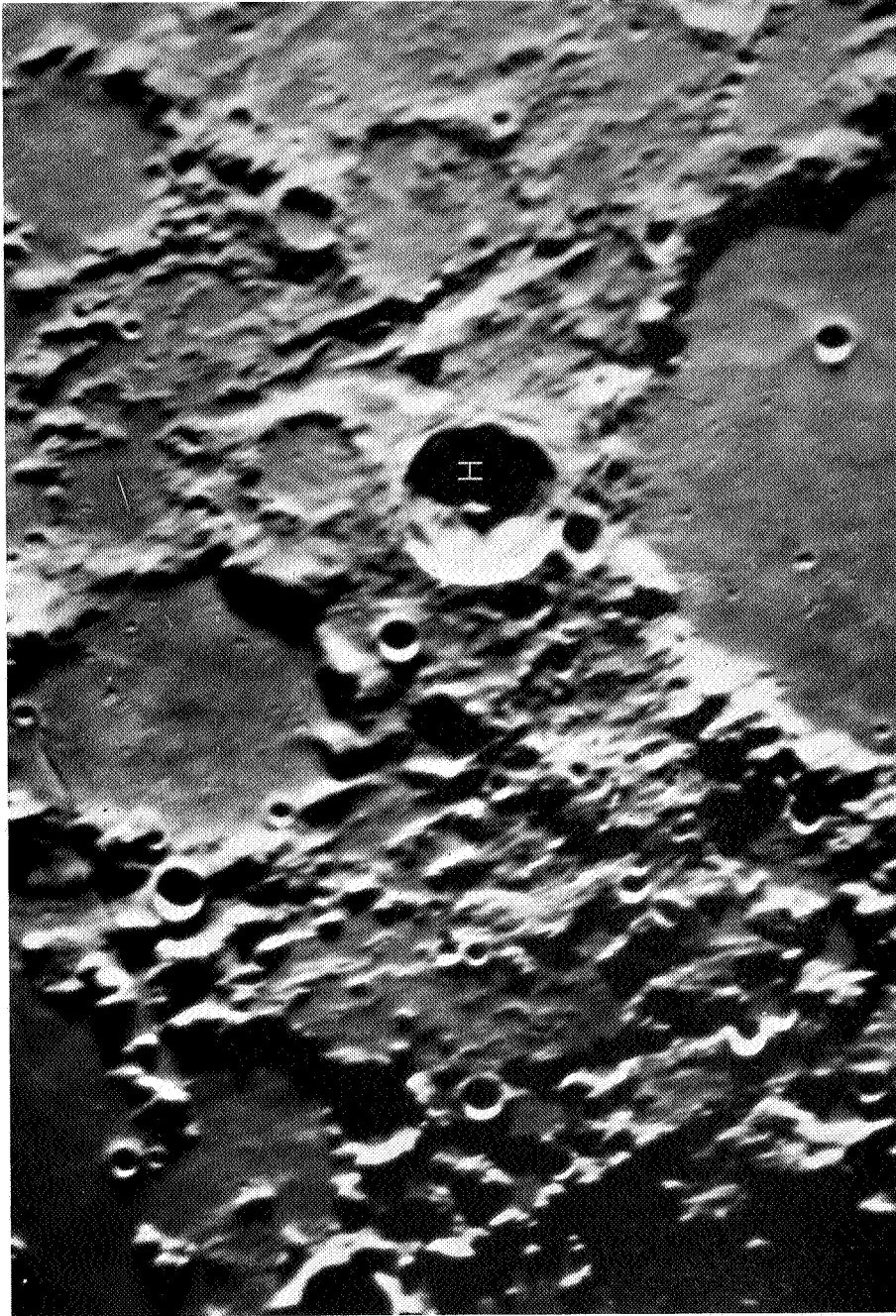


Figure 6.--Central part of Moon showing "Imbrian sculpture" trending N. 30° W., radial to the Imbrium basin. Large flat-floored crater at bottom of picture is Ptolemaeus, 145 km in diameter; fresh crater to right of center is Herschel (H), 40 km in diameter. The rims of Ptolemaeus and many other flat-floored craters are cut by the Imbrian sculpture, but the floors of these craters and the rim of Herschel are not cut. Geologic map of this area by Masursky (1965b). (Photo. 1907, Catalina Observatory.)

The assumption that much of the Imbrian sculpture pattern originated at the moment of basin formation seems valid and has been used to date the transected units. The criterion based on the above assumption is particularly helpful because the Imbrian sculpture pattern can be traced farther from the basin than the Fra Mauro Formation. The close geometric relation between the radial sculpture pattern and circular basin implies a genetic relation. While some faults probably were preexisting fractures and only emphasized by the presumed Imbrian impact, and others have been rejuvenated since the impact, most of them must have been produced by the shock wave proceeding outward from the basin-forming impact (Shoemaker, 1962, p. 349; additional bibliography is given in this reference). Therefore, a crater or other object close to the Imbrium basin and cut by many fractures radial to the Imbrium basin is likely to be pre-Imbrian even though one or two such fractures do not prove pre-Imbrian age.

Lunar surface units beyond the limits of the Fra Mauro Formation and Imbrian sculpture are dated and correlated with units of known age near the basin largely by comparison of crater densities and general freshness of appearance. Other criteria lacking, craters (pIc and its subunits<sup>6</sup>) are dated as pre-Imbrian which have many other large craters superposed on them, and which have very low, narrow rims and shallow broad floors.

Some of the most extensive pre-Imbrian materials are those in arcs like those near the Imbrium basin but concentric to other basins. Examples are the Altai Scarp (Rupes Altai) and several lesser highs around the Mare Nectaris basin, and the two prominent arcs bounded by steep jagged scarps around the Crisium basin (fig. 7) (Wilhelms and others, 1965; Hartmann and Kuiper, 1962). Arcs around three other circular basins--Serenitatis, Humorum (fig. 8),

---

<sup>6</sup>Unit pIc is sometimes divided in the manner of younger craters as discussed in footnote 10 on p. 273, but commonly only a central peak, pIcp, is discriminated in view of the rather amorphous nature of pre-Imbrian craters.



Figure 7.--Mare Crisium to right (east). Large crater at top of picture is 140 km in diameter. Crater Yerkes (Y) is at bottom, younger than the Crisium structural basin but older than the mare material (Masursky, 1965a). Topographic high arcs and low troughs concentric with the basin occur in alternation around it. Troughs (shown by dashed) are filled with mare material (Procellarum Group) and light plains-forming material (unit IpIp); mare is in the southern part of middle' trough and northern part of eastern one; light plains-forming material occurs in the rest (Pohn, 1965b; Binder, 1965). Inner Crisium basin probably lies inside ridges and scarps marked by arrows. See rectified photographs of region in Hartmann and Kuiper (1962). (Photo. 687, Catalina Observatory.)

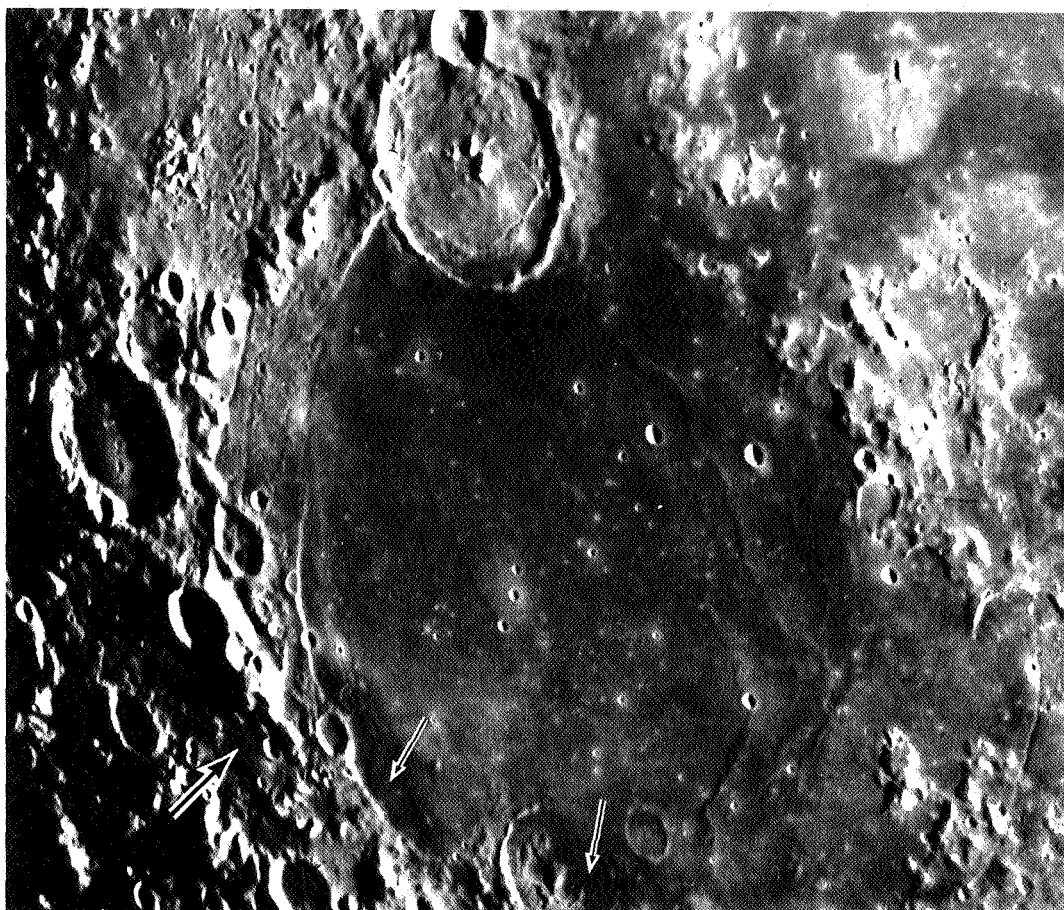


Figure 8.--Mare Humorum. Large crater at top of picture is Gassendi., 110 km in diameter. Southern rim of Gassendi is embayed by mare material (Procellarum Group). Rugged terrane to left of Gassendi is mostly the Vitello Formation (pIv). Dark terrane at bottom of picture (small arrows) is Doppelmayer Formation (EId); east occurrence of this formation overlies part of the rim and interior of the crater Doppelmayer. . Note ridges and mare-filled trough (large arrow) concentric with the basin. Inner basin probably lies between southernmost part of Gassendi rim and northernmost part of Doppelmayer rim. Geologic map of this area is by Titley (1967). (Photo. 1607, Catalina Observatory.)

and Fecunditatis--are less well defined. The Fra Mauro Formation has not been identified on any of these arcs so their dating is indirect. The surfaces of the arcs are pocked by many more large craters than is the surface of the Fra Mauro; hence, they must be pre-Imbrian unless the formation of craters is uncommonly localized. Further evidence of their age, though still more indirect, is the relatively subdued topography of the arcs. Only the Altai Scarp and the arcs of Crisium approach the Apennines in elevation and ruggedness.<sup>7</sup> Like the Apennine Mountains and other elements of the Imbrium ring, the topographic expression of the pre-Imbrian basin rings must have been imprinted at the time of basin formation upon prebasin (that is, upon pre-Imbrian) rocks. These rocks are designated mostly as pre-Imbrian undifferentiated (pIu), but also as pre-Imbrian ridge and hill material (Humorum basin--Trask and Titley, 1966; Titley, 1967), or simply as pre-Imbrian crater material (pIc) (Crisium basin inner arc, on 1:1,000,000 maps--Masursky, 1965a; Binder, 1965; Wilhelms, 1965b; Pohn, 1965b; in table 1 of this report and on the 1:5,000,000 compilation (Wilhelms and Trask, 1965a) the inner and outer ring of Crisium are together shown as Crisium rim material (pIkr) to distinguish them from other units of pIc and pIu).

The surface materials on these rings differ from basin to basin and are assigned rock-stratigraphic status and interpreted with varying degrees of confidence. Hummocky material like the Fra Mauro Formation but having less continuous exposures is present around the Humorum basin (fig. 8), where it is named the Vitello Formation (pIv) (Trask and Titley, 1966; Titley, 1967). This unit is believed with some confidence to be a blanket of ejected debris. Around the Crisium, Serenitatis, Nectaris and Fecunditatis basins, hummocky material and smooth material have patchy distribution, and

---

<sup>7</sup>The structures associated with another basin, Mare Orientale, are fresher than those of the Imbrium basin; this and other evidence suggests that the Orientale basin is Imbrian.

recognition of stratigraphic units and interpretations of origin are only tentative. Around the Crisium basin a few hummocky patches are mapped (and assigned noncommittal pre-Imbrian or Imbrian ages) (Pohn, 1965b), but as mentioned the inner raised ring is mapped simply as crater material (pIc), and the outer ring is mapped as pIu (Masursky, 1965a; Binder, 1965) or regional material (pIr) (Wilhelms, 1965b; Pohn, 1965b) [or the two rings together as Crisium rim material (pIkr) (Wilhelms and Trask, 1965a)]. Around the Serenitatis basin, except for additional patches of hummocky material (Pohn, 1965b; Carr, 1965a), the only unit is again the vague regional material (pIr, with numerical subdivisions) (Pohn, 1965b). High tracts of smooth material called the Censorinus Formation (pIce) (Elston, 1965a) between Mare Nectaris and Mare Tranquillitatis and material with considerable relief called the Pyrenees Formation (pIpy) (Elston, 1965a; formerly Pyrenees Group, Elston, 1964) which overlies large craters near Nectaris, may be composed of ejecta from Nectaris or some other basin. Hummocky material called the Secchi Formation (pIse) (Wilhelms, 1965b) that occurs near the Nectaris and Fecunditatis basins has a texture that grades outward from the Fecunditatis basin as the texture of crater rim material grades outward from craters, but the patchy distribution of the Secchi places its identification as ejecta in doubt. If hummocky material like the Fra Mauro ever surrounded the pre-Imbrian basins continuously, it is now nearly completely covered, or else its characteristic hummocky texture has been obliterated by mass wasting and prolonged meteorite bombardment. Until better photographs are available and impact ejecta and volcanic and erosional materials are differentiated, most geologists will map materials around basins and between basins as morphologic units and not assign rock-stratigraphic status to them. This procedure has been applied extensively in the Rupes Altai quadrangle, for example, where four morphologic units--three variations of hummocky and one pitted and hummocky--have been recognized (and assigned Imbrian or pre-Imbrian ages); none, one, or all of these may be composed

of ejecta from the Nectaris basin (Rowan, 1965). One plains-forming unit has been dated as pre-Imbrian because it is highly cratered, the Pitted Plains Formation (pIpp) east of Mare Nectaris (Elston, 1965a).

#### Pre-Imbrian and (or) Imbrian Units

Many lunar units are designated pre-Imbrian or Imbrian, meaning that they are older than the top of the Imbrian System but that their relation to the base of the Imbrian is unknown. Other units are designated pre-Imbrian and Imbrian, meaning that they are older than the top of the Imbrian, but that some individual occurrences of the unit are known or believed to be older and some younger than the base of the Imbrian. Most of the units of these categories that are discussed here are associated with pre-Imbrian mare basins and are younger than the basins, and their stratigraphic relations to the basins are similar to those of the Imbrian units to the Imbrium basin. Some pre-Imbrian or Imbrian morphologic units located near the eastern basins and possibly contemporaneous with those basins have been mentioned under "pre-Imbrian units" and will not be discussed again here.

The blanket designation of pre-Imbrian or Imbrian (IpI) has come into wide use in lunar geologic mapping because of the limited extent of the Fra Mauro Formation and the Imbrian sculpture, and because of the uncertain validity of sculpture as a criterion for dating. The approximate top of the Imbrian System is determinable over a larger area, because many rock-stratigraphic units are in contact with the widespread Procellarum Group (see p. 276) and can be dated relative to it by embayment relations; in addition, the age of some materials relative to the Procellarum can be estimated by density of superposed craters.

Crater material (IpIc) is a common pre-Imbrian or Imbrian material. This age designation may seem nearly meaningless but is useful for those craters which are much less fresh, and have superposed craters, than Eratosthenes and other Eratosthenian craters, but are

not sufficiently cratered, subdued, and degraded to remove all doubt that they are pre-Imbrian.

Another common type of pre-Imbrian or Imbrian material forms light flat smooth surfaces and resembles the Cayley Formation of Imbrian age (see p. 270). Such materials occur over much of the lunar surface, mostly in depressions. They are common in the troughs surrounding each pre-Imbrian mare basin (fig. 7), and on the shelf between the inner basin and the first high ring (figs. 4 and 5). They embay the rugged terrain of the circumbasin structures and are not cut by faults which cut the structures, so they are younger than the basins. Although they resemble the Cayley, they are not datable relative to the Fra Mauro Formation or Imbrian sculpture and so cannot be correlated with Cayley. They are given the symbol IpIp, for pre-Imbrian or Imbrian plains-forming material.<sup>8</sup>

The slightly different designation pre-Imbrian and Imbrian (also IpI) has a more definite meaning. This designation refers to the age of groups of craters which, like unit IpIp, are younger than a pre-Imbrian basin but older than the Procellarum Group which fills the basin; an example is the crater Gassendi in the Humorum basin (fig. 8). The position of these crater materials in the local basin stratigraphy is thus analogous to that of the materials of the crater Archimedes in the Imbrium basin stratigraphy--younger than the basin but older than the basin-filling Procellarum. While no individual crater can be dated any more closely than Imbrian or pre-Imbrian, the groups probably include

---

<sup>8</sup>The occurrences of these materials near each of the mare basins were given separate formal names on preliminary open-file maps. The common informal designation is now used because of the similar appearance of all occurrences, including some between the basins which cannot be related to the basin sections. The names on preliminary maps are: Humorum Bench material (Titley, 1964) or Formation (Wilhelms and Trask, 1965a), Nectaris Bench Formation (Wilhelms and Trask, 1965a), Bond Formation (on the Serenitatis bench)(Pohn, 1965a, b), and Somni Formation (on the bench and troughs around Crisium and dated as Imbrian) (Wilhelms, 1965b).

craters of both pre-Imbrian and Imbrian age, because near every basin, craters are more numerous per unit area than Archimedes Group craters are near the Imbrium basin. Pre-Imbrian and Imbrian crater materials for each of the basins are named as follows (see table 1): Gassendi Group (IpIg and its subdivisions<sup>9</sup>) (Trask and Titley, 1966; Titley, 1964, 1967); Humorum basin; Yerkes Group (IpIy) (Masursky, 1965b); Crisium basin (see fig. 7); Fracastorius Group (IpIf) (Wilhelms and Trask, 1965a), Nectaris basin. Some crater materials that Wilhelms and Trask call Fracastorius Group are shown as the Gutenberg Group (pIgu) of pre-Imbrian age by Elston (1964, p. 106; 1965a, b). No groups have yet been named in the Serenitatis, Fecunditatis, and other basins because crater materials formed after the basin are difficult to distinguish from those formed before; all are called merely pre-Imbrian or Imbrian crater materials.

Separate symbols and colors are used for "or" crater materials and "and" crater materials. In explanations, the former are shown to the left of the main column, while the latter are incorporated in the main column above units formed contemporaneously with the basin and below the Procellarum Group.

## Imbrian System

### General features

The units of the Imbrian System are well represented in a clear stratigraphic sequence in the Archimedes area, as discussed on p. 272. The name Imbrian is derived from Mare Imbrium; the system includes essentially all the rocks formed between the time of formation of the Imbrium basin and the time of completion of most of its filling. However, the type areas of the rock-stratigraphic units which define the Imbrian System, the Fra Mauro Formation at the base and the Procellarum Group at the top, are outside the basin.

---

<sup>9</sup>See footnotes 10 and 11 on p. 273 concerning subdivision of crater materials and use of formational letters such as "g" in place of "c" for "crater material."

### Fra Mauro Formation

The terra surrounding the Imbrium basin has a hummocky surface which is generally the same in belts concentric with the basin but changes progressively with respect to distance from the basin; it is coarsely hummocky close to the basin and less hummocky or smoother farther out (fig. 9). This regularity suggests that the surface material is a true rock-stratigraphic formation; that is, the hummocky morphology is intrinsic to the unit and the unit forms a laterally continuous bed of material (whose exposure is interrupted in many places by younger material). The unit is named the Fra Mauro Formation (If) (Eggleton, 1964, p. 52) for the crater Fra Mauro, a pre-Imbrian crater buried by the formation. Two members are recognized by Eggleton, one of which is hummocky and the other smooth (fig. 9). On two published maps (Eggleton, 1965; Hackman, 1966) and several preliminary ones, a dark hummocky facies is distinguished (Ifhd, not on table 1) but most mappers now regard the dark coloration as that of a superposed unit, the Sulpicius Gallus Formation (EIs, table 1; see discussion under Imbrian or Erasthenian materials).

The present Fra Mauro Formation was originally called simply the Imbrian System, because of its obvious relation to the Imbrium basin (Shoemaker and Hackman, 1962, p. 293, 294), and thus was equated to a time-stratigraphic system. Later (Shoemaker and others, 1962), it was called the regional material of the Imbrian System (Ir, Hackman, 1962; Marshall, 1963) and was equated to the time-stratigraphic unit the Apenninian Series, the older of two series of the Imbrian System, after the Apennine Mountains (Montes Apenninus) where the unit is well developed. But stratigraphic practice requires basic units to be lithologic and not time-stratigraphic units, and the Fra Mauro Formation was set up later by Eggleton with specific type localities and a more exact lithologic definition than the earlier one (Eggleton, 1964). Materials resembling the type Fra Mauro and having lateral continuity with the formation at its type area or in the Apennines are mapped as Fra Mauro,

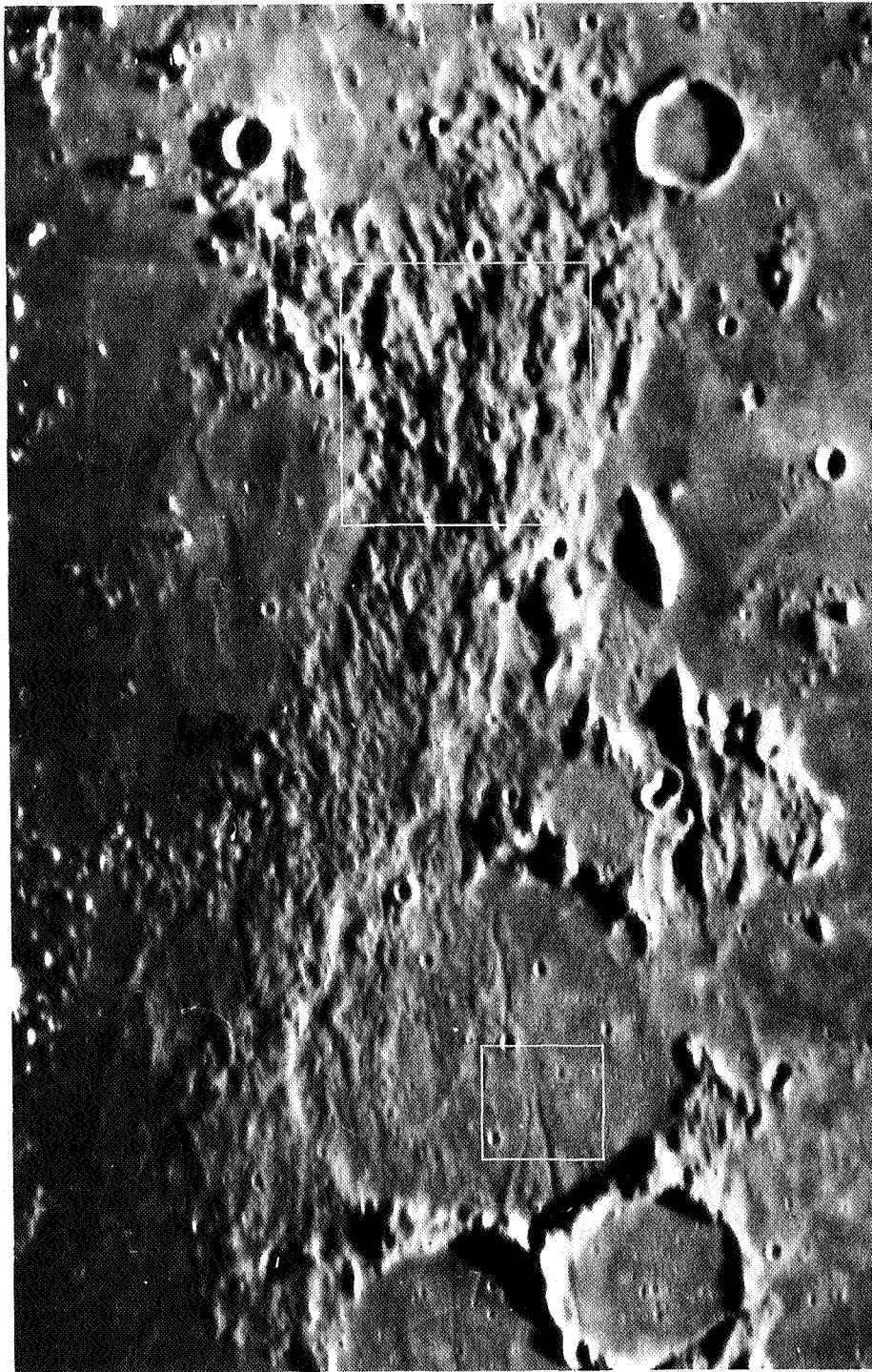


Figure 9.--Type area of the Fra Mauro Formation--hummocky member (upper box) and smooth member (lower **box**) (Eggleton, 1964, 1965). Lower box *is* within crater Fra Mauro, 95 km in diameter. **Hummocky** member grades to smooth from north (nearest Imbrium basin) to south. (Photo. 1994, Catalina Observatory.)

whereas other materials are mapped separately even if they may be contemporaneous with the Fra Mauro.

The Fra Mauro, like all lunar rock-stratigraphic units can be delineated objectively on the basis of physical properties, and age relations can be determined objectively from superposition and transection relations. However, the thought process that led to its recognition as a unit included an interpretation of its origin and history of emplacement. The interpretation was based on the observation that Mare Imbrium occupies a basin that has many characteristics of a giant crater. The basin is circular and is surrounded by circular rings of rugged topography. The surface material of these rings, the Fra Mauro, resembles rim material of fresh young craters in that its inner part is coarsely hummocky and its outer part smoother; and it seems to be thickest close to the basin since very few old craters are visible there, probably because the Fra Mauro mantles pre-Imbrian craters progressively more deeply toward the basin. The crater Julius Caesar is most heavily mantled by Fra Mauro on slopes facing the Imbrium basin as it would be if debris traveling in low trajectories piled up against obstacles (Morris, 1964; Morris and Wilhelms, 1967). The outer part of the Fra Mauro is lineated radially to the basin as is the outer part of crater rim material, although this linearity may be due to underlying structure and not the result of the depositional process as is (most likely) the linearity of crater rim material. A further conjectural similarity is a belt of pitted terrain about one crater (basin) diameter from the basin (Wilhelms, 1965a). Since large craters are probably produced by impact, the Fra Mauro is interpreted as the ejecta from a great impact which excavated the Imbrium basin. However, much of the Fra Mauro may well prove to be pre-Imbrian bedrock which is highly shattered but not laterally transported, and much of its surface may be covered by younger, presently unrecognized volcanic materials.

#### Cayley Formation

Light plains-forming material is abundant and widely distributed

on the Moon's surface. Much of this material in the central and northern parts of the Moon is believed to be of Imbrian age because it is younger than the Fra Mauro Formation but is apparently older than the Procellarum Group. One occurrence already mentioned is the light plains-forming material on the Apennine bench near the crater Archimedes. Another is the material in a circum-Imbrian trough near the crater Cayley (lat 4" N., long 15° E.) (Wilhelms, 1965a; Morris and Wilhelms, 1967). In the latter area the material is unaffected by the Imbrian sculpture which has greatly modified the adjacent terrain; the unit appears to be embayed by the Procellarum Group of Mare Tranquillitatis and has a higher crater density than the Procellarum. Except for the Apennine Bench Formation, all lunar plains-forming materials in the central part of the Moon which resemble this occurrence and are of demonstrable Imbrian age are designated the Cayley Formation (Ica; on preliminary maps, Icy). Near the Orientale basin, such materials may be called plains-forming materials of Imbrian age (Ip, table 1). On early maps, materials now called Cayley were also designated simply plains-forming materials of Imbrian age (In, Milton, 1964a, b; or Ip, Rowan, 1965; Holt, 1965).

Most Cayley, as well as other plains-forming material, is smooth and level and occurs in depressions. Like mare material, Cayley is probably composed of bedded materials. Contacts are sharp in places and gradational in places. Where contacts are sharp the Cayley may consist mostly of flows; where contacts are gradational, it may consist largely of free-fall tuff, possibly modified by downslope movement and interbedded with erosional debris.

Many occurrences of smooth, level Cayley merge without a detectable discontinuity in albedo into tracts of subdued topography. Many believe that these tracts are covered with material either identical with level Cayley but thinner or a pyroclastic facies of it, and the tracts are designated the hilly member of the Cayley Formation (Icah; formerly, Int or Ipt--thin plains

material). A pitted member has also been mapped (Inp, Milton, 1964a, b).

The Cayley Formation very likely includes beds that differ in age and lithology. A map made from a Ranger VIII photograph shows three subunits of Imbrian plains-forming material, which is probably Cayley (Milton and Wilhelms, 1966). Much of the material on the floor of Alphonsus that is lumped as Cayley in telescopic mapping is divided into numerous units on maps made from Ranger IX photographs (McCauley, 1966; Carr, 1966b). Even at telescopic resolution, differences in albedo and crater density are apparent from area to area. Post-Imbrian materials may be present within some areas mapped as Cayley, because at high telescopic resolution small spots are seen which are less densely cratered than the Procellarum Group. [One such spot was mapped as Eratosthenian or Copernican plains-forming material, CEp (Elston, 1965a).] Accordingly, subdivisions of the Cayley Formation will be required on future large-scale maps.

#### Archimedes Group

Although within the Imbrium basin, the crater Archimedes (fig. 4 and 5) is not overlain by Fra Mauro Formation nor cut by Imbrian sculpture and is thus younger than the basin and the Fra Mauro. On the other hand, it is older than the upper strata of the Procellarum Group, as shown by its embayment and filling by Procellarum and by the absence on the Procellarum of satellitic craters, which are plentiful on the older Apennine Bench Formation.

The name Archimedes Group is used informally in this paper and will eventually be proposed formally for material of all craters which like Archimedes are younger than Fra Mauro Formation and older than the uppermost unit of the Procellarum Group. Craters of the Archimedes Group can be contemporaneous with, younger than, or older than the Cayley Formation. These craters have previously been called Archimedian Series craters (see "Apenninian and Archimedian Series") or simply Imbrian System craters (unit Ic and its

subdivisions).<sup>10</sup> Satellites craters are symbolized by Isc. Some crater materials of the Archimedes Group which are contemporaneous with the Procellarum Group have been named the Diophantus Formation (Id)<sup>11</sup> (Moore, 1965a).

#### Cordillera and Hevelius Formations

The surface surrounding the Orientale basin, whose center lies on the west limb of the earthside disk, resembles the surface of the Fra Mauro Formation. It is coarsely hummocky close to the basin and smoother farther out; no hummocks are seen on available photographs beyond a distance of about 900 km from the basin center (compared with about 1,000 km for the Fra Mauro. Prebasin craters seem to be almost completely filled close to the basin and progressively less filled farther out (as seen on Zond 3 photographs of the averted hemisphere; see McCauley, in press). The density of postbasin craters around the Orientale basin is much less than on

---

<sup>10</sup>Unit IC--Crater material, undivided--and parallel units of other ages (Cc, CEc, Ec, EIC, IpIc, and sometimes pIc) are divided in large craters into morphologic subunits considered to be members of the formation "c". Subunits include rim material (cr, for example, Icr), wall material (cw) or slope material (s), floor material (cf) and peak material (cp). These members are further subdivided in the largest craters: rim material hummocky (crh) and radial (crr), floor material hummocky (cfh) and smooth (cfs), etc. An outer rim facies where some positive relief occurs together with many satellitic craters has been called crc, cratered rim (Ecrc) (Trask and Titley, 1966) or shown with a special contact symbol and the color of the underlying material (Schmitt, Trask, and Shoemaker, 1967). Examples of special units are material of the central ridge in Alphonsus (IpIr) (Masursky, 1965b) and ring material in Taruntius (Ctr) (Wilhelms, 19658) and in two craters in the Pitatus quadrangle (Ecfr) (Trask and Titley, 1966). Instead of by topography, subdivision can also be by albedo: crd, dark rim (Hackman, 1962); cfd, dark floor (Ryan and Wilhelms, 1965).

\*Where crater materials are given a formal name, the letter symbol for the name ordinarily replaces "c" for "crater" in symbols for the formation, its members, and submembers (though a "c" was added through oversight in the case of the Diophantus Formation in the reference cited).

the surrounding terra.

The surface material has been separated into two rock-stratigraphic units that are believed to be made up of blanketlike deposits. The hummocky unit is called the Cordillera Formation (Ico) (formerly Cordillera Group, McCauley, 1964a, b), and the smoother, possibly laterally continuous unit is the Hevelius Formation (Ih) (McCauley, 1967). These formations are believed to be younger than the Fra Mauro primarily on the basis of preliminary crater counts (McCauley, 1967). The Hevelius is embayed by dark mare material of questionable Imbrian age (Ipmd) and is therefore tentatively assigned an Imbrian age. The Cordillera and, tentatively, the Hevelius Formations are interpreted to be debris ejected by an impact which formed the Orientale basin. The Hevelius is believed genetically similar to the smooth member of the Fra Mauro Formation and similarly may consist locally of bedrock older than the Orientale basin and presently unrecognized younger volcanic units.

Under the basin-ejecta interpretation, the relative youth of the formations is supported by the apparent youth of the Orientale basin; the scarps concentric with the Orientale basin appear very fresh and there is comparatively little mare filling in the basin and along the base of the scarps. The upper age limit of pre-Eratosthenian is supported by the absence of Orientale sculpture or secondary craters or stringers of ejecta on the mare material of possible Imbrian age 1,000 km from the basin center; at this distance from the center of the Imbrium basin, there is much Imbrian sculpture in the pre-Imbrian materials. However, this mare material could be post-Imbrian and the Orientale basin could have a highly asymmetric peripheral structural pattern, as suggested by the Zond 3 photographs, so that the basin and the Cordillera and Hevelius Formations could be Eratosthenian in age (McCauley, written commun.).

### Crüger Group

Craters which are superposed on the Cordillera and Hevelius Formations and embayed and filled by mare material are dated as Imbrian on the assumptions that the Cordillera and Hevelius are Imbrian and that the mare material is correlative with the Procellarum Group (the mare could be younger; it was mapped as dark mare, EImd, by Trask, 1965b). Such craters are related to the Orientale basin and Procellarum Group as the craters of the Archimedes Group are related to the Imbrium basin and Procellarum. The Orientale craters have been tentatively named the Crüger Group (Ik) (McCauley, 1964a), although the relations of the crater Crüger are not entirely clear.

### Miscellaneous noncrater units

Three units that appear to have considerable intrinsic relief and are unlike any discussed above have been tentatively assigned to the Imbrian System. The first is the Auzout Formation (Iaz), which consists of large (average, 10 km diameter) sugarloaf hills surrounding smooth to hilly material (Masursky, 1965a). The sugarloaf hills resemble large stratovolcanoes more than do any other known lunar hills. However, the hills could be remnants of the Crisium rim which have been shaped by extensive downslope movement.

Two terra units occurring mostly in the Theophilus quadrangle have been called plateau-forming materials (Milton, 1964a, b). The first unit (It) forms a broad plateaulike arc around part of the Nectaris basin. Unlike plains-forming material, it does not conform to preexisting topography. The material is much like that mapped as Censorinus Formation (pIce) by Elston, illustrating the point that mapping of units is sometimes more reproducible than their age assignment and interpretation. Another unit mapped by Milton is hummocky plateau-forming material (Ith). This occurs as a very rugged and very bright patch centered at about lat  $10^{\circ}30' S.$ , long  $16^{\circ} E.$  (Neither unit is shown on table 1 because of doubts about their age; they may have formed over a long span of time.)

### Procellarum Group

The widespread Procellarum Group (Ipm) (Hackman, 1964, p. 4; U.S. Geological Survey, 1964, p. A141) is an important lunar stratigraphic datum and accordingly has been referred to often in the preceding discussion. In this section, the group is defined and its crater density and albedo, by which it is distinguished from other materials and subdivided, are discussed.

As lunar geologic studies have progressed, lunar mare material--that is, all lunar material which is dark, flat, and smooth--has been increasingly subdivided. Originally, all mare material was thought to be homogeneous and of about the same age, on the basis of crater counts from photographs with poor resolution, and was assigned time-rock status as the Procellarian System, whose type area is in the Copernicus region (Shoemaker and Hackman, 1962, p. 294; Shoemaker, 1962, p. 346). Subsequently, differences of crater density and albedo among mare surface areas became apparent, and certain crater rims (Diophantus, lat 27°30' N. , long 34° W. , Moore, 1965a; Lichtenberg, lat 32" N. , long 67°30' W. , Moore, 1965b) were found to be superposed on mare material in one sector but overlapped by it in another. To handle such complexities, and to follow correct stratigraphic practice by avoiding built-in premature age assumptions, the Procellarian System was dropped and the units of mare material were designated formations and groups--rock-stratigraphic units. Most material traditionally called mare is in the Procellarum Group, but a few occurrences of very dark material are mapped as post-Procellarum rock units. The type area of the Procellarum is the general area of the Kepler region in Oceanus Procellarum (Hackman, 1964, p. 4), but the type areas for subunits of the group are in Mare Serenitatis (Carr, 1966a), where there is less ray cover to obscure relations between the subunits.

Several physical characteristics set mare units apart from other smooth, flat rock units such as Cayley Formation and serve to define the Procellarum Group and its subdivisions. The most obvious properties on present-day photographs are crater density

and albedo. Polarization properties apparently correlate with albedo (Wilhelms and Trask, 1965b). Also, there seem to be slight color differences among patches of Procellarum which can be greatly enhanced by compositing of photographs taken through different filters, notably ultraviolet and infrared (Kuiper, 1965, fig. 13).

Procellarum areas of different albedo, color, and crater density may be underlain by discrete beds, or groups of beds. Commonly the contact between surface units is lobate, suggesting embayment of one flat-lying layer by another (fig. 5). Some surfaces appear higher than others and are bounded by a topographic scarp closely resembling the front of a volcanic flow. Some such scarps coincide with color changes (Kuiper, 1965, p. 29-32). Structures and units may be covered, partly buried, or partly filled by one surface unit but not by another.

Crater density has often been used as a criterion of age of Procellarum subunits and other materials as well. The validity of this depends on the two assumptions that the cratering rate is a function of time and that is constant areally. There may be more or less steady background count of impacting bodies from space forming craters on the lunar surface. However, telescopically detectable secondary impact craters may be distributed quite irregularly. Moreover, volcanic craters are present, and the distribution and rate of formation of these depend on the geologic milieu and will vary with time and place. The use of crater density as a criterion of age therefore depends on identification of primary impact craters. This is possible up to a point, and estimates of relative age can be made from crater counts as a first approximation.

Tentative age estimates of Procellarum units and other materials have been made from albedo on many maps because of an apparent correlation in some areas between crater counts and albedo: the more craters, the higher the albedo (the lighter the surface). Some surface areas which appear to embay other areas, or lie as pools within them, are darker and less cratered than the materials

they appear to overlie. An example is the sparsely cratered surface material of Palus Putredinis, which embays lighter, more cratered mare material and the Apennine Bench Formation (fig. 4). However, exceptions to this correlation between albedo and crater density are numerous, and age estimates based on it are hazardous. More directly, albedo may be a function of exposure of blocky material, which in turn is a function of both age and slope, so that not only old heavily cratered units are light but also units of all ages with any volcanic craters, fault scarps, and slump scars. Albedo may also be a function of chemical composition at least in part.

In many areas the Procellarum Group is subdivided on the basis of differences in albedo into formations whose symbols bear numerical suffixes. Only the sharpest contacts, most likely to represent contacts between beds, are mapped. Each unit so delineated is then assigned a number from the subunit of the type locality in Mare Serenitatis (Carr, 1966a) whose albedo is most nearly the same. Ipm1 has the highest albedo (lightest); Ipm4 the lowest albedo (darkest). [In one area there is a very light unit, Ipm0 (Pohn, 1965b).] A simpler breakdown of light (Ipm with no suffix) and dark (Ipm4) has been used in some areas (McCauley, 1967) and in rayed areas is more satisfactory than the fourfold breakdown. Much dark mare material, however, could well be post-Imbrian in age (McCauley, 1967).

Not all contacts between albedo units are sharp. Some albedo units may represent zones of hydrothermal or other internally produced alteration rather than different rock-stratigraphic units. Straight narrow bands of light material which resemble crater rays are possible examples. Where boundaries of albedo units do not appear to represent edges of beds, a special line symbol is used for them (Carr, 1966a). Boundaries of this type are drawn at albedo levels that most nearly approximate the transitions between albedo subunits in the type locality.

Most Procellarum is flat, and its boundaries terminate

abruptly at the slightest rise in topography. However some smooth dark material which overlies barely perceptible craters (ghosts) and other objects is apparently gradational to flat Procellarum material and has been mapped as Procellarum Group. On one map (Rowan, 1965) an extensive tract of it was mapped as thin mare material (Ipmt), a formation of the Procellarum Group. This Procellarum may be composed of free-fall pyroclastic material or of ash-flow tuff, which is emplaced as fluid flows. Both kinds of material may differentially compact upon cooling, so that the topography of the surface is a subdued form of the subjacent topography.

A type of material different from the Procellarum thus far discussed--mare dome material (Ipd)--is also considered a formation of the Procellarum Group. Domes are low and round or elliptical in plan, and they have convex-upward profiles; some have summit craters. Their surface is similar in fine texture and albedo to that of smooth Procellarum. The contact between most domes and adjacent mare is marked by a sharp topographic break. The domes, especially those with craters, resemble terrestrial shield volcanoes and are probably volcanoes superposed on the mare surface, but some merge gradually into the adjacent mare and may be subsurface intrusions, possibly laccoliths. Both kinds of domes may be younger than the uppermost strata of the smooth mare material nearby, but because of their similar surface texture and albedo they are included in the Procellarum Group. The possible laccoliths are transitional to some gentle mare ridges, which may be sills.

Three more units of the Procellarum Group remain to be discussed. Several domes having rough summits or discrete summit hills are known, and so far have been mapped in one area separately from other domes, as unit Ipr (Moore, 1965a). Second, hummocky material (Iph) is mapped tentatively as another formation of the Procellarum Group in some areas because of its low albedo (Carr, 1965b; Moore, 1965a; Wilhelms, 196513). Such material may be clusters of small domes. Finally, cratered cone material (Ipcc) which lies largely along mare ridges has been mapped as Procellarum by

Elston (1965a, b). All these domes and cones, however, could be younger than the Procellarum Group and unrelated to it.

#### Apenninian and Archimedian Series

In many reports and maps of the Survey the Imbrian System has been divided into the Apenninian and Archimedian Series. At present the base of Apenninian Series is defined as the base of the Fra Mauro Formation and the top as the top of the Apennine Bench Formation (Iab) (Hackman, 1966).<sup>12</sup> The Archimedian Series includes all post-Apenninian Imbrian materials.

The original definitions of the series, not published formally, were somewhat different (Shoemaker and others, 1962). The Apenninian Series included only the "regional material of the Imbrian System," now called the Fra Mauro Formation, and the Archimedian Series comprised only the crater-rim materials that are superimposed on the Apenninian Series and are overlapped by the Procellarian System. Thus the two units defined as series were in fact rock units.

These series names should be dropped. As presently defined they are practical units only in the vicinity of Archimedes and the Apennine bench, because only there can rock-stratigraphic units be assigned to the series; elsewhere, the age of a plains-forming unit or crater relative to the Apennine Bench Formation or the crater Archimedes cannot be determined yet. At best, all that is known is that they belong to the Cayley Formation or Archimedes Group respectively (that is, they resemble these units in their type localities and are younger than the Fra Mauro Formation and older than youngest Procellarum Group).

An alternative is to return to the original definition of the Apenninian Series by restricting it to the Fra Mauro Formation, and place all the remaining Imbrian rock units in the Archimedian

---

<sup>12</sup>These series were not explicitly defined in the publication cited but were employed in this way. The definition appears only in an open-file report (Hackman, 1964, p. 4).

Series. This, however, would produce an undesirable imbalance of the two series and would serve no practical purpose. There would be only one formation in one series--Fra Mauro--and four large units in the other--the Apennine Bench and Cayley Formations and the Archimedes and Procellarum Groups. If the interpretation is correct that the Fra Mauro Formation consists of ejecta, the two series could represent vastly disparate time spans--minutes as against tens of millions of years.

The Cordillera and Hevelius Formations might serve as more meaningful rock units to define a series break if they can be demonstrated conclusively to be Imbrian in age.

#### Summary of Mare Basin Stratigraphy

Most of the units discussed to this point are associated with mare basins. In summary, the stratigraphic column of each basin comprises the following in order of decreasing age: (1) crater materials and undifferentiated bedrock older than the basin and designated as pre-Imbrian; (2) materials interpreted as impact ejecta which accumulated contemporaneously with the creation of the basin; (3) light plains-forming materials and craters such as Archimedes and Gassendi; (4) mare material of the Procellarum Group, deposited in all the basins. The remainder of the section on the lunar stratigraphic column is devoted to units which are less localized by mare basins and their associated structures or not at all.

#### Imbrian or Eratosthenian Systems

Materials which cannot be dated relative to the Procellarum Group but which are believed to be fairly young are assigned to the Imbrian or Eratosthenian Systems (EI). These include crater materials, dark terra-mantling materials, and probable volcanic materials with intrinsic relief.

#### Crater materials

Crater materials that resemble known Eratosthenian ones but are superposed on terra instead of mare are by convention mapped

as Imbrian or Eratosthenian (E1c and its subdivisions). Such craters are topographically sharp and are rayless.

#### Dark terra-mantling units

An important type of Imbrian or Eratosthenian material is darker than or as dark as the Procellarum Group and occurs mainly in the terra. This material is believed to occur as a thin surficial covering because its relief is similar to that of adjacent materials or gentler; ridges, craters, and other topographic forms that pass under the contacts are only slightly subdued if at all. Its topographic expression suggests that the material is largely pyroclastic. Material of this kind adjacent to Mare Serenitatis is named the Sulpicius Gallus Formation (E1s) (Carr, 1966a). Large conspicuous areas of similar materials adjacent to Mare Vaporum and Sinus Aestuum and near Copernicus (Schmitt, Trask, and Shoemaker, 1967) also have been mapped as Sulpicius Gallus (fig. 11), although formerly regarded as a dark hummocky facies of the Fra Mauro Formation (Ifhd) (Hackman, 1966). The type Sulpicius Gallus is thickest along rilles, which are probably its source (Carr, 1965a). The source of other parts may be small craters and domes which are seen as dark spots on very high resolution full-Moon photographs of some areas.

Similar material adjacent to Mare Humorum is called the Doppelmayer Formation (E1d) (Titley, 1967) (fig. 8). Many other occurrences of terra material that are darker than their surroundings are being discovered on new high-quality full-Moon photographs and are being mapped as either of the above formations or as new formations, or shown by an overlay pattern.

Embayment relations suggest that the rugged parts of the Sulpicius Gallus Formation are mainly older than the Procellarum Group, but in some areas parts of this unit and much of the Doppelmayer Formation appear to be younger than the Procellarum. In those areas, flat material adjacent to rugged parts of Sulpicius Gallus or Doppelmayer Formations appears to be continuous with

the surface material of the rugged parts because both have the same low albedo; the mantle presumably extends over both the rugged terrain and the flat Procellarum.

Such flat areas would not be distinguishable from Procellarum if they were not laterally gradational to rugged areas of Sulpicius Gallus or Doppelmayer; the question thus arises, what is the difference between Procellarum on one hand and dark mantling material on the other? The difference may be that Procellarum, which tends to accumulate in available depressions, consists predominantly but not entirely of flows whereas the mantling type consists predominantly of ash.

#### Units with intrinsic relief

Some units mapped as Imbrian or Eratosthenian have considerable intrinsic relief. The best example of these is the Harbinger Formation (E1h) east of the Aristarchus plateau (fig. 10) (Moore, 1964, 1965a). Some of this formation's relief may be due to underlying Fra Mauro Formation, but some is formed by volcanic domes, cones and craters within and on the formation. The Harbinger Formation is characterized by numerous sinuous rilles (E1sr, not shown in table 1) whose high ends terminate at craters within the formation and whose low ends terminate on Procellarum. The rilles may have been cut principally by flowing volcanic material; the direction of flow may have been controlled partly by structure. The Harbinger Formation is designated Imbrian or Eratosthenian because parts of it may interfinger with the Procellarum Group whereas other parts seem to embay Procellarum; material that flowed out of the sinuous rilles may form part of the Procellarum. The Harbinger is part of an extensive volcanic province in the vicinity of the crater Aristarchus (fig. 10; table 1), some formations of which (units CEv, Ch, Csr) may be as young as Copernican (see below).

Another unit having intrinsic relief is the Boscovich Formation (E1b) (not shown in table 1) in the Julius Caesar quadrangle (Morris and Wilhelms, 1967). This unit forms long stringy ridges



Figure 10.--Aristarchus plateau (large parallellogram shaped raised area in left half of picture ); Harbinger Mountains (Montes Harbinger) are the smaller complex in the east half; large fresh crater is Aristarchus, 40 km in diameter; largest of the many sinuous lunar rilles is Schroter's Valley (Vallis Schroteri). Note large cone (28 km long) with summit crater (arrow). Probable volcanic material of several kinds forms the plateau (Vallis Schroteri Formation, Cobra Head Formation, sinuous rille material) and Harbinger Mountains (mainly Harbinger Formation) Geologic maps of this area are by Moore (1965a, b). (Photo. 369, Catalina Observatory.)

approximately parallel with Imbrian sculpture; near it are terra domes of probable volcanic origin. The Boscovich and the domes may consist of viscous volcanic materials extruded from the sculpture fractures.

#### Eratosthenian and Copernican Systems

The next youngest lunar time-stratigraphic system is the Eratosthenian, and the youngest is the Copernican. The two systems are discussed together here because of doubt that they can be validly separated in many areas. The base of the Eratosthenian System is defined as the top of the Procellarum Group.

#### Crater material's

Chief among rock-stratigraphic units of the Eratosthenian System are materials of rayless craters (unit Ec and its subdivisions); chief among Copernican units are materials of light-ray craters (unit Cc and its subdivisions).<sup>13</sup> (Craters that are staellitic to large Eratosthenian and Copernican craters are labeled Esc and Csc, respectively.) Craters that do not have telescopically resolvable light rays, but that have light halos which may be formed of unresolvable rays, are shown on some maps as Eratosthenian or Copernican (unit CEc and its subdivisions). The basis for assignment of rayed and rayless craters into time-rock systems is that rays appear to be among the most recent materials on the Moon and are superimposed on most other materials; for example, the rays of Copernicus overlie the materials of the nearly rayless crater Eratosthenes (fig. 11) (Shoemaker and Hackman, 1962, p. 295-298; Carr, 1964, p. 12-15). It has been supposed that rays darken with time because of external processes, possibly solar radiation and micrometeorite mixing (Shoemaker, 1962, p. 345). (Rays are shown with a stipple pattern on lunar geologic maps.)

---

<sup>13</sup> See footnote 10, p. 273, for discussions of crater-material subunits.

The presence or absence of visible light rays, however, is not entirely a function of age. There are rayless craters with circular dark halos--as Copernican dark-halo craters (Ccd)--clearly superimposed on the ray and rim materials of light-ray craters, including Copernicus (fig. 11) (Shoemaker and Hackman, 1962, p. 297-298, Carr, 1964, p. 16). Presumably similar dark craters of Copernican age are present in areas with no light rays; probably many have been mapped erroneously as Eratosthenian because of the absence of nearby Copernican ray material to determine their relative age. Differences in brightness may represent differences in origin--dark-halo craters may be volcanic, light-rayed craters may be impact. Another factor controlling the presence of rays may be the nature or composition of the material in which the crater formed; for example, there appear to be more light-rayed craters on terrae than on maria. Furthermore, regardless of where the crater formed, rays may form or be preserved more easily on some materials than others; a given ray that is superposed on both light and dark materials is usually brighter on the light materials than on the dark. Possibly the disappearance of rays is due in part to later events, such as burial by a localized ash fall. Finally, to complicate the picture further, the crater Dionysius (lat 3" N., long 17°30' E.) has dark rays as well as light. Probably the best statement of the situation is that the presence of rays is indicative of a young crater, but the absence of rays is not necessarily indicative of an old crater (Carr, 1964, p. 16).

There are therefore serious reservations about the assignment of craters to time-stratigraphic systems solely on the basis of the presence or absence of rays, and Copernican and Eratosthenian should properly be regarded as rock-stratigraphic designations. However, to assure uniformity among new and old maps, the division of post-Procellarum craters into Copernican and Eratosthenian will continue for the present on 1:1,000,000 and smaller scale maps. The younger subdivisions of the lunar time scale can be redefined later when the stratigraphic position of post-Imbrian rock units

other than crater materials is worked out, and when more is known about the formation and preservation of ray materials.

### Slope materials

Slope materials are mapped on the walls of craters and on other steep slopes. If for some reason it is desirable to show that talus, or other material, is younger than the crater on whose walls it occurs, it is mapped as slope material instead of wall material by convention. Otherwise the geologist maps the wall material as being the same age as the crater, either as a wall material subunit or as part of an undivided crater material unit.<sup>14</sup>

Copernican slope material (Cs) is commonly mapped because it has a special significance. It is defined as slope material which is markedly brighter than the adjacent unit. It may be material that was originally light and whose overall high albedo has been preserved by continued exposure of fresh material at a faster rate than the material can be darkened by external processes. Copernican slope material is believed to consist of both talus and exposed bedrock; it is therefore a morphologic unit.

### Probable volcanic units

Several units confidently interpreted to be composed of volcanic materials are recognized and mapped in the Eratosthenian and Copernican Systems. The ages of some of these materials are based on superposition on Eratosthenian and Copernican crater materials and thus are only as reliable as the estimated ages of the craters.

Some of these materials are mare materials (that is, they are smooth, flat, and dark). An example is mare material (unit Cmd) that embays the rayed crater Lichtenberg in the Seleucus quadrangle (Moore, 1965b) (fig. 12). The mare material apparently issued from part of a very long linear fracture, along which patches of rays

---

<sup>14</sup>On early maps (Carr, 1965b; Hackman, 1966) slope material (s) not wall material (cw) was shown as having the same age as the crater.

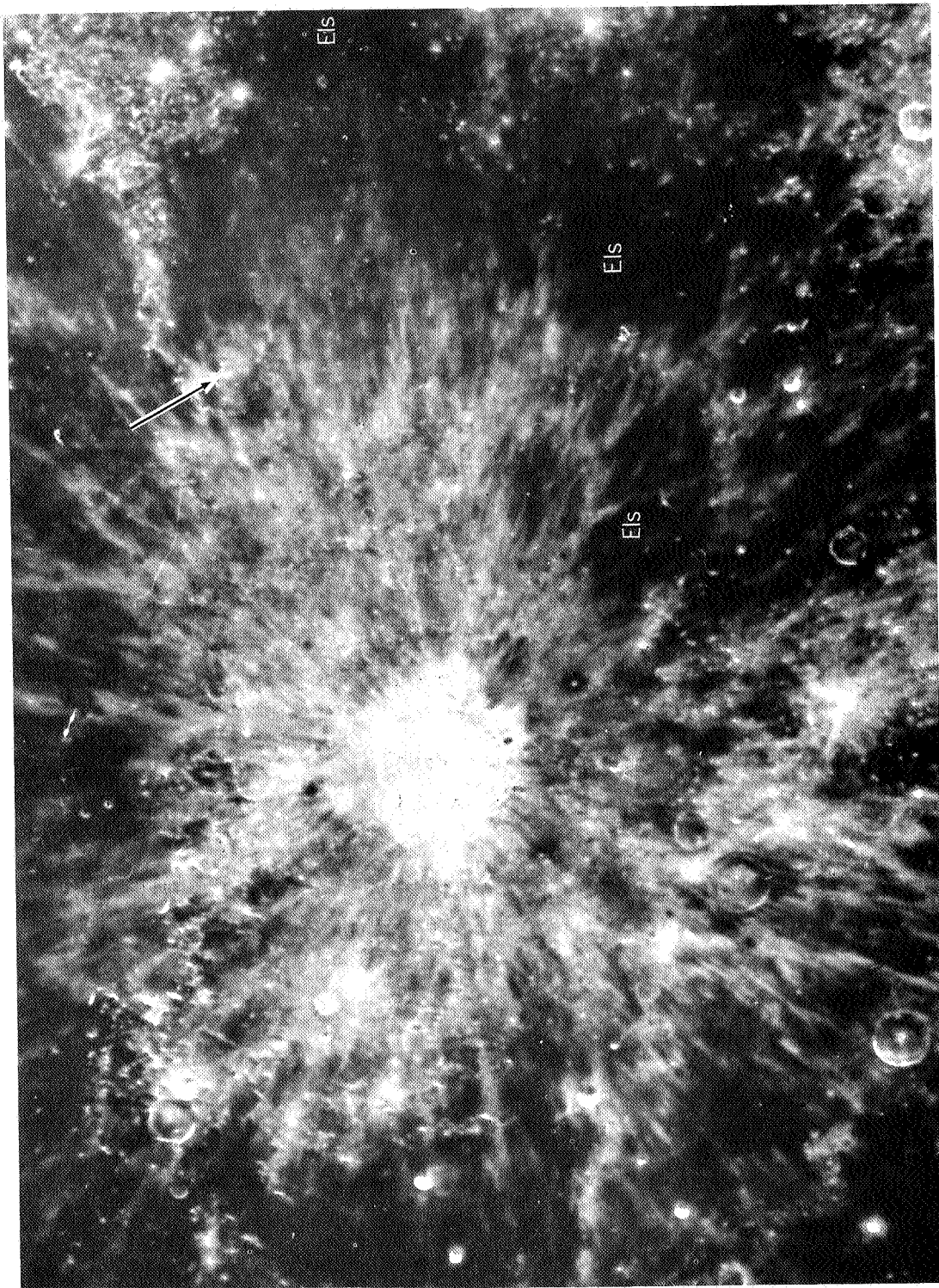


Figure 11 -- Copernicus (left center, 90 km in diameter) and Eratosthenes (its center marked by arrow) under near-full-Moon illumination. Copernicus has a bright ray system; Eratosthenes' rays are barely visible. The rays of Copernicus are clearly superimposed on Eratosthenes' spiral dark-halo craters younger than Copernicus are present; a conspicuous large one is southeast (below and to the right) of Copernicus about a crater diameter away. The dark patches are exposures of the Sulcioidis Gallus Formation (Sims). Compare photograph with the low-illumination photograph of figure 3, in which relief is much more conspicuous. (Unpub. photo. 5818, U.S. Naval Observatory, Flagstaff, Ariz.)

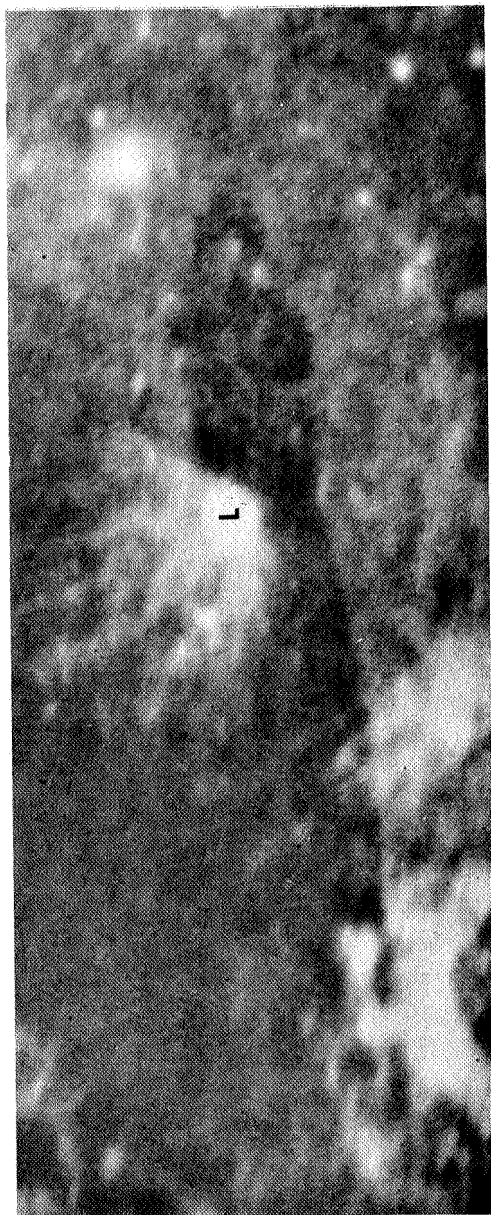


Figure 12.--Rayed crater Lichtenberg (L) and rays of other craters embayed by part of a dark mare deposit that lies along a long lineament. Picture includes an area approximately 500 km east-west. Geologic map of southeast quarter of picture by Moore (1965). (Rectified photo. from Whitaker and others, 1963, pl. 4c.)

of Copernicus are obscured. In addition, mare materials in many mare basins and in places on the terrae are assigned Eratosthenian and Copernican ages because of low crater density and low albedo; CEmd--mare, dark--is a common designation for these materials. The darkest mare material yet recognized is along the east margin of Mare Serenitatis; it is mapped as Eratosthenian mare material, dark (Emd) (Carr, 1966b) because it has very few craters but is apparently overlain by Copernican ray material.

Other, lighter materials which form plains are clearly superposed on crater rim material. In depressions of the rim material of the craters Theophilus and Petavius (lat 25° S., long 61° E.) are flat smooth-surfaced materials which are obviously younger than the craters, and are named for the craters. The Theophilus Formation (Ct) (fig. 13) is Copernican in age because the crater Theophilus is Copernican; the Petavius Formation could also be Copernican, but rather arbitrarily it is assigned to the Imbrian or Eratosthenian (EIp) because the crater Petavius is probably Imbrian. Around areas occupied by the plains-forming materials of both formations, the topography of the crater rim material is subdued, probably by thinner material related in origin to the plains-forming materials. The thinner materials are mapped as hilly member of the Theophilus Formation (Cth) and thin member of the Petavius Formation (EIpt).

Other more extensive thin units, morphologically and probably lithologically like the Sulpicius Gallus and Doppelmayer Formations and apparently covering subjacent terrain and adding little relief of their own, are assigned Eratosthenian and Copernican ages. A thin member of the Apollonius Formation (Ea) (Masursky, 1965a), at the boundary between Mare Fecunditatis and the flank of the Crisium basin, partly covers mare assigned to the Procellarum Group and is dated as Eratosthenian. The Cavalerius Formation of Copernican age (Cca) (McCauley, 1967) is superposed both on the rim material of the postmare crater Cavalerius and on the adjacent mare surface and interrupts Copernican rays. The Cavalerius Formation

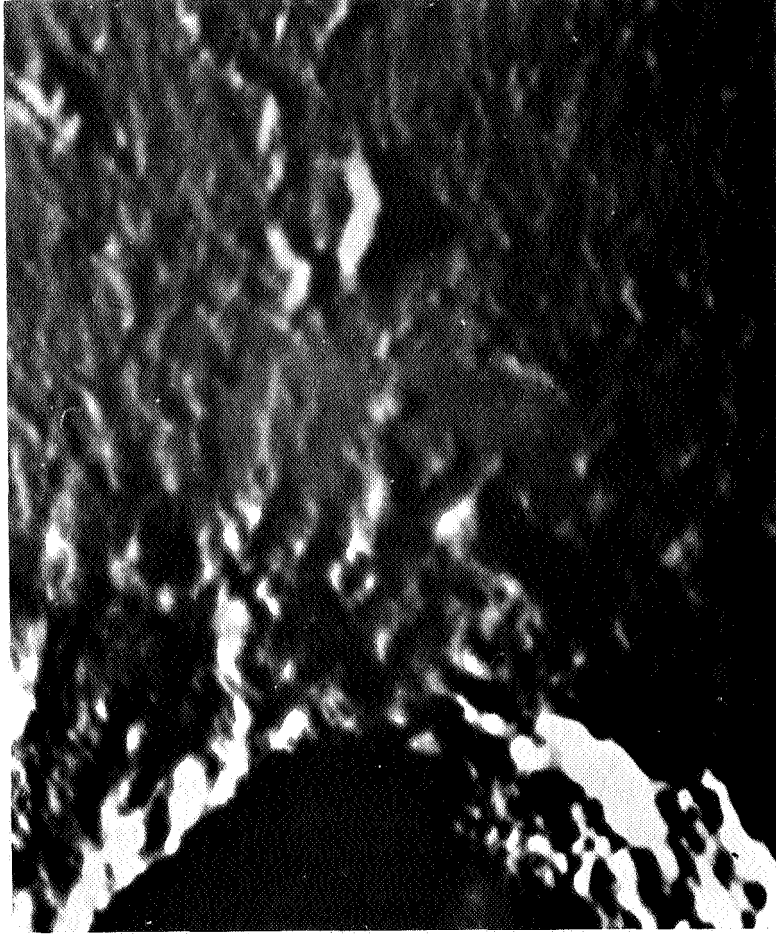


Figure 13.--Crater Theophilus at bottom of picture; its rim material extends over most of remainder of picture. Main occurrence of the Theophilus Formation (Milton, 1964a, b), a plains unit lying on the rim material and therefore younger than the crater, is in the center of picture. Picture includes area approximately 90 km east-west. (Unpub. photo. ECD 37 taken with 120-in. reflector, Lick Observatory.)

is the unit the Soviet probe Luna 9 probably landed on. A similar unit--dark veneering material (Cdv)--obscures rays of Theophilus without modifying the rim topography (Elston, 1965a). Several other units of Copernican age are so thin that subjacent topography is not modified at all; in order not to obscure the more important subjacent units on the map, the covering materials are shown with an overprint pattern and the subjacent units are shown in color (Schmitt, Trask, and Shoemaker, 1967).

At least one thin unit of covering material--the Reiner ~~Gamma~~ Formation (Cre) (lat 7" N., long 59" W.) west of the crater Reiner and south of the Marius Hills (McCauley, 1967)--is brighter than the adjacent material. This peculiar formation is tentatively explained as consisting of ash-flow tuff or an irregular area of surface alteration. Attention is now being given to other areas of light covering materials not associated with craters, but mapping conventions have not yet been established.

Some probable volcanic materials have considerable intrinsic relief. One is the Tacquet Formation (Et) along the southern edge of Mare Serenitatis (Carr, 1966a). The formation forms an elongate low bulbous dark ridge surrounded by lighter probably older material with lower relief. Rilles, some with raised rims which grade into the rest of the formation, run the length of the dark ridge and were probably the source of the material of the formation. Another Eratosthenian unit having relief is the dome-materia? member of the Apollonius Formation.<sup>15</sup>

In the northwest quadrant of the Moon are two complexes of domes and other materials that are believed from superposition relations to be younger than the Procellarum Group. One is the

---

<sup>15</sup>Most isolated small morphologic features of all ages such as domes (d), cones with summit craters (cc), etc., are not given formal names. Some may be given system assignments (CEcc, IpId, etc.), but superposition relations that are obvious from the map suffice to show age for most.

Marius Group (Em) (McCauley, 1967) west of the crater Marius. The Marius Group consists of undulating material forming a plateau and two kinds of domes, one low and convex in profile like mare domes, the other steeper and concave in profile. By analogy with terrestrial morphologic forms the domes are interpreted as volcanic in origin. Some steep domes are superimposed on low domes, as in certain terrestrial volcanic provinces. In some provinces, magma when first extruded is fluid and builds low domes, then with little change in composition loses its volatile components and builds steep cones of pumice and other fragmental debris. In other areas, basaltic magmas build shield volcanoes, and later magmas of alkaline or intermediate composition build steep cones. Steep Pelean spines may also protrude through older low volcanoes.

The other varied volcanic complex in the northwest quadrant of the Moon is the Vallis Schr'dteri Formation (CEv) in the Aristarchus plateau (Moore, 1965 a, b), an area also known as Wood's spot (fig. 10). Besides containing thin blanketing material that does not visibly subdue the underlying topography, the formation includes plains-forming materials, domes, and cratered cones; one elongate cone is as large as **13x28** km. Sinuous rilles head in the formation, as do those in the Harbinger Formation, and terminate in the mare. The two formations are similar and probably represent continued volcanism of the same type.

Transecting the Vallis Schr'dteri Formation is the feature from which the formation is named, the largest of all sinuous lunar rilles, Vallis Schr'dteri. The topographically higher end or head of the rille, called the Cobra Head, is a crater in a very large dome, the material of which is called the Cobra Head Formation (Ch). The Cobra Head Formation and the material in the floor of the rille (Csr, sinuous rille material) are assigned Copernican age because of their apparent topographic freshness and because of the light raylike pattern around the Cobra Head. Like the other sinuous rilles, Vallis Schr'dteri may have been formed partly by erosion as fluid material flowed from the crater at the head to the low end of the rille,

which is in an area mapped as Procellarum Group. The Procellarum Group may thus include Eratosthenian and Copernican materials in this area. Obviously, lunar volcanic stratigraphy is more complex than shown on maps at a scale of 1:1,000,000.

The more thoroughly the Moon's surface is examined, the more small areas are found that can be distinguished from their surroundings by differences in texture, albedo, and crater density. Materials in most of these small areas are post-Imbrian, and the stratigraphy of the Eratosthenian and Copernican Systems will doubtless soon become very complex. However, it is beyond the scope of this paper to describe units that had not been mapped and named, at least on preliminary maps, as of mid-1966.

#### INTERPRETATIVE SUMMARY

Geologic principles have been applied successfully in mapping the lunar surface from Earth-based observations. Surface areas are mapped that are believed to be conterminous with underlying three-dimensional rock-stratigraphic units. The rock units have been arranged in order of relative age in a lunar stratigraphic column. The column is divided provisionally into four parts: pre-Imbrian materials, and the Imbrian, Eratosthenian, and Copernican Systems; the system boundaries, however, are inexact.

The lunar history as read from the stratigraphic units is summarized as follows: In pre-Imbrian time many large craters and mare basins formed that are now subdued, heavily cratered and faulted, and partly or completely buried by younger materials. The estimated order of formation of the more distinct pre-Imbrian basins from oldest to youngest is Fecunditatis, Serenitatis, Nectaris, Humorum, Crisium. The Imbrian Period begins with the formation of the Imbrian basin, and the youngest basin, Orientale, formed later in this period. In Imbrian and also probably pre-Imbrian time, plains-forming materials that are now light (unit IpIp and the Cayley Formation) filled the basins, their peripheral structures, large craters, and other depressions. Craters (Gassendi Group and others) also

formed. Possibly simultaneously with emplacement of the plains-forming materials, the terrae were mantled by related materials that are now light (hilly member of the Cayley and others). Toward the end of the Imbrian Period a great volume of dark plains-forming materials (mare, Procellarum Group) nearly completed the filling of mare basins and other depressions and dark terramantling materials (Sulpicius Gallus Formation and others) were emplaced. All through the Imbrian Period craters formed, and many of these (Archimedes Group) are partly buried by light and dark plains-forming materials. In the Eratosthenian and Copernican Periods additional dark plains-forming and terramantling materials formed, though probably in lesser quantities than in the Imbrian, and other materials formed domes and other features with intrinsic positive relief. Craters formed in these periods are rayless (provisionally, Eratosthenian) and light rayed or dark haloed (provisionally, Copernican).

Although the principle immediate goal of lunar stratigraphic studies is the determination of the sequence of formation of materials, the ultimate goal includes discovery of the origin of materials. Interpretations of origin are not the main purpose of this paper, and deduction of the stratigraphic section proceeds largely without them but some preliminary interpretations have been made.

The lunar crust is largely a succession of interstratified plains-forming materials of volcanic origin, relatively thin mantling materials of mixed origin, and crater materials predominantly of impact origin.

Plains-forming materials range from dark (mare material) to light in brightness, and from pre-Imbrian to Copernican in age. Most dark and many light materials accumulated in preexisting depressions and terminate abruptly against higher topographic forms, suggesting that they consist chiefly of lava or ash flows.

Light and dark terramantling materials, which cover rugged terra and subdue but do not obliterate the subjacent relief,

probably consist of pyroclastic volcanics, farflung impact ejecta, and mass-wasted debris.

Plains-forming and terra-covering materials probably inter-finger; some pyroclastics are interbedded in mare and terra basins and may occur on the surface in many places, and some flows are present in the rugged terrae. Contact relations and crater density counts suggest that the dark mare and terra-mantling units are younger than most light plains-forming and terra-mantling materials, and dark subunits of the mare are younger than lighter ones. Dark and light lunar plains-forming and terra-covering materials may therefore have been dark when first emplaced and became lighter with time, possibly by exposure of blocky material through cratering and downslope movement; thus, the light plains-forming Cayley may be "old Procellarum", and hilly Cayley may be "old Sulpicius Gallus".

Most rugged lunar topographic features are probably parts of craters, young and old, large and small. The stratigraphic position of crater materials is worked out in large part independently of interpretations of their origin, but beyond this, the origin of many lunar craters can be deduced from comparison with natural and experimental terrestrial craters. Many lunar craters perfectly aligned along a fault or a graben or situated exactly on the summit of domes are unquestionably volcanic. Other craters are much more likely to be of impact origin, and these probably include the majority of large lunar craters. The rough steep rims of fresh craters like Copernicus are unlike rims of any large terrestrial caldera and are best accounted for as ejecta emplaced by an explosive mechanism. Most craters satellitic to large fresh lunar craters probably formed by the impact of clusters of fragmental debris excavated from a large explosive crater. The explosive process probably was not an explosion of volcanic gases because sufficient gases could hardly have accumulated and not have been dissipated in advance of one great release. Old craters, however, whose rim material occupies only a narrow subdued band, could have formed in a variety of ways.

In many respects mare basins are morphologically similar to large impact craters, and several are surrounded by deposits resembling impact crater ejecta. These facts plus the great areal extent of radial and concentric structures around the basins suggest they are of impact origin.

The stratigraphy of terra materials between mare basins is not yet well known. The Southern Highlands obviously consist of many large old craters with plains-forming material in and among them.

A brief summary of the results of lunar geologic studies to date and an answer--a foreseeable one--to the old question of whether the lunar crustal features result from impact or volcanism, is: The Moon's crust is a volcanic terrain that is constantly active and is constantly bombarded and deformed by the impact of solid bodies.

Lunar stratigraphy will of course continue to evolve and be refined beyond its status as described in this paper. The rate of progress will accelerate when ground exploration supplies field checks and when more and better spacecraft photographs supply detailed data on the regional relations. But we have gained valuable knowledge from preliminary telescopic work. We know that the Moon's crust is highly heterogeneous, possibly as complex as the Earth's, and knowing this, we will not plan future exploration on the basis that all points on the surface are the same, and that one trip will tell us all about "the" composition of the crust and therefore the history of the Moon. In working out the structure and history of the Moon, we must, as in terrestrial work, think in terms of individual stratigraphic building blocks, and a preliminary insight into these has been gained which will allow us to ask further meaningful questions.

#### REFERENCES

- Binder, A. B., 1965, Preliminary geologic map of the Cleomedes quadrangle of the Moon, *in* Astrogeol. Studies Ann. Prog. Rept., July 1964-July 1965, map supp.: U.S. Geol. Survey open-file report.

- Carr, M. H., 1964, The geology of the Timocharis quadrangle, in Astrogeol. Studies Ann. Prog. Rept., August 1962-July 1963, pt. A: U.S. Geol. Survey open-file report, p. 9-23.
- \_\_\_\_\_ 1965a, Dark volcanic materials and rille complexes in the north-central region of the Moon, in Astrogeol. Studies Ann. Prog. Rept., July 1964-July 1965, pt. A: U.S. Geol. Survey open-file report, p. 35-43.
- \_\_\_\_\_ 1965b, Geologic map of the Timocharis region of the Moon: U.S. Geol. Survey Misc. Geol. Inv. Map 1-462.
- \_\_\_\_\_ 1966a, Geologic map of the Mare Serenitatis region of the Moon: U.S. Geol. Survey Misc. Geol. Inv. Map 1-489.
- \_\_\_\_\_ 1966b, The structure and texture of the floor of Alphonsus, in Ranger VIII and IX, pt. 11--Experimenters' analyses and interpretations: California Inst. Technology, Jet Propulsion Lab. Tech. Rept. 32-800, p. 270-285.
- Cohee, G. V., ed., 1962, Stratigraphic nomenclature in reports of the U.S. Geological Survey: Washington, U. S. Geol. Survey, 35 p.
- Danes, Z. F., 1965, Rebound processes in large craters, in Astrogeol. Studies Ann. Prog. Rept., July 1964-July 1965, pt. A: U.S. Geol. Survey open-file report, p. 81-100.
- Eggleton, R. E., 1964, Preliminary geology of the Rhipaeus quadrangle of the Moon and definition of the Fra Mauro Formation, in Astrogeol. Studies Ann. Prog. Rept., August 1962-July 1963, pt. A: U.S. Geol. Survey open-file report, p. 46-63.
- \_\_\_\_\_ 1965, Geologic map of the Rhipaeus Mountains region of the Moon: U.S. Geol. Survey Misc. Geol. Inv. Map 1-458.
- Eggleton, R. E., and Marshall, C. H., 1962, Notes on the Apenninian Series and pre-Imbrian stratigraphy in the vicinity of Mare Humorum and Mare Nubium, in Astrogeol. Studies Semiann. Prog. Rept., February 1961-August 1961, pt. A: U.S. Geol. Survey open-file report, p. 132-137.

- Elston, D. P., 1964, Pre-Imbrian stratigraphy of the Colombo quadrangle, **&** *Astrogeol. Studies Ann. Prog. Rept.*, August 1962-July 1963, pt. A: U.S. Geol. Survey open-file report, p. 99-109.
- \_\_\_\_ 1965a, Preliminary geologic map of the Colombo quadrangle of the Moon, in *Astrogeol. Studies Ann. Prog. Rept.*, July 1964-July 1965, map supp.: U.S. Geol Survey open-file report.
- \_\_\_\_ 1965b, Preliminary geologic map of the Fracastorius quadrangle of the Moon, in *Astrogeol. Studies Ann. Prog. Rept.*, July 1964-July 1965, map supp. : U.S. Geol. Survey open-file report.
- Gilbert, G. K., 1893, The moon's face, a study of the origin of its features: *Philos. Soc. Washington Bull.* , v. 12, p. 241-292.
- Hackman, R. J., 1962, Geologic map of the Kepler region of the Moon: U.S. Geol. Survey Misc. Geol. Inv. Map 1-355.
- \_\_\_\_ 1964, Stratigraphy and structure of the Montes Apenninus quadrangle of the Moon, in *Astrogeol. Studies Ann. Prog. Rept.* , August 1962-July 1963, pt. A: U.S. Geol Survey open-file report, p. 1-8.
- \_\_\_\_ 1966, Geologic map of the Montes Apenninus region of the Moon: U.S. Geol. Survey Misc. Geol. Inv. map 1-463.
- Hartmann, W. K., 1963, Radial structures surrounding lunar basins, I--The Imbrium system: *Arizona Univ. Lunar and Planetary Lab. Commun.*, v. 2, no. 24, p. 1-15.
- \_\_\_\_ 1964, Radial structures surrounding lunar basins, 11--Orientale and other systems, conclusions: *Arizona Univ. Lunar and Planetary Lab. Commun.*, v. 2, no. 36, p. 175-191.
- Hartmann, W. K., and Kuiper, G. P., 1962, Concentric structures surrounding lunar basins: *Arizona Univ Lunar and Planetary Lab. Commun.*, v. 1, no. 12, p. 51-66.
- Holt, H. E., 1965, Preliminary geologic map of the Purbach quadrangle of the Moon, in *Astrogeol. Studies Ann. Prog. Rept.*, July 1964-July 1965, map supp. : U.S. Geol. Survey open-file report.

- Kuiper, G. P. , 1965, Interpretation of Ranger VII records, in Ranger VII, pt. 11--Experimenters' analyses and interpretations: California Inst. Technology, Jet Propulsion Lab. Tech. Rept. 32-700, p. 9-73.
- McCauley, J. F. , 1964a, The stratigraphy of the Mare Orientale region of the Moon, in Astrogeol. Studies Ann. Prog. Rept. , August 1962-July 1963, pt. A: U.S. Geol. Survey open-file report, p. 86-98.
- \_\_\_\_\_ 1964b, Preliminary geologic map of the Grimaldi quadrangle of the Moon, in Astrogeol. Studies Ann. Prog. Rept. , July 1963-July 1964, map supp. : U.S. Geol. Survey open-file report.
- \_\_\_\_\_ 1965, The Marius Hills volcanic complex, in Astrogeol. Studies Ann. Prog. Rept. , July 1964-July 1965, pt. A: U.S. Geol. Survey open-file report, p. 115-122.
- \_\_\_\_\_ 1966, Intermediate-scale geologic map of a part of the floor of Alphonsus, in Ranger VIII and IX, pt. 11--Experimenters' analyses and interpretations: California Inst. Technology, Jet Propulsion Lab. Tech. Rept. 32-800, p. 313-319.
- \_\_\_\_\_ 1967, Geologic map of the Hevelius region of the Moon: U.S. Geol. Survey Misc. Geol. Inv. Map 1-491.
- \_\_\_\_\_ in press, The nature of the lunar surface **as** determined by systematic geologic mapping, in Mantles of the Earth and terrestrial planets: New York and London, John Wiley & Sons, p. 431-460.
- Marshall, C. H. , 1963, Geologic map of the Letronne region of the Moon: U.S. Geol. Survey Misc. Geol. Inv. Map I-385.
- Masursky, Harold, 1964, A preliminary report on the role of isostatic rebound in the geologic development of the lunar crater Ptolemaeus, in Astrogeol. Studies Ann. Prog. Rept. , July 1963-July 1964, pt. A: U.S. Geol. Survey open-file report, p. 102-134.
- \_\_\_\_\_ 1965a, Preliminary geologic map of the Mare Undarum quadrangle of the Moon, in Astrogeol. Studies Ann. Prog. Rept. , July 1964-July 1965, map supp. : U.S. Geol. Survey open-file report.

- Masursky, Harold, 1965b, Preliminary geologic map of the Ptolemaeus quadrangle of the Moon, in Astrogeol. Studies Ann. Prog. Rept. , July 1964-July 1965, map supp. : U.S. Geol. Survey open-file report.
- Milton, D. J. , 1964a, Stratigraphy of the terra part of the Theophilus quadrangle , in Astrogeol. Studies Ann. Prog. Rept. , July 1963-July 1964, pt. A: U.S. Geol. Survey open-file report, p. 17-27.
- \_\_\_\_\_ 1964b, Preliminary geologic map of the Theophilus quadrangle of the Moon, in Astrogeol. Studies Ann. Prog. Rept. , July 1963-July 1964, map supp. : U.S. Geol. Survey open-file report.
- Milton, D. J. , and Wilhelms, D. E. , 1966, Geology from a relatively distant Ranger VIII photograph, in Ranger VIII and IX, pt. 11--Experimenters' analyses and interpretations: California Inst. Technology, Jet Propulsion Lab Tech. Rept. 32-800, p. 302-313.
- Moore, H. J. , 1964, A possible volcanic complex near the Harbinger Mountains of the Moon, in Astrogeol. Studies Ann. Prog. Rept. , July 1963-July 1964, pt. A: U.S. Geol. Survey open-file report, p. 42-51.
- \_\_\_\_\_ 1965a, Geologic map of the Aristarchus region of the Moon: U.S. Geol. Survey Misc. Geol. Inv. Map 1-465.
- \_\_\_\_\_ 1965a, Preliminary geologic map of the Seleucus quadrangle of the Moon, in Astrogeol. Studies Ann. Prog. Rept. , July 1964-July 1965, map supp.: U. S. Geol. Survey open-file report.
- Morris, E. C., 1964, Stratigraphic relations in the vicinity of the crater Julius Caesar, in Astrogeol. Studies Ann. Prog. Rept. , August 1962-July 1963, pt. A; U.S. Geol. Survey open-file report, p. 31-32.
- Morris, E. C. , and Wilhelms, D. E. , 1967, Geologic map of the Julius Caesar quadrangle of the Moon: U.S. Geol. Survey Misc. Geol. Inv. Map I-510.

- Pohn, H. A., 1965a, The Serenitatis Bench and the Bond Formation, in Astrogeol. Studies Ann. Prog. Rept., July 1964-July 1965, pt. A: U.S. Geol. Survey open-file report, p. 9-12.
- \_\_\_\_\_ 1965b, Preliminary geologic map of the Macrobius quadrangle of the Moon, in Astrogeol. Studies Ann. Prog. Rept., July 1964-July 1965, map supp.: U.S. Geol. Survey open-file report.
- Rowan, L. C., 1965, Preliminary geologic map of the Rupes Altai quadrangle of the Moon, in Astrogeol. Studies Ann. Prog. Rept., July 1964-July 1965, map supp. : U. S. Geol. Survey open-file report.
- Ryan, J. D., and Wilhelms, D. E., 1965, Preliminary geologic map of the Langrenus quadrangle of the Moon, in Astrogeol. Studies Ann. Prog. Rept., July 1964-July 1965, map supp. : U.S. Geol. Survey open-file report.
- Schmitt, H. H., Trask, N. J., and Shoemaker, E. M., 1967, Geologic map of the Copernicus quadrangle of the Moon: U.S. Geol. Survey Misc. Geol. Inv. Map 1-515 (in press).
- Shoemaker, E. M., 1962, Interpretation of lunar craters, in Kopal, Zdenek, ed., Physics and astronomy of the Moon: New York, Academic Press, p. 283-359.
- \_\_\_\_\_ 1964, The geology of the Moon: Sci. American, v. 211, no. 6, p. 38-47.
- Shoemaker, E. M., and Hackman, R. J., 1962, Stratigraphic basis for a lunar time scale, in Kopal, Zdenek, and Mikhailov, Z. K., eds., The Moon--Symposium 14, Internat. Astron. Union: London, Academic Press. p. 289-300.
- Shoemaker, E. M., Hackman, R. J., Eggleton, R. E., and Marshall, C. H., 1962, Lunar stratigraphic nomenclature, in Astrogeol. Studies Semiann. Prog. Rept., February 1961-August 1961: U.S. Geol. Survey open-file report, p. 114-116.

- Titley, S. R., 1964, A summary of the geology of the Mare Humorum quadrangle of the Moon, in Astrogeol. Studies Ann. Prog. Rept., August 1962-July 1963, pt. A: U.S. Geol. Survey open-file report, p. 64-73.
- \_\_\_\_\_ 1967, Geologic map of the Mare Humorum region of the Moon: U.S. Geol. Survey Misc. Geol. Inv. Map 1-495.
- Trask, N. J., 1965a, Preliminary report on the geology of the Byrgius quadrangle of the Moon, in Astrogeol. Studies Ann. Prog. Rept. , July 1964-July 1965, pt. A: U.S. Geol. Survey open-file report, p. 3-8.
- \_\_\_\_\_ 1965b, Preliminary geologic map of the Byrgius quadrangle of the Moon, in Astrogeol. Studies Ann. Prog. Rept., July 1964-July 1965, map supp. : U.S. Geol. Survey open-file report.
- Trask, N. J., and Titley, S. R. , 1966, Geologic map of the Pitatus region of the Moon: U.S. Geol. Survey Misc. Geol. Inv, Map I-485.
- U.S. Geological Survey, 1964, Lunar geologic mapping, in Geological Survey research 1964: U.S. Geol. Survey Prof. Paper 501-A, p. A140-A142.
- Whitaker, E. A. , Kuiper, G. P., Hartmann, W. K. , and Spradley, L. H. , eds. , 1963, Rectified lunar atlas--Supp. 2 to the Photographic Lunar Atlas: Tucson, Univ. Arizona Press, 30 p.
- Wilhelms, D. E., 1964, Preliminary geologic map of the Mare Vaporum quadrangle of the Moon, in Astrogeol. Studies Ann. Prog. Rept. , July 1963-July 1964, map supp.: U.S. Geol. Survey open-file report.
- \_\_\_\_\_ 1965a, Fra Mauro and Cayley Formations in the Mare Vaporum and Julius Caesar quadrangles, in Astrogeol. Studies Ann. Prog. Rept. , July 1964-July 1965, pt. A: U.S. Geol Survey open-file report, p. 13-28.

- Wilhelms, D. E., 1965b, Preliminary geologic map of the Taruntius quadrangle of the Moon, in Astrogeol. Studies Ann. Prog. Rept., July 1964-July 1965, map supp. : U.S. Geol. Survey open-file report.
- \_\_\_\_\_ 1965c, Preliminary geologic map of the Petavius quadrangle of the Moon, in Astrogeol. Studies Ann. Prog. Rept., July 1964-July 1965, map supp. : U.S. Geol. Survey open-file report.
- Wilhelms, D. E., and Trask, N. J., 1965a, Compilation of geology in the lunar equatorial belt, in Astrogeol. Studies Ann. Prog. Rept., July 1964-July 1965, pt. A: U.S. Geol. Survey open-file report, p. 29-34 and map supp.
- \_\_\_\_\_ 1965b, Polarization properties of some lunar geologic units, in Astrogeol. Studies Ann. Prog. Rept., July 1964-July 1965, pt. A: U.S. Geol. Survey open-file report, p. 63-80.
- Wilhelms, D. E., Masursky, Harold, Binder, A. B., and Ryan, J. D., 1965, Preliminary geologic mapping of the easternmost part of the lunar equatorial belt, in Astrogeol. Studies Ann. Prog. Rept., July 1964-July 1965, pt. A: U.S. Geol. Survey open-file report, p. 45-53.